Instytut Inżynierii Chemicznej
POLSKIEJ AKADEMII NAUK

ROZPRAWA DOKTORSKA

mgr inż. Agnieszka Ciemięga

Monolityczne, przepływowe mikroreaktory krzemionkowe z centrami kwasowymi. Otrzymywanie, właściwości i zastosowanie w wybranych procesach katalitycznych.

Promotor: dr hab. inż. Julita Mrowiec-Białoń

Promotor pomocniczy: dr inż. Katarzyna Maresz

Gliwice 2018

Środki na realizację badań zostały pozyskane z Narodowego Centrum Nauki w ramach projektów „Opus” oraz „Preludium”

Projekt „Opus” nr. 011/01/B/ST8/03855 pt. „Inżynieria otrzymywania ciągłych, wysokowydajnych, monolitycznych mikroreaktorów”, 2011-2014

Projekt „Preludium” nr. 014/15/N/ST8/03171 pt. „Nowe ciągłe monolityczne mikroreaktory do chemoselektywnej redukcji związków karbonylowych”, 2015-2017

Składam serdeczne podziękowania

Pani dr hab. inż. Julicie Mrowiec-Białoń za cenne uwagi merytoryczne, owocne dyskusje i wszechstronną pomoc.

Pragnę również wyrazić wdzięczność

Pani dr inż. Katarzynie Maresz za życzliwość i zaangażowanie na wszystkich etapach powstawania niniejszej pracy

oraz

Panu Prof. dr hab. inż. Andrzejowi Jarzębskiemu za wsparcie i poświęcony czas.

SPIS TREŚCI

WYKAZ PUBLIKACJI STANOWIĄCYCH ROZPRAWĘ DOKTORSKĄ, O KTÓRYCH MOWA W ART. 13.2 USTAWY

P1. **Agnieszka Koreniuk**, Katarzyna Maresz, Klaudia Odrozek, Andrzej B. Jarzębski, Julita Mrowiec-Białoń, *Highly effective continuous-flow monolithic silica microreactor for acid catalyzed processes,* Applied Catalysis A, General 489 (2015) 203-208. $IF_{5\text{-}year}$= 4,403

Udział w syntezie i funkcjonalizacji monolitów, badaniach fizykochemicznych, katalitycznych oraz w opracowaniu wyników i pisaniu publikacji.

P2. Małgorzata Berdys, **Agnieszka Koreniuk**, Katarzyna Maresz, Wojciech Pudło, Andrzej B. Jarzębski, Julita Mrowiec-Białoń, *Fabrication and performance of monolithic continuous-flow silica microreactors*, Chemical Engineering Journal 282 (2015) 137-141. $IF_{5\text{-}year}$= 5,439

Udział w syntezie materiałów, badaniach fizykochemicznych oraz opracowywaniu wyników.

P3. **Agnieszka Koreniuk**, Katarzyna Maresz, Julita Mrowiec-Białoń, *Supported zirconium-based continuous-flow microreactor for effective Meerwein-Ponndorf-Verley reduction of cyclohexanone*, Catalysis Communications 64 (2015) 48-51. $IF_{5\text{-}year}$= 3,646

Udział w syntezie i funkcjonalizacji monolitów, badaniach fizykochemicznych, katalitycznych oraz w opracowaniu wyników i pisaniu publikacji.

P4. **Agnieszka Koreniuk**, Katarzyna Maresz, Klaudia Odrozek, Julita Mrowiec-Białoń, *Titania-silica monolithic multichannel microreactors. Proof of concept and fabrication/structure/catalytic properties in the oxidation of 2,3,6-trimethylphenol*, Microporous and Mesoporous Materials 229 (2016) 98-105. $IF_{5\text{-}year}$=3,660

Udział w syntezie i funkcjonalizacji monolitów, badaniach hydrodynamicznych, fizykochemicznych i katalitycznych oraz w opracowaniu wyników i pisaniu publikacji.

P5. **Agnieszka Ciemięga**, Katarzyna Maresz, Julita Mrowiec-Białoń, *Continuous-flow chemoselective reduction of cyclohexanone in a monolithic silica-supported $Zr(OPr^i)_4$ multichannel microreactor*", Microporous and Mesoporous Materials 252 (2017) 140-145. $IF_{5\text{-year}}$=3,660

Zaplanowanie i realizacja badań. Udział w opracowaniu wyników i pisaniu publikacji.

P6. **Agnieszka Ciemięga**, Katarzyna Maresz, Janusz J. Malinowski, Julita Mrowiec-Białoń, *Continuous-Flow Monolithic Silica Microreactors with Arenesulphonic Acid Groups: Structure-Catalytic Activity Relationships*, Catalysts 7 (2017) 255-265. $IF_{5\text{-year}}$=3,947

Synteza materiałów monolitycznych o różnych strukturach, badania właściwości strukturalnych, fizykochemicznych i katalitycznych. Udział w opracowaniu wyników i pisaniu publikacji.

P7. **Agnieszka Ciemięga**, Katarzyna Maresz, Janusz J. Malinowski, Julita Mrowiec-Białoń, *Comparative study of continuous-flow microreactors based on silica monoliths modified with Lewis acid centres*, Chemical and Process Engineering 39 (2018) 33–38. $IF_{5\text{-year}}$=0,925

Zaplanowanie i realizacja badań. Udział w opracowaniu wyników i pisaniu publikacji.

P8. **Agnieszka Ciemięga**, Katarzyna Maresz, Julita Mrowiec-Białoń, *Meerwein-Ponndorf-Verley reduction of carbonyl compounds in monolithic siliceous microreactors doped with Lewis acid centres*, Applied Catalysis A, General 560 (2018) 111–118. $IF_{5\text{-year}}$=4,354

Zaplanowanie i realizacja badań. Udział w opracowaniu wyników i pisaniu publikacji.

P9 Katarzyna Maresz, **Agnieszka Ciemięga**, Julita Mrowiec-Białoń, *Selective Reduction of Ketones and Aldehydes in Continuous-Flow Microreactor - Kinetic Studies*, Catalysts 8 (2018) 221. $IF_{5\text{-year}}$=3,947

Udział w syntezie i funkcjonalizacji monolitów, badaniach fizykochemicznych, katalitycznych oraz w opracowaniu wyników i pisaniu publikacji.

WYKAZ POZOSTAŁYCH PUBLIKACJI

1. **Agnieszka Ciemięga**, Katarzyna Maresz, Janusz J. Malinowski, Julita Mrowiec-Białoń, *Efektywne katalizatory funkcjonalizowane palladem do reakcji sprzęgania Suzukiego*, Prace Naukowe Instytutu Inżynierii Chemicznej PAN 21 (2017) 33-44.

2. Katarzyna Szymańska, Monika Pietrowska, Jacek Kocurek, Katarzyna Maresz, **Agnieszka Koreniuk**, Julita Mrowiec-Białoń, Piotr Widłak, Edmond Magner, Andrzej Jarzębski, *Low back-pressure hierarchically structured multichannel microfluidic bioreactors for rapid protein digestion - Proof of concept*, Chemical Engineering Journal 287 (2016) 148-154.

3. **Agnieszka Ciemięga**, Katarzyna Maresz, Janusz J. Malinowski, Julita Mrowiec-Białoń, *Monolityczne hybrydowe sorbenty ditlenku węgla*, Prace Naukowe Instytutu Inżynierii Chemicznej PAN 20 (2016) 127-136.

4. Katarzyna Maresz, **Agnieszka Koreniuk**, Janusz J. Malinowski, Julita Mrowiec-Białoń, *Badania porównawcze przepływowych monolitycznych mikroreaktorów i reaktorów ze złożem stałym w reakcji estryfikacji*, Prace Naukowe Instytutu Inżynierii Chemicznej PAN 19 (2015) 37-48.

5. Klaudia Odrozek, Katarzyna Maresz, **Agnieszka Koreniuk**, Krystian Prusik, Julita Mrowiec-Białoń, *Amine-stabilized small gold nanoparticles supported on AlSBA-15 as effective catalysts for aerbic glucose oxidation*, Applied Catalysis A: General 475 (2014) 203-210.

6. Klaudia Odrozek, Katarzyna Maresz, **Agnieszka Koreniuk**, Janusz J. Malinowski, Julita Mrowiec-Białoń, SBA-15 modyfikowany tlenkiem glinu jako nośnik nanocząstek złota, Prace Naukowe Instytutu Inżynierii Chemicznej PAN 18 (2014) 27-37.

7. Katarzyna Maresz, Janusz J. Malinowski, Klaudia Odrozek, **Agnieszka Koreniuk**, Julita Mrowiec-Białoń, Andrzej B. Jarzębski, *Kinetic of acetic acid –methanol esterification reaction over sulphonic acid-functionalized MCF catalyst*, Prace Naukowe Instytutu Inżynierii Chemicznej PAN 17 (2013) 35-46.

8. Klaudia Odrozek, Katarzyna Maresz, **Agnieszka Koreniuk**, Julita Mrowiec-Białoń*, Gold nanoparticles as active catalyst of glucose oxidation,* Prace Naukowe Instytutu Inżynierii Chemicznej PAN 17 (2013) 5-15.

STRESZCZENIE

Przedmiotem badań było opracowanie innowacyjnych, efektywnych, przepływowych mikroreaktorów do zastosowań w syntezie wybranych związków organicznych. Rdzeniami aktywnymi mikroreaktorów były modyfikowane monolity krzemionkowe otrzymane metodą zol-żelową z jednoczesną separacją fazową oraz szablonowaniem za pomocą związku powierzchniowo czynnego. Hierarchiczną strukturę monolitów tworzyły transportowe, przelotowe makropory, a obecne w szkielecie krzemionkowym mezopory o bi- lub monomodalnym rozkładzie wielkości decydowały o rozwinięciu powierzchni właściwej materiałów.

Otrzymano cylindryczne monolity o średnicy 4,5 mm oraz długości od 1 do 8 cm, o trzech znacząco różnych morfologiach, wynikających z zastosowania odmiennych procedur syntezy tych materiałów. Przeprowadzono szczegółowe badania właściwości strukturalnych materiałów metodami: niskotemperaturowej adsorpcji azotu, porozymetrii rtęciowej, skaningowej mikroskopii elektronowej. Monolity z dużymi przepływowymi makroporami, o wielkościach w zakresie 30-50 μm, oraz bimodalnym rozkładem mezoporów (2,5/20 nm) cechowała powierzchnia właściwa S_{BET} wynosząca około 300 m^2/g i całkowita objętość porów ok. 4 cm^3/g. Materiały syntetyzowane bez związku powierzchniowo-czynnego oraz z zastosowaniem łagodniejszych warunków obróbki hydrotermalnej (niższa temperatura i/lub stężenie amoniaku tj. 80^oC i 40^oC, stosując odpowiednio 1M i 0,1M roztwór NH_3; warunki standardowej obróbki: 90 ^oC i 1M NH_3) wyróżniały mniejsze makro- i mezopory (4-6 μm/15 nm i 1-3 μm/9 nm) oraz większa powierzchnia właściwa, do 575 m^2/g.

W pracy wyznaczono opory przepływu cieczy przez monolity oraz obliczono współczynniki przepuszczalności. Ich wartość silnie zależała od wielkości makroporów.

Monolity modyfikowano w celu nadania im właściwości kwasowych. Centra aktywne o charakterze kwasów Brönsteda uzyskano przez funkcjonalizację materiału grupami arenosulfonowymi. Właściwości fizykochemiczne określono stosując metody spektroskopii FTIR oraz termograwimetrii. Największe stężenie centrów aktywnych, wynoszące 0,97 mmol/g, uzyskano w monolicie o największej powierzchni właściwej. Zbadano wpływ stężenia grup organicznych, długości monolitycznego rdzenia, natężenia przepływu reagentów, temperatury i stosunku molowego substratów na konwersję oraz produktywność mikroreaktorów w modelowych reakcjach estryfikacji kwasów octowego i mlekowego butanolem. Wykazano, że mikroreaktory mogą stabilnie

pracować przez wiele godzin, w temperaturze 140^{o}C. Stwierdzono, że zaproponowane rozwiązanie umożliwia efektywne prowadzenie procesu estryfikacji, przy jednoczesnym znacznym jego uproszczeniu, wynikającym z eliminacji separacji katalizatora.

Zbadano właściwości katalityczne i transportowe mikroreaktora typu „monolit w monolicie", wykonanego metodą wprowadzenia hierarchicznej krzemionki do szkieletu monolitycznego nośnika kordierytowego z kapilarnymi kanałami. Celem tych działań było powiększenie skali z jednoczesnym zwiększeniem wytrzymałości mechanicznej reaktora. Reaktor, w porównaniu z monolitycznymi mikroreaktorami, charakteryzował się większymi o 40% spadkami ciśnienia.

Monolity z centrami kwasowymi o charakterze Lewisa otrzymano wykorzystując do funkcjonalizacji prekursory metali: cyrkonu, glinu i tytanu. Przeprowadzono kompleksową charakterystykę właściwości fizykochemicznych katalizatorów. Znaleziono zależności pomiędzy rodzajem centrów aktywnych, ich chemicznym otoczeniem oraz stężeniem i wydajnością procesu selektywnej redukcji związków karbonylowych metodą Meerweina-Ponndorfa-Verleya (MPV) w opracowanych mikroreaktorach. Badania katalityczne przeprowadzono dla szeregu ketonów i aldehydów, wyznaczono parametry kinetyczne reakcji, a wyniki porównano z danymi dostępnymi w literaturze. Mikroreaktory zawierające cyrkon, z przyłączonymi ligandami propylowymi, okazały się najbardziej efektywne spośród badanych. Cechami, które wyróżniają zaproponowane mikroreaktory, poza wysoką produktywnością, są łatwość przygotowania, regeneracji, magazynowania i kontroli parametrów procesowych.

Porównano właściwości monolitycznych tytanokrzemianów syntetyzowanych metodą impregnacji oraz współkondensacji, tj. wprowadzenia centrów aktywnych podczas syntezy monolitów. Materiały tytanokrzemianowe otrzymane metodą współkondensacji charakteryzowały się znakomitym rozproszeniem jonów tytanu w szkielecie krzemionkowym, co jest warunkiem koniecznym ich aktywności w procesach selektywnego utleniania związków organicznych. Właściwości te zweryfikowano w reakcji utleniania 2,3,6-trimetylofenolu do 2,3,5-trimetylo-1,4-benzochinonu, ważnego półproduktu do syntezy witaminy E. Pokazano złożone zależności między aktywnością centrów i produktywnością a strukturą porowatą mikroreaktorów.

Stwierdzono, że kręta struktura przepływowych kanałów w monolitach, odpowiadającą za intensyfikację mikromieszania i transportu masy, wraz z łatwo dostępną, rozwiniętą powierzchnią właściwą, odpowiadają za wysoką aktywność i efektywność monolitycznych mikroreaktorów.

Zaproponowane mikroreaktory mogą być z powodzeniem stosowane w wielu ważnych procesach chemicznych, zastępując reaktory okresowe oraz przepływowe ze złożem upakowanym. Otwiera to szerokie możliwości ich praktycznego wykorzystania, zwłaszcza do syntezy związków chemicznych o specjalnych właściwościach oraz farmaceutyków.

ABSTRACT

The aim of the work was to elaborate innovative, highly effective continuous-flow microreactors for organic synthesis purposes. Modified silica monoliths were applied as catalytically reactive cores of micoreactors. The monoliths were prepared by an aggregate of the sol-gel, surfactant tempting and phase separation methods. The materials featured a hierarchical pore structure of i. interconnected flow-through macropores, and ii. mesopores, located in the silica skeleton, with mono- or bi-modal size distribution, providing large specific surface area.

Cylindrical monoliths, with diameter of 4.5 mm and lengths of 1 to 8 cm, with three different morphologies resulting from the use of various synthesis protocols, were obtained. Detailed studies of the structural properties of materials were carried out by means of low-temperature nitrogen adsorption, mercury porosimetry, scanning electron microscopy. Monoliths with large flow-through macropores, in the range of 30-50 μm and a bimodal mesopore size distribution (2.5/20 nm) were characterised by specific surface area of about 300 m^2/g and a total pore volume ca. 4 cm^3/g. When surfactant was not added and the synthesis was performed under mild hydrothermal treatment conditions (lower temperature and/or ammonia concentration i.e. at 80 ^oC and 40 ^oC, and using 1M and 0.1 M NH_3 solution, respectively; standard conditions were 90 ^oC and 1M NH_3) monoliths featured smaller macro- and mesopores (i.e. 4-6 μm/15 nm and 1-3 μm/9 nm) but larger specific surface area, up to 575 m^2/g. The flow resistance of liquids was measured and the permeability coefficients were calculated. The values strongly depended on the size of macropores.

The surface of monoliths was modified with various moieties to impart acidic properties. Brönsted acid centres were obtained by functionalization with arenesulfonic groups. The physicochemical properties of materials were determined using spectroscopic and thermogravimetric methods. The highest concentration of centres, 0.97 mmol/g, was reached in the sample of the largest specific surface area. The performance of the microreactors was studied in continuous-flow model esterification reactions of acetic and lactic acids with butanol. Effects of organic group concentration, length of monolith, flow rate of reactants, temperature and molar ratio of the substrates on a conversion and thus microreactor productivity (space-time yield) were determined. Long-term catalytic stability of the microreactor at 140 ^oC has been confirmed. It was found that microreactors boost the

esterification process and additional important assets are continuous operation with no need for catalyst separation and recycling.

The catalytic and flow-through properties of the "monolith in monolith" microreactor, made by introducing hierarchically structured silica into the channels of typical cordierite monolith were also studied. The modification increased the mechanical strength of the reactor, its size and enhanced reaction capacities, as well. However, that reactor featured enlarged (by 40%) pressure drop than recorded in the monolithic microreactors.

Comparative studies of the monolithic silica microreactors modified with different Lewis sites were performed in the Meerwein-Ponndorf-Verley (MPV) selective reduction of the carbonyl compounds. Lewis acid centres were obtained by monolith's modification using various zirconium, aluminium and titanium precursors. A comprehensive characterization of the physicochemical properties of the catalysts was performed. The effects of different active centres, chemical environment and concentration on the efficiency of the MPV reaction were shown.

Catalytic studies were carried out for a number of ketones and aldehydes. Reactions kinetics was determined and the results were compared with literature data. Microreactors containing zirconium sites surrounded by propoxy ligands, appeared to be the most effective. The facile preparation, regeneration, storage, control of process parameters and high productivity were found to be inherent features of the proposed microreactors.

The properties of monolithic titanosilicates, synthesized by impregnation and co-condensation method were compared. Those prepared by co-condensation were characterised by excellent dispersion of titanium ions over the silica skeleton, required for their high activity in the selective oxidation of organic compounds. Catalytic performance of the microreactors was verified in the selective oxidation of 2,3,6-trimethylphenol to 2,3,5-trimethyl-1,4-benzoquinone, an important intermediate for vitamin E synthesis. Activity of the centres, productivity and structural properties of the microreactors were determined.

It was concluded that a waving, tortuous structure of flow-through channels present in the monoliths, which induce intensive micromixing and enhance external mass transport, plus an easily accessible, large surface area stand behind a very high activity and efficacy of the monolithic microreactors.

The performed studies demonstrate that the continuous-flow microreactors can be successfully applied in many important chemical processes, and replace batch and packed

bed flow reactors in multi-kilogram scale fabrication of fine chemicals, complex intermediates and pharmaceuticals.

1. WSTĘP

1.1 Materiały porowate

Inżynieria materiałów porowatych począwszy od lat 90-tych XX wieku stanowi ogromny, szybko rozwijający się obszar badawczy, skupiający zainteresowanie naukowców z wielu grup badawczych. Rozwój nauk dotyczących otrzymywania uporządkowanych, porowatych materiałów z „zaprojektowaną" teksturą zainicjował postęp technologiczny w dziedzinach takich jak: adsorpcja, separacja, kataliza, medycyna i nanotechnologia. Możliwości ich zastosowań silnie zależą zarówno od właściwości strukturalnych, chemicznych, jak i ich morfologii. Materiały, przyjmujące postać proszków, granulek, włókien, cienkich filmów czy monolitów, mogą cechować się strukturą mikro-, mezo-, makro-porowatą, hierarchiczną, o charakterze uporządkowanym lub chaotycznym.

Najlepiej poznaną i najczęściej wykorzystywaną w przemyśle grupą materiałów porowatych są zeolity. Ich krystaliczna struktura, z porami o średnicach mniejszych niż 1,5 nm, generującymi duże powierzchnie właściwe, powoduje, że są one atrakcyjne w obszarze selektywnej adsorpcji, opartej na niewielkich różnicach w wielkości cząsteczek gazu. Niemniej jednak, mikroporowata natura zeolitów i związane z nią ograniczenia dyfuzyjne, są czynnikami ograniczającymi ich wykorzystanie w wielu procesach katalitycznych, zwłaszcza z udziałem dużych molekuł [1-3]. Przełomem w inżynierii materiałowej była synteza i charakterystyka uporządkowanego materiału M41S, przez naukowców z firmy Mobil Oil Corporation [4]. Zastosowanie metod szablonowania związkami amfifilowymi dało początek nowej rodzinie materiałów krzemionkowych, a także w syntezie wielu tlenkowych i hybrydowych materiałów [5]. Oddziaływania pomiędzy szablonem i prekursorem tlenku umożliwiają otrzymanie materiałów o strukturach dwu- (2D) i trójwymiarowych (3D), o różnym zakresie rozmiarów porów i wielkości ziaren. Wiele uwagi poświęcono modyfikacji i zastosowaniom mezoporowatych sit krzemionkowych o strukturze heksagonalnej (MCM-41, SBA-15), regularnej (MCM-48, SBA-16), warstwowej (MCM-50) [6, 7], a także mezostrukturalnym piankom komórkowym (MCFs) [8-10]. Pomimo zalet związanych z możliwością precyzyjnej kontroli struktury i właściwości chemicznych, proszkowa postać tych materiałów stwarza trudności związane z separacją, regeneracją i ponownym wykorzystaniem, co ogranicza ich zastosowanie w przemyśle.

Monolityczne materiały, posiadające właściwości sit molekularnych i/lub mezoporowatych są rozwiązaniem pozwalającym na wyeliminowanie części kłopotliwych operacji, a tym samym redukcję kosztów aparaturowych i eksploatacyjnych. Warunkiem użyteczności monolitów jest obecność systemu kanałów, tworzonych przez połączone ze sobą makropory, umożliwiające transport mediów do rozbudowanej wewnętrznej sieci mikro/mezoporów.

Krzemionkowe materiały monolityczne o ściśle zdefiniowanej ciągłej, bimodalnej strukturze porów po raz pierwszy zaproponował Nakanishi. Porowate monolity otrzymano z wykorzystaniem połączonych metod: zol-żelowej oraz separacji fazowej, pod kątem zastosowania ich jako wysokosprawnych kolumn do chromatografii cieczowej [11-13]. Znaczący wkład w poprawę właściwości strukturalnych i przepływowych monolitów wnieśli Smått [14] i Pudło [15], stosując kationowe związki powierzchniowo-czynne, jako matryce struktury mezoporowatej oraz hydrotermalną obróbkę w amoniaku, co zaowocowało otrzymaniem materiałów o bimodalnym rozkładzie mezoporów oraz istotnym powiększeniem średnic makroporów, aż do wielkości ok. 50 μm.

1.2 Mikroreaktory

W ostatniej dekadzie miniaturyzacja procesów i opracowywanie nowych katalizatorów zmieniły koncepcję produkcji związków chemicznych o specjalnych właściwościach. Tradycyjne, duże, drogie oraz energochłonne instalacje pilotażowe w niektórych przypadkach mogą być zastąpione przez mniejsze, bardziej elastyczne, efektywniejsze, wielofunkcyjne mikro-instalacje, złożone z układów mikroreaktorów, które charakteryzują się mniejszymi kosztami inwestycyjnymi i operacyjnymi. Wiele prac poświęcono możliwym zastosowaniom małych reaktorów strukturalnych w przemyśle farmaceutycznym oraz różnych gałęziach przemysłu chemicznego, spożywczego i kosmetycznego [16, 17].

Mikroprzepływowe reaktory w przemyśle są stosowane głównie do produkcji małotonażowej, wysokiej jakości chemikaliów *(fine chemicals),* niebezpiecznych lub mających krótki okres przydatności związków chemicznych. Technologie wykorzystujące mikroreaktory są przyjaznym dla środowiska rozwiązaniem, oferującym zredukowane zużycie odczynników, a tym samym wytwarzanie mniejszych strumieni odpadów. Technologie te są już stosowane w wielu zakładach farmaceutycznych i chemicznych np. DSM i Corning Incorporated wykorzystują je do selektywnego nitrowania [18], Xi'an Huian Industrial Group wytwarza nitroglicerynę o wysokiej czystości [19],

FMC Corporation, będący jednym z największych producentów nadtlenku wodoru, był zaangażowany w projekt dotyczący jego produkcji bezpośrednio w miejscu, gdzie stanowi półprodukt do dalszych syntez [20]. Sigma-Aldrich oferuje wygodne rozwiązanie typu *all-in-one* pod nazwą handlową Microreactor Explorer Kit [21].

Mikroreaktory zazwyczaj są wytwarzane w formie płytek lub stosu płytek z kanałami kapilarnymi o średnicy 50-500 μm i długości mniejszej niż 2000 μm, metodami odlewania taśmowego, żelowego oraz bardziej zaawansowanymi technikami dwu- i trójwymiarowymi (2D i 3D), tj. sitodruku lub stereolitografii [22-25]. Istotną zaletą tych reaktorów jest duży stosunek powierzchni do objętości, osiągający wartość 20000 m^2/m^3, podczas gdy w konwencjonalnych reaktorach wielkość ta nie przekracza 1000 m^2/m^3 [16]. Mikroraktory, w porównaniu z konwencjonalnymi reaktorami, cechują się lepszą wymianą ciepła oraz masy, co znacząco wpływa na poprawę wydajności i selektywności prowadzonych reakcji chemicznych [26].

W mikroreaktorach z upakowanym złożem, jako wypełnienie, stosuje się nośniki tlenkowe oraz polimerowe. Pomimo, że nośniki polimerowe są zazwyczaj stosunkowo tanie i proste do otrzymania, ich zastosowanie jest ograniczone z powodu tendencji do pęcznienia i wrażliwości na wysoką temperaturę. Ponadto niejednorodność uziarnienia skutkuje brakiem regularności dynamiki przepływu przez złoże, co jest niekorzystne z punktu widzenia inżynierii procesowej. Tych wad pozbawione są tlenkowe wypełnienia monolityczne. Monolityczny nośnik stanowiący rdzeń mikroreaktora powinien być neutralny chemicznie, stabilny w warunkach reakcji, nietoksyczny i posiadać zdolność trwałej immobilizacji aktywnych indywiduów chemicznych. Porowata krzemionka spełnia wszystkie te wymagania. Modyfikacja powierzchni grupami organicznymi lub nieorganicznymi, którą umożliwia obecność silanoli, pozwala na nadanie nośnikom nowych właściwości fizykochemicznych. Monolityczne mikroreaktory krzemionkowe są stosunkowo nowym rozwiązaniem procesowym [27], a do tej pory otrzymywano je poprzez modyfikację monolitów grupami organicznymi [28, 29], zeolitami [30] oraz enzymami [31-33]. Stosunek powierzchni do objętości w tych reaktorach jest o ponad rząd wielkości większy niż w mikroreaktorach strukturalnych, co bezpośrednio przekłada się na intensyfikację procesów wymiany masy i ciepła.

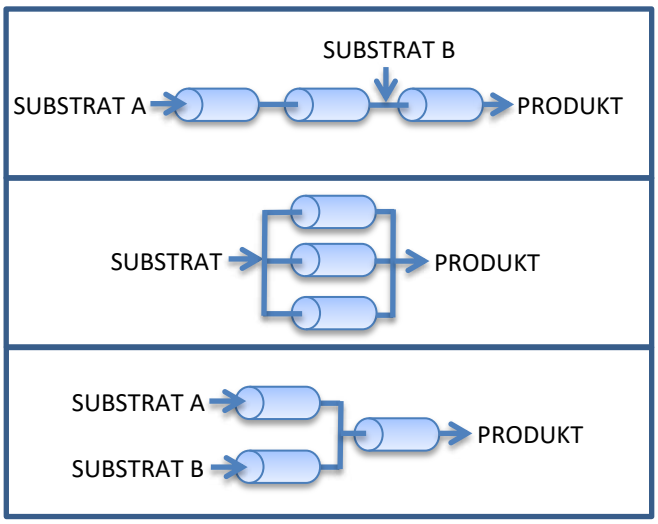

Rysunek 1. Przykładowe moduły katalityczne złożone z mikroreaktorów

Praktyczne aspekty, takie jak prostota i elastyczność konstrukcji instalacji doświadczalnej, zmniejszone zużycie reagentów i poprawa bezpieczeństwa pracy powodują, że mikroreaktory są niezwykle obiecujące w procesach, w których zapotrzebowanie na określony produkt jest czasowe i zmienne. Jedną z ważniejszych ich zalet jest możliwość łączenia w większe segmenty, tworzące mikro-instalacje (rys. 1), a także możliwość prowadzenia złożonych procesów chemicznych w połączonych układach kilku reaktorów. Mikroreaktory umożliwiają szybką implementację wyników badań otrzymanych w laboratorium do praktyki przemysłowej, bez zmiany istotnych warunków procesowych (rys. 2). Zastosowanie metody powiększania skali „numbering-up" ułatwia dostosowanie rozmiaru instalacji do wymaganej wielkości produkcji [17-19].

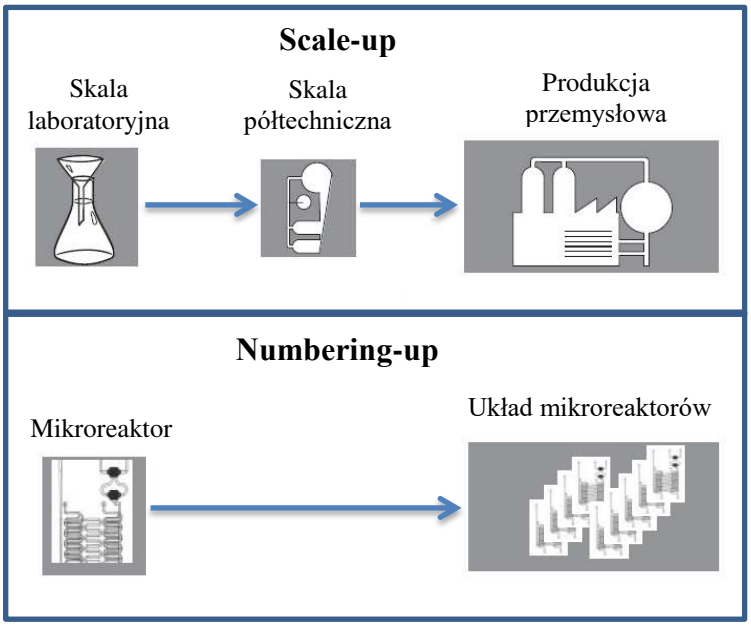

Rysunek 2. Uproszczone schematy metod powiększania skali: scale up vs. numbering-up [16]

2. CEL PRACY

Celem pracy było otrzymanie przepływowych, monolitycznych mikroreaktorów, opartych na materiałach krzemionkowych o hierarchicznej strukturze porów, modyfikowanych centrami kwasowymi. Zakres pracy obejmował:

- syntezę monolitów różniących się rozmiarami porów przepływowych i dyfuzyjnych,
- wprowadzenie centrów aktywnych metodą jedno lub dwustopniowej modyfikacji z wykorzystaniem różnych prekursorów,
- charakterystykę właściwości strukturalnych i fizykochemicznych materiałów,
- weryfikację właściwości katalitycznych w procesach: estryfikacji, chemoselektywnej redukcji związków karbonylowych oraz selektywnego utleniania związków organicznych,
- zbadanie wpływu struktury nośnika (wielkości powierzchni, rozmiaru porów), rodzaju i ilości centrów katalitycznych oraz ich prekursora, a także zastosowanych warunków syntezy na aktywność katalityczną.

Uzyskanie zależności pomiędzy aktywnością katalityczną i wydajnością a właściwościami strukturalnymi i przepływowymi mikroreaktorów, miało na celu dostarczenie nowej wiedzy, niezbędnej do projektowania wydajnych i elastycznych układów katalitycznych do syntezy związków chemicznych o specjalnych właściwościach, do zastosowań w procesach przemysłu farmaceutycznego, spożywczego oraz kosmetycznego.

3. METODYKA

Monolity krzemionkowe, będące nośnikiem centrów aktywnych oraz równocześnie rdzeniami mikroreaktorów, otrzymano z wykorzystaniem połączonych metod zol-żelowej oraz separacji fazowej. Zmiany składu mieszaniny, warunków syntezy oraz odpowiedni dobór form pozwoliły na uzyskanie materiałów o pożądanych właściwościach, kształcie i wymiarach. Parametry tekstury wyznaczone zostały na podstawie izoterm niskotemperaturowej adsorpcji azotu oraz porozymetrii rtęciowej. Ciągła struktura makroporów, determinująca przepływ cieczy przez monolit, została zweryfikowana za pomocą skaningowej mikroskopii elektronowej. Monolity, wraz z odpowiednimi króćcami doprowadzającymi media reakcyjne, umieszczone były w teflonowych osłonkach termokurczliwych. Opory przepływu cieczy dla tak otrzymanych mikroreaktorów zostały wyznaczone za pomocą manometru różnicowego. Centra aktywne były wprowadzone na powierzchnię krzemionki metodą impregnacji, w reakcji prekursora z izolowanymi powierzchniowymi hydroksylami w atmosferze suchego gazu obojętnego, bądź metodą jednostopniową – współkondensacji. Stężenie, stabilność temperaturowa, sposób związania z powierzchnią, stopień dyspersji centrów aktywnych były określone za pomocą metod: ICP-MS, termograwimetrii, spektroskopii FTIR i UV-Vis. Stanowisko badawcze do badań katalitycznych składało się z: zbiornika zasilającego, pompy membranowej, mikroreaktora, termostatu, odbieralnika produktu oraz chromatografu gazowego do analizy stężeń substratów i produktów.

3.1 Właściwości strukturalne

Do opisu struktury monolitów zastosowano kilka technik badawczych, które umożliwiły uzyskanie danych o porowatości tych materiałów w różnych skalach.

Na podstawie izoterm adsorpcji azotu, otrzymanych w temperaturze -196^{o}C, wyznaczano właściwości monolitów w mikro- i mezo- skali (średnica porów do 50 nm). Powierzchnię właściwą, S_{BET}, obliczano metodą Braunauera-Emmeta-Tellera [34], a rozkłady wielkości mezoporów i mikroporów odpowiednio metodą Barretta-Joynera-Halendy (BJH) [35], i Dubinina-Astakhova [36]. Przed przystąpieniem do badań próbki poddano odgazowaniu w podwyższonej temperaturze. Pomiary wykonano w aparacie Micromeritics ASAP 2020.

Przelotowa struktura makroporów była weryfikowana na podstawie obrazów uzyskanych metodą skaningowej mikroskopii elektronowej (Hitachi HD-2300A).

Całkowitą objętość porów i średnice makroporów wyznaczano metodą porozymetrii rtęciowej (Quantachrome PoreMaster 60).

3.2 Właściwości fizyko-chemiczne

Próbki po modyfikacji centrami aktywnymi poddawano badaniom metodą spektroskopii w podczerwieni (FTIR). Pomiary wykonano w aparacie Nicolet 4700. W pracy wykorzystywano dwie techniki: transmisyjną i rozproszonego odbicia (DRIFT). Zastosowanie techniki transmisyjnej wymagało rozcieńczenia próbek w materiale transparentnym dla promieniowania IR (2 mg próbki/748 mg KBr). Homogeniczną mieszaninę formowano w postać pastylek, przy użyciu prasy hydraulicznej. Na podstawie charakterystycznych pasm w uzyskanych widmach identyfikowano obecność grup funkcyjnych w próbkach.

W technice DRIFT do pomiarów zastosowano komorę próżniową z możliwością regulacji temperatury, wyposażoną w okna ZnSe. Komorę wykorzystano do oznaczenia kwasowości próbek metodą adsorpcji pirydyny (Py). Odgazowane i wysuszone w temperaturze 110^{o}C próbki poddawano adsorpcji par Py w temperaturze otoczenia, pod ciśnieniem atmosferycznym przez 2 godziny. W komorze pod obniżonym ciśnieniem, w temperaturze 150^{o}C następowała desorpcja fizycznie zaadsorbowanej pirydyny. Pozostała część pirydyny, zależnie od rodzaju centrum, była zaadsorbowana w postaci jonu pirydynowego (PyH^{+}) na centrach kwasowych Brönsteda lub kompleksu (PyL) na centrach kwasowych Lewisa, których obecność stwierdzano na podstawie pasm adsorpcyjnych, obserwowanych, odpowiednio przy liczbach falowych 1540 cm^{-1} oraz 1445 cm^{-1}. Moc centrów wyznaczano na podstawie zmiany intensywności danego pasma, zarejestrowanego w temperaturach 150^{o}C i 200^{o}C.

Na podstawie analizy termograwimetrycznej określono stężenie grup organicznych w sfunkcjonalizowanych materiałach oraz stabilność termiczną otrzymanych mikroreaktorów. Badania prowadzono w termograwimetrze STAR (Mettler Toledo) w zakresie temperatur 25-800^{o}C, w przepływie powietrza wynoszącym 60 cm^{3}/min, stosując szybkość grzania 10 K/min.

Spektroskopię DRS UV-Vis zastosowano do zbadania koordynacji jonów metali wbudowanych w strukturę materiału krzemionkowego. Próbki przed analizą odgazowano, wysuszono i rozproszono w KBr. Badania przeprowadzono w aparacie Varian Carry 100, wyposażonym w komorę przystosowaną do badania ciał stałych (Labsphere DRA-CA-3300), w zakresie długości fali 190-500 nm.

Skład chemiczny próbek oznaczano metodą spektrometrii mas sprzężoną z plazmą wzbudzaną indukcyjnie (ICP-MS).

3.3 Właściwości hydrodynamiczne

Spadki ciśnienia w mikroreaktorach mierzono za pomocą manometru różnicowego (UNIK 5000 Ex-Calibra), w zakresie natężeń przepływu cieczy 0,01-16 cm^3/min, a współczynniki przepuszczalności obliczono z równania Darcy'ego [37]:

$$\frac{\Delta P}{L} = \frac{1}{K}\frac{\eta}{A}\dot{V} \qquad [1]$$

gdzie:

ΔP- spadek ciśnienia [Pa],

L- długość reaktora [m],

K- współczynnik przepuszczalności [m^2],

η – współczynnik dynamiczny lepkości cieczy [Pa·s],

A – pole przekroju poprzecznego [m^2],

$\dot{V}$ – objętościowe natężenie przepływu [m^3/s].

3.4 Właściwości katalityczne

Właściwości mikroreaktorów weryfikowano w reakcjach: estryfikacji, chemoselektywnej redukcji związków karbonylowych Meerweina-Ponndorfa-Verleya (MPV) oraz selektywnego utleniania.

Mikroreaktory sfunkcjonalizowane grupami arenosulfonowymi badano w reakcjach estryfikacji kwasów octowego oraz mlekowego butanolem. Reakcje prowadzono w zakresie temperatur 75^{o}C-140^{o}C, dla stosunków molowych kwas:alkohol wynoszących 1:1, 1:6, 1:12, natężeń przepływu 0,03-0,09 cm^3/min, i długości reaktorów 1, 2, 4 cm.

Reakcję redukcji MPV wybranych ketonów i aldehydów prowadzono w mikroreaktorach modyfikowanych kompleksami cyrkonu, glinu i tytanu. Stosowano następujące warunki reakcji: temperatura: 65-95^{o}C, stosunek molowy substratów 1:6; 1:12, 1:26, 1:52, 1:78, 1:104; długość reaktorów: 1-8 cm, natężenie przepływu reagentów: 0,03-0.24 cm^3/min.

Utlenianie 2,3,6-trimetylofenolu do 2,3,5-trimetylo-1,4-benzochinonu badano w mikroreaktorach aktywowanych tlenkiem tytanu, który wprowadzano do monolitów stosując metodę impregnacji oraz współkondensacji. Czynnikiem utleniającym był nadtlenek wodoru zastosowany w 3,5 krotnym nadmiarze w stosunku do substratu. Temperatura reakcji wynosiła 80^{o}C, natężenie przepływu 0,03 cm^3/min.

Postęp wszystkich reakcji oraz ich selektywność monitorowano za pomocą chromatografu gazowego (Agilent 7890A, detektor: FID, kolumna: HP-5). Na podstawie wyznaczonych konwersji obliczano produktywność mikroreaktorów zgodnie ze wzorem [38]:

$$P = C_0 K \frac{V_T}{\tau} \quad [2]$$

gdzie:

P- produktywność [mmol/g_{kat}min],

C_0- stężenie początkowe roztworu [mmol/cm^3],

K-konwersja [-],

V_T – całkowita objętość porów [cm^3/g],

τ – czas kontaktu [min],

$$\tau = \frac{m_k V_T}{\dot{V}} \quad [3]$$

gdzie:

m_k- masa katalizatora [g],

$\dot{V}$ – objętościowe natężenie przepływu [cm^3/min].

4. WYNIKI BADAŃ

4.1 Synteza i charakterystyka monolitycznych nośników krzemionkowych [P2, P6]

Cechy materiału krzemionkowego, stanowiącego stały szkielet nośnika, takie jak porowatość, średnia wielkość, rozkład, kształt i krętość porów oraz ich wzajemne połączenie, ściśle determinują ich przydatność do określonych zastosowań. Hierarchiczna struktura porów, zawierająca pory o rozmiarach w dwóch lub więcej skalach (od nano do makro) zapewnia pożądane właściwości w wymiarze procesowym, związane z transportem substratów, a także intensywną wymianą masy i ciepła, oraz katalitycznym, obejmującym dostępność centrów aktywnych, wysoką selektywność, chemiczną stabilność oraz efektywne wykorzystanie objętości katalizatora. Obecność mikro i mezoporów wpływa na wielkość powierzchni właściwej, a tym samym na stężenie oraz dyspersję centrów aktywnych, z kolei otwarte, połączone makropory pozwalają na przepływ płynów przez materiał.

W pracy otrzymano monolityczne nośniki krzemionkowe o hierarchicznej strukturze porów. Proces syntezy jest kilkuetapowy i opiera się na jednocześnie zachodzących procesach separacji fazowej oraz zol-żelowym w kwasowym środowisku.

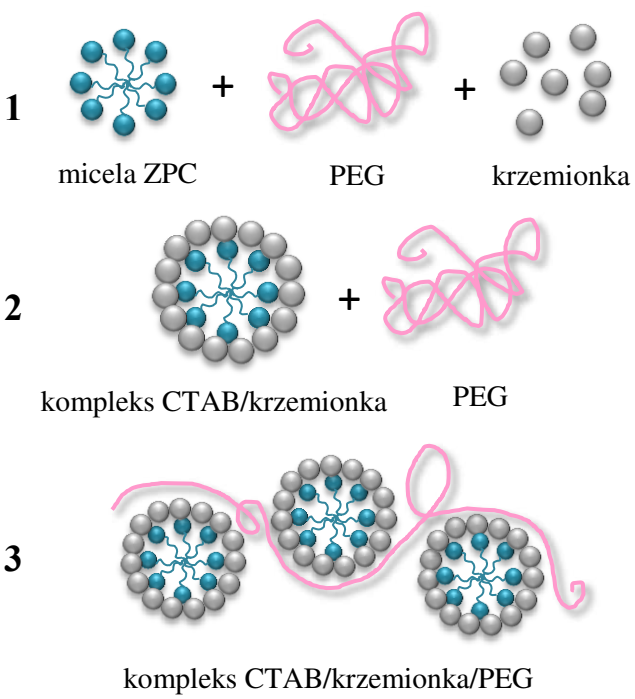

Rysunek 3. Etapy tworzenia porowatej struktury materiałów monolitycznych [14]

Na rys. 3 zaprezentowano schematycznie etapy tworzenia struktury materiałów monolitycznych. Pierwszy etap to otrzymywanie mezofazy, zawierającej prekursor krzemionki – tetraetoksysilan, kwas azotowy, kationowy związek powierzchniowo-czynny (ZPC) - bromek cetylotrimetyloamoniowy oraz rozpuszczalny w wodzie polimer – glikol polietylenowy. Związki powierzchniowo-czynne w odpowiednich warunkach tworzą micele, które oddziałują z cząsteczkami krzemionki. Związki te pełnią rolę szablonu mezoporów ulokowanych w ściankach materiału.

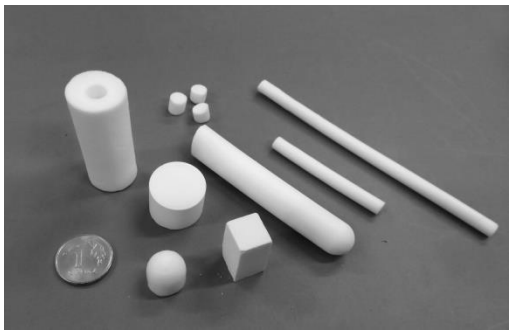

Rysunek 4. Monolity krzemionkowe o różnych kształtach

Separacja fazowa jest inicjowana przez polimeryzację alkoksylanu oraz odpychające oddziaływania zachodzące pomiędzy cząsteczkami wody i krzemionki otoczonej przez polimer. Utworzona przejściowa struktura, składająca się z fazy bogatej w krzemionkę oraz fazy wodnej jest utrwalana w wyniku procesu żelowania. Po tym etapie szkielet krzemionkowy jest jeszcze niecałkowicie skondensowany, co przekłada się na jego małą mechaniczną stabilność. Dalsza kondensacja grup silanolowych zachodzi podczas starzenia. Istotnym etapem w procesie otrzymywania monolitów jest obróbka hydrotermalna w wodnym roztworze amoniaku. Środowisko zasadowe sprzyja przeorganizowaniu struktury wskutek zjawiska nazywanego dojrzewaniem Ostwalda [14], polegającego na rozpuszczaniu i ponownym strącania krzemionki na powierzchniach o różnej krzywiźnie. Ostatnim etapem jest usunięcie organicznego szablonu w procesie kalcynacji w temperaturze 550^{o}C. Kształt i wielkość monolitu zależy od formy, w której umieszczony jest zol (rys. 4).Właściwości strukturalne monolitów silnie zależą od warunków ich syntezy. Ze względu na wrażliwość procesu na jakiekolwiek wahania parametrów (składu mieszaniny, temperatury, czasu) ważne jest rygorystyczne przestrzeganie ustalonej procedury.

W pracy [P6] przedstawiono sposób otrzymywania materiałów o trzech istotnie różnych strukturach (rys. 5). Monolityczne materiały krzemionkowe charakteryzowały się obecnością przelotowych makroporów oraz mezoporów o monomodalnym lub bimodalnym rozkładzie ich wielkości (tabela 1).

Tabela 1. Właściwości strukturalne monolitów

Monolit	S_{BET} (m^2/g)	Vp_{mezo} (cm^3/g)	V_T (cm^3/g)	D_{makro} (μm)	D_{mezo} (nm)
M1	328	1,15	4	30-50	2,5/20
M2	413	1,12	3,27	4-6	15
M3	575	1,04	2,98	1-3	8,7

Monolity wykazywały różnice w wielkości powierzchni właściwej (S_{BET}), bezpośrednio związane z rozmiarem (D_{mezo}) i objętością mezoporów (Vp_{mezo}); obecność mniejszych mezoporów przekładała się na większą powierzchnię właściwą. Zastosowanie związku powierzchniowo-czynnego skutkowało wygenerowaniem

bimodalnej mezostruktury złożonej z małych porów o średnicach ok. 2,5 nm, które są wynikiem szablonowania za pomocą miceli ZPC, oraz dużych teksturalnych mezoporów, o średniej średnicy około 20 nm. Wielkość teksturalnych mezoporów zależała przede wszystkim od warunków obróbki hydrotermalnej w roztworze amoniaku; zwiększeniu ich rozmiarów sprzyjała podwyższona temperatura, 90^{o}C i stosunkowo wysokie stężenie amoniaku (1M).

Na podstawie obrazów otrzymanych metodą skaningowej mikroskopii elektronowej i wyników analizy metodą porozymetrii rtęciowej stwierdzono znaczące różnice

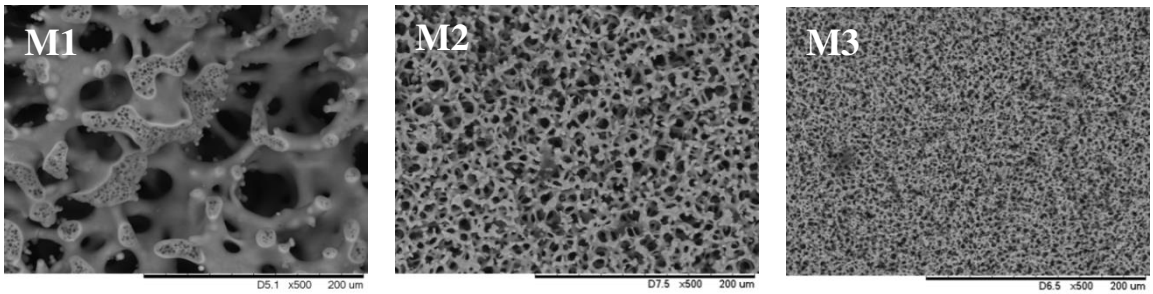

Rysunek 5. Obrazy SEM monolitów o różnych strukturach

w wielkości makroporów (D_{makro}) oraz całkowitej objętości porów (V_T). W monolitach otrzymanych przy zastosowaniu łagodniejszych warunków obróbki posyntezowej makropory były zdecydowanie mniejsze i wynosiły, odpowiednio ok. 5 μm i 1 μm, jednak charakteryzowały się większą jednorodnością grubości ścian. Tymczasem w monolicie z dużymi makroporami (30-50 μm) w krzemionkowym szkielecie dobrze widoczne były elementy struktury (mostki) o różnej grubości, w zakresie od kilku do kilkudziesięciu mikrometrów. Całkowita objętość porów w monolitach mieściła się w zakresie 3-4 cm^3/g, podczas gdy objętość mezoporów była porównywalna, osiągając średnią wartość ok. 1,1 cm^3/g.

Wielkość makroporów (przelotowych kanałów) jest niezwykle istotna w przypadku zastosowania tych materiałów, jako przepływowych mikroreaktorów, ponieważ od ich rozmiarów zależą opory przepływu mediów, co z kolei bezpośrednio wiąże się z kosztami prowadzenia procesu. Zależność pomiędzy spadkiem ciśnienia a natężeniem przepływu cieczy zaprezentowano w pracy [P6]. Przepływ cieczy przez złoże o krętej strukturze porów jest złożony i najczęściej zgodny z założeniami prawa Darcy`ego [37]. Prostoliniowy przebieg wskazuje na przepływ laminarny, który jest specyficzną cechą mikroprzepływowych układów.

Na podstawie otrzymanych danych obliczono współczynnik przepuszczalności badanych monolitów. Stwierdzono, że zmniejszenie średnicy makroporów z 50 µm do 1 µm spowodowało wzrost oporów o kilka rzędów wielkości oraz zmniejszenie przepuszczalności materiałów z $11{,}3 \cdot 10^{-12}$ m^2 do $25 \cdot 10^{-15}$ m^2. Warto podkreślić, że najwyższa wartość współczynnika przepuszczalności, wyznaczona dla monolitu, znaleziona w źródłach literaturowych wynosi $2.3 \cdot 10^{-13}$ m^2 i dotyczy materiału polimerowego modyfikowanego trypsyną [39]. Uzyskane wyniki wskazują, że zastosowanie opracowanych mikroreaktorów o największych makroporach (30-50 µm) umożliwia pracę w szerokim zakresie natężeń przepływu przy małych oporach i może być konkurencyjne w stosunku do innych proponowanych rozwiązań.

Pomimo, że kształt i wielkość monolitów hierarchicznych, będących przedmiotem pracy, zależą od formy zastosowanej w trakcie syntezy, to przy średnicach większych niż 2 cm obserwuje się pękanie materiału. W pracy [P2] wykorzystano koncepcję wzmocnienia szkieletu monolitów, w celu rozszerzenia ich potencjału aplikacyjnego, zaproponowaną przez Jarzębskiego i Pudło [40]. Idea rozwiązania („monolit w monolicie") polega na wypełnieniu monolityczną krzemionką kanałów komercyjnego, kordierytowego monolitu (rys. 6).

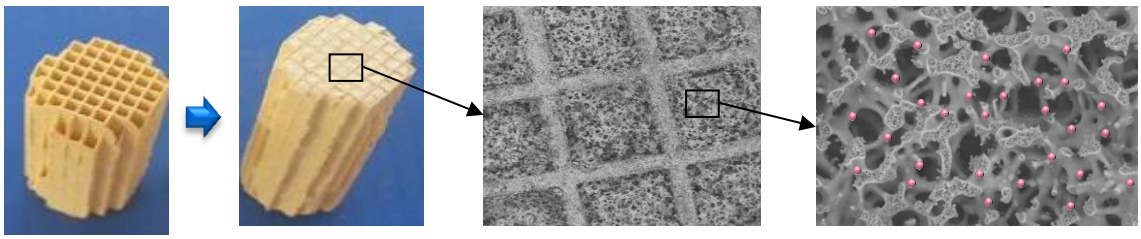

Rysunek 6. Koncepcja mikroreaktora typu „monolit w monolicie"

Zasadniczym wyzwaniem było zapewnienie dobrego kontaktu pomiędzy materiałami przy zachowaniu właściwości przepływowych i powierzchniowych monolitu hierarchicznego. Koniecznym było poddanie kordierytu obróbce, dla zwiększenia powierzchni kontaktu oraz wygenerowania większej ilości silnych, powierzchniowych hydroksyli zdolnych do utworzenia wiązań z kondensującą krzemionką. W tym celu kordieryt poddano obróbce w roztworach wodorotlenku sodu lub piranii (mieszanina nadtlenku wodoru i kwasu siarkowego (VI)) w różnych warunkach (temperatura, czas, stężenie). Na podstawie badań EDS, FTIR oraz SEM stwierdzono, że najtrwalsze połączenie pomiędzy powierzchniami materiałów uzyskano dla kordierytu poddanego obróbce w 10% wodnym roztworze NaOH w 20°C, przez 0,5 godziny. Potwierdzono zachowanie trimodalnej struktury monolitycznej krzemionki po jej syntezie

w kanałach kordierytowego monolitu. Porowatość krzemionki wbudowanej w strukturę kordierytu była ok. 20% mniejsza niż monolitycznego materiału, i wynikała z obecności mniejszych makroporów. Krzemionka charakteryzowała się natomiast większą powierzchnią właściwą oraz większą objętością mezoporów.

„Monolit w monolicie" cechowała większa stabilność mechaniczna, jednak opory przepływu były o ok. 40% wyższe niż w monolitycznym materiale krzemionkowym.

Opisane powyżej monolityczne materiały krzemionkowe sfunkcjonalizowano centrami kwasowymi (Brönsteda i Lewisa) i zastosowano jako rdzenie przepływowych mikroreaktorów.

4.2 Mikroreaktory sfunkcjonalizowane centrami kwasowymi Brönsteda [P1, P6]

Katalizatory kwasowe są szeroko wykorzystywane w procesach syntezy organicznej takich jak hydratacja, alkilowanie, eteryfikacja lub estryfikacja. Katalizatorami tych reakcji są kwasy mineralne, żywice jonowymienne, zeolity, ciecze jonowe oraz modyfikowane materiały porowate [41-45]. Do ostatniej z wymienionych grup zaliczamy materiały krzemionkowe różnych dwu- i trójwymiarowych strukturach, sfunkcjonalizowane grupami sulfonowymi, tworzącymi centra kwasowe Brönsteda.

W badaniach przedstawionych w pracy [P1] monolity krzemionkowe, o trójmodalnym rozkładzie porów (40 μm, 20 nm, 2,5 nm), powierzchni S_{BET} równej 328 m^2/g, aktywowano grupami arenosulfonowymi z wykorzystaniem metody impregnacji. Zbadano wpływ zastosowanej metody modyfikacji na zmianę właściwości strukturalnych nośnika. Stwierdzono zmniejszenie powierzchni S_{BET}, wynikające z preferencyjnego osadzania się grup funkcyjnych w małych mezoporach. Nie stwierdzono natomiast zmian w wielkościach i objętości porów teksturalnych.

Przyłączenie grup organicznych do powierzchni krzemionki potwierdzono metodą spektroskopii w podczerwieni. Na widmach próbek sfunkcjonalizowanych obserwowano pasma charakterystyczne dla drgań w pierścieniu aromatycznym, piki odpowiadające drganiom deformacyjnym grupy C-H, oraz piki odpowiedzialne za asymetryczne rozciągające drgania grup metylenowych łączących pierścień aromatyczny z nośnikiem.

Metodą termograwimetryczną wyznaczono stabilność temperaturową, sięgającą 350^oC, oraz stężenie grup funkcyjnych w próbkach. Stwierdzono, że maksymalna ilość grup, jaką można trwale związać z badanym nośnikiem wyniosła 0,65 mmol/g.

Monolity z wprowadzonymi grupami arenosulfonowymi zastosowano, jako rdzenie przepływowych mikroreaktorów, a ich aktywność katalityczną zbadano w reakcjach

estryfikacji kwasu octowego i mlekowego butanolem. W celu wyeliminowania wpływu oporów dyfuzji zewnętrznej porównano konwersje otrzymane w mikroreaktorach o różnej długości z zachowaniem stałego czasu przebywania reagentów wynoszącego 155 s. Jednakowa wartość konwersji uzyskana w 1-, 2- i 4-centymetrowych mikroreaktorach świadczyła o przebiegu procesu w obszarze kinetycznym. Przeprowadzone eksperymenty potwierdziły wysoką efektywność opracowanego mikroreaktora oraz stabilność jego właściwości katalitycznych, strukturalnych i fizykochemicznych wykazaną w 3-dniowym cyklu reakcyjnym. Struktura monolitu po reakcji, w skalach mikrometrycznej i nanometrycznej, została zachowana. Badania procesu estryfikacji kwasu mlekowego przeprowadzone w temperaturze 140^{o}C dowiodły, że mikroreaktory mogą stabilnie pracować w wysokich temperaturach.

Wpływ struktury monolitycznego rdzenia mikroreaktora na efektywność procesu estryfikacji kwasu octowego butanolem przedstawiono w pracy [P6]. W badaniach wykorzystano monolity opisane w punkcie 4.1.

Rzeczywiste stężenie grup funkcyjnych – arenosulfonowych zostało wyznaczone na podstawie analizy termograwimetrycznej. Stwierdzono, że stężenie grup trwale przyłączonych do krzemionki było proporcjonalne do jej powierzchni właściwej, co dobrze korelowało z ilością dostępnych hydroksyli.

Na podstawie badań adsorpcji/desorpcji pirydyny określono charakter i moc centrów aktywnych. Na widmach po adsorpcji obserwowano jedynie pasma charakterystyczne dla jonów pirydynowych skoordynowanych z centrami kwasowymi Brönsteda. Obecność tych pasm zarejestrowana po desorpcji w 150^{o}C i 200^{o}C, potwierdziła występowanie centrów o dużej mocy.

Porównano właściwości katalityczne mikroreaktorów i reaktora rurowego, o średnicy 4,5 mm (odpowiadającej średnicy monolitów), wypełnionego żywicą jonowymienną – Amberlyst-15, o masie równej masie monolitu. We wszystkich mikroreaktorach, niezależnie od typu rdzenia, uzyskano zbliżoną konwersję wynoszącą 42%, w reaktorze ze stałym złożem konwersja była niższa - 38%, stąd produktywność reaktorów, odniesiona do jednostki masy katalizatora była podobna. Natomiast największą produktywność, odniesioną do jednostkowej ilości centrów aktywnych, uzyskano w mikroreaktorze o największych porach, mimo, że charakteryzował się on najmniejszym stężeniem centrów kwasowych. Efekt ten został przypisany zintensyfikowanej wymianie masy reagentów z rdzenia do powierzchni krzemionkowego szkieletu oraz ułatwionemu dostępowi

reagentów do miejsc aktywnych. Produktywność reaktora ze złożem Amberlyst-15 stanowiła około 13% tej uzyskanej w najlepszym mikroreaktorze.

W mikroreaktorze typu „monolit w monolicie" uzyskano konwersję kwasu octowego mniejszą o ok. 6% niż w mikroreaktorze, którego rdzeń stanowił monolit krzemionkowy, wynikającą z krótszego czasu przebywania reagentów w reaktorze, spowodowanego mniejszą porowatością układu.

Biorąc pod uwagę produktywność uzyskaną w mikroreaktorach oraz duże różnice w wartościach współczynnika przepuszczalności, przekładającego się bezpośrednio na spadek ciśnienia, a tym samym na zapotrzebowanie energetyczne i bezpieczeństwo procesu stwierdzono, że zastosowanie mikroreaktora o największych porach jest najbardziej efektywne.

4.3 Mikroreaktory sfunkcjonalizowane centrami kwasowymi Lewisa [P3, P5, P7, P8, P9]

Centra kwasowe Lewisa są katalizatorami wielu reakcji chemicznych, między innymi redukcji Meerweina-Ponndorfa-Verleya (MPV) [46-50], utleniania Baeyera-Villigera [51, 52], reakcji Friedela-Craftsa [53, 54]. Redukcja nienasyconych związków karbonylowych do ich alkoholi ma duże znaczenie w przemyśle farmaceutycznym, kosmetycznym oraz spożywczym [55]. Reakcja przeprowadzona klasycznie, z udziałem wodoru, posiada istotne ograniczenia: z jednej strony związane z bezpieczeństwem przeprowadzanego procesu, z drugiej z małą selektywnością reakcji, zależną od wielu czynników: rodzaju metalu używanego jako katalizatora, nośnika tego metalu, rozpuszczalnika, temperatury reakcji oraz ciśnienia wodoru [56]. Alternatywną ścieżką dla syntezy niektórych związków chemicznych jest reakcja MPV, wykorzystująca mechanizm przeniesienia wodoru, która pozwala zarówno wyeliminować koszty związane z pracą pod ciśnieniem, jak i znacznie ograniczyć zużycie drogich katalizatorów. Ponadto, dobór odpowiednich warunków prowadzenia procesu może zapewnić wysoką selektywność reakcji. Reakcja MPV jest reakcją redukcji związków karbonylowych (aldehydów lub ketonów), w której jako źródło wodoru wykorzystuje się drugorzędowe alkohole [57]. Początkowo reakcja ta była prowadzona w obecności katalizatorów homogenicznych – alkoksylanów metali [58], które poza zaletami takimi jak: wysoka selektywność, możliwość prowadzenia procesu w łagodnych warunkach posiadały istotne ograniczenia, między innymi konieczność stosowania ich w ilościach stechiometrycznych w stosunku do substratu oraz trudności z separacją katalizatora z mieszaniny reakcyjnej.

Zastąpienie katalizatorów homogenicznych heterogenicznymi pozwoliło na wyeliminowanie niektórych wad, niemniej jednak problem stanowi duża wrażliwość katalizatorów (immobilizowanych alkoksylanów metali) na wilgoć, powodująca spadek ich aktywności bądź dezaktywację [59]. Zapewnienie izolacji katalizatora od kontaktu z niepożądanymi czynnikami zewnętrznymi możliwe jest w przypadku zastosowania zaproponowanego mikroreaktora. Jego konstrukcja znacząco ułatwia wprowadzenie centrów aktywnych na powierzchnię, prowadzenie procesu, regenerację katalizatora, oraz przechowywanie, co jest znacznie trudniej osiągnąć w przypadku stosowania proszkowych katalizatorów heterogenicznych reakcji MPV. W literaturze przedmiotu znaleziono zaledwie jedną pracę poświęconą prowadzeniu tej reakcji w procesie przepływowym w reaktorze wypełnionym złożem tlenku cyrkonu [60].

W pracach [P3], [P5], [P7], [P8], oraz [P9] opublikowano wyniki badań nad innowacyjnymi, monolitycznymi mikroreaktorami do reakcji MPV. Jako centra kwasowe Lewisa do tej reakcji zastosowano następujące metale: cyrkon, glin oraz tytan. Modyfikację powierzchni krzemionki wykonano metodą impregnacji. Zbadano wpływ typu metalu, rodzaju prekursora oraz otoczenia centrum aktywnego na właściwości fizykochemiczne i katalityczne materiałów oraz efektywność otrzymanych na ich bazie mikroreaktorów.

W pracy [P3] przedstawiono wyniki badań mikroreaktorów zmodyfikowanych cyrkonem w formie i) kompleksów zawierających ligandy propoksylowe i/lub hydroksylowe oraz ii) tlenku. Stwierdzono, że aktywność jonów cyrkonu Zr^{4+}, zależy od ich otoczenia chemicznego. Konwersja w mikroreaktorach, w których jony cyrkonu były kompleksowane przez ligandy propoksylowe i/lub hydroksylowe była o ok. 20% wyższa niż w reaktorze modyfikowanym tlenkiem cyrkonu. Wykazano stabilną prace mikroreaktora w 48 godzinnym eksperymencie (długość reaktora 8 cm, konwersja 100%). Stwierdzono wpływ śladowych ilości wody w substratach na stabilność właściwości katalitycznych. W badaniach, w których nie zastosowano sit molekularnych do osuszania substratów przed reakcją, obserwowano znaczny spadek aktywności w kolejnych cyklach reakcyjnych.

Do dalszych szczegółowych badań wybrano mikroreaktor sfunkcjonalizowany cyrkonem z ligandami propoksylowymi [P5]. Zbadano wpływ ilości cyrkonu na stężenie centrów kwasowych oraz aktywność katalityczną w reakcji redukcji cykloheksanonu. Do pełnej charakterystyki strukturalnej i fizykochemicznej wykorzystano termograwimetrię, spektroskopię FTIR i UV-Vis, niskotemperaturową adsorpcję azotu,

oraz ICP-MS. Stosunek Zr/Si zmieniano w zakresie od 0,01-0,28. Struktura monolitu po funkcjonalizacji została zachowana, zmniejszeniu uległa jedynie objętość mezoporów, proporcjonalnie do ilości wprowadzonych grup. Badania wykazały, że stężenie centrów kwasowych zależało od zawartości cyrkonu, osiągając maksimum dla próbki, w której stosunek Zr/Si wynosił 0,14, co bezpośrednio przełożyło się na jej najlepszą aktywność katalityczną. Dalsze zwiększanie tego stosunku powodowało zmniejszenie ilości centrów Lewisa i mniejszą produktywność w mikroreaktorze. Z uwagi na brak danych literaturowych dotyczących redukcji cykloheksanonu w procesie ciągłym, produktywność mikroreaktora porównano z wynikami otrzymanymi przez innych badaczy w reaktorach zbiornikowych. Wykazano, że zaproponowany mikroreaktor pracuje znacznie wydajniej niż reaktory, w których stosowano katalizatory zeolitowe czy modyfikowane materiały mezostrukturalne.

W pracach [P7, P8] pokazano wpływ typu metalu, jego otoczenia chemicznego oraz rodzaju zastosowanego prekursora na właściwości katalityczne mikroreaktorów. Zastosowano różne prekursory metali - alkoksylany, chelatowane alkoksylany oraz sole. Wynikiem tych modyfikacji były materiały z różnymi centrami katalitycznymi, o różnym otoczeniu chemicznym. We wszystkich zmodyfikowanych materiałach nominalny stosunek masowy metal/Si wynosił 0,05. Stwierdzono, że reaktywność prekursorów wpływała na stężenie grup funkcyjnych trwale związanych z powierzchnią krzemionki. W materiałach aktywowanych alkoksylanami metali rzeczywiste ilości metali były zbliżone do wartości nominalnych. Zastosowanie chelatowanych prekursorów glinu i tytanu, ze względu na ich większe rozmiary oraz sferyczne ograniczenia i mniejszą reaktywność, skutkowało obniżeniem stężenia tych centrów o połowę. Stwierdzono, że spośród soli, tylko zastosowanie chlorku tlenku cyrkonu (IV) ($ZrOCl_2 \cdot 8H_2O$) i azotanu (V) glinu ($Al(NO_3)_3 \cdot H_2O$) powala na uzyskanie znaczących zawartości metalu w próbce. Sposób związania metalu z powierzchnią krzemionki zbadano metodą spektroskopii UV-Vis. Na podstawie analizy widm stwierdzono, że glin oraz cyrkon występują w koordynacji tetraedrycznej. Ta konfiguracja jest najbardziej korzystana z punktu widzenia mechanizmu reakcji MPV. Badania adsorpcji/desorpcji pirydyny, przeprowadzone techniką spektroskopii w podczerwieni, potwierdziły obecność kwasowych centrów Lewisa, niezbędnych do przeprowadzenia reakcji redukcji MPV [61, 62]. Stwierdzono brak centrów Brönsteda, które mogłyby obniżać selektywność procesu. Monolity sfunkcjonalizowane glinem charakteryzowały się największą ilością centrów kwasowych, a ich moc była dwukrotnie większa niż moc centrów cyrkonowych.

Właściwości katalityczne mikroreaktorów, zawierających metale w postaci tlenków oraz kompleksów, zbadano w modelowych reakcjach redukcji cykloheksanonu lub benzaldehydu 2-butanolem.

Mikroreaktory modyfikowane tlenkami metali wykazywały mniejszą aktywność w obu reakcjach niż te sfunkcjonalizowane kompleksami metalo-organicznymi, co potwierdza, że w reakcji MPV powierzchniowe grupy OR/OH sprzyjają wymianie ligandów pomiędzy grupą karbonylową a alkoholem.

Największą aktywnością charakteryzowały się materiały modyfikowane cyrkonem zawierające grupy propoksylowe. Wysoka aktywność wynikała z obecności słabych centrów kwasowych i mocnych zasadowych, które są odpowiedzialne za aktywację grupy metylenowej alkoholu. Konwersje i produktywności uzyskane w mikroreaktorach modyfikowanych glinem były mniejsze w stosunku do ich cyrkonowych odpowiedników, a w szczególności tych modyfikowanych i-propoksylanem glinu (zarówno w formie kompleksów metaloorganicznych jak i tlenków). Takie zachowanie może być przypisane występowaniu tego prekursora w formie oligomerycznych struktur oraz jego dużej reaktywności w obecności śladowych ilości wody, a tym samym silnej tendencji do tworzenia agregatów tlenku glinu.

Mikroreaktory aktywowane Ti wykazywały bardzo małą aktywność w reakcji MPV, co wynikało z małego stężenia centrów kwasowych, tendencji do tworzenia oligomerycznych struktur TiO_2 oraz wymywania Ti z nośnika w kontakcie z polarnymi rozpuszczalnikami.

Potwierdzono stabilność wiązania pomiędzy centrum aktywnym i nośnikiem przez oznaczenie zawartości metalu w roztworze poreakcyjnym oraz w teście polegającym na śledzeniu postępu reakcji po wydzieleniu katalizatora z mieszaniny reakcyjnej. Analiza ICP-MS potwierdziła wymywanie jedynie tytanu (ok. 3% po 8 godzinach pracy) oraz nie obserwowano postępu reakcji po usunięciu katalizatora.

Wykazano, że w procesie redukcji cykloheksanonu oraz benzaldehydu prowadzonym w mikroreaktorach można osiągnąć wyższe produktywności niż w reaktorach okresowych (z wykorzystaniem sproszkowanych monolitycznych materiałów), a także z udziałem innych katalizatorów, opisanych w literaturze.

Przeprowadzono eksperymenty w reaktorze zbiornikowym z wykorzystaniem sproszkowanych monolitów. Produktywności uzyskane w tym reaktorze, przy zachowaniu tych samych warunków procesowych, były mniejsze niż w reaktorze przepływowym, co wynikało z intensywniejszego transportu masy w warstwach cieczy w mikrokanałach,

w szczególności tych znajdujących się w bezpośrednim kontakcie z powierzchną katalizatora.

W pracy [P9] wyznaczono parametry kinetyczne reakcji MPV dla układu cykloheksanon:2-butanol w mikroreaktorze sfunkcjonalizowanym propanolanem cyrkonu (stosunek masowy Zr/Si wynosił 0,14). Reakcję prowadzono w mikroreaktorach o długości 1-8 cm. Wykazano brak wpływu zewnętrznych oporów transportu masy. Uzyskano liniową zależność szybkości reakcji od czasu w stosowanym zakresie temperatur 65-95^{o}C. Dane eksperymentalne były zgodne z obliczonymi z założeniem kinetyki pierwszego rzędu. Wyznaczona energia aktywacji wynosiła 52 KJ/mol. Badania rozszerzono dla innych ketonów i aldehydów. Alkohole będące produktami selektywnego uwodornienia związków karbonylowych, wybrane zostały ze względu na ich znaczenie praktyczne. Są stosowane głównie jako składniki zapachowe, ale również jako półprodukty do produkcji leków. Na przykład produkty estryfikacji alkoholu cynamonowego i kwasu indolo-3-octowego lub kwasu α-liponowego badano pod kątem ich właściwości przeciwutleniających i przeciwzapalnych, geraniol do zastosowań w leczeniu raka jelita grubego. Określono wpływ struktury substratu oraz wpływ rodzaju i stężenia alkoholu - donora wodoru na postęp reakcji. Wykazano, że aldehydy są bardziej podatne na redukcję niż ketony. Jako główny czynnik wpływający na uzyskiwanie mniejszych konwersji w przypadku wielkocząsteczkowych, nienasyconych związków karbonylowych wskazano zawadę steryczną. Stwierdzono, że ilości produktów uzyskiwane w mikroreaktorze są ok. czterokrotnie większe niż w reaktorze przepływowym z upakowanym złożem ZrO_2 [60]. Nie stwierdzono występowania produktów ubocznych, które mogłyby powstać pochodzących w reakcji Tischenko lub kondensacji aldolowej.

4.4 Mikroreaktory modyfikowane tlenkiem tytanu [P4]

Tytanokrzemiany ze względu na wyjątkowe właściwości fizykochemiczne znajdują zastosowanie w fotokatalizie, reakcjach utleniania, redukcji, oraz jako nośniki katalityczne, o wysokiej termicznej i mechanicznej wytrzymałości [63-65].

W pracy [P4] zbadano właściwości fizykochemiczne i katalityczne monolitycznych mikroreaktorów modyfikowanych tlenkiem tytanu. Zastosowano dwa sposoby wprowadzania tytanu do szkieletu krzemionkowego: metodę jednostopniową (współkondensacji - D) oraz posyntezową (impregnacji- I). Ti wprowadzano w ilości 1, 2, 5% masowych. Próbki (I) otrzymano w sposób identyczny jak materiały modyfikowane kompleksami cyrkonu: nośniki krzemionkowe sfunkcjonalizowano za pomocą

diisopropoksy bis(acetyloacetonianu) tytanu(IV), a następnie kalcynowano w celu uzyskania tlenku tytanu. Zgodnie z oczekiwaniami, zastosowana metoda modyfikacji posyntezowej nie wpłynęła na makroporowatą strukturę monolitu, natomiast obserwowano zmiany w mezostrukturze materiału, tj. zmniejszenie powierzchni właściwej, wielkości i objętości mezoporów, które były proporcjonalne do ilości wprowadzonych centrów.

Metodą jednostopniową, polegającą na wprowadzeniu atomów tytanu w trakcie syntezy materiału, możliwe było otrzymanie monolitów o jednorodnej bimodalnej strukturze porów tylko w przypadku próbek zawierających 1% i 2% tytanu. Próbki zawierające 5% tytanu nie wykazywały cech materiału monolitycznego (rozpadły się podczas suszenia). Parametry strukturalne monolitów (D) znacząco różniły się od tych otrzymanych metodą posyntezową i zależały od ilości Ti wbudowanego w szkielet krzemionkowy. Całkowita objętość porów wyraźnie się zmniejszyła – cztero- i siedmiokrotnie w stosunku do krzemionkowego monolitu. W szkielecie wygenerowane zostały jedynie mikropory o średnicach ok. 1,5 nm, co wpłynęło na zwiększenie powierzchni właściwej do wartości powyżej 500 m^2/g. Ciągłość przepływowej struktury monolitu została zachowana, a średnice makroporów wynosiły 3 μm oraz 9 μm, odpowiednio dla próbek zawierających 1% i 2% Ti. Wyraźne różnice związane z zastosowaniem prekursora tytanu na etapie syntezy, wynikały ze zmiany mechanizmu polikondensacji krzemionki i z opóźnienia wystąpienia zjawiska separacji fazowej w stosunku do procesu zol-żelowego [66]. W przypadku tych materiałów nie stosowano obróbki hydrotermalnej w roztworze amoniaku. Porowatość materiałów typu D była mniejsza o około 20% w porównaniu z monolitami impregnowanymi. Wszystkie monolity posiadały ciągłą strukturę makroporów, co umożliwiło ich zastosowanie, jako rdzeni mikroreaktorów. Jednakże, mniejsza porowatość i znacząco mniejsze rozmiary makroporów w monolitach otrzymanych metodą jednostopniową spowodowały zwiększenie spadków ciśnienia nawet o dwa rzędy wielkości. Badania przeprowadzone z wykorzystaniem techniki ICP-MS wykazały, że ilość tytanu w próbkach była mniejsza od wartości nominalnej. Dla próbek serii I różnice pomiędzy tymi wielkościami były nieznaczne, natomiast dla monolitów otrzymanych metodą współkondensacji sięgały 40%. Metodą EDS (pomiar wielopunktowy) potwierdzono, że zarówno całkowite jak i powierzchniowe stężenie tytanu w monolitach D było zbliżone, co świadczyło o równomiernym rozkładzie metalu w szkielecie krzemionkowym. Z kolei w monolitach otrzymanych metodą impregnacji, powierzchniowe stężenie Ti było wyższe, niż to

wyznaczone metodą ICP-MS, a pomiary uzyskane w kilku punktach wskazały na niejednolite pokrycie powierzchni krzemionki.

Katalityczne właściwości materiałów krzemionkowo-tytanowych zależą m.in. od stężenia tytanu, jego otoczenia chemicznego i stopnia dyspersji [67]. Na podstawie badań metodą spektroskopii UV-Vis i FTIR potwierdzono dobrą dyspersję izolowanych, tetraedrycznie skoordynowanych atomów tytanu w próbkach otrzymanych metodą jednostopniową. Natomiast na powierzchni krzemionek modyfikowanych przez impregnację stwierdzono występowanie małych, oligomerycznych cząstek tlenku tytanu. Wielkości przerw energetycznych, wyznaczonych na podstawie widm UV-Vis, z wykorzystaniem funkcji Kubelki-Munka [68], wskazywały na podobny sposób wbudowania tytanu do krzemionki w materiałach serii D jak w zeolicie TS-1 [69], a w serii I obserwowano oligomeryczne struktury tlenku tytanu w formie anatazu [70].

Aktywność katalityczną materiałów zweryfikowano w reakcji utleniania 2,3,6-trimetylofenolu do 2,3,5-trimetylo-1,4-benzochinonu. Produkt tej reakcji jest kluczowym półproduktem do syntezy witaminy E [71]. Badania przeprowadzone w mikroreaktorach, dla założonego czasu przebywania lub stałego natężenia przepływu, pozwoliły na uzyskanie zależności pomiędzy właściwościami materiałów a ich aktywnością katalityczną.

Badania reakcji utleniania w przepływowych mikroreaktorach oraz w reaktorze okresowym, z wykorzystaniem sproszkowanych monolitów, pokazały złożone zależności między strukturą materiału, stężeniem Ti i jego dyspersją a aktywnością katalityczną i efektywnością procesu. Izolowane jony tytanu o tetraedrycznej koordynacji, wbudowane w strukturę krzemionki z użyciem metody współkondensacji, charakteryzowały się większą aktywnością katalityczną (wyrażoną jako początkowa szybkość reakcji, TOF_{Tisurf} odniesiona do liczby powierzchniowych atomów Ti) w procesie prowadzonym w reaktorze okresowym w porównaniu z ich odpowiednikami syntetyzowanymi metodą dwustopniową. Natomiast, w procesie przepływowym, w mikroreaktorach których rdzenie stanowiły monolity modyfikowane dwustopniowo, dla identycznych czasów kontaktu, uzyskano zdecydowanie większe konwersje, większą produktywność (odniesioną zarówno do stężenia Ti jak i masy reaktora), niż w mikroreaktorach, w których rdzenie syntetyzowano metodą jednostopniową. Jednocześnie obserwowano zwiększenie tych wielkości z rosnącym stężeniem tytanu. Znacząco mniejsza efektywność reaktorów, syntetyzowanych z użyciem metody jednostopniowej, związana jest z utrudnionym

dostępem reagentów do centrów, wbudowanych w szkielet krzemionkowy oraz ograniczeniami dyfuzyjnymi, wynikającymi z mikroporowatej struktury tych materiałów.

5. PODSUMOWANIE

W pracy przedstawiono wyniki badań nad innowacyjnymi, monolitycznymi mikroreaktorami przepływowymi, w których jako reaktywne rdzenie zastosowano monolity krzemionkowe o hierarchicznej strukturze porów modyfikowane centrami kwasowymi. Monolity, dzięki możliwości projektowania ich porowatej struktury, zapewniają, z jednej strony, pożądane właściwości hydrodynamiczne tj. niskie opory przepływu, a równocześnie, poprzez odpowiednie modyfikacje, wprowadzenie dużej liczby centrów aktywnych, co bezpośrednio skutkuje wysoką efektywnością procesów chemicznych prowadzonych w mikroreaktorach.

Otrzymano trzy rodzaje mikroreaktorów: a) z centrami kwasowymi Brönsteda do reakcji estryfikacji, b) z centrami Lewisa do selektywnej redukcji związków karbonylowych metodą Meerweina-Ponndorfa-Verleya (MPV), c) z centrami Ti do selektywnego utleniania związków organicznych.

Aktywność katalityczną mikroreaktorów z centrami kwasowymi Brönsteda potwierdzono w reakcjach estryfikacji kwasów octowego i mlekowego, wykazując efektywność zaproponowanego rozwiązania, przy jednoczesnym znacznym uproszczeniu procesu, wynikającym z wyeliminowania etapu separacji katalizatora. Ponadto, na podstawie uzyskanych wyników badań, jednoznacznie stwierdzono, że duża porowatość rdzeni mikroreaktorów umożliwia nie tylko zmniejszenie oporów przepływu, ale również uzyskanie wysokich wydajności przy mniejszym stężeniu centrów aktywnych [P1, P6]. W badaniach opisanych w pracy [P2] wykorzystano koncepcję wzmocnienia szkieletu mikroreaktora przez wprowadzenie krzemionki do monolitycznego nośnika kordierytowego.

Mikroreaktory z centrami kwasowymi Lewisa zastosowano w selektywnej redukcji związków karbonylowych MPV. Wykazano, że mikroreaktory mogą stabilnie pracować przez wiele godzin, z dobrą wydajnością. Przeprowadzono szereg reakcji, w których substratami były ketony i aldehydy o różnej budowie molekularnej. Efektywność mikroreaktorów silnie zależała od rodzaju centrum i jego otoczenia chemicznego. Zaletami opracowanych mikroreaktorów, poza wysoką produktywnością, są łatwość przygotowania, regeneracji, magazynowania i kontroli parametrów procesowych. Wymienione właściwości mają decydujące znaczenie przy prowadzeniu procesów, takich jak reakcja MPV, w których centra katalityczne wymagają zapewnienia specjalnych warunków, np. odpowiedniej atmosfery przechowywania. [P3, P5, P7, P8, P9].

Opracowano metodę syntezy monolitycznych tytanokrzemianów, charakteryzujących się dobrym rozproszeniem jonów tytanu w szkielecie krzemionkowym, co jest warunkiem ich aktywności w procesach selektywnego utleniania związków organicznych. Właściwości te zweryfikowano w reakcji utleniania 2,3,6-trimetylofenolu do 2,3,5-trimetylo-1,4-benzochinonu. Kompleksowe badania aktywności katalitycznej monolitycznych nośników i odpowiadających im proszków, działających odpowiednio w procesach przepływowym i okresowym, pozwoliły na ukazanie związków między strukturą katalizatora, jego właściwościami fizykochemicznymi oraz wydajnością [P4].

Opublikowane wyniki dostarczają nowej wiedzy w zakresie projektowania, otrzymywania i efektywnej funkcjonalizacji monolitów krzemionkowych, szczególnie w kierunku ich wykorzystania, jako rdzeni aktywnych przepływowych reaktorów, do zastosowań w wysokospecjalistycznych syntezach przemysłu chemicznego i farmaceutycznego.

LITERATURA

[1] J. Coronas, Present and future synthesis challenges for zeolites, Chem. Eng. J., 156 (2010) 236-242.

[2] E. Koohsaryan, M. Anbia, Nanosized and hierarchical zeolites: A short review, Chinese J. Catal., 37 (2016) 447-467.

[3] A.F. Masters, T. Maschmeyer, Zeolites - From curiosity to cornerstone, Microporous Mesoporous Mater., 142 (2011) 423-438.

[4] C.T. Kresge, M.E. Leonowicz, W.J. Roth, J.C. Vartuli, J.S. Beck, Ordered Mesoporous Molecular-Sieves Synthesized by a Liquid-Crystal Template Mechanism, Nature, 359 (1992) 710-712.

[5] P. Gómez-Romero, C. Sanchez, Functional Hybrid Materials, Wiley-VCH Verlag GmbH & Co. KGaA (2005).

[6] V. Meynen, P. Cool, E.F. Vansant, Verified syntheses of mesoporous materials, Microporous Mesoporous Mater., 125 (2009) 170-223.

[7] A. Taguchi, F. Schuth, Ordered mesoporous materials in catalysis, Microporous Mesoporous Mater., 77 (2005) 1-45.

[8] M. Trejda, J. Kujawa, M. Ziółek, J. Mrowiec-Białoń, Nb-containing mesoporous materials of MCF type-Acidic and oxidative properties, Catal. Today, 139 (2008) 196-201.

[9] P. Schmidt-Winkel, W.W. Lukens, P.D. Yang, D.I. Margolese, J.S. Lettow, J.Y. Ying, G.D. Stucky, Microemulsion templating of siliceous mesostructured cellular foams with well-defined ultralarge mesopores, Chem. Mater., 12 (2000) 686-696.

[10] K. Szymańska, J. Bryjak, J. Mrowiec-Białoń, A.B. Jarzębski, Application and properties of siliceous mesostructured cellular foams as enzymes carriers to obtain efficient biocatalysts, Microporous Mesoporous Mater., 99 (2007) 167-175.

[11] N. Tanaka, H. Kobayashi, K. Nakanishi, H. Minakuchi, N. Ishizuka, Monolithic LC columns, Anal. Chem., 73 (2001) 420a-429a.

[12] K. Nakanishi, Y. Kobayashi, T. Amatani, K. Hirao, T. Kodaira, Spontaneous formation of hierarchical macro-mesoporous ethane-silica monolith, Chem. Mater., 16 (2004) 3652-3658.

[13] K. Nakanishi, R. Takahashi, T. Nagakane, K. Kitayama, N. Koheiya, H. Shikata, N. Soga, Formation of hierarchical pore structure in silica gel, J. Sol-Gel Sci. Technol., 17 (2000) 191-210.

[14] J.H. Smått, S. Schunk, M. Linden, Versatile double-templating synthesis route to silica monoliths exhibiting a multimodal hierarchical porosity, Chem. Mater., 15 (2003) 2354-2361.

[15] W. Pudło, W. Gawlik, J. Mrowiec-Białoń, T. Buczek, J.J. Malinowski, A.B. Jarzębski, Materials with multimodal hierarchical porosity, Inż. Chem. Procesowa, 27 (2006) 177-185.

[16] W. Ehrfeld, V. Hessel, H. Lowe, Microeactors: New Technology for Modern Chemistry, Weinheim: Willey-VCH (2000).

[17] K. Jahnisch, V. Hessel, H. Lowe, M. Baerns, Chemistry in microstructured reactors, Angew. Chem. Int. Edit., 43 (2004) 406-446.

[18] S. Braune, P. Pochlauer, R. Reintjens, S. Steinhofer, M. Winter, O. Lobet, R. Guidat, P. Woehl, C. Guermeur, Selective nitration in a microreactor for pharmaceutical production under cGMP conditions, Chim. Oggi., 27 (2009) 26-29.

[19] V. Hessel, P. Lob, H. Lowe, Micro Process Engineering - A Comprehensive Handbook, Vol. 3, Wiley-VCH Verlag GmbH & Co.KGaA (2009).

[20] M. Freemantle, Microprocessing on a large scale, Chemical & Engineering News, 82 (2004) 39.

[21] Sigma-Aldrich, The Sigma-Aldrich Microreactor Explorer Kit - Made by Chemists for Chemists, ChemFiles, 9 (2009).

[22] X. Wang, J. Zhu, H. Bau, R.J. Gorte, Fabrication of micro-reactors using tape-casting methods, Catal. Lett., 77 (2001) 173-177.

[23] G. Kolb, V. Hessel, Micro-structured reactors for gas phase reactions, Chem. Eng. J., 98 (2004) 1-38.

[24] B. Jiang, T. Maeder, A.J. Santis-Alvarez, D. Poulikakos, P. Muralt, A low-temperature co-fired ceramic micro-reactor system for high-efficiency on-site hydrogen production, J. Power Sources, 273 (2015) 1202-1217.

[25] V. Hessel, H. Lowe, A. Muller, G. Kolb, Chemical Micro Process Engineering. Processing and Plans, Wiley-VCH Verlag GmbH & Co.KGaA 2005.

[26] A. Tanimu, S. Jaenicke, K. Alhooshani, Heterogeneous catalysis in continuous flow microreactors: A review of methods and applications, Chem. Eng. J., 327 (2017) 792-821.

[27] A. El Kadib, R. Chimenton, A. Sachse, F. Fajula, A. Galarneau, B. Coq, Functionalized Inorganic Monolithic Microreactors for High Productivity in Fine Chemicals Catalytic Synthesis, Angew. Chem. Int. Edit., 48 (2009) 4969-4972.

[28] A. Sachse, A. Galarneau, F. Fajula, F. Di Renzo, P. Creux, B. Coq, Functional silica monoliths with hierarchical uniform porosity as continuous flow catalytic reactors, Microporous Mesoporous Mater., 140 (2011) 58-68.

[29] A. Koreniuk, K. Maresz, K. Odrozek, A.B. Jarzębski, J. Mrowiec-Białoń, Highly effective continuous-flow monolithic silica microreactors for acid catalyzed processes, Appl. Catal. A., 489 (2015) 203-208.

[30] J. Babin, J. Iapichella, B. Lefevre, C. Biolley, J.P. Bellat, F. Fajula, A. Galarneau, MCM-41 silica monoliths with independent control of meso- and macroporosity, New J. Chem., 31 (2007) 1907-1917.

[31] K. Szymańska, W. Pudło, J. Mrowiec-Białoń, A. Czardybon, J. Kocurek, A.B. Jarzębski, Immobilization of invertase on silica monoliths with hierarchical pore structure to obtain continuous flow enzymatic microreactors of high performance, Microporous Mesoporous Mater., 170 (2013) 75-82.

[32] K. Szymańska, K. Odrozek, A. Zniszczoł, G. Torrelo, V. Resch, U. Hanefeld, A.B. Jarzębski, MsAcT in siliceous monolithic microreactors enables quantitative ester synthesis in water, Catal. Sci. Technol., 6 (2016) 4882-4888.

[33] K. Szymańska, M. Pietrowska, J. Kocurek, K. Maresz, A. Koreniuk, J. Mrowiec-Białoń, P. Widłak, E. Magner, A. Jarzębski, Low back-pressure herarchically structured multichannel microfluidic bioreactors for rapid protein digestion - Proof of concept, Chem. Eng. J., 287 (2016) 148-154.

[34] S. Braunauer, P.H. Emmet, E. Teller, Adsorption of Gases in Multimolecular Layers, J. Am. Chem. Soc., (1938) 309-319.

[35] E. Barrett, L. Joyner, P. Halenda, The Determination of Pore Volume and Area Distributions in Porous Substances. Computations from Nitrogen Isotherms, J. Am. Chem. Soc., 73 (1951) 373-380.

[36] M.M. Dubinin, V.A. Astakhov, Description of Adsorption Equilibria of Vapors on Zeolites over Wide Ranges of Temperature and Pressure, Adv. Chem. Ser., (1971) 69-85.

[37] S. Whitaker, Advances in Theory of Fluid Motion in Porous Media, Ind. Eng. Chem., 61 (1969) 14-28.

[38] A. Sachse, V. Hulea, A. Finiels, B. Coq, F. Fajula, A. Galarneau, Alumina-grafted macro-/mesoporous silica monoliths as continuous flow microreactors for the Diels-Alder reaction, J. Catal., 287 (2012) 62-67.

[39] S.B. Wu, L.L. Sun, J.F. Ma, K.G. Yang, Z. Liang, L.H. Zhang, Y.K. Zhang, High throughput tryptic digestion via poly (acrylamide-co-methylenebisacrylamide) monolith based immobilized enzyme reactor, Talanta, 83 (2011) 1748-1753.

[40] A. Jarzębki, W. Pudło, Sposób wzmacniania wytrzymałości mechanicznej monolitów krzemionkowych zwłaszcza o multimodalnej strukturze porowatej otrzymywanych metodą zol-żel, Polish Patent P.217560 (2011).

[41] H.H. Zhang, R.X. Liu, Z.Q. Yang, F. Huo, R.R. Zhang, Z.H. Li, S.J. Zhang, Y.J. Wang, Alkylation of isobutane/butene promoted by fluoride-containing ionic liquids, Fuel, 211 (2018) 233-240.

[42] S. Soltani, U. Rashid, S.I. Al-Resayes, I.A. Nehdi, Recent progress in synthesis and surface functionalization of mesoporous acidic heterogeneous catalysts for esterification of free fatty acid feedstocks: A review, Energy Convers. Manage., 141 (2017) 183-205.

[43] L. Xiao, J.B. Mao, J.X. Zhou, X.W. Guo, S.G. Zhang, Enhanced performance of HY zeolites by acid wash for glycerol etherification with isobutene, Appl. Catal. A., 393 (2011) 88-95.

[44] M.A. Tejero, E. Ramirez, C. Fite, J. Tejero, F. Cunill, Esterification of levulinic acid with butanol over ion exchange resins, Appl. Catal. A., 517 (2016) 56-66.

[45] Y.C. Lin, Y.W. Huang, K.H. Sung, T.H. Lin, S. Cheng, Hydration of DCPD over sulfonic acid-functionalized SBA-15 catalyst, J. Ind. Eng. Chem., 44 (2016) 60-66.

[46] A. Koreniuk, K. Maresz, J. Mrowiec-Białon, Supported zirconium-based continuous-flow microreactor for effective Meerwein-Ponndorf-Verley reduction of cyclohexanone, Catal. Commun., 64 (2015) 48-51.

[47] J. Wang, K. Okumura, S. Jaenicke, G.K. Chuah, Post-synthesized zirconium-containing Beta zeolite in Meerwein-Ponndorf-Verley reduction: Pros and cons, Appl. Catal. A., 493 (2015) 112-120.

[48] G. Ahmed, K. Nickisch, Thermodynamic Meerwein-Ponndorf-Verley reduction in the diastereoselective synthesis of 17 α-estradiol, Steroids, 113 (2016) 1-4.

[49] Z.H. Xiao, Insight into the Meerwein-Ponndorf-Verley reduction of cinnamaldehyde over MgAl oxides catalysts, Mol. Catal., 436 (2017) 1-9.

[50] B. Zhang, F. Xie, J. Yuan, L. Wang, B.X. Deng, Meerwein-Ponndorf-Verley reaction of acetophenone over ZrO_2-La_2O_3/MCM-41: Influence of loading order of ZrO_2 and La_2O_3, Catal. Commun., 92 (2017) 46-50.

[51] A. Corma, H. Garcia, Lewis acids as catalysts in oxidation reactions: From homogeneous to heterogeneous systems, Chem. Rev., 102 (2002) 3837-3892.

[52] X.H. Yang, Y.Q. Jiang, Y.D. Li, X.Z. Xu, D.F. Li, K.F. Lin, Mesoporous silica beads containing active and stable tin species for the Baeyer-Villiger oxidations of cyclic ketones, Microporous Mesoporous Mater., 253 (2017) 40-48.

[53] F. Adam, K.L. Sęk, Heterogenization of Indium for the Friedel-Craft Benzoylation of Toluene, Chinese J. Catal., 33 (2012) 1802-1808.

[54] A. Vinu, D.P. Sawant, K. Ariga, K.Z. Hossain, S.B. Halligudi, M. Hartmann, M. Nomura, Direct synthesis of well-ordered and unusually reactive FeSBA-15 mesoporous molecular sieves, Chem. Mater., 17 (2005) 5339-5345.

[55] K. Bauer, D. Garbe, H. Surbung, Common Fragrance and Flavor Materials: Preparation Properties and Uses, Wiley-VCH Verlag GmbH & Co.KGaA (2001).

[56] P. Mäki-Arvela, J. Hájek, T. Salmi, D.Y. Murzin, Chemoselective hydrogenation of carbonyl compounds over heterogeneous catalysts, Appl. Catal. A., 292 (2005) 1-49.

[57] R.A.W. Johnstone, A.H. Wilby, I.D. Entwistle, Heterogeneous Catalytic Transfer Hydrogenation and Its Relation to Other Methods for Reduction of Organic Compounds, Chem. Rev., 85 (1985) 129-170.

[58] H. Meerwein, R. Schmidt, Ein neues Verfahren zur Reduktion von Aldehyden und Ketonen, Justus Liebigs Ann. Chem., 444 (1925) 221-238.

[59] F. Quignard, O. Graziani, A. Choplin, Group 4 alkyl complexes as precursors of silica anchored molecular catalysts for the reduction of ketones by hydrogen transfer, Appl. Catal. A, 182 (1999) 29-40.

[60] C. Battilocchio, J.M. Hawkins, S.V. Ley, A Mild and Efficient Flow Procedure for the Transfer Hydrogenation of Ketones and Aldehydes using Hydrous Zirconia, Org. Lett., 15 (2013) 2278-2281.

[61] J.F. Minambres, A. Marinas, J.M. Marinas, F.J. Urbano, Chemoselective crotonaldehyde hydrogen transfer reduction over pure and supported metal nitrates, J. Catal., 295 (2012) 242-253.

[62] V.V. Srinivasan, A. Ranoux, R. Maheswari, U. Hanefeld, A. Ramanathan, B. Subramaniam, Potential applications of Zr-KIT-5: Hantzsch reaction, Meerwein-Ponndorf-Verley (MPV) reduction of 4-tert-butylcyclohexanone, and Prins reaction of citronellal, Res. Chem. Intermed., 42 (2016) 2399-2408.

[63] R.Y. Zhang, A.A. Elzatahry, S.S. Al-Deyab, D.Y. Zhao, Mesoporous titania: From synthesis to application, Nano Today, 7 (2012) 344-366.

[64] D. Elhamifar, O. Yari, B. Karimi, Highly ordered mesoporous organosilica-titania with ionic liquid framework as very efficient nanocatalyst for green oxidation of alcohols, J. Colloid Interface Sci., 500 (2017) 212-219.

[65] I. Lazar, J. Kalmar, A. Peter, A. Szilagyi, E. Gyori, T. Ditroi, I. Fabian, Photocatalytic performance of highly amorphous titania-silica aerogels with mesopores: The adverse effect of the in situ adsorption of some organic substrates during photodegradation, Appl. Surf. Sci., 356 (2015) 521-531.

[66] K. Nakanishi, S. Motowaki, N. Soga, Preparatio of SiO_2-TiO_2 Gels with Controlled Pore Structure via Sol-Gel Route, Bulletin ot the Institute for Chemical Research, Kyoto Univeristy, 70 (1992) 144-151.

[67] K.M. Choi, R. Wakabayashi, T. Tatsumi, T. Yokoi, K. Kuroda, Usefulness of alkoxyltitanosiloxane for the preparation of mesoporous silica containing a large amount of isolated titanium, J. Colloid Interface Sci., 359 (2011) 240-247.

[68] C. Beck, T. Mallat, T. Burgi, A. Baiker, Nature of active sites in sol-gel TiO_2-SiO_2 epoxidation catalysts, J. Catal., 204 (2001) 428-439.

[69] M. Taramasso, G. Perego, B. Notari, US Pat 4 410 501, (1983).

[70] Z.M. Liu, L. Peng, A.W. Tang, Fluoride-assisted synthesis of anatase TiO_2 nanocrystals with tunable shape and band gap via a solvothermal approach, Chin. Chem. Lett., 27 (2016) 1801-1804.

[71] W. Bonrath, T. Netscher, Catalytic processes in vitamins synthesis and production, Appl.Catal. A., 280 (2005) 55-73.

PUBLIKACJE

Applied Catalysis A: General 489 (2015) 203–208

Contents lists available at ScienceDirect

Applied Catalysis A: General

journal homepage: www.elsevier.com/locate/apcata

Highly effective continuous-flow monolithic silica microreactors for acid catalyzed processes

A. Koreniuk[a], K. Maresz[a], K. Odrozek[b], A.B. Jarzębski[a,b], J. Mrowiec-Białoń[a,b,*]

[a] Institute of Chemical Engineering, Polish Academy of Sciences, Bałtycka 5, 44-100 Gliwice, Poland
[b] Department of Chemical Engineering and Process Design, Silesian University of Technology, Ks. M. Strzody 7, 44-100 Gliwice, Poland

ARTICLE INFO

Article history:
Received 28 August 2014
Received in revised form 21 October 2014
Accepted 23 October 2014
Available online 1 November 2014

Keywords:
Microreactors
Silica monoliths
Acid catalysis
Esterification
Hierarchical materials

ABSTRACT

This work reports the performance of a new monolithic silica microreactor, activated with sulphonic acid groups in the continuous-flow synthesis of *n*-butyl acetate and *n*-butyl lactate. A reactive core of the reactor was made of a single silica rod with bi-continuous structure, containing flow-through pores with diameter in the range of 20–50 μm and mesopores of ca. 20 nm localized in silica struts. This structure resulted in low pressure drop, even at flow rates large enough to eliminate external mass transfer effect on the reaction kinetics. The microreactor functionalized with 0.65 mmol/g of $-SO_3H$ groups showed high activity and productivity in both esterification reactions carried out in temperatures up to 140 °C. Structural and catalytic stability of the microreactor was confirmed to demonstrate its process viability.

1. Introduction

Synthesis of most fine chemicals is typically carried out in a liquid phase and batch operation. Their replacement by continuous processes using microreactor-based technologies can make them more effective, safer and to give products with stable properties. Catalysts beads, currently applied as column reactor packings in fine chemicals' synthesis, are usually of 50–100 μm diameter. Therefore, their application often leads to serious operational problems; excessive backpressure results in a maldistribution of fluids, and thus formation of stagnant zones and hot spots, which in addition to a fairly long diffusion path, leads to lower yields, poorer selectivity and reduced catalyst life [1]. Continuous-flow monolithic polymeric microreactors show important advantages: defined system of flow-through pores and facile modification of the surface using ample arsenals of chemical tools [2,3]. But their thermal sensitivity and propensity to swell are serious drawbacks [4]. Typical ceramic (e.g. cordierite) monoliths, which feature bunch of channels of 1–5 mm sizes, connected with smaller ones of ca. 0.1–1.0 mm, are aimed at gas-phase reactions [5].

Silica-based continuous-flow monolithic microreactors, first proposed by the Montpellier group, appeared to be extremely promising for the cost-effective production of fine chemicals [6]. This stems from a unique, bi-continuous structure of the monoliths in which flow-through macropores are connected to an extensive network of meso- and micro-pores present in the silica skeleton [6–8]. In effect, pressure drops are fairly small, even at considerable throughputs, whereas easily accessible large surface area offers very large concentration of active sites per unit volume. Initially, such microreactor was made of a single monolith–MonoSil, the surface of which was functionalized with $-NH_2$ or $-HSO_3$ groups [6]. Control of its meso- and macro-porosity was obtained by combining phase separation method, elaborated by Nakanishi [9–11], with pseudomorphic synthesis [12,13], to obtain an ordered mesoporosity of the silica skeleton. But more importantly perhaps, the productivity of MonoSil microreactors in Knovenagel reaction and acid transesterification was shown to be 13 and 18 times larger than in the corresponding batch processes.

The original Nakanishi method was later modified [14,15] to give silica monoliths with notably larger macropores (30–50 μm) and more isotropic structure. Their pore structure was not destroyed after immobilization of ionic liquids and the catalysts obtained from the crushed monoliths were very active, selective and stable in the Baeyer–Villiger reaction and also in aerobic oxidation of primary alcohols [16–18].

The up to date methods of silica modification [19] offer huge potentials to develop microreactors with the structure

* Corresponding author at: Polish Academy of Sciences, Institute of Chemical Engineering, Bałtycka 5, 44-100 Gliwice, Poland. Tel.: +48 32 2310811; fax: +48 32 2310318.
E-mail address: jmrowiec@polsl.pl (J. Mrowiec-Białoń).

http://dx.doi.org/10.1016/j.apcata.2014.10.047
0926-860X/

purposely designed to meet specific catalytic and process engineering demands. Most recently these monoliths were successfully converted into a miniaturized multichannel enzymatic reactor [20] which could operate at flow rates up to about 20 cm^3/min at backpressure not exceeding 2.5 bar. Worth noting, the sucrose hydrolysis catalysed by invertase appeared to proceed in this microreactor with maximum rate over 1000 times faster than in the MCF-based slurry system, and the enzyme confined in mesopores showed notably larger affinity to substrate than the native one, a clear signature of hyperactivity effect.

For this reason we deemed it important to test the potentials of continuous-flow microreactors made of similar silica monoliths with ultra large (20–50 μm) macropores, but activated with sulphonic acid groups, in the esterification of acetic acid and lactic acid with *n*-butanol. While considered here as model reactions [21–25], they are both of a major practical interest. The *n*-butyl acetate is commonly used as a solvent in the manufacturing of lacquer, artificial perfume, photographic films, plastics and safety glass, and also as synthetic fruit flavouring in foods [26]. Typically, the esterification of lactic acid is applied to recover and purify the acid obtained by bacterial fermentation of carbohydrates [27,28]. But as all previous experiments with the reactors of this type were carried out in relatively benign conditions [7,20], we considered it also important to test whether they can effectively operate at elevated temperature.

2. Experimental part

2.1. Synthesis of silica monoliths

Silica rods of 4.5 mm diameter were synthesized using Nakanishi method [9–11] with the modifications described in [15,16]. In brief, 0.91 g of polyethylene glycol (PEG 35000) was dissolved in 10.5 cm^3 of 1 M HNO_3, next 7.6 cm^3 of TEOS was added slowly, followed by addition 0.4 g of cetyltrimethylammonium bromide (CTAB). The solution was mixed at room temperature for 1 h and then polypropylene tubes (5.7 mm i.d.) were filled with the sol. After gelation at 40 °C (12 h) they were aged at the same temperature for seven days. Then the samples were treated in 1 M ammonia aqueous solution at 90 °C for 9 h and after washing with water the monoliths were dried at 40 °C for three days and finally calcined at 550 °C for 5 h. During the processing shrinkage of about 20% of the size of mold was observed.

Single rods (1, 2 and 4 cm long) were embedded into a heat-shrinkable PTFE tubes (DSG-Canusa), equipped with connectors to obtain microreactors suitable for a continuous-flow operation. Then these microreactors were functionalized under flow (48 h, 60 °C) with arenesulphonic acid groups using solutions of 2-(4-chlorosulfonylphenyl)ethyltrimethoxysilane (CSPTMS; 50 wt% solution in CH_2Cl_2) dissolved in anhydrous ethanol (99.6%) to prevent uncontrolled hydrolysis.

2.2. Characterization of materials

Macropore structure of the monoliths thus obtained was investigated by mercury porosimetry (Quantachrome, PoreMaster 60), and by scanning electron microscopy (SEM, TM 30000 Hitachi). Low temperature nitrogen sorption (ASAP Micromeritics 2010) was applied to evaluate specific surface area (S_{BET}), mesopore volume and mesopore size distribution using desorption branch of isotherm and BJH method. Before analysis the samples were degassed for 24 h at 200 °C. The incorporation of functional groups was confirmed by FT-IR analysis (samples were prepared by KBr technique). Thermal properties and an amount of incorporated active groups were determined by thermogravimetric method

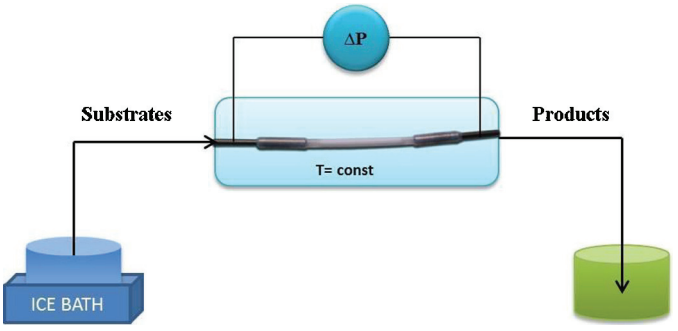

Fig. 1. Scheme of microreactor setup.

(Mettler Toledo STAR 850). The weight loss and thermal effects during heating with ramp of 10 deg/min and air flow of 60 cm^3/min were recorded in the range of 25–800 °C. Additionally, drop pressure was measured in the continuous reaction conditions using pressure controller (UNIK 5000, Ex-Calibra).

2.3. Catalytic measurements

The microreactor was tested in esterification of acetic acid and lactic acid with *n*-butanol (pure p.a, Chempur, Poland). The reactor setup is shown schematically in Fig. 1. The substrates solution was stored in ice bath to prevent any further reaction.

The experiments with acetic acid were performed for the molar ratio of substrates 1:1, at 75 °C using flow rates of 0.03, 0.06 and 0.09 cm^3/min. Esterification of lactic acid was carried out at 120 °C and 140 °C (measured with accuracy of ±0.1 °C) with flow rates of 0.03–0.4 cm^3/min. The molar ratio of lactic acid to *n*-butanol was 1:12, 1:6 and 1:1. The reaction progress was evaluated from the amount of acetic/lactic acid in the mixture. Acid concentration at the inlet and outlet of the microreactor was measured by titration method and additionally confirmed by gas chromatography (Agilent 7890 A, FID detector, HP-5 column).

Productivity of the microreactor and residence time was calculated from Eq. (1) and (2) [29]:

$$P = C_0 \times \mathrm{Conv} \times \frac{V_T}{\tau} \quad (1)$$

$$\tau = \frac{V_T \times m}{F} \quad (2)$$

where C_0 is initial concentration of substrate [mmol/cm^3], Conv is the conversion coefficient, V_T is the total pore volume [cm^3/g], τ is the residence time [min], m is the mass of monolith [g], F is the flow rate [cm^3/min]. The esterification of acetic acid was also carried out in batch reactor using round bottom flask (75 cm^3) equipped with a heating jacket and condenser. The reaction was performed under agitation at 1000 rpm using the same temperature and molar ratio of substrates as in the continuous process. The functionalized monolith was crushed and particles of ca. 50 μm were applied as catalyst at concentration of 0.74 wt%.

3. Results and discussion

Crack free silica rods displayed in Fig. 2 featured three types of pores detected by mercury porosimetry, nitrogen adsorption and scanning electron microscopy: (i) small mesopores with diameters ca. 3 nm and larger ones with maximum at 20 nm, originating from the presence of CTAB micelles, applied as soft pore templates, and a hydrothermal treatment of monoliths in ammonia solution, and (ii) ultra large macropores (flow-through channels) with diameters in the range of 20–50 μm (Figs. 3 and 4) obtained by

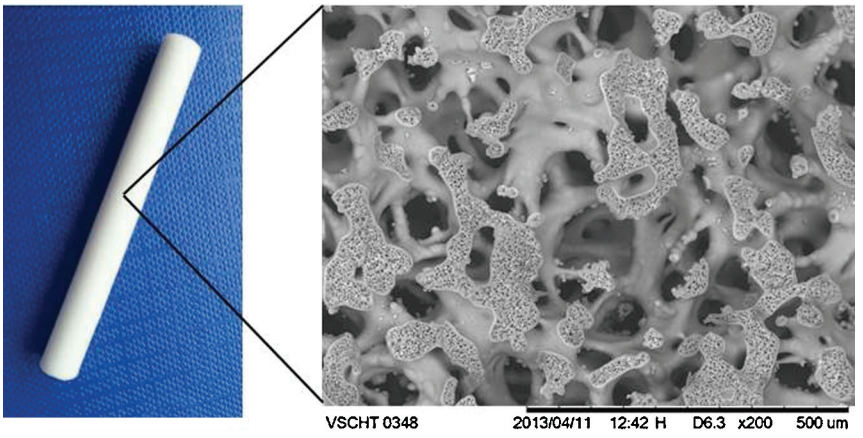

Fig. 2. Silica monoliths and SEM image of their structure.

Table 1
Texture parameters of monoliths.

Description	S_{BET} (m^2/g)	V_{mes} (cm^3/g)	V_{mac} (cm^3/g)	V_{total} (cm^3/g)	d_{mes} (nm)	d_{mac} (nm)
Monolith (M)	328	1.15	2.45	3.5	3.5/20	20–50
Functionalized monolith (MF)	245	0.91	2.45	3.25	20	20–50
Monolith after reaction (MFR)	275	0.91	2.44	3.25	20	20–50

PEG-induced phase separation. The bi-continuous structure of voids (macropores) and silica struts is well seen in the SEM image displayed in Fig. 2. Separated spherical voids of ca. 1 μm could also be observed in the silica skeleton, yet they were hardly detected by mercury porosimetry owing to their inaccessibility (Fig. 4). We believe that they originate from small PEG droplets. A pristine monolith (M) exhibited surface area of about 328 cm^2/g and mesopore volume of 1.15 cm^3/g (Table 1). After its functionalization with arenesulphonic groups (MF) smaller mesopores disappeared and this can be explained by a preferential deposition of functional groups' precursor in that space [30]. Clearly, it resulted in a decrease of specific surface area (ca. 17%). The monoliths thus obtained appeared to possess larger meso- and macropores compared to those reported before [6–8].

The presence of arenesulphonic groups on the monoliths' surface was investigated by FT-IR spectroscopy to obtain the spectra shown in Fig. 5. In all materials the asymmetric and symmetric stretching vibrations of the Si—O—Si framework occur in the range of 1000–1250 cm^{-1} and also 800 and 470 cm^{-1}. Weak absorption peak at around 960 cm^{-1} is attributed to stretching vibration of Si—OH group. Broad band in the range of 3000–3700 cm^{-1} corresponds to asymmetric stretching of hydrogen bonded OH groups. In the arenesulphonic-functionalized samples typical absorption bands from aromatic ring are observed at 700 cm^{-1}, 1403 cm^{-1}

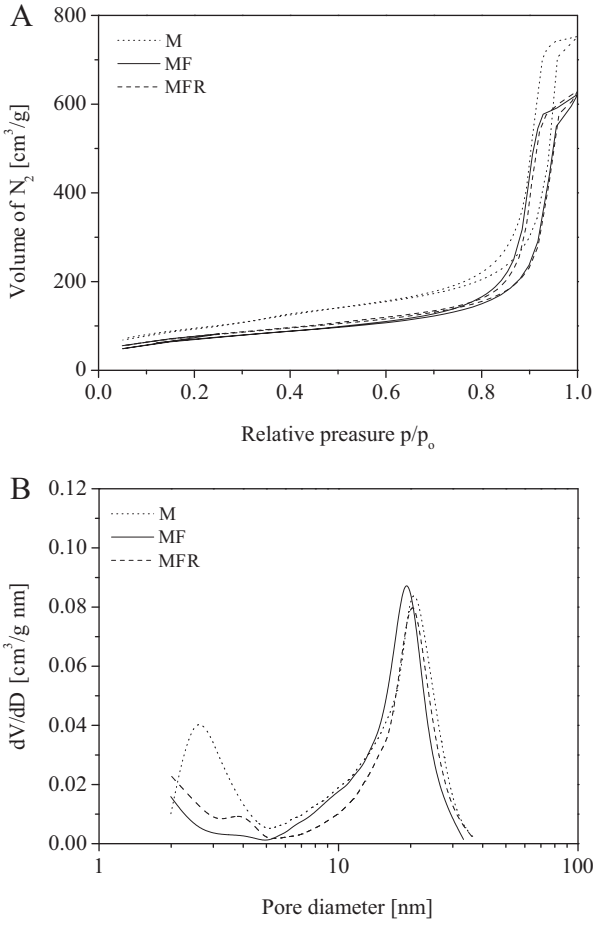

Fig. 3. Nitrogen adsorption/desorption isotherms (A) and pore size distributions (B) of pristine monolith (M), after its activation (MF) and after 3-day operation (MFR).

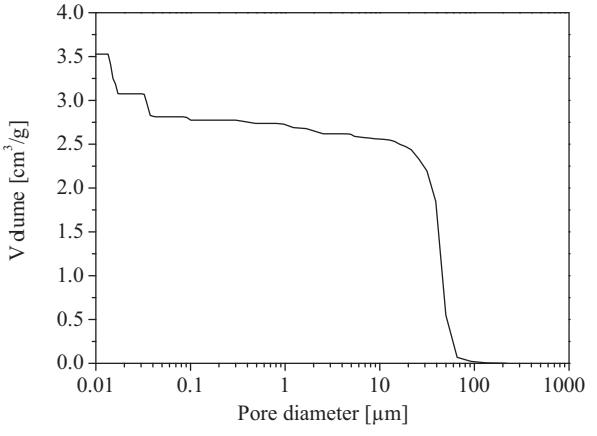

Fig. 4. Cumulative pore size distribution in a pristine monolith obtained by mercury porosimetry.

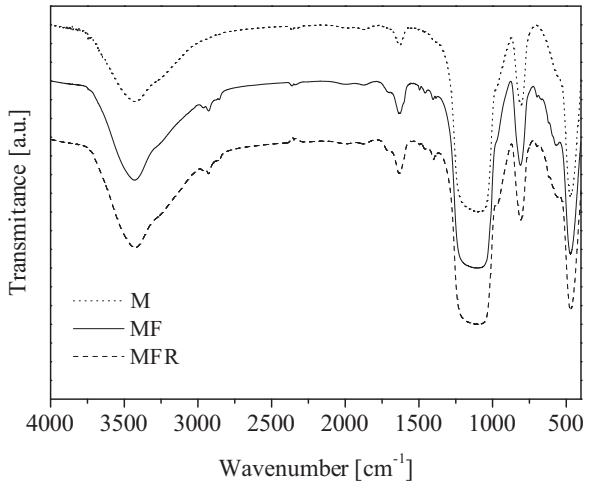

Fig. 5. FT-IR spectra of M, MF and MFR samples (the spectra were shifted for clarity).

and 1498 cm^{-1}. Absorption in the range of 2850–3000 cm^{-1} and the peak at 1457 cm^{-1} can be assigned to asymmetric stretching and bending vibration of C—H in methylene group connecting the aromatic ring. The S=O stretching vibrations of sulphonic groups normally occur in the range of 1000–1200 cm^{-1}. In the case of silica-based materials those vibrations overlap with Si—O—Si bands.

The amount of functional groups attached to the monoliths' surface and also their thermal stability were determined by thermal analysis. TG curves of the samples activated with different amounts of acidic groups are shown in Fig. 6A. Two steps of weight loss are clearly visible on the TG curve, especially from the sample with the

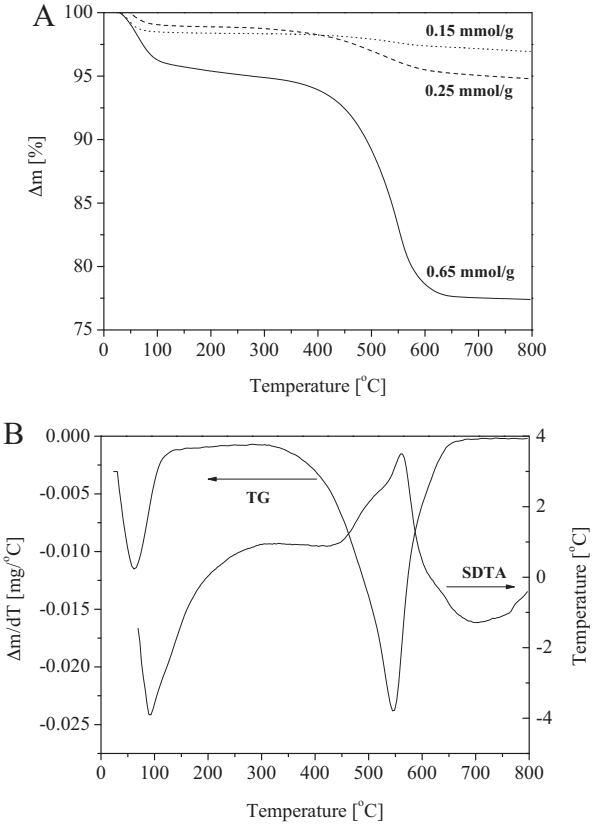

Fig. 6. TG curves of samples with different amount of incorporated acidic groups (A) and DTG and SDTA curves recorded for MF with 0.65 mmol/g of active groups (B).

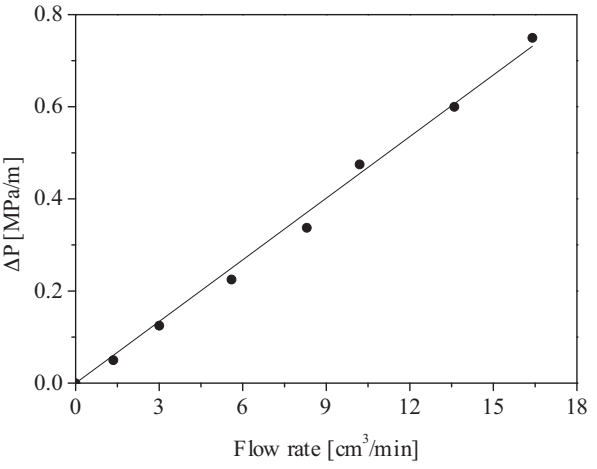

Fig. 7. Drop pressure vs. flow rate for 4 cm microreactor.

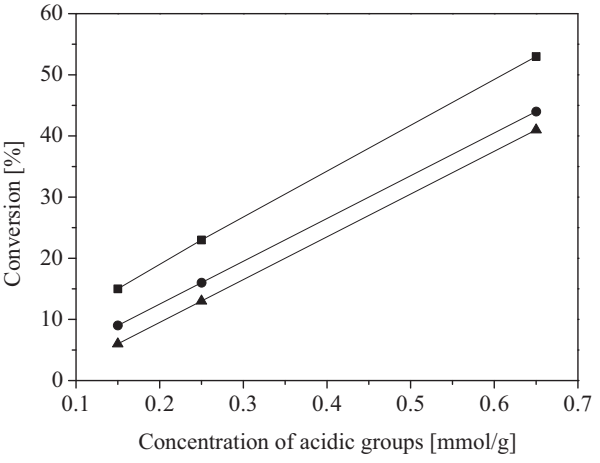

Fig. 8. Conversion of acetic acid vs. concentration of acidic groups for different flow rates: (■) 0.03 cm^3/min; (●) 0.06 cm^3/min and (▲) 0.09 cm^3/min.

largest content of functional groups. The sharp weight loss below 120 °C is assigned to the removal of physisorbed water, whereas the loss between 350 and 600 °C, corresponds to the decomposition of organic groups. Desorption of water and decomposition of organics appeared to be portrayed by two thermal effects; the endothermic peak with maximum at 100 °C and the exothermic (550 °C), are well seen on SDTA curve (Fig. 6B). The amount of incorporated groups was calculated from mass loss in the range of 350–600 °C and the values obtained were 0.15, 0.25 and 0.65 mmol/g. The largest value is consistent with the reported dependence between the maximum number of organic group, which could effectively be bound, and the concentration of hydroxyl groups present on the silica surface [31,32].

For the continuous-flow microreactors the relationship between pressure drop and the flow rate through the monoliths is of practical significance. As can be inferred from Fig. 7, which shows the effect of liquid flow rate on pressure drop in the 4-cm reactor, the pressure drop in this microreactor was significantly smaller than that recorded before [7], due to the presence of much larger flow-through channels. This eliminates the need for the use of high-pressure metering pumps, typically applied in columns packed with fine beads, with a positive effect on process economy.

As indicated, catalytic properties of the microreactor were investigated in the esterification of acetic acid and lactic acid with *n*-butanol. First, the relationship between the amount of acidic groups and conversion was checked in esterification of acetic acid, at

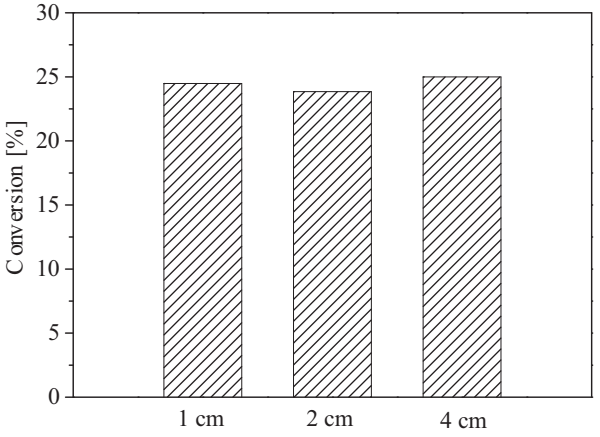

Fig. 9. Conversion of acetic acid in microreactors of different length for the residence time equal 155 s.

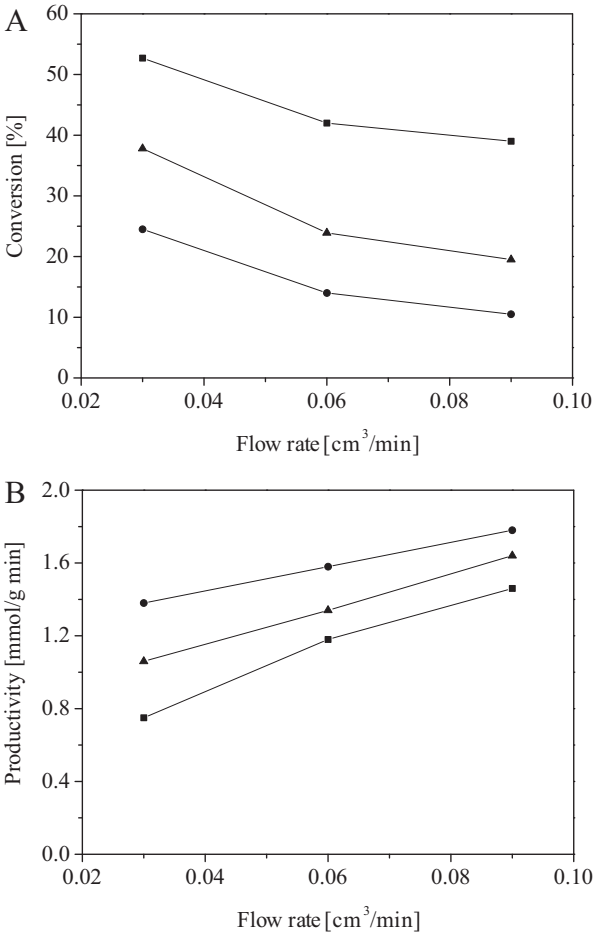

Fig. 10. Conversion of acetic acid (A) and productivity of ester (B) vs. flow rate in microreactors 1 cm (●), 2 cm (▲) and 4 cm (■) long.

different flow rates, to find a linear dependence (Fig. 8). Therefore, the bulk of experiments were performed for the monoliths with the highest concentration of acid groups, i.e. 0.65 mmol/g.

In order to check and eliminate the effect of external mass transfer on reaction kinetics, the reactors of different lengths were compared for the same residence time (155 s) to obtain similar values of conversion (ca. 25%, cf. Fig. 9); a clear proof of the lack of those limitations.

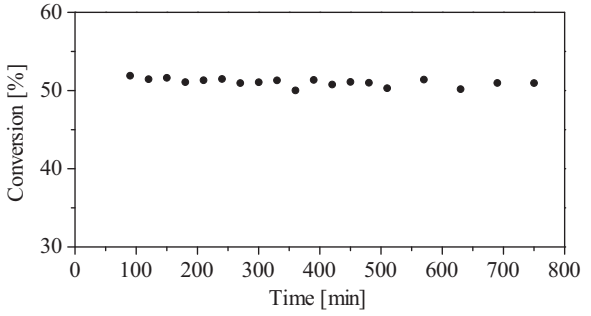

Fig. 11. Catalytic stability of microreactor in esterification of acetic acid with *n*-butanol (reaction conditions: 75 °C, molar ratio 1:1, flow rate 0.03 cm^3/min).

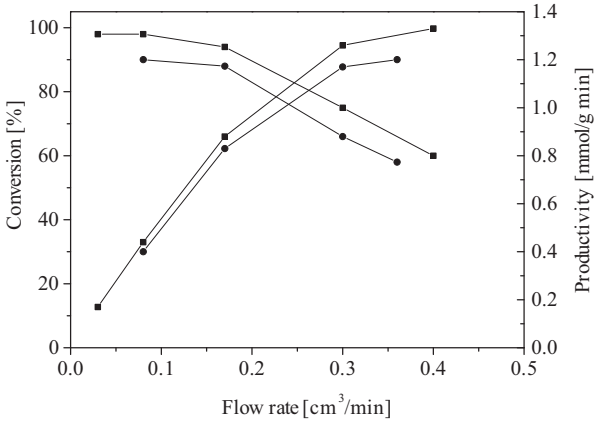

Fig. 12. Conversion of lactic acid and productivity of ester vs. flow rate in reactions carried out at (■) 140 °C and (●) 120 °C.

Fig. 10 shows the relationship of ester productivity and conversion of acetic acid against the flow rate for microreactors of different length (1–4 cm). As can be seen, the highest productivity (1.78 mmol/g min) was achieved in the shortest one (1 cm) and for the largest value of flow rate (0.09 cm^3/min), and this is in accord with expectations. An opposite relationship was observed for the case of conversion; the highest value, of ca. 53%, was received for 4 cm reactor and the lowest value of flow rate.

The performance of the monolithic and batch reactors was compared under identical conditions: the catalysts of 0.1444 g load, had either the form of monolith or powder, reaction time was 6 h and the volume of substrates was 21.6 cm^3. The conversion of acid was found to be ca. 42.5% and the productivity of ester reached the value of 1.2 mmol/g min in the both cases. This confirms that diffusion had no effect on the rate of reaction, unlike observed before for Diels–Alder reaction study, in which productivity in batch reactor was only half of that determined for the flow system [29]. But not less importantly, good catalytic stability during 800 min-long process was observed (Fig. 11).

To check the possibility of application these microreactors under more severe conditions, the esterification of lactic acid with *n*-butanol was performed. The results shown in Figs. 12 and 13 demonstrate almost full (99%) conversion of the acid when the process was carried out at 140 °C, the molar ratio of lactic acid to *n*-butanol equalled to 1:12 and the flow rate was in the range of 0.03–0.15 cm^3/min. This conversion is similar to that reported for batch process carried out over TiO_2–Al_2O_3 catalyst under the same conditions [24]. However, the productivity obtained in the monolithic microreactor under study (for flow rate of 0.15 cm^3/min) reached the value of 0.874 mmol/g min, i.e. four times more than reported. The increase in the flow rate to 0.3 cm^3/min decreased the conversion to 75%, but productivity increased by ca. 50%, to

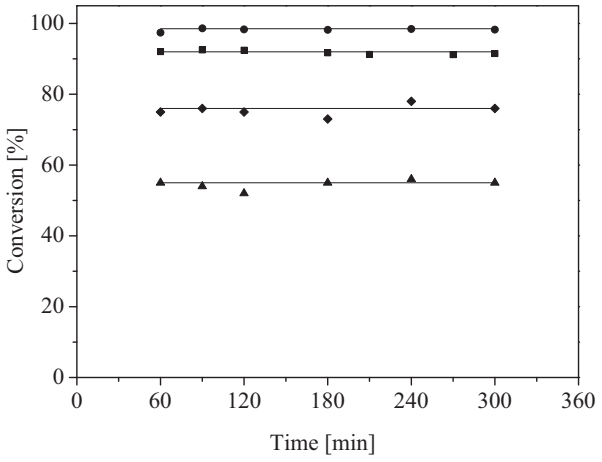

Fig. 13. Conversion of lactic acid vs. time at different reaction conditions: (●) 140 °C, 1:12; (■) 120 °C, 1:12; (♦) 120 °C, 1:6; (▲) 140 °C, 1:1.

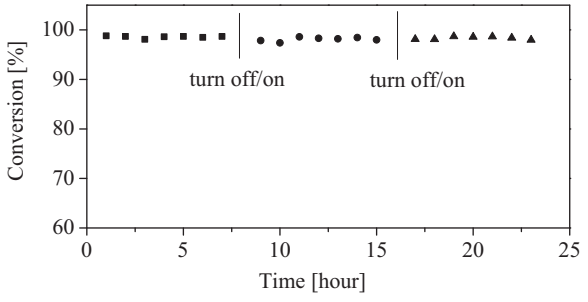

Fig. 14. Catalytic stability of microreactor in esterification of lactic acid with *n*-butanol: (■) 1st; (●) 2nd; (▲) 3rd day (reaction conditions: 140 °C, molar ratio 1:12, flow rate 0.15 cm^3/min).

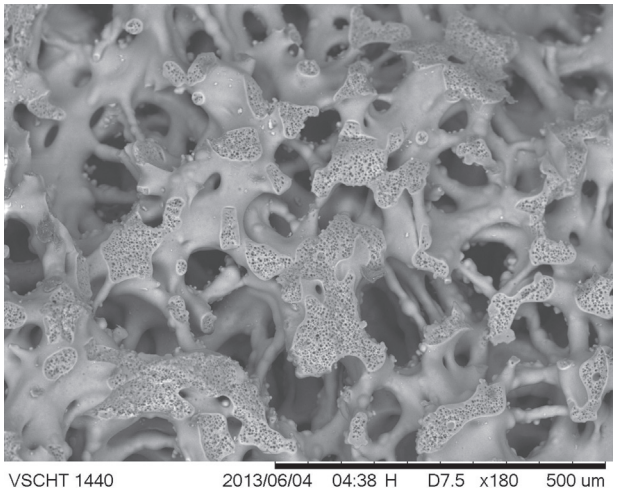

Fig. 15. SEM image of MFR monolith after esterification of lactic acid (reaction conditions: 140 °C, molar ratio 1:12, flow rate 0.15 cm^3/min).

the value of 1.25 mmol/g min. Further increase in the flow rate had a small affect on the increase of productivity. At lower temperature (120 °C) and with less excess of *n*-butanol (1:6 and 1:1) the efficiency of esterification was smaller, owing to reverse reaction effect.

The stability of microreactor was checked during three-day operation, discontinued for nights, to find that microreactor's performance did not change after the breaks (Fig. 14). The structure of the monolith also appeared to be well preserved both at the nanometric (Fig. 3) and micrometric scale (Fig. 15) and no change in the acidic groups content was detected by IR and thermogravimetric analysis after that period (data not shown).

4. Conclusions

A facile procedure to prepare an effective continuous-flow monolithic silica microreactor functionalized with arenesulphonic acid groups was proposed. Due to the presence of flow-through pores of 20–50 μm sizes these reactors can operate at low pressure drops which eliminate the need for the use of high pressure pumps. The relatively large specific surface area, ca. 250 m^2/g, exhibited by mesopores of ca. 20 nm present in silica skeleton allowed to attaching acidic groups in amount of 0.65 mmol/g. The microrector demonstrated very high activity and productivity and also good stability of catalytic and structural properties in the continuous esterification of acetic and lactic acid with *n*-butanol, even carried out at the temperature as high as 140 °C.

Acknowledgements

The support of the National Science Center for this project under the project UMO-2011/01/B/ST8/03855 is gratefully acknowledged.

References

[1] A. Stankiewicz, Chem. Eng. Sci. 56 (2001) 359–364.
[2] T.-H. Yoon, L.-Y. Hong, D.-P. Kim, Chem. Eng. J. 167 (2011) 666–670.
[3] J.F. Ng, Y. Nie, G.K. Chuah, S. Jaenicke, J. Catal. 269 (2010) 302–308.
[4] C. Viklund, F. Svec, J.M. Fréchet, K. Irgum, Chem. Mater. 8 (1996) 744–750.
[5] A. Cybulski, J.A. Moulijn, Catal, Rev. Sci. Eng. 36 (1994) 179–270.
[6] A. El Kadib, R. Chimenton, A. Sachse, F. Fajula, A. Galarneau, B. Coq, Angew. Chem. Int. Ed. 48 (2009) 4969–4972.
[7] A. Sachse, A. Galarneau, F. Fajula, F. Di Renzo, P. Creux, B. Coq, Microporous Mesoporous Mater. 140 (2011) 58–68.
[8] A. Sachse, A. Galarneau, B. Coq, F. Fajula, New J. Chem. 35 (2011) 259–264.
[9] K. Nakanishi, H. Minakuchi, N. Soga, N. Tanaka, J. Sol-Gel Sci. Technol. 13 (1998) 163–169.
[10] K. Nakanishi, Y. Kobayashi, T. Amatani, K. Hirao, T. Kodaira, Chem. Mater. 16 (2004) 3652–3658.
[11] N. Tanaka, H. Kobayashi, K. Nakanishi, H. Minakuchi, N. Ishizuka, Anal. Chem. 73 (2001) 420A–429A.
[12] A. Galarneau, J. Iapichella, K. Bonhomme, F. Di Renzo, P. Kooyman, O. Terasaki, F. Fajula, Adv. Funct. Mater. 16 (2006) 1657–1667.
[13] T. Martin, A. Galarneau, F. Di Renzo, F. Fajula, D. Plee, Angew. Chem. Int. Ed. 41 (2002) 2590–2592.
[14] J.H. Smått, S. Schunk, M. Linden, Chem. Mater. 16 (2003) 2354–2361.
[15] W. Pudło, W. Gawlik, J. Mrowiec-Białoń, T. Buczek, J.J. Malinowski, A.B. Jarzębski, Inż. Chem. Proc. 27 (2006) 177–185 (in Polish).
[16] A. Chrobok, S. Baj, W. Pudło, A.B. Jarzębski, Appl. Catal., A: Gen. 366 (2009) 22–28.
[17] A. Chrobok, S. Baj, W. Pudło, A.B. Jarzębski, Appl. Catal., A: Gen. 389 (2010) 179–185.
[18] A. Drożdż, A. Chrobok, S. Baj, K. Szymańska, J. Mrowiec-Białoń, A.B. Jarzębski, Appl. Catal., A: Gen. 467 (2013) 163–170.
[19] F. Hoffmann, M. Cornelius, J. Morell, M. Fröba, Angew. Chem. Int. Ed. 45 (2006) 3216–3251.
[20] K. Szymańska, W. Pudło, J. Mrowiec-Białoń, A. Czardybon, J. Kocurek, A.B. Jarzębski, Microporous Mesoporous Mater. 170 (2013) 75–82.
[21] B. Rabindran Jeremy, A. Pandurangan, J. Mol. Catal. A: Chem. 237 (2005) 146–154.
[22] G. Mitran, É. Makó, Á. Rédey, Catal. Lett. 140 (2010) 32–37.
[23] E. Sert, F.S. Atalat, React. Kinet. Catal. Lett. 99 (2010) 125–134.
[24] K.-T. Li, Ch.-K. Wang, Appl. Catal., A: Gen. 433–434 (2012) 275–279.
[25] K.-T. Li, Ch.-K. Wang, I. Wang, Ch.-M. Wang, Appl. Catal., A: Gen. 392 (2011) 180–183.
[26] Data K., in: Encyclopedia of Chemical Technology, Wiley, New York, 13 (1997) 1042-1058.
[27] D. Garlotta, J. Polym. Environ. 9 (2001) 63–84.
[28] S.P. Kamble, P.P. Barve, J.B. Joshi, I. Rahman, B.D. Kulkarni, Ind. Eng. Chem. Res. 51 (2012) 1506–1514.
[29] A. Sachse, V. Hulea, A. Finiels, B. Coq, F. Fajula, A. Galarneau, J. Catal. 287 (2012) 62–67.
[30] A. Zuka, H. Silklova, J. Cejka, Langmuir 24 (2008) 9837–9842.
[31] J. Mrowiec-Białoń, Thermochim. Acta 443 (2006) 49–52.
[32] L.T. Zhuravlev, Colloids Surf., A: Physicochem. Eng. Aspects 173 (2000) 1–38.

Chemical Engineering Journal 282 (2015) 137–141

Contents lists available at ScienceDirect

Chemical Engineering Journal

journal homepage: www.elsevier.com/locate/cej

Fabrication and performance of monolithic continuous-flow silica microreactors

Małgorzata Berdys [a], Agnieszka Koreniuk [b], Katarzyna Maresz [b], Wojciech Pudło [a], Andrzej B. Jarzębski [a,b], Julita Mrowiec-Białoń [a,b,*]

[a] Department of Chemical Engineering and Process Design, Faculty of Chemistry, Silesian University of Technology, Ks. M. Strzody 7, 44-100 Gliwice, Poland
[b] Institute of Chemical Engineering, Polish Academy of Sciences, Bałtycka 5, 44-100 Gliwice, Poland

HIGHLIGHTS

- Monolith-in-monolith topology of microreactor was realized and tested.
- Cordierite reinforcement of silica monolith facilitates its scale-up.
- Good contact of both monoliths can be achieved after a surface treatment.
- The operational viability of microreactor was demonstrated in model reaction.

GRAPHICAL ABSTRACT

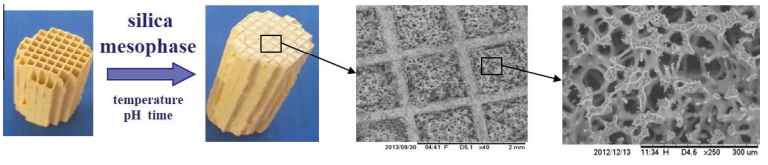

ARTICLE INFO

Article history:
Available online 18 February 2015

Keywords:
Monolith-in-monolith
Cordierite
Surface treatment
Monolithic microreactor
Catalytic activity

ABSTRACT

Monolith-in-monolith reactor (MiM) was obtained by embedding monolithic silica with the hierarchical pore structure into the channels of conventional honeycomb monolith made of cordierite. Surface treatment of the cordierite with alkaline and acidic solution was applied to increase its surface area and generate strong silanols, to ensure good adherence between the monoliths. Application of 10 wt% NaOH solution at room temperature for 0.5 h was found to offer the best contact between two materials. Both structure and flow characteristics of the embedded silica proved to be quite similar to those obtained for pure silica rods, considered as reference. Performance of MiM microreactor functionalised with sulphonic groups was shown to be similar to that of a single silica rod microreactor in the esterification of acetic acid with butanol. The elaboration of fabrication procedure for monolithic silica microreactors may open new venue in the engineering of cost-effective production of fine chemicals.

1. Introduction

The mesoporous silicas have been on the forefront of research since their discovery over two decades ago. However, the separation of their fine particles, typically 10–50 μm in size, but quite often sub micrometric sizes, e.g., as obtained from the flow synthesis [1] may be a major problem. An ingenious method proposed to overcome this difficulty is to incorporate magnetic nanoparticles into their structure [1–3]. But even more effective approach is the use of silica monoliths with the pore structure in micrometric scales similar to that displayed by the mesoporous materials. Indeed, the silica-based continuous-flow monolithic microreactors were more recently shown to be extremely promising for the cost-effective production of *fine chemicals* [4]. Owing to the unique hierarchical pore structure, in which flow-through macropores are connected to an extensive network of meso- and micro-pores [4], the back-pressure could be reduced, permeability increased and the accessibility of substrates to catalytic sites improved, giving in overall much better performance compared to packed columns [5]. The monoliths, typically obtained, feature high porosity and large surface area, but their mechanical strength is low. So far, these microreactors were fabricated by embedding the monolith

* Corresponding author at: Department of Chemical Engineering and Process Design, Faculty of Chemistry, Silesian University of Technology, Ks. M. Strzody 7, 44-100 Gliwice, Poland. Tel.: +48 322310811.
E-mail address: jmrowiec@polsl.pl (J. Mrowiec-Białoń).

http://dx.doi.org/10.1016/j.cej.2015.01.132
1385-8947/

either into a heat-shrinkable PTFE tube [4] or a polymeric body [6], which limited the scope of their operation.

To achieve more robust structure of the monoliths the concept of monolith-in-monolith (MiM) was proposed [7]. It relies on embedding silica monoliths with the hierarchical pore structure into the channels of conventional ceramic monolith, e.g. made of cordierite. The cordierite is a crystalline magnesium aluminosilicate ($2MgO{\cdot}2Al_2O_3{\cdot}5SiO_2$) widely applied for high-temperature applications in the form of honeycomb monoliths, serving as supports in industrial catalytic systems. However, as the surface area of these monoliths is low <0.5 m^2/g, therefore it has to be extended and also activated, and this is achieved by a washcoat [8–10]. The acid treatment is often applied, prior to deposition of the washcoat, to increase the monolith's surface area and to improve adhesion of the coating to the support [11].

The concept of monolith-in-monolith is clear. However, it appeared somewhat difficult to fabricate it, and especially to achieve a good contact between these two materials. It is critical for the effective operation of the reactor; otherwise maldistribution of the fluid flow will follow. However, this contact is exposed to a considerable stress, caused by shrinkage of the silica monolith during drying and calcination and this poses a need for its reinforcement. The latter can be achieved by extension of the contact surface area and also the formation of strong bonds between the two solids using chemical methods.

In this paper we propose a treatment of the cordierite surface to increase the contact surface area and generate strong surface silanols for its firm binding with the siliceous monolith. The composition of the solution applied, temperature and time of the treatment were investigated. The changes in surface area, its composition and morphology were studied by nitrogen adsorption, XPS and SEM. The hydrodynamic properties of MiMs were compared with those determined for a single silica monolith. Finally, practical potentials of the MiM-type of microreactor functionalised with arenesulphonic acid groups were examined in a model reaction of acetic acid esterification with butanol to demonstrate its operational viability.

2. Experimental

2.1. Materials

Tetraethoxysilane (TEOS, 99%, ABCR) was used as a silica precursor. Polyethylene glycol (PEG 35000, Fluka) induced phase separation during monoliths synthesis and acted as a matrix of macropore structure. Nitric acid (65%, Avantor Performance Materials) was used as the catalyst for hydrolysis and condensation of TEOS. Cetyltrimethylammonium bromide (CTAB, Aldrich) was applied as a mesopores template. Ammonia aqueous solution (25%, Avantor Performance Materials) was employed during post-synthesis treatment of monoliths. The precursor of acidic groups was 2-(4-chlorosulfonylphenyl)ethyltrimethoxysilane (CSPTMS, 50% in methylene chloride, ABCR). Cordierite honeycomb monolith (Corning) with channel dimension of 1.1 mm and wall thickness of 0.17 mm was used as support for monolithic silica. Sodium hydroxide and piranha solution ($H_2SO_4 + H_2O_2$) (Avantor Performance Materials) were applied for a cordierite treatment. Acetic acid (99.5%) and n-butanol (99.5%), both from Chempur were applied as reactants in evaluation of the catalytic performance. All the chemicals were used without further purification.

2.2. Fabrication of microreactors

The monolith-in-monolith structure was obtained by filling the cordierite honeycomb rods (12 × 40 mm) with a silica sol. First, the cordierite rods were treated with sodium hydroxide solution (10, 20, and 30 wt%) or piranha for 30, 60 or 120 min, at different temperature. After treatment, they were washed with excess of deionised water and dried at 110 °C overnight. Next, silica sol was prepared using a modified Nakanishi method [6]. Briefly, mixture of TEOS, PEG and nitric acid (1 M) was stirred in an ice bath for 1 h, followed by addition of CTAB. Molar ratio of TEOS:PEG:HNO_3:-H_2O:CTAB was 1:0.53:0.26:14:0.0275. Then the honeycomb channels were filled with the transparent sol, which was left to gel and age at 40 °C for 7 days. After that, the MiM was treated in a 1 M ammonia solution at 90 °C for 9 h. Finally, organic templates were decomposed during calcination at 550 °C for 6 h. The weight ratio of silica to cordierite was 0.32. For comparison, pure silica rods of the same length were synthesized using the procedure described above.

The single MiM piece was embedded into a heat-shrinkable polytetrafluoroethylene tube (PTFE, DSG-Canusa), equipped with connectors [12]. To impart catalytic properties to the microreactor the arenesulfonic groups were incorporated into silica surface. The functionalization was performed by passing (and recycling) the solution of CSPTMS dissolved in dry ethanol for 48 h at 60 °C. The amount of functional groups (determined by thermogravimetry) was 0.6 mmol/g.

2.3. Characterization

Scanning electron microscopy (SEM, TM 3000 Hitachi) was used to examine the macroporous structure and morphology of the monoliths, and the surface of the cordierite before and after the treatment with sodium hydroxide and piranha solution. The specific surface area, mesopore volume and pore size distribution were determined from the low temperature nitrogen adsorption (ASAP Micromeritics 2010). The size distributions of pores larger than 50 nm and total pore volume of silica monoliths were measured by a mercury porosimetry (Quantachrome, PoreMaster 60). The surface composition of cordierite was determined by XPS technique. The spectra were recorded by a VG Scientific ESCALAB-210 photoelectron spectrometer using a non-monochromatized Al Kα ($E_{h\nu}$ = 1486.6 eV) radiation (14.5 kV; 20 mA). The binding energy (E_b) scale was calibrated against the position of C 1s (E_b = 284.6 - eV). The analysis chamber was operated under an ultrahigh vacuum with a pressure of 5×10^{-7} Pa. The spectra were recorded with 0.4 eV resolution and deconvolution was made using AVANTAGE programme (Thermo Electric ver. 4.84), the background was fitted by a Shirley's model.

The esterification of acetic acid with butanol was carried out at 75 °C, for substrates ratio 1:1, and using the flow rate of 0.03 cm^3/min in all reactors. Concentrations of the substrates and product were measured using gas chromatography (Agilent 7890A, FID detector, HP-5 column). Error of the evaluated activities was smaller than 3%. The pressure drop was measured using a pressure controller (UNIK 5000, Ex-Calibra).

3. Results and discussion

As it can be seen from Fig. 1, the proposed concept can indeed be realized by filling the channels of the cordierite honeycomb with silica monoliths to obtain a monolith-in-monolith type of structure.

As already mentioned, the surface of the honeycomb was treated with sodium hydroxide solutions of different concentration and also piranha solution prior to introduction of the silica sol. Fig. 2 shows SEM images of its surface after such treatment for 0.5 h at 20 °C. Appreciable changes in surface morphology can be observed. The edges and corners of the pristine crystalline structure were

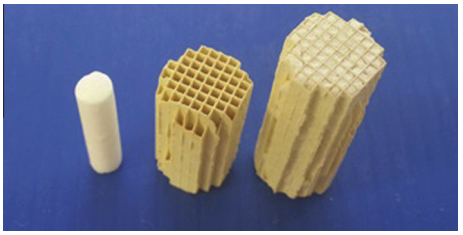

Fig. 1. Images of silica monolith (M), cordierite rod and monolith-in-monolith (MiM).

notably smoothed, roughly in proportion to concentration of the applied NaOH solution.

However, in the nanometric scale the surface became rougher. It is reflected in the increase in the specific surface area detected by nitrogen adsorption measurements. Pristine cordierite featured the S_{BET} value of ca. 0.2 m^2/g, whereas it increased to 0.36 m^2/g and 0.62 m^2/g after the treatment with 10 wt% and 30 wt% sodium hydroxide solution, respectively. The surface composition has also changed, as the XPS analysis indicated (Table 1). The concentration of silicon decreased as a result of silica etching by alkaline solution, and this caused the increase in aluminium and magnesium content. The alkaline treatment was expected to facilitate the hydrolysis of siloxane bonds, and the increase in hydroxyls' concentration was confirmed by FTIR spectroscopy and thermogravimetry (data not shown here). The treatment in the strong acid solution (piranha) resulted in similar changes in the surface properties as in the case of 30 wt% NaOH solution, whereas that at higher temperature (60 °C) and for a longer time resulted in a fairly pronounced destruction of the cordierite surface (Fig. 3).

The best connection between honeycomb surface and silica monolith was obtained for the cordierite treated with 10 wt% sodium hydroxide solution at 20 °C for 0.5 h (Fig. 2b). Large voids could be seen when untreated cordierite was used (Fig. 2a) and also after treatment with strong basic and acidic conditions (Fig. 2c–e). The gap between the walls of cordierite and silica monoliths was up to 150 μm.

Comparative studies of physico-chemical properties of the silica monolith (M) and MiM confirmed that a careful introduction of the silica monoliths, by the sol–gel process, into the cordierite's

Table 1
Surface composition determined by XPS analysis.

Element	Pristine cordierite	Cordierite after treatment[a]	
		10 wt% NaOH	30 wt% NaOH
	Atomic (%)		
O	58.84	57.51	57.22
Si	20.06	19.38	19.04
Al	11.46	12.27	13.47
Mg	7.40	7.84	8.20

[a] *Conditions*: time 0.5 h; room temperature.

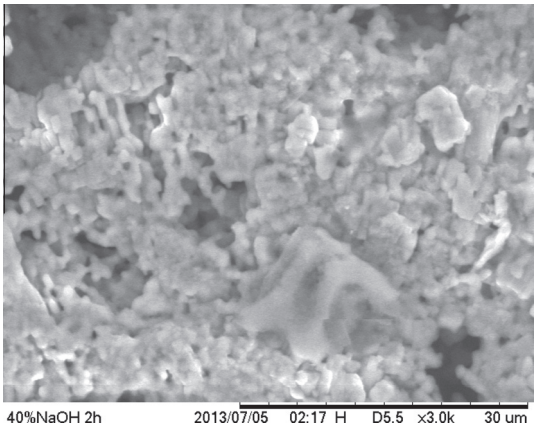

Fig. 3. SEM image of cordierite treated in 30 wt% NaOH solution at 60 °C for 2 h.

channels does not affect the silica structure. Both the nitrogen adsorption analysis (Fig. 4) and mercury porosimetry (Fig. 5) clearly evidenced this fact. Interestingly enough, MiM sample featured a larger specific surface area, ca. 20%. This increase is associated with a larger volume (ca. 13%) of the mesopores than seen in the silica monolith (Table 2) and a slightly larger contribution of the smaller mesopores in the 2–4 nm range (Fig. 4). The continuous macropore structure was very well preserved, but diameter of the macropores (flow-through channels) was slightly reduced; they were in the range of 10–40 μm, and of about 20–50 μm in the reference silica

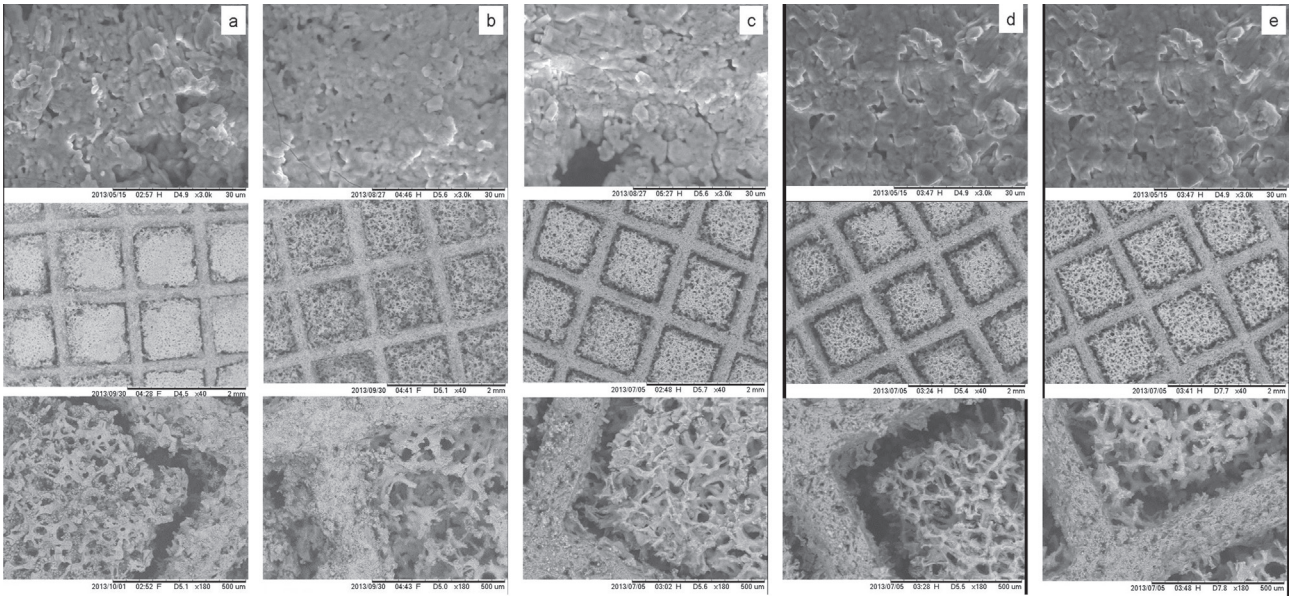

Fig. 2. SEM images of cordierite surface (top row): pristine (a) and after treatment with sodium hydroxide solution of 10 wt% (b), 20 wt% (c), 30 wt% (d) and piranha (e). Middle and bottom rows – images of MiMs (cross section; obtained at different magnifications) fabricated using the specified cordierite samples.

monolith. The thickness of silica struts in the MiM monoliths was also a bit smaller. Clearly, a considerable part of the MiM's volume was occupied by honeycomb walls. Overall, the MiM's porosity was lower by ca. 20%.

In terms of permeability and mass transfer the MiM microreactor was found to be quite similar to the single rod monolithic microreactor, but the fluid flow hindrance appeared to be slightly larger than that determined for a single silica rod (Fig. 6). This increase can be explained by the slightly smaller flow-through pores present in MiM. But the effect of honeycomb's walls cannot be precluded, as their thickness is more than one order larger that the size of struts present in the silica monolith. However, this pressure drop is still considerably smaller than that reported for the silica monolithic (capillary) microreactor proposed earlier [13].

Preliminary tests of the MiM reactor, functionalised with arenesulphonic acidic groups in amount of 0.6 mmol/g of silica, in a model reaction of acetic acid esterification with n-butanol showed that its catalytic performance is similar to that obtained using the single silica rod counterpart (M) (Fig. 7, inset). All catalytic experiments were performed under the same flow rate. Therefore, the residence time in the reactor 1 cm of length was a quarter of that four times longer. Consequently, a smaller conversion was observed in the former, in line with expectations [9]. But more interestingly, conversion achieved in the MiM reactor was ca. 6% lower than in the silica monolith (M) counterpart, perhaps due to a shorter residence time caused by the smaller porosity. Good catalytic stability of MiM reactor was confirmed during a continuous 8 h experiment (Fig. 7).

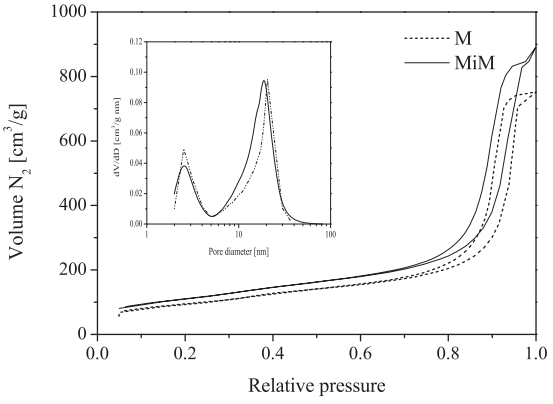

Fig. 4. Nitrogen adsorption/desorption isotherm and pore size distribution in silica monolith (M) and monolith-in-monolith (MiM).

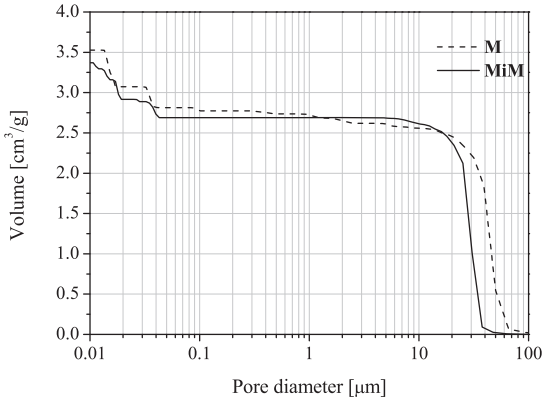

Fig. 5. Pore volume *vs.* pore diameter for silica monolith (M) and monolith-in-monolith (MiM) obtained by mercury porosimetry.

Table 2
Structure parameters of silica monolith (M) and monolith in cordierite (MiM).

Sample	S_{BET} [m^2/g]	V_{meso} [cm^3/g]	$d_{p(meso)}$ [nm]	$d_{p(macro)}$ [μm]	V_{total} [cm^3/g]
M	330 ± 3.0	1.15	2.5/20	20–50	3.5
MiM	393 ± 1.2	1.30	2.5/19	10–40	3.3

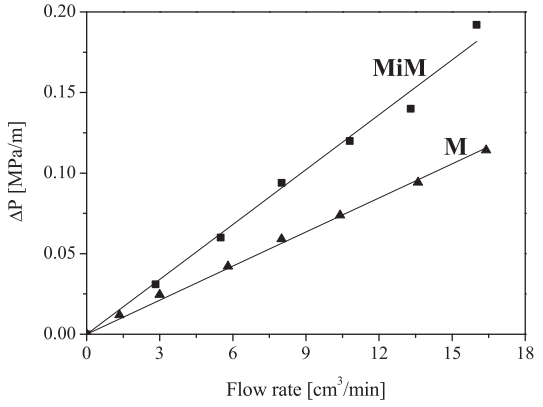

Fig. 6. Pressure loss *vs.* flow rate for silica monolith (M) and monolith-in-monolith (MiM).

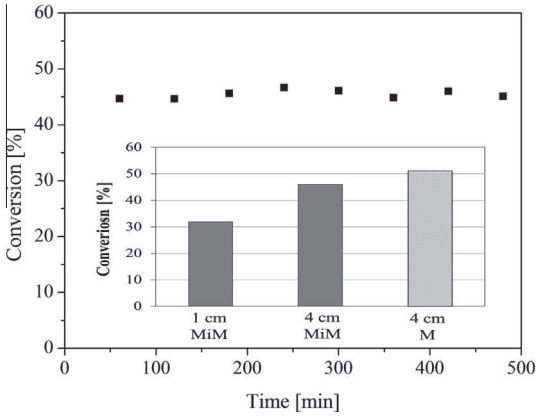

Fig. 7. Conversion of acetic acid *vs.* time obtained in the MiM reactor.

4. Conclusions

The performed studies clearly demonstrate that silica monoliths with a hierarchical pore structure can be build into channels of most typical cordierite honeycomb monoliths to obtain microreactors of the monolith-in-monolith topology which feature vastly enlarged reaction capacities compared to the conventional monolithic devises.

A crucial stage in the fabrication of monolith-in-monolith appeared to be the cordierite surface treatment. The increase in surface area and concentration of silanols, responsible for the formation of strong bonds between cordierite and silica, depended on the applied solution, its concentration and temperature of the treatment.

The operational properties of thus obtained continuous-flow microreactors (MiM) are quite similar to those of the high-performance monolithic silica microreactors (M) with the same pore structure, reported before. Therefore, we believe that the microreactors devised may find an application in the cost-effective production of fine chemicals in small and medium size companies.

Acknowledgment

This work was financed by the National Science Centre – Poland, Project No. DEC-2011/01/B/ST8/03855.

References

[1] X. Chen, M. Arruebo, K.L. Yeung, Flow-synthesis of mesoporous silicas and their use in the preparation of magnetic catalysts for Knoevenagel condensation reactions, Catal. Today 204 (2013) 140–147.
[2] M. Arruebo, W.Y. Ho, K.F. Lam, X. Chen, J. Arbiol, J. Santamaría, K.L. Yeung, Preparation of magnetic nanoparticles encapsulated by an ultrathin silica shell via transformation of magnetic Fe-MCM-41, Chem. Mater. 20 (2008) 486–493.
[3] J. Lee, S.Y. Lee, S.H. Park, H.S. Lee, J.H. Lee, B.-Y. Jeong, S.-E. Park, J.H. Chang, High throughput detection and selective enrichment of histidine-tagged enzymes with Ni-doped magnetic mesoporous silica, J. Mater. Chem. B 1 (2013) 610–616.
[4] A. El Kadib, R. Chimenton, A. Sachse, F. Fajula, A. Galarneau, B. Coq, Functionalized inorganic monolithic microreactors for high productivity in fine chemicals catalytic synthesis, Angew. Chem. Int. Ed. 48 (2009) 4969–4972.
[5] A.-M. Siouffi, Silica gel-based monoliths prepared by the sol–gel method: facts and figures, J. Chromatogr. A 1000 (2003) 801–818.
[6] K. Szymańska, W. Pudło, J. Mrowiec-Białoń, A. Czardybon, J. Kocurek, A. Jarzębski, Immobilization of invertase on silica monoliths with hierarchical pore structure to obtain continuous enzymatic microreactors of high performance, Microporous Mesoporous Mater. 170 (2013) 75–79.
[7] A. Jarzębski, W. Pudło, Polish Patent P.217560 (2011).
[8] J.M. Zamaro, M.A. Ulla, E.E. Miró, Zeolite washcoating onto cordierite honeycomb reactors for environmental applications, Chem. Eng. J. 106 (2005) 25–33.
[9] A. Cybulski, J.A. Moulijn, Monoliths in heterogeneous catalysis, Catal. Rev. Sci. Eng. 36 (1994) 179–270.
[10] A. Cybulski, J.A. Moulijn (Eds.), Structured Catalysts and Reactors, CRC Press Taylor & Francis, 2006.
[11] A.N. Shigapov, G.W. Graham, R.W. McCabe, M.P. Peck, H.K. Plummer Jr., The preparation of high-surface-area cordierite monolith by acid treatment, Appl. Catal. A Gen. 182 (1995) 137–146.
[12] A. Koreniuk, K. Maresz, K. Odrozek, A.B. Jarzębski, J. Mrowiec-Białoń, Highly effective continuous-flow monolithic silica microreactors for acid catalysed processes, Appl. Catal. A Gen. 489 (2015) 203–208.
[13] J. Ma, Z. Liang, X. Qiao, Q. Deng, D. Tao, L. Zhang, Y. Zhang, Organic-inorganic hybrid silica monolith based immobilized trypsin reactor with high enzymatic activity, Anal. Chem. 80 (2008) 2949–2956.

Catalysis Communications 64 (2015) 48–51

Contents lists available at ScienceDirect

Catalysis Communications

journal homepage: www.elsevier.com/locate/catcom

Short communication

Supported zirconium-based continuous-flow microreactor for effective Meerwein–Ponndorf–Verley reduction of cyclohexanone

Agnieszka Koreniuk [a], Katarzyna Maresz [a], Julita Mrowiec-Białoń [a,b,*]

[a] Institute of Chemical Engineering Polish Academy of Sciences, Bałtycka 5, 44-100 Gliwice, Poland
[b] Department of Chemical Engineering and Process Design, Faculty of Chemistry, Silesian University of Technology, Strzody 7, 44-100 Gliwice, Poland

ARTICLE INFO

Article history:
Received 24 November 2014
Received in revised form 21 January 2015
Accepted 22 January 2015
Available online 30 January 2015

Keywords:
Monolithic continuous-flow microreactors
Active zirconium species
Chemoselective MPV reduction
Stability

ABSTRACT

Continuous-flow monolithic silica microreactor activated with anchored isolated zirconium species was shown to be a very convenient and efficient system for chemoselective Meerwein–Ponndorf–Verley reduction. It was shown that isolated Zr^{4+} ions covalently bonded to the silica surface and terminated with isopropoxy/hydroxo ligands can be much more catalytically active than supported zirconia. Conversion of cyclohexanone approached 100% and excellent catalytic selectivity and stability were obtained in 8 cm long microreactor during 8 catalytic cycles. The microreactors also enable better control of undesired hydrolysis of highly reactive metal precursors during functionalisation of the monoliths.

1. Introduction

The Meerwein–Ponndorf–Verley (MPV) reduction of carbonyl compounds to alcohols is a chemoselective reaction which can be performed under mild conditions. Typically, it is activated by metal alkoxides, such as aluminium or zirconium isopropoxide, using secondary alcohols as hydrogen donors. However, to obtain reasonable product yields stoichiometric amounts of this homogeneous catalyst are required [1]. This necessitates its separation downstream and moisture sensitivity limit is another drawback to overcome. A number of heterogeneous catalysts have also been considered for this reaction, to name: Sn-, Ti-, Zr- and Al-beta-zeolites [2,3], magnesium oxide [4,5], Mg/Al hydroxides [6–8], zirconia and metal modified zirconia [9–11]. Zirconium and aluminium propoxide supported on mesostructured silicas were also found to be active in the reduction carbonyl compounds [12–14]. The mechanism of MPV reduction over the heterogeneous catalysts proposed by Creyghton [15] involves a six-membered transition state, with oxidant and reducer coordinating to the same Lewis acid site, and activity of the catalysts is related to their acidic character and ligand exchange ability [13,16]. The presence of the metal alkoxide species resulted in a high conversion of ketones. However, moisture sensitivity appeared to hinder both the preparation and reuse of these catalysts [16].

To the best of our knowledge there is no report on the MPV reaction in conventional flow reactors, and the application of the monolithic type continuous-flow microreactors, which offer exceptional efficiencies of fine chemical synthesis [17,18]. Flow systems offer precise control of process parameters (temperature, contact time, etc.) with positive effects on selectivity and productivity. In microreactors, small dimensions of channels additionally induce large gradients of temperature and concentrations, which promote rapid heat and mass transport. Moreover, owing to facile isolation and continuous removal of deterimental agents, e.g. of water, the microreactors provide better control of the hydrolysis of highly reactive metal precursors during surface modification and continuous operation. Thus not surprisingly perhaps, they also appeared to be an attractive solution for setting suitable operating conditions to enable faster transfer of the lab-scale results to commercial production, especially related to fine chemicals and pharma industry [19].

Herein, we propose a new continuous-flow monolithic microreactor for MPV reduction process.

2. Experimental

2.1. Microreactor preparation

Silica monoliths (M) with hierarchical pore structure were obtained using the procedure described previously in Refs. [20,21]. Active zirconium species were grafted onto silica surface using $Zr(OPr^i)_4$ (Zirconium (IV) propoxide, Aldrich) solution in ethanol. Prior to modification the moisture adsorbed onto monolith surface was removed by passing dry nitrogen through the microreactor, placed in an oven at 200 °C, to avoid uncontrolled hydrolysis of zirconium precursor and ZrO_2 precipitation. Functionalisation was carried out at 70 °C for 24 h. The solvent was removed also by passing dry nitrogen through the microreactor

* Corresponding author at: Institute of Chemical Engineering Polish Academy of Sciences, Bałtycka 5, 44-100 Gliwice, Poland.
E-mail address: jmrowiec@polsl.pl (J. Mrowiec-Białoń).

http://dx.doi.org/10.1016/j.catcom.2015.01.021
1566-7367/

(Zr–M). Microreactors modified with ZrO_2 (Zr–M–C) and Zr–OH species (Zr–M–H) were fabricated to obtain some insight into the role of zirconium species to the catalyst performance. The first one was obtained by calcination of the modified monolith at 500 °C in air and the second one by passing an aqueous solution of ethanol through the monolith grafted with $Zr(OPr^i)_4$.

2.2. Characterisation methods

The textural characteristics of the monoliths were determined from low temperature nitrogen adsorption isotherms (Micromeritics ASAP 2020). Total pore volume and flow-through macropore diameters were evaluated from mercury porosimetry. The structure of the monoliths in micrometric size scale was also verified using scanning electron microscopy (Hitachi HD-2300A).

Spectroscopic methods: FT-IR (Nicolet 6700) and UV–Vis (Varian), thermogravimetry (STAR 851, Metler Toledo) and ICP–MS technique provided information about physicochemical properties of metal species-doped catalyst. Pressure drop was measured using pressure controller (UNIK 5000, Ex-Calibra).

2.3. Catalytic experiments

Catalytic performance of the microreactors was investigated in the reduction of cyclohexanone with 2-butanol. Microreactors with diameter of 4.5 mm and 4 or 8 cm long were tested at 95 °C using ketone:alcohol molar ratio of 1:52. The flow rate was fixed to achieve contact times of 17.5 and 35 min, in 4 and 8 cm long microreactors, respectively. Substrates and products were analysed by GC (Agilent 7890 A, HP-5 column, FID detector). After each reaction cycle the microreactor was washed with dry ethanol to remove all the residues. The substrates were dried using molecular sieves and one experiment was made without drying.

3. Results and discussion

3.1. Structure parameters

The textural properties of the monoliths are displayed in Table 1. Mesopores with bimodal pore distribution (pore diameters of about 3 nm and 20 nm) provided high specific surface area (320 m^2/g). Smaller pores arose from the presence of cationic surfactant, used as a pore template, whereas the larger ones were formed during ammonia treatment. The contribution of small pores to the total mesopore volume appeared to be low (3.5%). However, their presence significantly increased the surface area, and thereby the amount of hydroxyls per gramme of the silica host, which controls surface concentration of the attached zirconium species. In consequence, these species were uniformly distributed over the whole silica surface, as could be inferred from the mesopore size distribution before and after modification. This uniformity was well preserved after catalytic experiments (Table 1, Fig. 1). The continuous structure of large macropores (flow-through channels) with diameters in the range of 20–50 μm (Fig. 2A) obtained by PEG-induced phase separation and isolated spherical voids of ca. 1 μm could be observed in the silica skeleton (Fig. 2B).

Low pressure drop was recorded in the reactor made of silica rod with dimensions 4.5 × 40 mm (18 Pa/cm for 0.03 cm^3/min flow rate)

Table 1
Properties of materials.

Monolith	S_{BET} [m^2/g]	Mesopore volume [cm^3/g]	Mesopore mean diameter [nm]	Zr [wt.%]
M	320	1.2	2.5/20	–
Zr–M	288	1.0	2.5/20	6.1
Zr–M–R	291	1.0	2.5/20	6.1

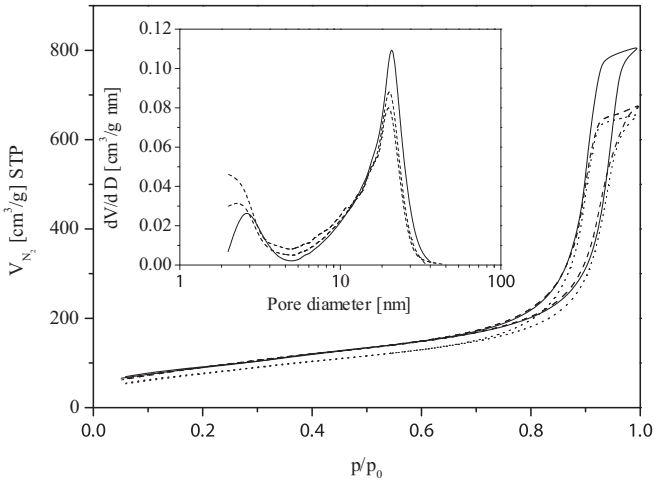

Fig. 1. Nitrogen adsorption isotherms and BJH pore size distribution (B) in pristine silica monolith (solid line), functionalised Zr–M (dots) and after reaction Zr–M–R (dashed line).

due to abundant presence of large flow-through macropores of total volume ca. 2.3 cm^3/g.

3.2. Catalyst characterisation

The amount of isopropoxy groups in the Zr–M microreactor was ca. 0.7 per zirconium molecule and determined by means of

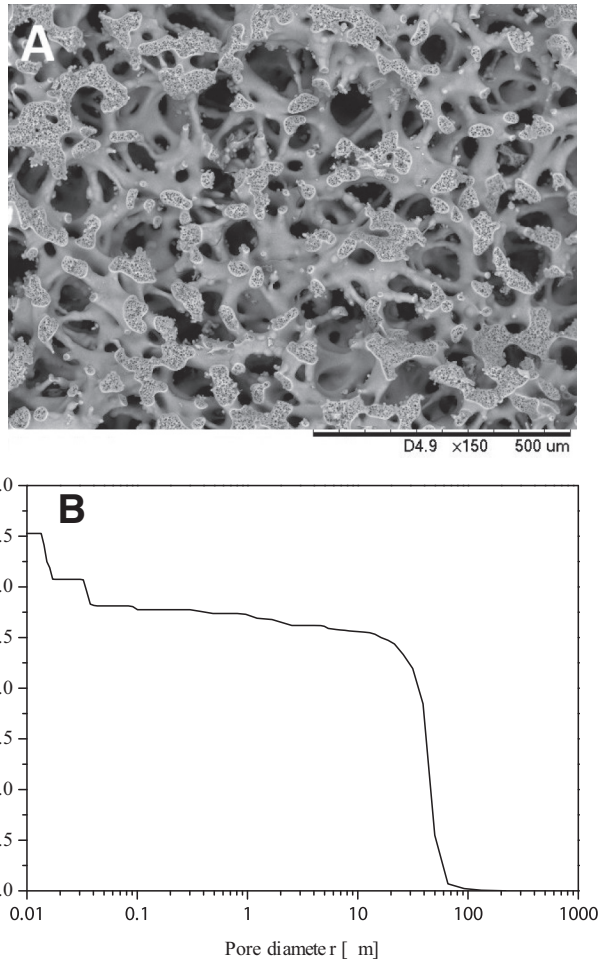

Fig. 2. SEM image of monolith (A) and cumulative pore size distribution in a pristine monolith obtained by mercury porosimetry (B).

thermogravimetry. Zirconium precursor with four isopropoxy groups can be attached to silica surface by one to three Si – O – Zr bonds, depending on the concentration and proximity of the surface silanols. However, a part of them hydrolysed, despite strict precautions to avoid the traces of water during functionalisation, or formed Zr – O – Zr bond, hardly detected by UV–Vis (Fig. 3B, curve b). Therefore, the zirconium atoms deposited onto the silica surface were terminated with both hydroxyls and isopropoxy entities. The latter presence was confirmed by FT-IR spectroscopy (Fig. 3A), wherein absorption at 2963 cm^{-1} and 2905 cm^{-1} is attributed to C – H stretching bands in the propyl chain. The decrease in intensity of hydroxyl vibrations in the range of 3000–3700 cm^{-1} signifies formation of Zr – O – Si bonds and hence the attachment of zirconium species to silica matrix.

The metal loading before and after reaction remained unchanged and it was 6.1 wt.%, which corresponds to surface coverage of 1.3 Zr/nm^2. UV–Vis spectroscopy was used to examine the nature of Zr species incorporated into silica matrix and ZrO_2 spectrum was recorded as reference (Fig. 3B). Absorption at ~200 nm (Fig. 3B, line b and c), attributed to ligand-to-metal charge transfer from O^{2-} to an isolated Zr^{4+} ion in a tetrahedral coordination, confirms that the grafted monoliths (Zr–M and Zr–M–H) contain only Lewis acidic atoms capable to activate carbonyl group of the reactants [3]. In Zr–M–C maximum absorption is shifted to 209 nm (line d), implying a possible formation of small ZrO_2 oligomers during calcination. In pure ZrO_2, i.e. the case of full connectivity of Zr–O–Zr linkages this charge transfer occurs at 230 nm (line a). Moreover, the values of absorption edge energy E_g, determined from the spectra, were equal to 5.40 eV for Zr–M and Zr–M–H and 5.33 eV for Zr–M–C and higher than the value recorded for pure zirconia (5.1 eV). This is an additional clear evidence of very good dispersion of Zr species over silica surface [22,23].

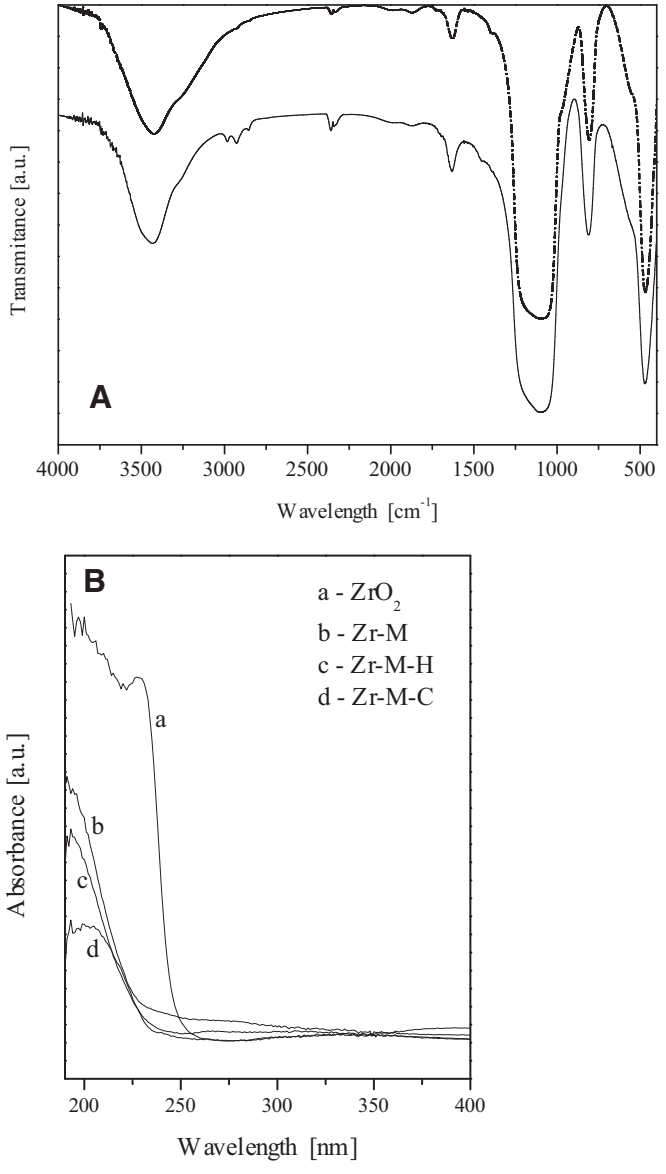

Fig. 3. FT-IR spectra of silica (dots) and Zr–M (solid line) monoliths (A) and UV–Vis spectra of ZrO_2 (a), Zr–M (b), Zr–M–H (c) and Zr–M–C (d) (B).

3.3. Catalytic experiments

Fig. 4 shows the results of catalytic experiments. The data clearly indicate that catalytic activity of the zirconium-modified silica monoliths depends on the type of ligands coordinating zirconium. The highest conversion, of ca. 90%, was obtained with those functionalised with uncalcined zirconium species; it was ~30% higher than that obtained in the microreactor subjected to calcination (Zr–M–C). This follows directly from the smaller content of isolated Zr^{4+} ions in the silica framework caused by: i. formation of oligomeric species during calcination, and ii. a smaller exchange rate of O^{2-} ligands in Zr–M–C. The performance of microreactors with partially (Zr–M) and fully hydrolysed (Zr–M–H) zirconium alkoxides was quite similar. Slightly larger conversion seen in Zr–M microreactor in the first cycle was probably due to the higher exchange rate of the isoporopoxy ligands with n-butanol in comparison to hydroxo ligands [16]. The isopropyl alcohol formed at the beginning of the continuous flow process, was later washed away from the microreactor together with the products. In effect, the isopropoxy ligands could impact the process only in the initial stage.

Productivities achieved in 4 cm reactors (contact time — 17.5 min) are shown in Table 2, and their changes correlate with the values of conversions obtained in these reactors. The largest productivity, ca. 3.5 mmol/h mmol Zr, was recorded for Zr–M and Zr–M–H for conversion ~90%. In 8 cm reactor, with contact time of 35 min, the productivity was ca. 1.9 mmol/h mmol Zr, and both the value of ketone conversion and selectivity of the product were ~100%. The observed decline in productivity with the increase in conversion is in good accord with earlier reports [21,24].

We also observed strong impact of the water traces present in the substrates on the reaction course (microreactor Zr–M*). Lower activity

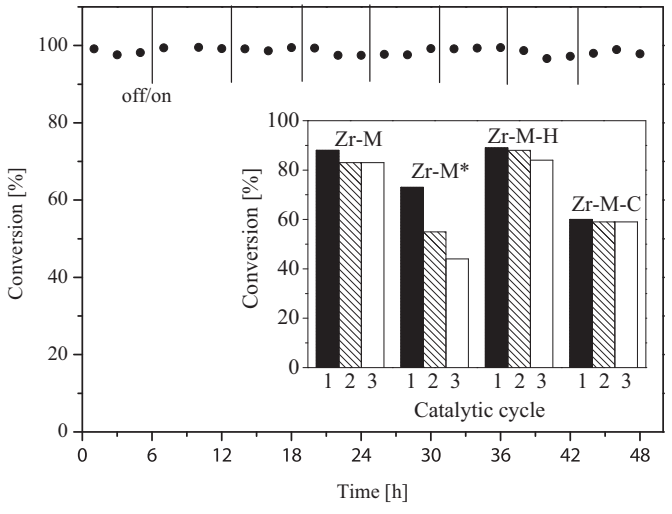

Fig. 4. Conversion of cyclohexanone in long term test in Zr–M microreactor (8 cm length) and conversion obtained in 4 cm microreactor (inset) with different Zr species on the silica surface in three catalytic cycles. (* — indicates that reaction was carried out without drying of substrates).

Table 2
Productivity of the microreactors in three runs.

Run	Productivity [mmol/mmol Zr h][a]			
	Zr–M	Zr–M–H	Zr–M–C	Zr–M*
1	3.48 (88)	3.51 (89)	2.32 (60)	2.65 (73)
2	3.30 (83)	3.48 (88)	2.27 (59)	2.00 (55)
3	3.30 (83)	3.32 (84)	2.27 (59)	1.65 (34)

[a] Conversion is shown in parenthesis; reactor length 4 cm, contact time 17.5 min.
* Indicates that reaction was carried out without drying of substrates.

was recorded in the first catalytic cycle and its decline was still seen in the second and third runs. This can be explained by a detrimental effect of adsorption of water molecules onto the zirconium centres and hindered access of substrates.

A longer stability test during 8 reaction cycles (6 h/day — discontinued for night) showed very good performance of the microreactor (Fig. 4).

Preliminary studies of the monoliths after eight catalytic cycles (data not shown here) tend to indicate that no agglomeration of zirconium species occurred during 48 h of the catalytic process. Further, more detailed studies are under way to confirm that.

4. Conclusions

Our studies demonstrate that the hydrogen-transfer reduction of carbonyl compounds to their corresponding alcohols can be efficiently carried out in the continuous-flow silica microreactors activated with zirconium hydroxide/isopropoxide species. The isoporopoxy ligands affect reaction rate only at the beginning of the continuous-flow process, because they are more easily exchanged with 2-butanol than hydroxo ligands and subsequently washed away together with products. Zirconia modified reactor features smaller amount of active surface zirconium species, which results in its lower activity and productivity. The developed microreactors exhibit stable structural and catalytic properties. They can be easily and reproducibly fabricated, stored and reused when needed.

Acknowledgments

This work was financed by the National Science Centre project No DEC-2011/01/B/ST8/03855.

References

[1] R.A.W. Johnstone, A.H. Wilby, I.D. Entwistle, Chem. Rev. 85 (1985) 129–170.
[2] A. Corma, M.E. Domine, S. Valencia, J. Catal. 215 (2003) 294–304.
[3] M. Boronat, A. Corma, M. Renz, J. Phys. Chem. B 110 (2006) 21168–21174.
[4] M.A. Aramendía, V. Borau, C. Jiménez, J.M. Marinas, J.R. Ruiz, F.J. Urbano, J. Colloid Interface Sci. 238 (2001) 385–389.
[5] M.A. Aramendía, V. Borau, C. Jiménez, J.M. Marinas, J.R. Ruiz, F.J. Urbano, Appl. Catal. A Gen. 244 (2003) 207–215.
[6] C. Jiménez-Sanchidrián, J.M. Hidalgo, J.R. Ruiz, Appl. Catal. A Gen. 303 (2006) 23–28.
[7] J.R. Ruiz, C. Jiménez-Sanchidrián, J.M. Hidalgo, Catal. Commun. 8 (2007) 1036–1040.
[8] J.M. Hidalgo, C. Jiménez-Sanchidrian, J.R. Ruiz, Appl. Catal. A Gen. 470 (2014) 311–317.
[9] G. Peng, X. Wang, X. Chen, Y. Jiang, Z. Mu, J. Ind. Eng. Chem. 20 (2014) 2641–2645.
[10] Y. Zhu, S. Jaenicke, G.K. Chuah, Catal. Today 97 (2004) 249–255.
[11] J.F. Miñambres, M. Aramendía, A. Marinas, J.M. Marinas, F.J. Urbano, J. Mol. Catal. A 338 (2011) 121–129.
[12] R. Anwander, C. Palm, G. Gerstberger, O. Groeger, G. Engelhardt, Chem. Commun. (1998) 1811–1812.
[13] M. De Bruyn, M. Lombourg, J. Denayer, G.V. Baron, V. Parvulescu, P.J. Grobet, D.E. De Vos, P.A. Jacobs, Appl. Catal. A Gen. 254 (2003) 189–201.
[14] Y. Zhu, S. Jaenicke, G.K. Chuah, J. Catal. 218 (2003) 396–404.
[15] E.J. Creyghton, S.D. Ganeshie, R.S. Downing, H. van Bekkum, J. Mol. Catal. A Chem. 115 (1997) 457–472.
[16] F. Quignard, O. Graciani, A. Choplin, Appl. Catal. A Gen. 182 (1999) 29–40.
[17] K. Szymańska, W. Pudło, J. Mrowiec-Białoń, A. Czardybon, J. Kocurek, A.B. Jarzębski, Microporous Mesoporous Mater. 170 (2013) 75–82.
[18] A.E. Kadib, R. Chimenton, A. Sachse, F. Fajula, A. Galarneau, B. Coq, Angew. Chem. 48 (2009) 1–5.
[19] A. Stankiewicz, Chem. Eng. Sci. 56 (2001) 359–364.
[20] A. Sachse, A. Galarneau, F. Fajula, F. Di Renzo, P. Creux, B. Coq, Microporous Mesoporous Mater. 140 (2011) 58–68.
[21] A. Koreniuk, K. Maresz, K. Odrozek, A.B. Jarzębski, J. Mrowiec-Białoń, Appl. Catal. A Gen. 489 (2015) 203–208.
[22] M.S. Morey, G.D. Stucky, S. Schwarz, M. Fröba, J. Phys. Chem. B 103 (1999) 2037–2041.
[23] T. Klimova, O. Gutiérrez, L. Lizama, J. Amezcua, Microporous Mesoporous Mater. 133 (2010) 91–99.
[24] A. Sachse, V. Hulea, A. Finiels, B. Coq, F. Fajula, A. Galarneau, J. Catal. 287 (2012) 62–67.

Microporous and Mesoporous Materials 229 (2016) 98–105

Contents lists available at ScienceDirect

Microporous and Mesoporous Materials

journal homepage: www.elsevier.com/locate/micromeso

Titania-silica monolithic multichannel microreactors. Proof of concept and fabrication/structure/catalytic properties in the oxidation of 2,3,6-trimethylphenol

Agnieszka Koreniuk [a], Katarzyna Maresz [a], Klaudia Odrozek [b], Julita Mrowiec-Białoń [a, b, *]

[a] Institute of Chemical Engineering Polish Academy of Sciences, Bałtycka 5, 44-100, Gliwice, Poland
[b] Department of Chemical Engineering and Process Design, Faculty of Chemistry, Silesian University of Technology, 44-100, Gliwice, ks. M. Strzody 7, Poland

ARTICLE INFO

Article history:
Received 17 December 2015
Received in revised form
12 April 2016
Accepted 14 April 2016
Available online 20 April 2016

Keywords:
Titania-silica monolithic microreactors
Fabrication method
Titanium dispersion
TMP oxidation

ABSTRACT

Titania-silica monoliths with 3D hierarchical porosity in μm and nm scales were fabricated using either direct or post-synthesis method, to find that they enable very fast continuous-flow oxidation of 2,3,6-trimethylphenol to 2,3,5-trimethyl-1,4-benzoquinone with hydrogen peroxide as the oxidant. Extensive characterization of the monoliths using N_2 adsorption, mercury porosimetry, SEM, energy dispersive X-ray mapping, FT-IR and UV–Vis spectroscopy showed a strong impact of the fabrication method on the structural properties and also coordination/dispersion of the titanium ions incorporated into the silica. Systematic study of the monolithic microreactors and corresponding powders in the continuous-flow and batch systems, revealed a large complexity of performance/structure/catalytic properties relationships. A direct method resulted in titanium active centres highly dispersed in microporous skeleton, and therefore larger TOF, compared to the surface titanium entities in monoliths obtained from the post-synthesis approach. However, owing to the lower porosity and much smaller flow-through (macro) pores the pressure drops were almost two orders of magnitude larger. The highly porous monolithic microreactors fabricated by the post-synthesis incorporation of titanium appeared to be superior; the substrate conversions of 85% were obtained in about 12 min compared to those of ca. 75% obtained in batch systems after 1 h. This could be explained by very intensive mass transport in macro- and mesopore size scales.

1. Introduction

Titania-silica oxides are known as active and selective catalysts in oxidation of organic compounds using molecular oxygen and aqueous solutions of hydrogen peroxide under mild conditions [1]. The catalytic systems are based on zeolite or amorphous mesoporous materials. Titanium silicalite (TS-1), discovered in 1983, was the first Ti-substituted zeolite, which exhibited unique activity and high selectivity in several oxidation reactions, and its high catalytic activity was attributed to isolated, tetrahedrally coordinated Ti(IV) sites associated to the hydrophobic silicalite structure [2–6]. Other Ti-substituted zeolites (i.e. TS-2, Ti-beta) were also reported to be efficient catalysts for selective oxidation of organic compounds [7,8]. However, applications of these microporous materials are limited to reactions with small molecules. Moreover, a slow diffusion of reactants and blocking of active sites by large molecules are additional drawbacks. In the past decades various titanium-containing mesoporous materials were obtained, i.e. mesoporous molecular sieves of different type [9–12] and titanium-silicate mixed oxides with xerogel and aerogel structure [13–17]. Catalytic properties of Ti-species dispersed in amorphous skeleton of mesoporous materials were found to be strongly dependant on their local structure. In these materials oligomeric domains are usually found along with the isolated, tetrahedrally coordinated Ti(IV) sites. The relative contribution of the isolated and oligomeric species depends, in particular, on the preparation procedure and amount of incorporated titanium [18]. The sol-gel method is usually used for synthesis of mesoporous materials, providing a good control over structural properties, especially in case of mesostructured materials synthesized with the use of soft templates [11]. However, significant differences between reactivity of

* Corresponding author. Institute of Chemical Engineering Polish Academy of Sciences, Bałtycka 5, 44-100, Gliwice, Poland.
E-mail address: jmrowiec@polsl.pl (J. Mrowiec-Białoń).

http://dx.doi.org/10.1016/j.micromeso.2016.04.020
1387-1811/

alkoxysilanes and titanium alkoxides are a major problem in the synthesis of materials with titanium ions highly dispersed in silica skeleton. Successfully, effective methods for the fabrication of well dispersed titania-silica materials were proposed, either with the use of chelated Ti alkoxides or prehydrolised silanes [15,19]. Of importance is also an appropriate choice of reaction conditions (pH, temperature, Ti concentration) and drying procedure. The post-synthesis incorporation of titanium to silica materials was also elaborated [20]. In Ref. [21] it was reported that Ti ions can be well dispersed onto the surface of MCF-type silica and high selectivity of α-pinene oxidation was reached.

More recently, silica monoliths with bi-modal pore structure of transport (flow-through) macropores and diffusional mesopores [22–26] were applied as flow microreactors. So far, these reactors have been prepared by activating monoliths with alumina [27], zirconia [28], organic groups [29,30], zeolites [31] and enzymes [32,33]. The microreactor-based technologies are an environmentally friendly solution, offering reduced reagents' consumption and thus, generating lower waste streams. Compared to the conventional reactors, the microreactors proposed have a surface-to-volume ratio more than two orders of magnitude larger, which directly translates into enhanced heat and mass transfer, and hence the reaction kinetics and overall performance.

In this paper we analyse the fabrication and properties of Ti-modified silica monoliths, converted into flow multichannel microreactors, in the selective oxidation of 2,4,6- trimethylphenol (TMP) to 2,3,5-trimethyl-1,4-benzoquinone (TMBQ) using hydrogen peroxide as the oxidant. TMBQ is a key intermediate in the synthesis of Vitamin E [34]. Titanium of different concentration was incorporated to the monoliths by a direct (co-condensation) and post-synthesis method. The monoliths were characterized by instrumental techniques to find structure/properties relationships, and to explain their catalytic performance. To the best of our knowledge it is the first report on the application of siliceous monolithic microreactors to oxidation of organics using hydrogen peroxide.

2. Experimental

2.1. Materials

Synthesis of materials: tetraethoxysilane (TEOS, 99 wt%, ABCR) polyethylene glycol (PEG 35000, Fluka) nitric acid (65 wt% Avantor) cetyltrimethylammonium bromide (CTAB, Aldrich) ammonia aqueous solution (25 wt% Avantor), isopropanol (Avantor), titanium diisopropoxide bis(acetylacetonate) (75 wt% in isopropanol, Sigma-Aldrich).

Catalytic experiments: 2,3,6-trimethylphenol (TMP, 95 wt%, Alfa Aesar), hydrogen peroxide (30 wt %, Avantor), acetonitrile (99.5 wt %, Chempur).

2.2. Synthesis of catalysts

2.2.1. Post synthesis method (I)

The silica monoliths (P0) were synthesized as described previously in much detail [29]. Shortly: TEOS, PEG, HNO_3, H_2O, and CTAB in molar ratio 1:0.53:0.26:14:0.0275 were homogenized, transferred into heat-shrinkable PTFE tubes (DSG-Canusa) and aged at 40 °C. Wet monolithic rods were immersed in 1 M ammonia aqueous solution and kept at room temperature for 9 h. After drying, the material was calcined at 550 °C. The pristine silica rods were soaked with a solution composed of titanium precursor dissolved in isopropanol and stored at 40 °C overnight. Then the solvent was allowed to evaporate, and the monoliths were calcined in air for 2 h at 500 °C. The nominal content of Ti in samples was 1, 2 and 5 wt%, and they were designated I1, I2 and I5.

2.2.2. Direct method (D)

In the direct method titanium precursor was added during monoliths' synthesis. First, PEG was dissolved in 1 M HNO_3 and stirred vigorously in ice bath, followed by TEOS addition. Next, a suitable amount of titanium diisopropoxide bis(acetylacetonate) was added to the mixture to obtain the samples with 1, 2 and 5 wt% Ti nominal content, designated D1, D2 and D5. The stirring was continued until homogeneous solution was obtained, and then the cetyltrimethylammonium bromide was added and the mixture was stirred for 1 h at room temperature. The clear sol was transferred into polypropylene tubes and aged at 40 °C for 8 days. The monolithic rods thus obtained were washed with an excess of distilled water, air-dried and calcined at 550 °C for 5 h.

2.3. Characterization methods

Low-temperature nitrogen adsorption measurements were carried out in an ASAP 2010 analyser (Micromeritics). The samples were previously outgassed for 24 h at 200 °C under vacuum. Specific surface area was determined using BET and Dubinin-Astakhov methods, depending on the size of pores present in the monoliths. The mesopore size distributions were obtained from desorption

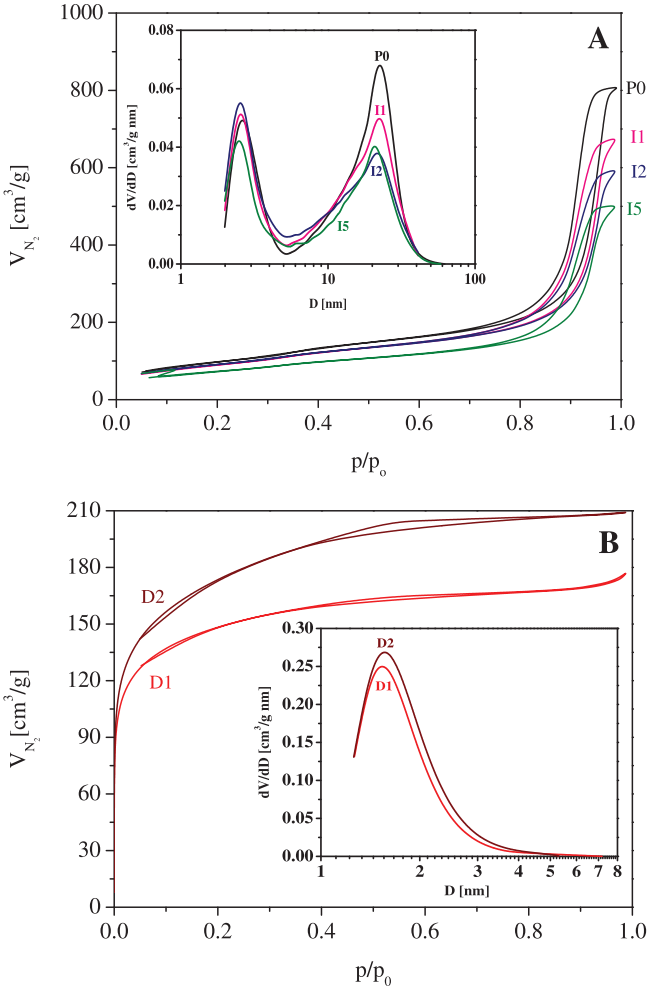

Fig. 1. Nitrogen adsorption/desorption isotherms of I (A) and D (B) series of the titania-silica monoliths and the pristine silica sample P0 (A).

isotherms using BJH method, and the Dubinin-Astakhov method was applied in case of microporous materials. Scanning Electron Microscopy (SEM, Hitachi HD-2300A) and mercury porosimetry (Quantachrome, PoreMaster 60) were employed to determine the sizes of flow-through channels created by macropores. The skeletal density was measured by a helium pycnometer (AccuPyc 1330, Micromeritics). Titanium analyses were carried out by inductively-coupled plasma mass spectrometry (ICP-MS). The state of titanium was evaluated from UV–Vis diffuse reflectance spectra measured on Varian Carry 100 spectrometer equipped with Labsphere DRA-CA-3300. The materials were calcined at 400 °C for 1 h prior to the measurement. The FT-IR spectra were recorded in a Nicolet 6700 spectrometer using KBr technique, and later used to estimate semi-quantitatively the Si–O–Ti connectivity, defined as [18].

$$D_{(Si-O-Ti)} = \frac{S_{(Si-O-Ti)}}{S_{(Si-O-Si)}} \cdot \frac{x_{Si}}{x_{Ti}} \quad (1)$$

where: $S_{(Si-O-Ti)}$ and $S_{(Si-O-Si)}$ 7 areas of the ν(Si–O–Ti) band at ca. 940 cm^{-1} and ν(Si–O–Si) band at ca. 1210 cm^{-1}, x_{Si} and x_{Ti} designate molar portions of Si and Ti, respectively.

The energy dispersive X-ray mapping (Phenom ProX of Phenom-World B.V.) was used to study the dispersion and surface concentration of titanium species in the samples.

2.4. Catalytic studies

The monolithic rods (3.5 × 40 mm) equipped with connectors and embedded into heat-shrinkable tubes constituted the reactive cores of continuous-flow microreactors. The catalytic oxidation of TMP was performed at 80 °C. In a typical reaction 0.1 M solution of TMP in acetonitrile was prepared. Hydrogen peroxide, used as the oxidizing agent, was added to the mixture stored in ice bath prior to experiments (molar ratio H_2O_2/TMP was 3.5). The solution was passed through the microreactor with the flow rate of 0.03 ml/min. The substrate conversion and product yield were quantified by GC-MS. The process was carried out in a laboratory set described in detail in Ref. [29].

The flow resistance was measured during catalytic experiments using a differential pressure controller (UNIK 5000, Ex-Calibra).

The batch experiments were carried out at 80 °C using 3 mmol of TMP dissolved in 30 ml of MeCN and 0.37 g of catalyst, and the molar ratio of H_2O_2:TMP was 3.5.

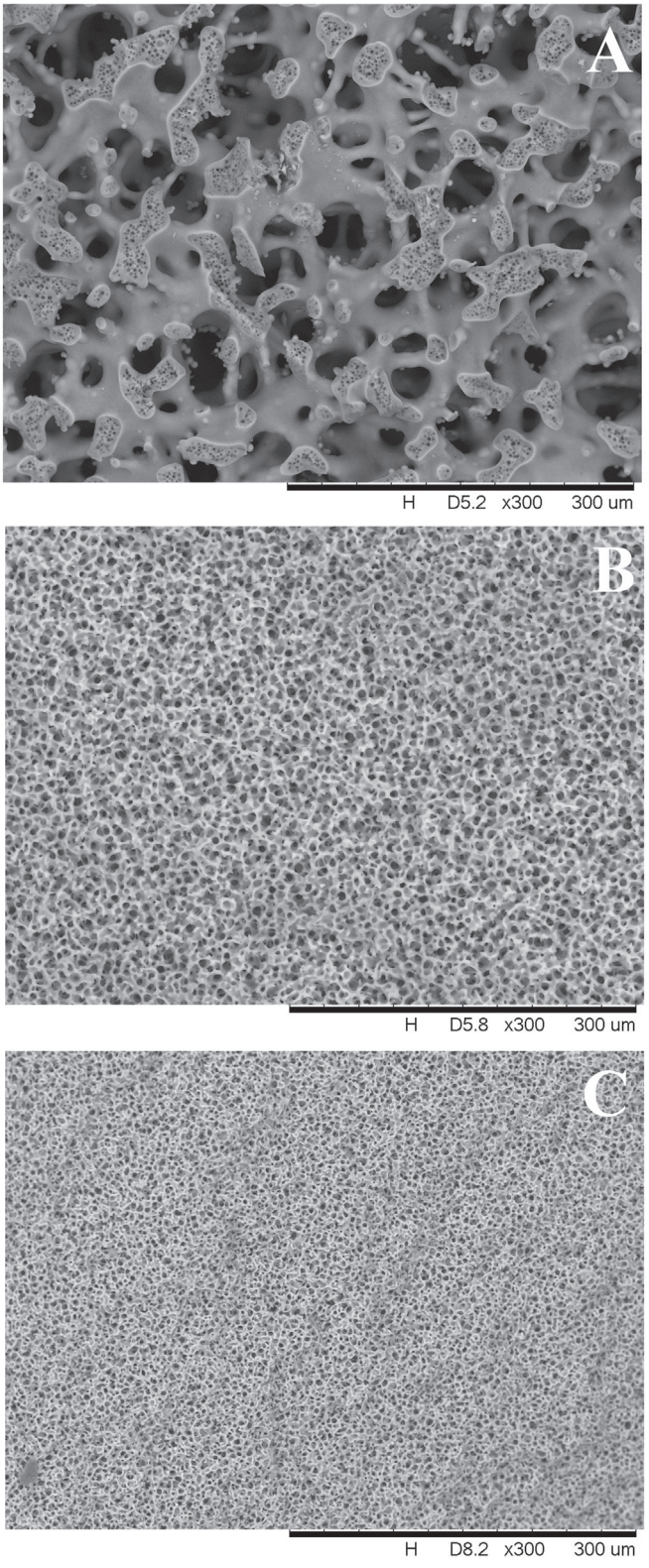

Fig. 2. SEM images of I1 (A), D1 (B) and D2 (C) monoliths.

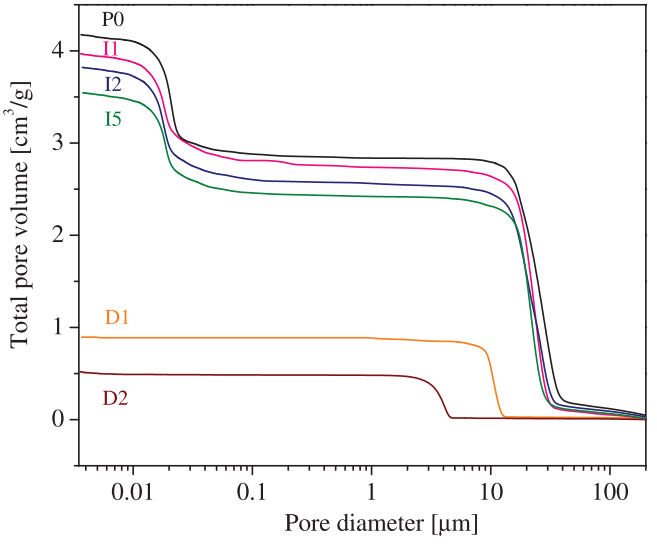

Fig. 3. Pore volume vs. pore diameter for the silica and titania-silica monoliths obtained by mercury porosimetry.

Table 1
Properties of monoliths.

Monolith	S_{BET} [cm^2/g]	$D_{micro/meso}$[a] [nm]	$V_{meso/micro}$ [cm^3/g]	D_{macro}[b] [μm]	V_{Hg}[c] [cm^3/g]	Ti[d] [%]
P0	344	2.53/24.0	1.25	10–30(28)	4.2	0
I1	319	2.54/23.4	1.03	10–30(28)	4.0	0.95(1.7)
I2	323	2.54/23.0	0.89	10–30(24)	3.8	1.66(2.6)
I5	261	2.52/20.7	0.77	10–30(21)	3.5	4.21(4.8)
D1	489/(538)[e]	1.56	0.24[f]	8–10.3	0.9	0.57(0.5)
D2	586/(611)[e]	1.54	0.28[f]	2–4	0.5	1.23(1.1)

[a] Maximum value on the pore size distribution.
[b] In parentheses maximum value on the macropore size distribution.
[c] Pore volume determined by mercury porosimetry.
[d] Ti concentration by ICP-MS and EDS (in parentheses).
[e] In parentheses micropore surface area calculated using Dubinin-Astakhov method.
[f] Micropore volume.

3. Results and discussion

3.1. Characterization of materials

The titanium atoms were incorporated into the silica skeleton using either a direct or grafting method to obtain monoliths with a nominal titanium content of 1, 2 and 5 wt%. In the direct approach the titanium precursor (titanium diisopropoxide bis(acetylacetonate)) was added to the reaction mixture prior to the monoliths' formation, whereas in the grafting method it was expected to react with the surface silanols of dry silica monoliths. Moreover, the samples of the D-series were not treated with ammonia solution, because it had been found to induce cracking of the titania-silica skeleton, perhaps owing to the facilitated hydrolysis of Si–O–Ti bonds. These two fundamental differences in the monoliths' synthesis produced two distinct pore structures; the micro/macropore structure appeared to prevail in the D-samples, and the original meso/macropore structure of the pristine monolith was perfectly preserved in the I-samples. The pore structure parameters could be estimated from the nitrogen isotherms displayed in Fig. 1, SEM images (Fig. 2) and also mercury intrusion measurements (Fig. 3).

The nitrogen adsorption/desorption isotherms for the P0 and I-samples belong to the IUPAC IV class, with capillary condensation steps occurring at a relative pressure above 0.8. The pristine silica monolith exhibited the mesopore morphology with a bi-modal pore size distribution of small mesopores, of ca. 2.5 nm, and large ones of about 23 nm in size, tailored by the cationic surfactants and ammonia treatment. The H1-type of hysteresis loop indicated a narrow pore size distribution of cylindrical pores. The incorporation of titania by grafting decreased both the specific surface area and the mesopore volume, more significantly for the larger Ti load (Table 1). This is portrayed by a slight shift in maximums of the pore size distributions towards lower diameters shown in Fig. 1A. All the materials possessed interconnected macropores, displayed in SEM image of I2 sample (Fig. 2A). The isolated spherical voids of ca. 1 μm clearly observed in the SEM images of the struts, were not detected by mercury porosimetry because of their inaccessibility (cf. Fig. 3). Probably, they are footprints of the polymer droplets entrapped in the silica skeleton during the spinodal decomposition process [29]. As expected, the grafting appeared not to affect the monoliths macropore structure, and hence macropores sizes (10–30 μm) remained much the same in all I-monoliths as in the parent sample (P0, Fig. 3).

In contrast, the direct incorporation of titania precursor during the monoliths' synthesis appeared to have a significant effect on their structure (Table 1). The bi-modal pore structure with an open and continuous network of flow-through channels was still retained (Fig. 2B, 2C), but both the size and the volume of macropores dramatically decreased. The pore volumes in D1 and D2, determined by mercury porosimetry, were respectively, 4 and 7 times lower than in the parent monolith (P0) and the isotherms of IUPAC type I provided a clear proof of the micropore presence. They were 1.5–1.6 nm in size and 0.24–0.28 cm^3/g of total volume, and possessed the specific surface area of ca. 600 m^2/g (Table 1). The size of macropores (flow-through channels) also appeared to depend strongly on the titania content; they were about 8–10 μm in the sample with 1 wt% of Ti and 2–4 μm in that with 2 wt%. The proposed synthesis afforded flawless monoliths only for 1 and 2 wt % of Ti but failed in the case of 5 wt%. Such dramatic difference in the macropore structure can be explained by the strong effect of titanium isopropoxide presence on the rate of the spinodal decomposition [35].

Apparently, the drastic differences in pore structure observed in D- and I-samples can be linked with the discrepancies in their

Table 2
Structural parameters of monoliths.

Sample	Skeletal density [g/cm^3]	Bulk density [g/cm^3]	Porosity [%]
P0	2.26	0.24	89
I1	2.39	0.23	90
I2	2.31	0.24	90
I5	2.49	0.24	90
D1	2.29	0.56	76
D2	2.23	0.65	71

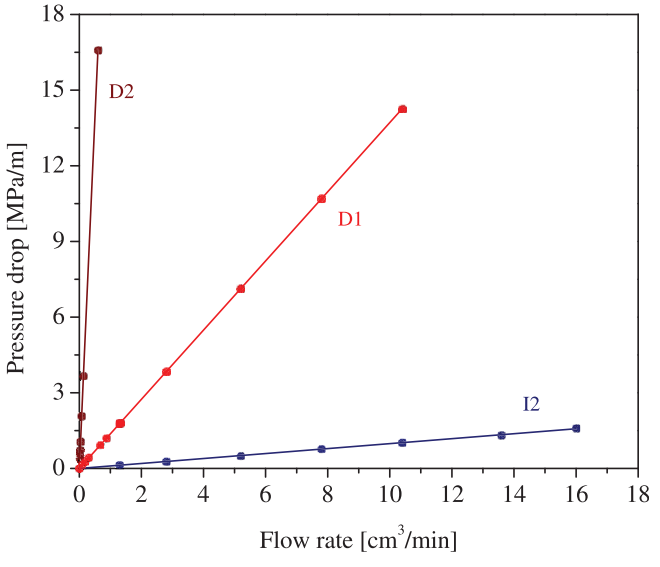

Fig. 4. Pressure loss. vs. flow rate for I2, D1 and D2 monoliths.

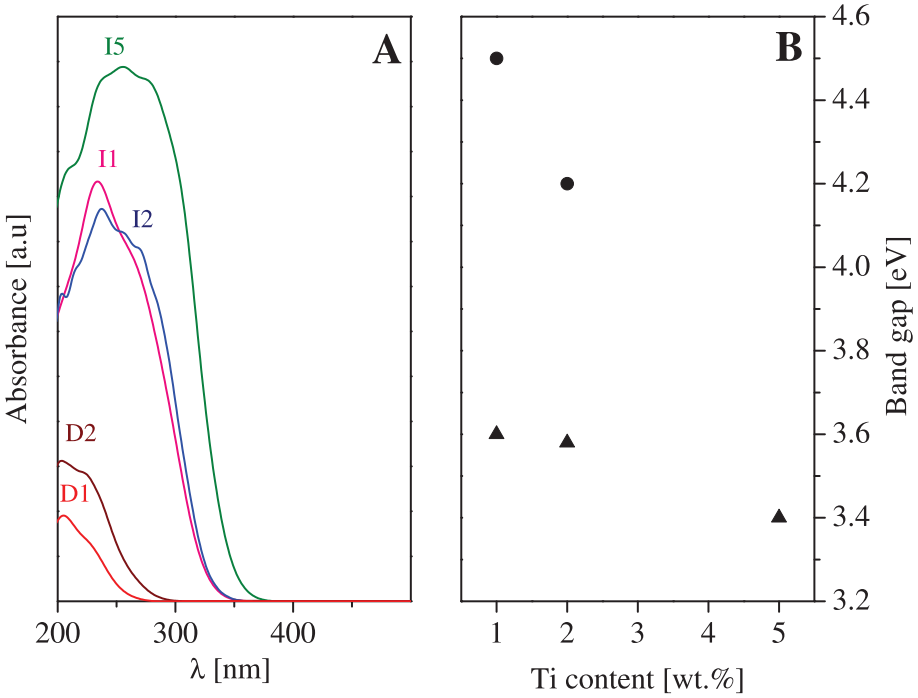

Fig. 5. UV–Vis spectra (A) and band gap of the titania-silica monoliths (B) of I- and D-series.

skeletal densities, directly affecting mechanical strength and hence also the shrinkage of the wet samples (Table 2).

All of the functionalized monoliths possessed structural features, indispensable for application as reactive cores of the continuous flow microreactors. However, appreciable differences in the size of flow-through channels significantly affected the flow rate-pressure drop relationship (Fig. 4). The pressure drop per unit length dramatically increased with the decrease in macropore size; it was about an order of magnitude higher for D1 and even two orders for D2, compared with the reference monolith (P0).

The titanium content in the monoliths determined by ICP-MS and EDS methods showed that the total concentration of titanium was slightly smaller than the nominal values for I-series, and even ca. 40% less in D-samples (Table 1). Moreover, both the total and the surface concentration of Ti was much the same in D-monoliths, and EDS multi point measurements (at least 10 points) confirmed its

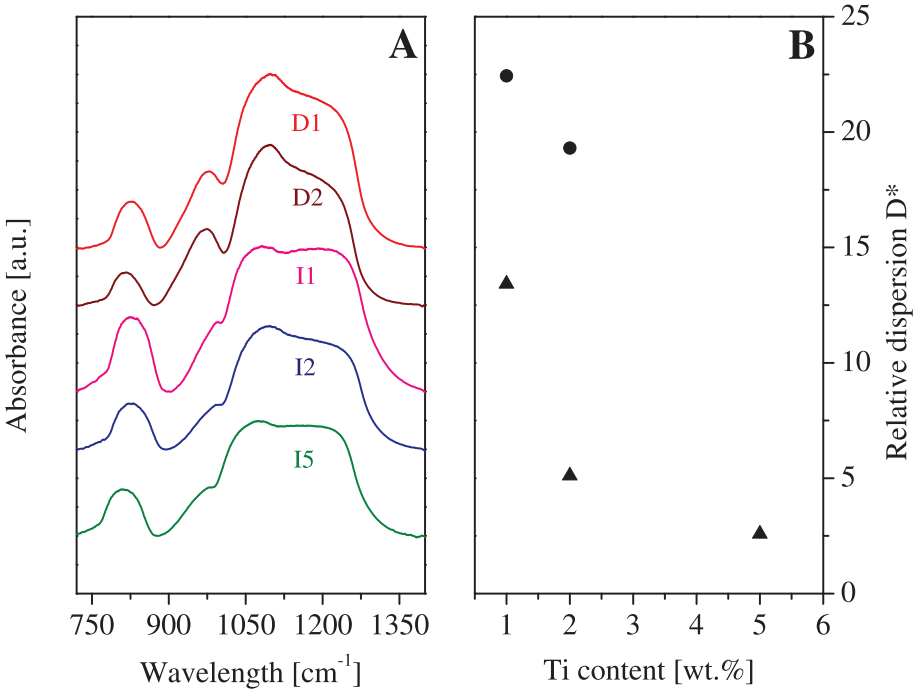

Fig. 6. FT-IR spectra of the titania-silica monoliths (A) and relative dispersion of titanium as a function of Ti content in monoliths of I- and D-series (B).

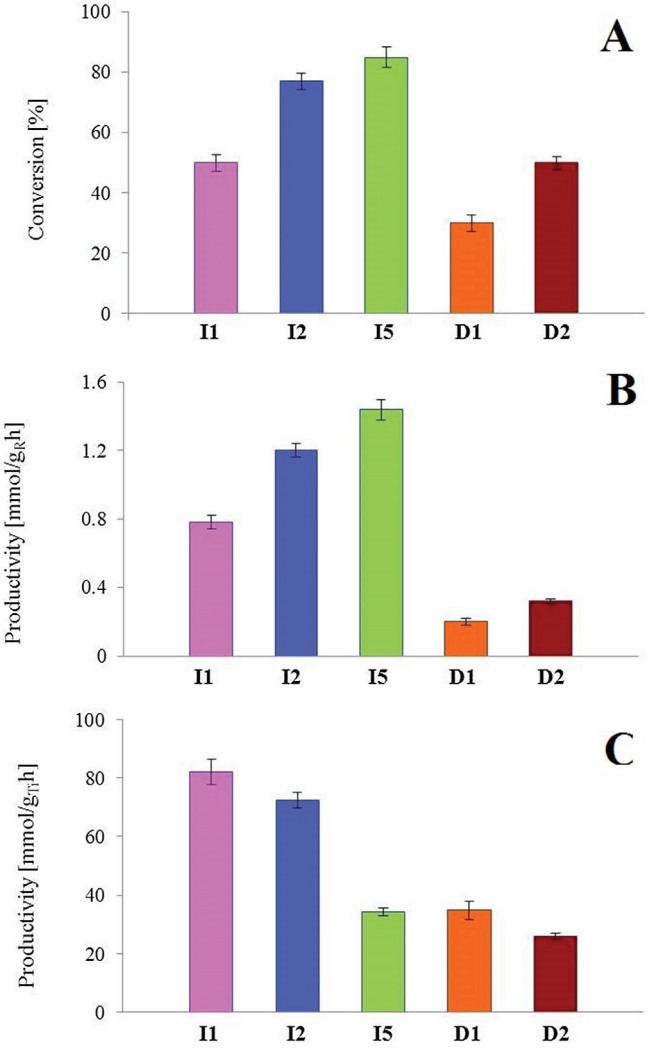

Fig. 7. TMP oxidation in the titania-silica microreactors. Conversion (A), productivity related to mass of reactors (B) and productivity related to Ti content (C) in I- and D-series.

uniform distribution all over the surface. As expected, the monoliths of I-series featured higher titanium surface concentration than the total value detected by ICP-MS method (Table 1), and the multi point measurements showed a broad distribution of titanium built-into the silica surface; for I1 the values ranged from 1.0 to 3.5 wt%. Similarly, large dispersions of Ti surface concentration were observed in I2 and I5. These differences are well seen in the images given in Supporting data (Figs. A1 and A2). Although EDS is not quite a quantitative technique, particularly on curved surfaces, the results obtained shed light on the distribution of Ti in the skeleton.

The UV–Vis spectra were recorded to investigate the titanium dispersion in the silica skeleton and its coordination. To preclude an artefact of the water presence, the monoliths were heat treated at 400 °C prior to analysis. The absorption maximum in the UV–Vis spectra of D1 and D2 at ca. 210 nm is characteristic for materials with isolated, tetrahedrally coordinated Ti species [36,37], whereas a significant shift to longer wavelengths was observed for materials obtained by the post synthesis method (I-series) (Fig. 5A). The UV absorption bands are broad between 200 and 350 nm, and shifted to higher values with increasing titanium content. It corroborates the presence of oligomerized titanium-oxygen species in these materials [20]. The diffuse reflectance spectra were transformed to function $[F(R) \times h\nu]^2$ vs. $h\nu$ (Supplementary data, Fig. A3), to obtain absorption edge energy E_g Ref. [36] (Fig. 5B). The location of absorption edge appeared to be shifted to lower values of photon energy with the increase in Ti content. A significant difference was observed between I- and D-series. For the I-monoliths the absorption edge is located closer to that characteristic for bulk anatase [19,38], whereas for the D1 and D2 the respective values of 4.5 eV and 4.17 eV approach the one found in TS-1 zeolite characterized by atomically dispersed titanium ions in silica skeleton [36].

The UV–Vis results are in a good agreement with the data obtained by FT-IR spectroscopy. A characteristic peak around 960 cm^{-1}, assigned to the bending vibration of Si–O–Ti bonds [20,39] is present in all of FT-IR spectra. However, its intensity is much greater for the monoliths obtained by the direct method (Fig. 6A). The FT-IR spectra deconvolution (see example in Supplementary data, Fig. A4) enabled to evaluate semi quantitatively the Ti dispersion, $D_{(Si-O-Ti)}$ using Eq. (1) [18]. Fig. 6B clearly demonstrates a strong impact of both the modification method and the titanium content on its dispersion in silica. The contribution of Si–O–Ti species decreased with the increase in Ti content, and this trend was more apparent in the monoliths of the I-series. The dispersion in I2 was ca. 60% smaller than in I1, whereas in the D-samples this decline was only 15%. It may be ascribed to the much higher concentration of titanium ions on the impregnated monoliths' surface, in contrast to those obtained from the direct synthesis in which Ti was uniformly distributed all over the silica skeleton (Table 1).

3.2. Catalytic properties in TMP oxidation

The oxidation of 2,3,6-trimethyl-phenol (TMP) to 2,3,5-trimethylbenzoquinone (TMBQ) using H_2O_2 as oxidant confirmed catalytic potentials of all the reactors. For the same flow rate (0.03 ml/min), thus different mean residence/reaction times determined by the pore volumes, the conversion of TMP strongly depended on both the type of material and the titanium content (Fig. 7A). A rapid increase in the conversion from 50% to 85% was observed for the I-series monoliths with the increase in the nominal titanium content from 1 wt% to 5 wt 2%, in spite of decreasing reaction time (14.3, 12.7 and 11.8 min, for I1, I2 and I5, respectively). This directly influenced the productivity seen as the amount of TMP converted during 1 h related to the mass of the monolith (Fig. 7B). The reverse trend was observed when the productivity was referred to the titanium content (Fig. 7C). Similar tendencies were also observed in two D-series reactors, but the corresponding values were lower owing to much shorter residence time (7.7 min for D1 and 4.5 min for D2). Table 3 compares the catalytic performance of D2 and I2 for residence time of 4.5 min. The conversion coefficient obtained for

Table 3
Catalytic properties of microreactors for the same contact time equal to 4.5 min.

Reactor	m_R [g]	Flow rate [cm^3/min]	Conv. [%]	Productivity			
				[mmol/cm^3 h]	[mmol/g_R h]	[mmol/g_{Ti} h]	[mmol/g_{Tisurf} h]
D2	0.2707	0.03	50	0.41	0.32	26	29
I2	0.1006	0.078	35	0.22	1.56	94	60

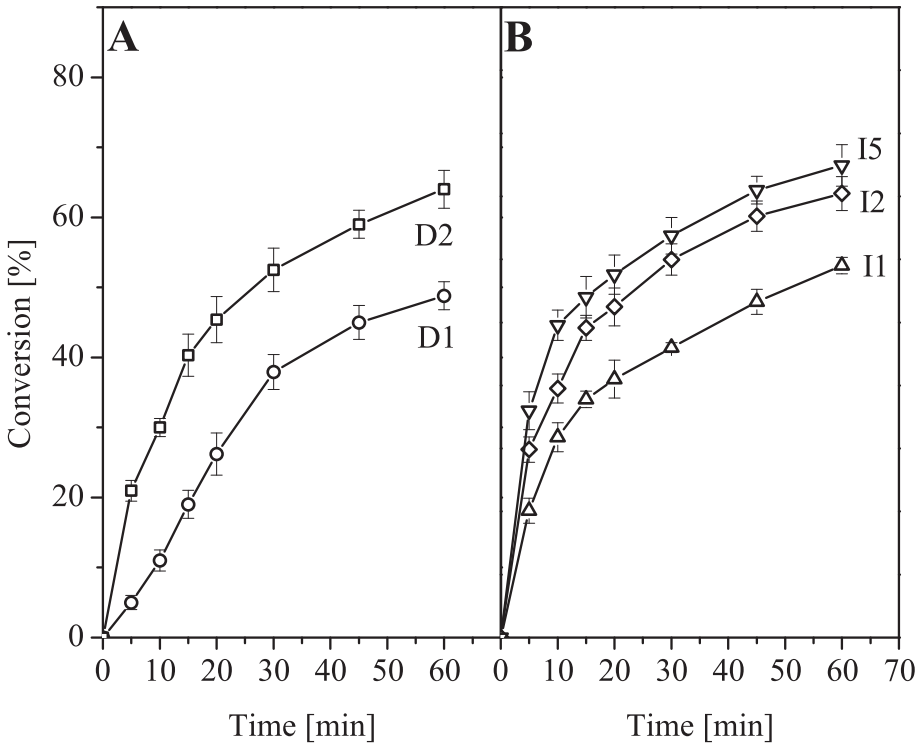

Fig. 8. Conversion vs. time in the batch process with powdered catalysts: D1 and D2 (A), and I1, I2, I3 (B).

Table 4
Catalytic properties of powdered monoliths in the batch process.

Catalyst	TOF [mol/mol$_{Ti}$ h]	TOF [mol/mol$_{(Tisurf)}$ h]	Ti surface concentration [Ti/nm^2]
I1	75	43	0.67
I2	54	34	1.0
I5	10	28	2.1
D1	50	57	0.13
D2	49	54	0.24

Reaction conditions: temperature 80 °C; 3 mmol of TMP in 30 ml of MeCN, catalyst 0.37 g, H_2O_2/TMP molar ratio 3.5.

the D2 appeared to be over 30% higher than for the I2, however, the mass of reactor- and titanium content-related productivities were much larger for the I2 owing to the application of much higher flow rate. This behaviour can be directly associated with bigger porosity of the I2 sample in all pore size scales. Not only it enabled larger flow rates of the substrates, but also their unhindered transport to the catalytic sites located in very large mesopores, and not micropores as in the D-monolith. But, the lower surface concentration of Ti centres in the D2 also contributed to this behaviour (cf. Table 1).

To obtain a deeper understanding of the effect of Ti concentration and dispersion on the catalytic properties of monoliths more systematic studies were performed in a batch reactor with the powdered monoliths used as the corresponding (slurry) catalysts. The conditions, including the catalysts loading, were the same in all experiments. It can be seen from Fig. 8 that the reaction took even an hour in the slurry system to approach the values of conversions obtained in the monolithic flow reactors in about 10 min. As expected, the increase in the titanium loading from 1 wt% to 2 wt% had a strong positive effect (see Fig. 8) on the reaction rate, regardless of the monolith synthesis, but further increase to 5 wt% (I5) had much smaller effect. Table 4 gives the estimated (initial) rates of TMP oxidation quantified as TOF numbers, related to either the total titanium content or its surface concentration. For the I-series the values decreased with the increase in Ti content, and thus the catalysts' specific activity appeared to be well correlated with the titanium dispersion (Fig. 6B). This is in a perfect agreement with the previous observations, in which a good Ti dispersion in the form of dimeric species, was found to be indispensable to ensure good catalytic properties [14–16]. Remarkably, the calculated values of surface concentration of Ti in the I1 and I2 (cf. Table 4) fall in the range of 0.7–1.0 Ti/nm^2, considered as optimal for this type of catalytic materials [16]. In the D-monoliths the TOF values related to total Ti were smaller than in the corresponding I-samples, but when related to the surface concentration they appeared to be larger, again in a very good agreement with the results of Ti dispersion analyses (Fig. 6). However, the positive effect of high titanium dispersion on the catalytic properties of the D-samples was diminished by a strong diffusion limitation of mass transport, caused by their micropore structure. This negative effect of the micropore structure, and of hindered accessibility of titanium sites was observed also before [14,15]. A more profound comparison of the corresponding samples of the I- and D-series is, however, obscured by different contents of both the total and the surface titanium caused by differences in their preparation and pore structure, despite the efforts to obtain the same Ti load. Finally, while different reaction conditions hinder a direct comparison of the TOF values for the monoliths with those determined for other titanium silicates in the same reaction, a closer inspection of

literature indicates that for the I1 and I2 they appear to be similar to those of mesoporous Ti-MMM-2, i.e. some of the most active catalysts reported so far [16].

4. Conclusions

It has been shown that monolithic titania-silica microreactors with a hierarchical pore structure can be very effective in the oxidation of TMP to TMBQ using H_2O_2 and enable high conversion of substrates in about 10 min and not an hour, as in the corresponding batch slurry systems. The catalytic activity of the reactors appeared to depend strongly on their structural properties, Ti content and its dispersion, and hence on the adopted preparation method. The post synthesis incorporation of titanium into the silica skeleton preserved the pristine meso/macroporous structure of the silica monoliths, whereas the incorporation of titanium during the monolith's synthesis resulted in much smaller flow-through macropores, which dramatically changed the flow properties of the microreactor and produced a drastic increase in the pressure drop. Additionally, the direct method gave materials with a micropore structure which hindered mass diffusion. The preparation method also strongly affected the titanium state in the silica skeleton. The spectroscopic investigations clearly evidenced a fine dispersion of tetrahedrally coordinated titanium atoms across the silica monoliths obtained by the direct method and showed a presence of small oligomeric titania species on the surface of silica monoliths functionalized by impregnation.

The catalytic studies of the monoliths performed in continuous-flow and of their powdered counterparts in the batch (slurry) process revealed a considerable complexity of the performance/properties relationships. The monoliths synthesized directly featured a higher activity of titanium centres, quantified by larger values of initial TOF_{Tisurf} (moles of substrates/moles of $Ti_{surf} \times h$) in the batch process, than their counterparts synthesized by the two-step method. This was mainly due to the positive impact of high titanium dispersion in these monoliths. In the flow synthesis, carried out in reactors of the same volume and contact time, both the conversion and the productivity related to the reactor volume were larger in the direct-type reactors, but when related to the mass of reactor and titanium content they were much smaller than in the highly porous reactors fabricated in the two-step process. Under the same flow conditions, better performance, i.e. significantly higher conversion and productivity related to the reactor mass, were achieved for the reactors fabricated in the two-step process. Moreover, a further progress of these two values was observed with the increase in titanium concentration. The presence of larger flow-through channels enabled the use of much lower overpressure and that affects process safety, as well as energy and capital inputs.

Acknowledgements

This work was financed by the National Science Centre – Poland, Project No. DEC-2011/01/B/03855. The authors wishes to thank Prof. A. Jarzębski for helpful discussion and G. Miodońska for technical assistance.

Appendix A. Supplementary data

Supplementary data related to this article can be found at http://dx.doi.org/10.1016/j.micromeso.2016.04.020.

References

[1] Handbook of Advanced Methods and Processes in Oxidation Catalysis, Imperial College Press, London, 2014.
[2] M. Taramasso, G. Perego, B. Notari, U. S. Pat. 4 410 501 (1983).
[3] B. Notari, Adv. Catal. 41 (1996) 253–334.
[4] G. Bellussi, A. Carati, M.G. Clerici, G. Maddinelli, R. Millini, J. Catal. 133 (1992) 220–230.
[5] R. Millini, E.P. Massara, G. Perego, G. Bellussi, J. Catal. 137 (1992) 497–503.
[6] C. Perego, A. Carati, P. Ingallina, M.A. Mantegazza, G. Bellussi, Appl. Catal. A Gen. 221 (2001) 63–72.
[7] A. Corma, M.A. Camblor, P. Esteve, A. Martinez, J. Perezpariente, J. Catal. 145 (1994) 151–158.
[8] A. Carati, C. Flego, E.P. Massara, R. Millini, L. Carluccio, W.O. Parker, G. Bellussi, Micropor. Mesopor. Mater. 30 (1999) 137–144.
[9] A. Corma, Chem. Rev. 97 (1997) 2373–2419.
[10] D.M. Antonelli, J.Y. Ying, Curr. Opin. Colloid. In. 1 (1996) 523–529.
[11] W.Z. Zhang, T.J. Pinnavaia, Catal. Lett. 38 (1996) 261–265.
[12] N. Lang, P. Delichere, A. Tuel, Micropor. Mesopor. Mater. 56 (2002) 203–217.
[13] O.A. Kholdeeva, M.S. Mel'gunov, A.N. Shmakov, N.N. Trukhan, V.V. Kriventsov, V.I. Zaikovskii, M.E. Malyshev, V.N. Romannikov, Catal. Today 91–2 (2004) 205–209.
[14] J. Mrowiec-Białoń, A.B. Jarzębski, O.A. Kholdeeva, N.N. Trukhan, V.I. Zaikovski, V.V. Kriventsov, Z. Olejniczak, Appl. Catal. A Gen. 273 (2004) 47–53.
[15] O.A. Kholdeeva, N.N. Trukhan, M.P. Vanina, V.N. Romannikov, V.N. Parmon, J. Mrowiec-Białoń, A.B. Jarzębski, Catal. Today 75 (2002) 203–209.
[16] O.A. Kholdeeva, I.D. Ivanchikova, M. Guidotti, N. Ravasio, M. Sgobba, M.V. Barmatova, Catal. Today 141 (2009) 330–336.
[17] X.T. Gao, I.E. Wachs, Catal. Today 51 (1999) 233–254.
[18] D.C.M. Dutoit, M. Schneider, A. Baiker, J. Catal. 153 (1995) 165–176.
[19] K.M. Choi, R. Wakabayashi, T. Tatsumi, T. Yokoi, K. Kuroda, J. Colloid. Interf. Sci. 359 (2011) 240–247.
[20] X.T. Gao, S.R. Bare, J.L.G. Fierro, M.A. Banares, I.E. Wachs, J. Phys. Chem. B 102 (1998) 5653–5666.
[21] N.V. Maksimchuk, M.S. Melgunov, J. Mrowiec-Białoń, A.B. Jarzębski, O.A. Kholdeeva, J. Catal. 235 (2005) 175–183.
[22] K. Nakanishi, J. Porous Mater. 4 (1997) 67–112.
[23] K. Nakanishi, H. Minakuchi, N. Soga, N. Tanaka, J. Sol-Gel Sci. Technol. 13 (1998) 163–169.
[24] K. Nakanishi, Y. Kobayashi, T. Amatani, K. Hirao, T. Kodaira, Chem. Mater. 16 (2004) 3652–3658.
[25] N. Tanaka, H. Kobayashi, K. Nakanishi, H. Minakuchi, N. Ishizuka, Anal. Chem. 73 (2001) 420A–429A.
[26] J.H. Smått, S. Schunk, M. Linden, Chem. Mater. 16 (2003) 2354–2361.
[27] A. Sachse, V. Hulea, A. Finiels, B. Coq, F. Fajula, A. Galarneau, J. Catal. 287 (2012) 62–67.
[28] A. Koreniuk, K. Maresz, J. Mrowiec-Białoń, Catal. Commun. 64 (2015) 48–51.
[29] A. Koreniuk, K. Maresz, K. Odrozek, A.B. Jarzębski, J. Mrowiec-Białoń, Appl. Catal. A Gen. 489 (2015) 203–208.
[30] A. Sachse, A. Galarneau, F. Fajula, F. Di Renzo, P. Creux, B. Coq, Micropor. Mesopor. Mater. 140 (2011) 58–68.
[31] A. Sachse, A. Galarneau, F.D.R.F. Fajula, B. Coq, Chem. Mater. 22 (2010) 4123–4125.
[32] K. Szymańska, M. Pietrowska, J. Kocurek, K. Maresz, A. Koreniuk, J. Mrowiec-Białoń, P. Widłak, E. Magner, A. Jarzębski, Chem. Eng. J. 287 (2016) 148–154.
[33] K. Szymańska, W. Pudlo, J. Mrowiec-Białoń, A. Czardybon, J. Kocurek, A.B. Jarzębski, Micropor. Mesopor. Mater. 170 (2013) 75–82.
[34] P. Schudel, H. Mayer, O. Isler, I.S. W.H, R.S. Harris, The Vitamines Vol. 5, Academic Press, New York, 1972.
[35] K. Nakanishi, S. Motowaki, N. Soga, Bull. Inst. Chem. Res. Kyoto Univ. 70 (1992) 144–151.
[36] C. Beck, T. Mallat, T. Burgi, A. Baiker, J. Catal. 204 (2001) 428–439.
[37] E. Escobedo Morales, E. Sanchez Mora, U. Pa, Rev. Mex. De. Fis. S 53 (2007) 18–22.
[38] J.L. Lu, K.M. Kosuda, R.P. Van Duyne, P.C. Stair, J. Phys. Chem. C 113 (2009) 12412–12418.
[39] J.M. Fraile, J.I. Garcia, J.A. Mayoral, E. Vispe, J. Catal. 189 (2000) 40–51.

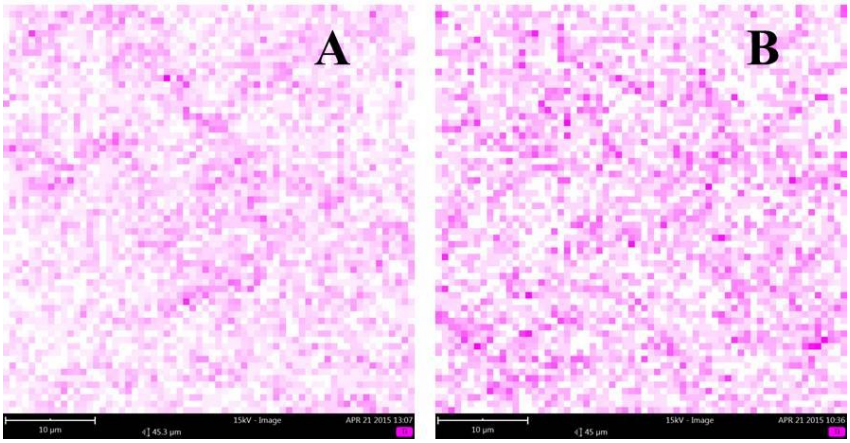

Fig. A1. SEM-EDS titanium mapping images of D1 (A) and D2 (B) monoliths.

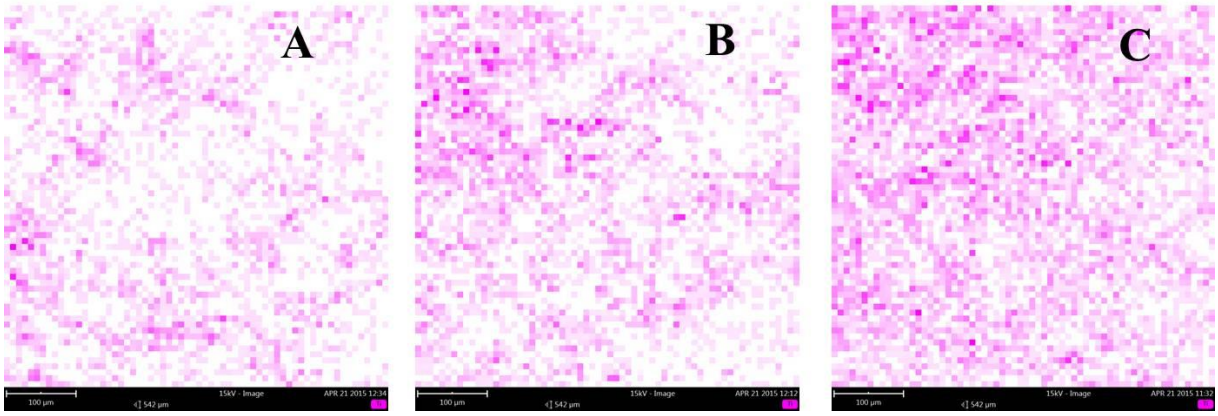

Fig. A1. SEM-EDS titanium mapping images of I1(A), I2 (B) and I3 (C) monoliths.

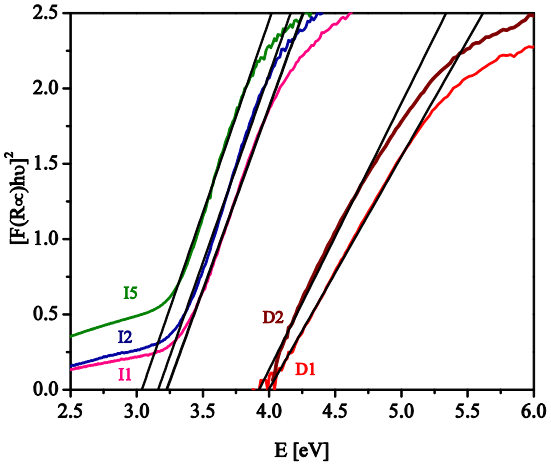

Fig. A2. Kubelka-Munk transformed reflectance spectra of titania silica monoliths of I- and D-series.

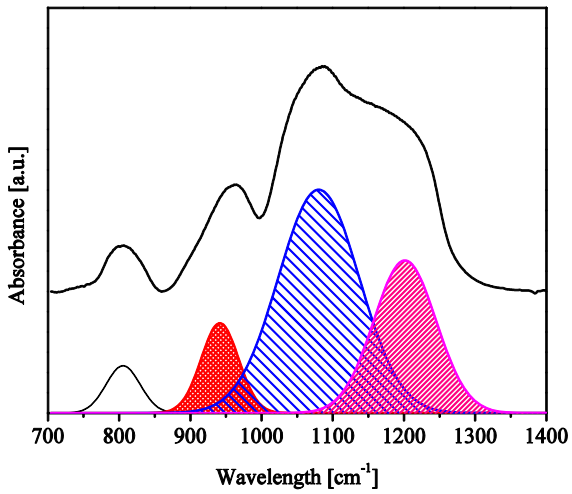

Fig. A4. Deconvolution of the FT-IR spectrum of D2 monolith.

Microporous and Mesoporous Materials 252 (2017) 140–145

Contents lists available at ScienceDirect

Microporous and Mesoporous Materials

journal homepage: www.elsevier.com/locate/micromeso

Continuous-flow chemoselective reduction of cyclohexanone in a monolithic silica-supported $Zr(OPr^i)_4$ multichannel microreactor

Agnieszka Ciemięga [a], Katarzyna Maresz [a], Julita Mrowiec-Białoń [a, b, *]

[a] Institute of Chemical Engineering Polish Academy of Sciences, Bałtycka 5, 44-100 Gliwice, Poland
[b] Department of Chemical Engineering and Process Design, Faculty of Chemistry, Silesian University of Technology, Strzody 7, 44-100 Gliwice, Poland

ARTICLE INFO

Article history:
Received 8 December 2016
Received in revised form
12 June 2017
Accepted 13 June 2017
Available online 13 June 2017

Keywords:
3D hierarchical monoliths
Lewis acid sites
Chemoselective reduction
Continuous-flow microreactor

ABSTRACT

Meerwein-Ponndorf-Vereley reduction of cyclohexanone using 2-butanol as hydrogen donor was studied in the multichannel monolithic silica microreactors modified with zirconium species to demonstrate their higher efficacy than of conventional batch systems with powdered catalysts. $Zr(OPr^i)_4$ species were attached onto the monoliths siliceous surface to obtain a nominal Zr/Si mass ratio in the range of 0.01–0.28. The value of 0.14 gave the largest concentration of Lewis acid sites and hence also the highest conversion (88%) after 20 min reaction/residence time and productivity of 2.22 mmol/g h. The monoliths prepared by the sol-gel process combined with phase separation were characterized using nitrogen adsorption, mercury porosimetry, thermogravimetry, SEM, FTIR and UV–Vis spectroscopy, pyridine adsorption and XRD. They featured very open 3D co-continuous structure of 20 nm textural meso- and flow-through macropores 30–60 μm in diameter (4 cm^3/g total pore volume) which was not appreciably changed after their modification with zirconium species. Diffraction peaks characteristic for crystalline zirconia were not detected even in materials with the highest Zr content.

1. Introduction

Structural microreactors are used in the pharmaceutical industry and the fine chemicals production [1]. They are cost-effective and eco-friendly, since they enable a reduction in energy and reagent consumption and also improve process safety. The microreactors are usually fabricated by casting, tape-casting, and most recently also by more advanced 2D and 3D techniques such as screen printing or stereolithography [2,3] to obtain plates with capillary channels 50–500 μm in diameter which can be assembled into stacks. They feature the surface-to-volume ratio of up to $2 \cdot 10^4$ m^2/m^3, whereas in conventional reactors it does not exceed 10^3 m^2/m^3. Monolithic silica microreactors with multitude of micrometric channels are relatively novel solution in process engineering [4]. But more importantly, in these reactors the value of surface-to-volume ratio can even be ca. 10^5 m^2/m^3, i.e. 5–10 fold higher than in the capillary-based devices, and it translates into more rapid reaction kinetics. In this light the need for further studies of application potentials of these reactors in the continuous-flow reaction systems is quite obvious. Up to now these microreactors were prepared by a modification of the siliceous monolith with organic groups [5], zeolites [6], enzymes [7–9] and transition metals [10].

Most recently we have shown that the monolithic silica microreactors activated with isolated zirconium species are a robust system for the continuous-flow Meerwein-Ponndorf-Verley reduction (MPV) [11]. The reduction of unsaturated carbonyl compounds to their alcohols is of great importance in the pharmaceutical, cosmetic and food industry [12]. The reaction, conventionally carried out with hydrogen, has significant limitations like process safety and low selectivity of the reaction. An alternative pathway for the synthesis of some compounds makes use of hydrogen transfer mechanism. It eliminates the work under pressure and significantly reduces the use of expensive catalysts. Furthermore, the selection of an appropriate active centre capable to polarize the carbonyl group during alcohol and ketone coordination and application of accurate process conditions can provide a high selectivity. The MPV reduction of α,β-carbonyl compounds (aldehydes or ketones), utilizes secondary alcohols as the hydrogen

* Corresponding author. Institute of Chemical Engineering Polish Academy of Sciences, Bałtycka 5, 44-100 Gliwice, Poland.
E-mail address: jmrowiec@polsl.pl (J. Mrowiec-Białoń).

http://dx.doi.org/10.1016/j.micromeso.2017.06.023
1387-1811/

source. Initially, the reaction was carried out in the presence of homogeneous catalysts - metal alkoxides. They appeared to be highly selective but have serious limitations, the major one being the need for the use in stoichiometric amounts to the substrate and difficulty in separation from the reaction mixture [13]. The applications of Zr [14], Al [15], Mg [16], Sn [17] and other metals immobilized onto mesoporous supports or incorporated into the crystal lattice of the zeolite [18] were also studied. The papers on the MPV reduction in continuous-flow systems are scarce, and report on selective reduction of unsaturated aldehydes in a mixture of supercritical isopropanol/CO_2 in the presence of alumina [19] or application of steel coil reactor with LiOtBu as catalyst [20]. A mild and efficient flow procedure was also proposed using hydrous zirconia in a packed-bed reactor and it allowed a clean and fast production of the alcohol within a few minutes [21].

A replacement of homogeneous catalysts with heterogeneous ones enabled to eliminate some of the drawbacks, but sensitivity of the catalysts (immobilized metal alkoxides) to moisture, which directly hampers their activity, still remains a major unresolved issue [22]. The use of the proposed microreactor enables to isolate the catalytic centres from a direct contact with the adverse external factors. Moreover, its construction significantly facilitates the introduction of active centres on to the surface, process operation, its regeneration and storage, which is much more difficult to achieve in the case of powder catalyst. Herein, we report the results of studies of the $Zr(OPr^i)_4$ supported silica monoliths and focus on the impact of zirconium content on the generation of Lewis acid sites, and ultimately on the catalytic performance of thus obtained microreactors. Catalytic activity was studied in a selective reduction of cyclohexanone with 2-butanol and compared with literature data for powdered materials to find and demonstrate its superior performance.

2. Experimental

2.1. Catalysts preparation

The silica monolithic materials were prepared using procedure described previously in Ref. [23]. Briefly, first polyethylene glycol (PEG 35000, Fluka) was dissolved in 1 M nitric acid. Next, the vessel was immersed in ice bath and then tetraethoxysilane (TEOS, ABCR) was added dropwise. The resulting mixture was stirred for one hour, and finally cetyltrimethylammonium bromide (CTAB, Sigma) was added. The molar composition of the prepared sol was: 1TEOS:0.26HNO_3:14H_2O:0.53PEG:0.028CTAB, where PEG is expressed as a molar ratio of ethylene oxide units to silica. Polypropylene tubes were filled with a transparent solution and transferred into oven. After 8 day thermal treatment at 40 °C, the solid rods were removed from the moulds, washed with distilled water and then immersed in 1 M ammonia solution at 90 °C for 9 h. Then they were washed with water, dried at room temperature, and finally calcined at 550 °C to remove organic template. Monoliths of cylindrical shape (ca. 4.5 × 40 mm), equipped with connectors were placed into heat shrinkable PTFE tubes. Afterwards, to remove the traces of moisture and thus prevent uncontrollable hydrolysis of zirconium precursor, the microreactors were dried by passing through nitrogen at 200 °C. The zirconium species were deposited onto silica surface by impregnation under flow using zirconium (IV) propoxide (70% in isopropanol, Aldrich) as precursor [11]. Functionalization was carried out at 70 °C for 24 h. Finally, the reactors were washed with anhydrous ethanol and dried again at 110 °C by passing through dry nitrogen. The microreactors with Zr/Si mass ratio of 0.01, 0.07, 0.14 and 0.28 were fabricated and designated as 1ZrM, 7ZrM, 14ZrM, 28ZrM, respectively.

2.2. Catalysts characterization

The monoliths were characterized using several instrumental techniques. Specific surface area, mesopore volume and mesopore size distribution were calculated from nitrogen adsorption data obtained using an ASAP 2020 (Micromeritics) apparatus. Before analysis the samples were degassed for 24 h at 110 °C under vacuum. The structure parameters were checked before and after functionalization. A continuous macropore structure of the monoliths was verified by scanning electron microscopy (TM 30000 Hitachi) and mercury porosimetry. Physicochemical properties of materials were investigated using FTIR DRIFT spectroscopy (Nicolet 6700, Thermo Line), DRS UV–Vis spectroscopy (Varian) and ICP technique (NexION 300D, PerkinElmer). Thermal properties and amount of propoxy ligands were determined by thermogravimetric method (STAR 850, Mettler Toledo). The weight loss during heating with ramp of 10 K/min and air flow rate of 60 cm^3/min were recorded in the range of 25–800 °C. The X-ray diffraction patterns of the samples were collected by a PAN analytical X'Pert Pro PW 3040/60 diffractometer for 2theta in the range of 10–60°. The samples were scanned with the increment of 0.03°/step.

Acid properties of modified samples were determined using FTIR spectroscopy and pyridine as probe molecule. Adsorption measurements were carried out at high temperature in vacuum chamber equipped with ZnSe windows (Thermo Scientific). Prior to pyridine adsorption, the samples were activated at 110 °C in dried nitrogen stream. The pyridine was adsorbed at room temperature during 2 h and next physically adsorbed molecules were desorbed under vacuum at 150 °C for 0.5 h. Afterwards, the FTIR spectra were collected.

2.3. Catalytic experiments

Catalytic performance of the monolithic microreactors was studied in the MPV reduction of cyclohexanone, using 2-butanol as a hydrogen donor. The experiments were carried out in a continuous flow rate of 0.03 cm^3/min, at 95 °C. Ketone to alcohol molar ratio was fixed at 1:52. GC technique (Agilent 7890 A, FID detector, HP-5 column) was applied to determine substrate and product concentrations. The analysis of samples was performed every 30 min. Each experiment was carried out at least for 6 h.

3. Results and discussion

3.1. Structural properties

The silica monoliths featured a hierarchical continuous pore structure consisting of flow-through macropores, and textural mesopores, which were expected to enable very fast access of reactants to the catalytic sites distributed over the surface area of mesopores. The macropore structure examined by SEM (Fig. 1) indicated that macropore diameters were in the range of 30–60 μm and their volume determined by mercury porosimetry, was ca. 2.8 cm^3/g. A total pore volume was ca. 4 cm^3/g and that is a typical value for the monolithic materials under study [8]. Note that it is about four times larger than that reported for the most representative mesoporous materials of SBA-15 or MCM-41 type [24].

The textural characteristics of materials were determined from nitrogen adsorption isotherms measured at 77 K, using Braunauer, Emmet, Teller method for calculation of specific surface area (S_{BET}), and Barrett-Joyner-Halenda (BJH) method to determine the mesopore size distributions from desorption branch of isotherm. The isotherms and cumulative volume distribution graphs are shown in Figs. 2 and 3, and the structural parameters for the parent (M) and modified samples (ZrM) are collected in Table 1.

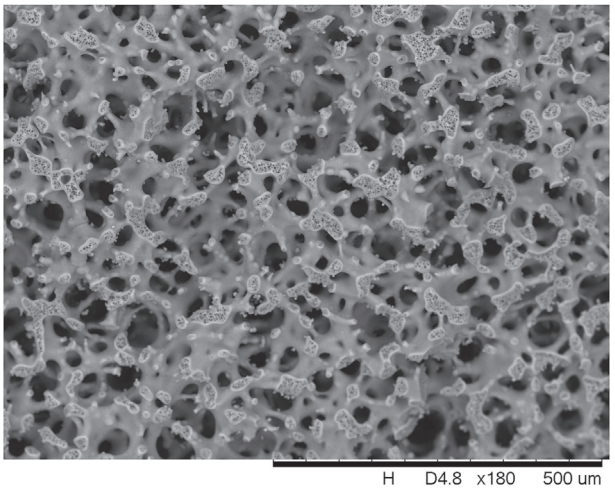

Fig. 1. SEM image of pristine silica monolith.

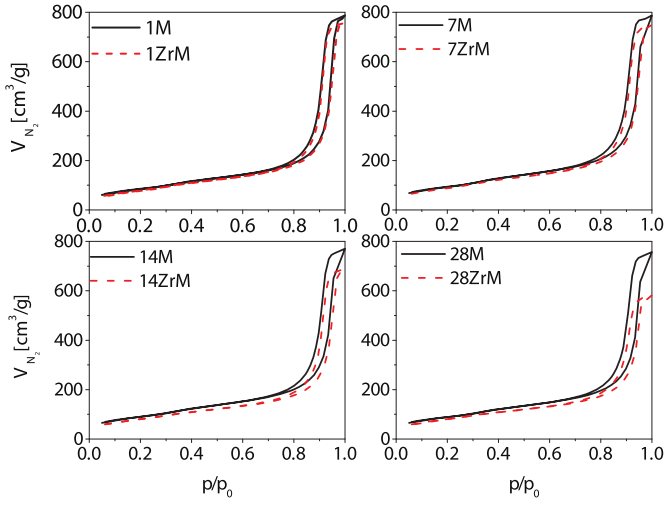

Fig. 2. Nitrogen adsorption/desorption isotherms at 77 K for pristine (M) and zirconium modified samples (ZrM).

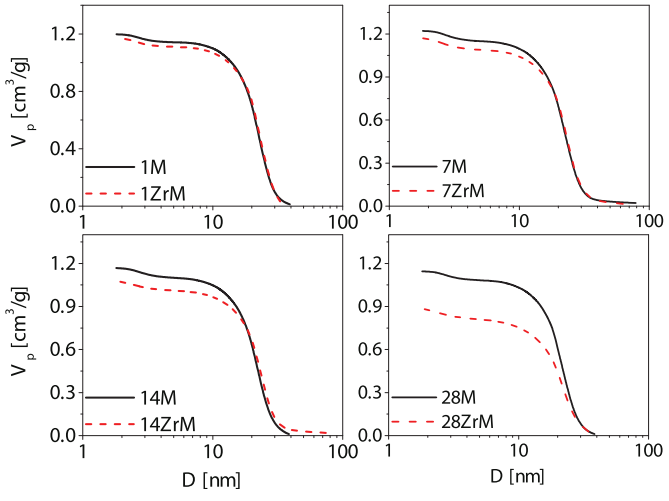

Fig. 3. Cumulative pore volume for pristine (M) and zirconium modified samples (ZrM).

Table 1
Parameters of parent and functionalized monolithic samples.

Sample	Zr/Si mass ratio	Zr/Si (ICP)	S_{BET} m^2/g	V_p[a] cm^3/g	C[b] %
1M	–	–	304	1.19	–
1ZrM	0.01	0.009	297	1.15	2.93
7M	–	–	333	1.2	–
7ZrM	0.07	0.09	328	1.14	3.2
14M	–	–	322	1.16	–
14ZrM	0.14	0.15	303	1.05	3.39
28M	–	–	315	1.15	–
28ZrM	0.28	0.21	305	0.88	4.1

[a] Volume of mesopores.
[b] Content of propoxy groups determined by thermogravimetry.

All pristine silica monoliths were characterized by a specific surface area S_{BET} slightly above 300 m^2/g, while their mesopore volumes were ca. 1.2 cm^3/g. The samples before functionalization were characterized by isotherms of type IV with H1 hysteresis loop characteristic for mesoporous materials, which confirmed that silica skeleton of the macroporous monoliths had a mesoporous structure. This structure was preserved after functionalization with zirconium species. However, the decrease in mesopore volume proportional to the amount of the incorporated Zr was observed. These changes were in the range of 3%–24% for samples 1ZrM and 28ZrM, respectively. On the whole, it confirmed that zirconium precursor was deposited mainly in the mesopores, but a minor part also covered the surface of macropores without noticeable effect on their volume and size. The specific surface area of pristine and functionalized monoliths was almost the same.

3.2. Physicochemical properties

The variation in the amount of active species in the modified samples was examined in a function of Zr/Si mass ratio. The nominal values were equal to 0.01, 0.07, 0.14, 0.28, whereas those determined by ICP technique, appeared to be slightly lower. The largest discrepancy (ca. 21%) was observed for 28ZrM sample, and it was probably caused by a larger amount of loosely attached zirconium species, which were removed during washing. Therefore, the ratio determined by ICP technique (Table 1) corresponds to the species permanently attached to the silica surface.

A primary study of the modified microreactors showed the strong impact of chemical environment of the Lewis acid sites on the process selectivity and efficiency [11]. Modification of the silica monoliths with zirconium (IV) propoxide, i.e. an extremely reactive precursor, led to the formation of zirconium complexes with mixed propoxy/hydroxy ligands on the silica surface. The preservation of organic moieties was proved by TG analysis (Fig. 4), and the amount of incorporated organic ligands, estimated from mass loss above 200 °C, varied from 2.9 to 4.1 wt% (Table 1). The mass loss below 200 °C comes from desorption of residual solvent.

The presence of organic ligands was also confirmed by FTIR spectroscopy. The spectra recorded for pristine and functionalized sample are depicted in Fig. 5. In all spectra, broad bands in the range of 3200 and 3700 cm^{-1} and 1000 and 1250 cm^{-1}, corresponding to vibration of different OH group and Si-O-Si bonds were recorded. Modification of silica surface with zirconium complexes containing propyl groups resulted in the presence of characteristic peaks of asymmetric and symmetric stretching vibrations of C–H bonds in CH_3 groups at 2962 and 2920 cm^{-1}, respectively, and at 2858 cm^{-1} for stretching vibration in CH_2 group. Absorption band cantered at 3745 cm^{-1} is attributed to isolated silanols. The highest intensity of this band was observed in pure silica sample. The gradual decrease in intensity of this band with the increase in concentration of Zr

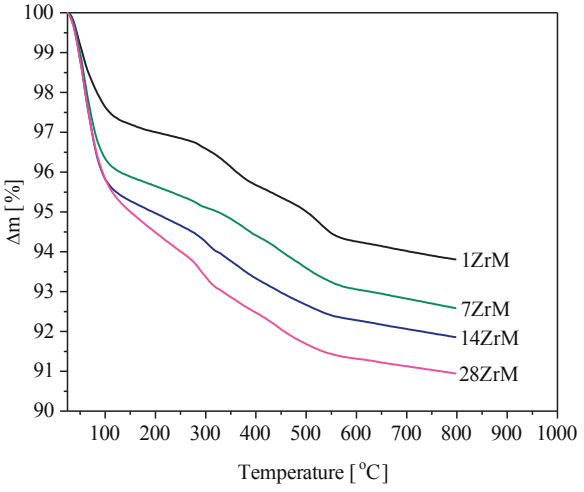

Fig. 4. TG curves of samples with different amount of incorporated zirconium species.

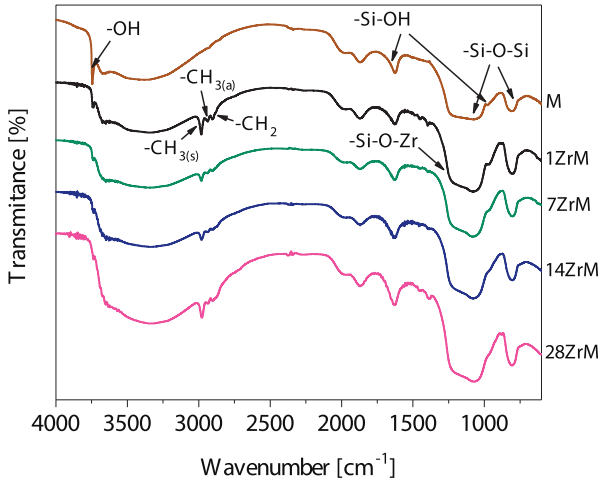

Fig. 5. FTIR spectra for pristine (M) and zirconium modified silica monoliths (ZrM).

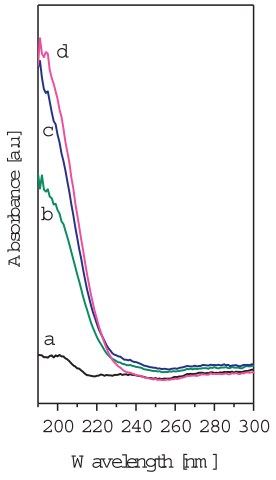

Fig. 6. UV–Vis spectra of modified samples: (a) 1ZrM, (b) 7ZrM, (c) 14ZrM, (d) 28ZrM.

clearly evidenced the attachment of zirconium species to silica surface. A similar trend can be observed for signal at 960 cm^{-1}, corresponding to Si-O-Zr bond formation [25,26].

UV–Vis spectra (Fig. 6) were recorded to determine the dispersion and coordination of zirconium ions grafted onto silica support. Sample 1ZrM with a low zirconium content shows a broad and very weak absorption band. It confirms quite good dispersion of Zr^{4+} ions on silica surface. Maximum absorption at ca. 200 nm in all materials confirmed the presence of zirconium in the tetrahedral coordination. The spectra of samples with higher zirconium concentration show sharp absorption edges in the region 200–220 nm, which suggests the presence of a very small amount of tetragonal ZrO_2 particles with coordination eight [27]. Thus the zirconium species are located mainly in the mesopores, in agreement with the data obtained from nitrogen adsorption, in which the mesopores volume decrease proved to be proportional to the amount of attached zirconium precursor. As expected, the XRD analysis (Fig. 7) showed the presence of amorphous silica evidenced by a broad band in the range of 15–30° for 2 theta. Diffraction peaks of crystalline zirconia were not detected, even in the catalyst with the highest Zr content (28ZrM). Moreover, an inspection of the spectra obtained using Raman spectroscopy (not shown here) excluded the presence of crystalline zirconium species. It should be noted that the presence of amorphous phase can be explained by a relatively low processing temperature (110 °C) of functionalized monoliths, applied to prevent decomposition of isopropoxy species.

The presence of Lewis acid sites on the surface of microreactors was confirmed using FTIR spectroscopy and pyridine as a probe molecule. Lewis coordinated pyridine shows strong signals at 1440-1460 cm^{-1} and 1580-1600 cm^{-1} [28–31]. The characteristic peaks of PyL complex appeared in all spectra at wavenumber ca. 1445 cm^{-1} and 1596 cm^{-1} (Fig. 8). Relative concentration of Lewis acid sites in each sample was determined by comparing surface area of the peak at 1445 cm^{-1} with that of 1ZrM sample, and dividing that value by a ratio of the surface area for that sample to the surface area of 1ZrM. The results obtained clearly showed that the surface concentration of acid sites strongly varied with the zirconium content and maximum value was observed in 14ZrM (Fig. 9).

MPV reduction of cyclohexanone was performed to elucidate the impact of the physicochemical properties of thus obtained materials on the catalytic activity. All the catalyst showed considerable activity in the proposed reaction. The residence time (20 min) was selected to ensure the conversion of cyclohexanone of less than 100% in all experiments, which enabled to find a direct relationship of catalytic activity vs. zirconium content. Conversion achieved in the microreactors changed (and increased) in the order: 1ZrM < 7ZrM <14ZrM >28ZrM in accord with the change

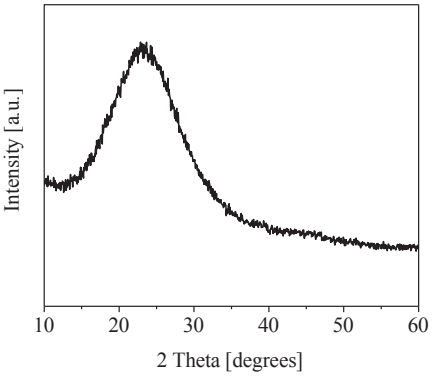

Fig. 7. XRD spectrum of 28ZrM sample.

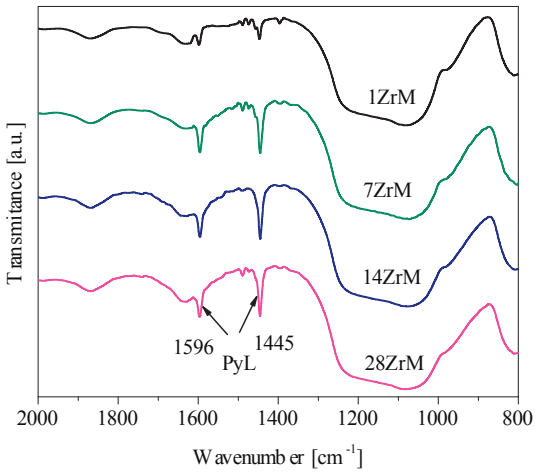

Fig. 8. FTIR spectra after adsorption of pyridine on Lewis acid sites.

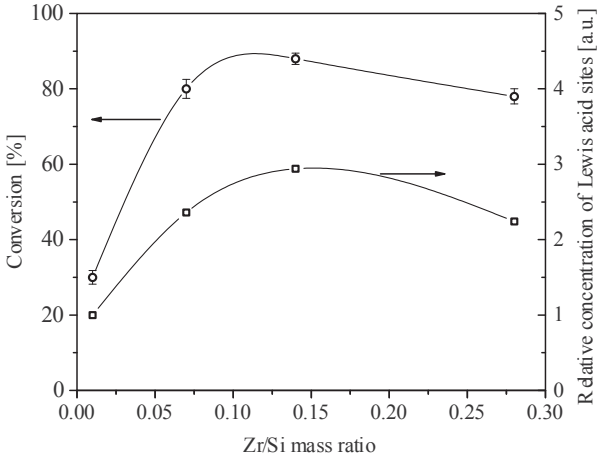

Fig. 9. Conversion of cyclohexane in microreactors with different content of zirconium and relative concentration of Lewis acid sites.

(increase/decrease) of Lewis acid sites concentration determined from pyridine adsorption (Fig. 9). Of importance is that an excessive content of Zr species did not result in the improved catalytic activity, conversely, it caused its decline. In sample 28ZrM the surface concentration of acid sites is lower than in 14ZrM. It is reasonable to assume that at lower content of zirconium species (ca. 0.01–0.14 Zr:Si molar ratio) acidic sites form a monolayer, whereas at higher concentrations the multilayer islands of zirconium occur and active sites become less accessible [32]. Moreover the selectivity was 100% in all of the experiments, as no by-products were detected by GC.

Table 2
Productivity of cyclohexanol in MPV reduction of cyclohexanone using different catalytic systems.

Catalyst	Productivity[a] mmol/g h	Conversion %	Reference
Flow process: 14ZrM	2.22	88	this paper
Batch process:			
ZrO_2	0.66	81	[31]
Sn-MCM-41 (Sn 10 wt%)	1.08	100	[35]
Zr-MCM-41 (Zr 10 wt%)	1.02	95	[33]
MgO	0.06	88.9	[36]
Sn-Beta (SnO_2 2 wt%)	0.22	98.6	[37]
ZS-5 (ZrO_2-SiO_2)	2.28	89.1	[34]

[a] Productivity is related to mass of material.

The productivity of cyclohexanol achieved in a 14ZrM microreactor was 2.22 mmol/g h at conversion 88% and, except for one case, it was significantly higher than reported for batch reactors with powdered catalysts (Table 2) applied in the same reaction. We believe, that much higher activity of 14ZrM than of Zr-MCM-41 [33], with fairly similar (10%) Zr content, can be ascribed to mass transport limitation of the reaction kinetics caused by small size of mesopores present in the applied MCM-41supports. But similar activity of ZS-5 [34] catalysts is a clear proof of very high catalytic activity of the silica-supported zirconium species in MPV reaction.

4. Conclusions

The performed studies clearly demonstrate that $Zr(OPr^i)_4$ species can be effectively attached to the silica monoliths' mesopore surface to obtain continuous-flow microreactors which were shown to be very active in the MPV reduction of a model carbonyl compound, and offered higher productivity than conventional batch reactors with powdered catalysts.

The attachment of isopropoxy species appeared to have little effect on the very open bi-modal pore structure of pristine siliceous monoliths. It enabled unhampered access of reactants from the larger flow-through pores to Lewis acid sites present in the mesopores and to express their very high catalytic activity.

Catalytic activity of the reactive monolith was proportional to the concentration of Lewis acid sites and it was the highest for Zr/Si mass ratio of 0.14. With that ca. 2.2 mmol/g h of cyclohexanol could be produced from cyclohexanone.

Acknowledgement

This work was financed by the National Science Centre project no DEC-2014/15/N/ST8/03171.

References

[1] L. Malet-Sanz, F. Susanne, J. Med. Chem. 55 (2012) 4062–4098.
[2] X. Wang, J. Zhu, H. Bau, R.J. Gorte, Catal. Lett. 77 (2001) 173–177.
[3] G. Kolb, V. Hessel, Chem. Eng. J. 98 (2004) 1–38.
[4] K. Nakanishi, R. Takahashi, T. Nagakane, K. Kitayama, N. Koheiya, H. Shikata, N. Soga, J. Sol Gel Sci. Technol. 17 (2000) 191–210.
[5] A. Koreniuk, K. Maresz, K. Odrozek, A.B. Jarzębski, J. Mrowiec-Białoń, Appl. Catal. A Gen. 489 (2015) 203–208.
[6] J. Babin, J. Iapichella, B. Lefevre, C. Biolley, J.P. Bellat, F. Fajula, A. Galarneau, New J. Chem. 31 (2007) 1907–1917.
[7] K. Szymańska, K. Odrozek, A. Zniszczoł, G. Torrelo, V. Resch, U. Hanefeld, A.B. Jarzębski, Catal. Sci. Technol. 6 (2016) 4882–4888.
[8] K. Szymańska, M. Pietrowska, J. Kocurek, K. Maresz, A. Koreniuk, J. Mrowiec-Białoń, P. Widlak, E. Magner, A. Jarzębski, Chem. Eng. J. 287 (2016) 148–154.
[9] K. Szymańska, W. Pudło, J. Mrowiec-Białoń, A. Czardybon, J. Kocurek, A.B. Jarzębski, Microporous Mesoporous Mater. 170 (2013) 75–82.
[10] A. Koreniuk, K. Maresz, K. Odrozek, J. Mrowiec-Białoń, Microporous Mesoporous Mater. 229 (2016) 98–105.
[11] A. Koreniuk, K. Maresz, J. Mrowiec-Białoń, Catal. Commun. 64 (2015) 48–51.
[12] K. Bauer, D. Garbe, H. Surbung, Common Fragrance and Flavor Materials: Preparation Properties and Uses, Wiley-VCH Verlag GmbH & Co.KGaA, 2001.
[13] P. Mäki-Arvela, J. Hájek, T. Salmi, D.Y. Murzin, Appl. Catal. A Gen. 292 (2005) 1–49.
[14] Y. Zhu, S. Liu, S. Jaenicke, G. Chuah, Catal. Today 97 (2004) 249–255.
[15] B. McNerney, B. Whittlesey, D.B. Cordes, C. Krempner, Chem. Eur. J. 20 (2014) 14959–14964.
[16] M.A. Aramendía, V. Borau, C. Jiménez, J.M. Marinas, J.R. Ruiz, F. Urbano, Appl. Catal. A Gen. 249 (2003) 1–9.
[17] C. Jiménez-Sanchidrián, J.R. Ruiz, Appl. Catal. A Gen. 469 (2014) 367–372.
[18] M. Boronat, A. Corma, M. Renz, J. Phys. Chem. B 110 (2006) 21168–21174.
[19] I.V. Il'ina, V.P. Sivcev, K.P. Volcho, N.F. Salakhutdinov, V.I. Anikeev, J. Supercrit. Fluids 61 (2012) 115–118.
[20] J. Sedelmeier, S.V. Ley, I.R. Baxendale, Green Chem. 11 (2009) 683–685.
[21] C. Battilocchio, J.M. Hawkins, S.V. Ley, Org. Lett. 15 (2013) 2278–2281.
[22] F. Quignard, O. Graziani, A. Choplin, Appl. Catal. A Gen. 182 (1999) 29–40.
[23] M. Berdys, A. Koreniuk, K. Maresz, W. Pudło, A.B. Jarzębski, J. Mrowiec-Białoń, Chem. Eng. J. 282 (2015) 137–141.
[24] A.T. Krzyzak, I. Habina, Microporous Mesoporous Mater. 231 (2016) 230–239.
[25] S.G. Chen, Y.S. Yin, D.P. Wang, J. Am. Ceram. Soc. 88 (2005) 1041–1045.

[26] G. Yu, L.Y. Zhu, X.Q. Wang, J.R. Liu, D. Xu, Microporous Mesoporous Mater. 130 (2010) 189–196.
[27] E. Rodriguez-Castellon, A. Jimenez-Lopez, P. Maireles-Torres, D.I. Jones, J. Roziere, M. Trombetta, G. Busca, M. Lenarda, L. Storaro, J. Solid State Chem. 175 (2003) 159–169.
[28] J. Datka, A.M. Turek, J.M. Jehng, I.E. Wachs, J. Catal. 135 (1992) 186–199.
[29] C. Ngamcharussrivichai, P. Wu, T. Tatsumi, J. Catal. 235 (2005) 139–149.
[30] I.M. Hill, S. Hanspal, Z.D. Young, R.J. Davis, J. Phys. Chem. C 119 (2015) 9186–9197.
[31] T. Komanoya, K. Nakajima, M. Kitano, M. Hara, J. Phys. Chem. C 119 (2015) 26540–26546.
[32] A. Zukal, H. Siklova, J. Cejka, Langmuir 24 (2008) 9837–9842.
[33] S. Shylesh, M.P. Kapoor, L.R. Juneja, P.P. Samuel, C. Srilakshmi, A.P. Singh, J. Mol. Catal. A Chem. 301 (2009) 118–126.
[34] G. Li, W.H. Fu, Y.M. Wang, Catal. Commun. 62 (2015) 10–13.
[35] P.P. Samuel, S. Shylesh, A.P. Singh, J. Mol. Catal. A Chem. 266 (2007) 11–20.
[36] M.A. Aramendia, V. Borau, C. Jimenez, J.M. Marinas, J.R. Ruiz, F.J. Urbano, Appl. Catal. A Gen. 244 (2003) 207–215.
[37] A. Corma, M.E. Domine, S. Valencia, J. Catal. 215 (2003) 294–304.

catalysts

MDPI

Article

Continuous-Flow Monolithic Silica Microreactors with Arenesulphonic Acid Groups: Structure–Catalytic Activity Relationships

Agnieszka Ciemięga [1], Katarzyna Maresz [1], Janusz J. Malinowski [1] and Julita Mrowiec-Białoń [1,2,*]

[1] Institute of Chemical Engineering Polish Academy of Sciences, Bałtycka 5, 44-100 Gliwice, Poland; akoreniuk@iich.gliwice.pl (A.C.); k.kisz@iich.gliwice.pl (K.M.); j.mal@iich.gliwice.pl (J.J.M.)

[2] Department of Chemical Engineering and Process Design, Silesian University of Technology, Ks. M. Strzody 7, 44-100 Gliwice, Poland

* Correspondence: jmrowiec@polsl.pl; Tel.: +48-32-231-08-11

Academic Editors: Tian-Yi Ma, Jian-Rong (Jeff) Li and Cláudia Gomes Silva
Received: 11 July 2017; Accepted: 28 August 2017; Published: 30 August 2017

Abstract: The performance of monolithic silica microreactors activated with sulphonic acid groups and a packed bed reactor with Amberlyst 15 resin were compared in the esterification of acetic acid with n-butanol. The monolithic microreactors were made of single silica rods with complex pore architecture, differing in the size of mesopores, and in particular, flow-through macropores which significantly affected the flow characteristic of the continuous system. The highest ester productivity of 105.2 $mol \cdot mol_H^{+-1} \cdot h^{-1}$ was achieved in microreactor M1 with the largest porosity, characterized by a total pore volume of 4 $cm^3 \cdot g^{-1}$, mesopores with 20 nm diameter, and large flow-through macropores 30–50 μm in size. The strong impact of the permeability of the monoliths on a reaction kinetics was shown.

Keywords: silica monoliths; continuous-flow microreactors; acid centres; structure/catalytic activity relationships

1. Introduction

Synthesis of most fine and specialty chemical—particularly pharmaceuticals—is typically carried out in a liquid phase and batch operation, despite the fact that batch processes cause a number of problems, especially with scaling up and producing within homogeneous processing conditions [1]. Flow reactors have many advantages over batch reactors: continuous production, better process control, easier automation, and reduced operation costs. Moreover, continuous-flow heterogeneous catalytic processes offer higher selectivity, productivity, and elimination of costly catalyst separation from the reaction media [2,3]. The application of reactors involving solid catalysts in the form of either stationary or moving particles often leads to serious operational problems associated with mass and heat transfer limitations, excessive backpressure, thermal instabilities in stationary beds, etc. [4]. The replacement of a continuous flow reactor by monolithic microreactor-based technology appeared to be promising for the effective production of fine chemicals.

Continuous microreactors allow a miniaturization of the apparatus, which is of particular importance in fine chemical synthesis, and in the pharmaceutical and chemical industries [2]. A high surface to volume ratio of the rectors enables high concentrations of active sites per unit volume and provides better heat and mass transfer. Furthermore, precise control of the reaction temperature and residence time has a beneficial effect on the productivity and selectivity.

Microreactors can be made from a wide range of materials, and a variety of fabrication techniques have been proposed [5,6], often requiring special equipment and skills. Continuous-flow monolithic

polymeric microreactors which have a well-defined system of flow-through pores show important advantages over packed bed reactors [7–9], but suffer from low thermal stability and a tendency to swell. More recently, however, it was shown [8] that highly cross-linked polymer monoliths do not suffer from the latter effects. In recent years, among the various types of microreactor, much attention has been paid to the reactors with reactive cores made of inorganic carriers—especially of monolithic silica. The silica-based microreactors were first proposed by the Montpellier group, and were made from a single monolith (MonoSil), the surface of which was functionalized with -NH_2 or -HSO_3 groups. Innovation of this approach stems from a unique hierarchical pore structure of the monolith in which flow-through macropores are connected to an extensive network of meso- and micropores present in the silica skeleton [10,11]. Owing to the unique hierarchical pore structure, the flow resistance could be reduced, permeability increased, and the accessibility of substrates to catalytic sites improved, giving an overall better performance compared to packed column [12]. The silica monoliths with hierarchical porosity were obtained by combining the phase separation method elaborated by Nakanishi [13,14] with pseudomorphic synthesis [15,16], to ensure an ordered mesoporous morphology of materials.

Hierarchically structuring both the porosity and the architecture of a material over a different length scale provides an opportunity to synthesize materials suitable for different applications, including catalysis and separation [17,18]. Recently, the synthesis strategies and catalytic performances exhibited by the hierarchically porous catalysts have been thoroughly reviewed [18].

Silica-based materials are extensively used in heterogeneous catalysis as an active site support due to the abundance of surface silanols, which allows the grafting of a wide variety of active species to meet specific catalytic demands [19] posed for the synthesis of fine chemicals [10]. Consequently, silica monoliths have been activated with organic groups [11,20], enzymes [21,22], or metal complexes [23], and successfully applied as active cores of continuous-flow microreactors.

In this work, we compare the performance of continuous-flow reactors fabricated using silica monoliths featuring different pore structure with that of the packed bed reactor filled with Amberlyst 15 resin. The reactors were tested in the esterification of acetic acid with n-butanol. The n-butyl acetate is the product of the model reaction which is of practical interest, being used as a solvent in the manufacturing of lacquer, artificial perfume, plastics, and safety glass, and also as a synthetic fruit flavouring in foods [24]. The silica monoliths were synthesized using four synthesis protocols to obtain carriers with significantly different structural parameters on both the meso- and macroscale. Subsequently, monoliths were functionalized with arenesulphonic acid groups in order to obtain monolithic microreactors with Brönsted acid centres. A strong impact of the macroporous structure on the flow characteristic of the microreactors was found, while the amount of anchored active groups correlated well with mesostructural properties (i.e., significant increase was recorded with increasing values of specific surface area). However, the structure of monoliths at macroscale decisively influenced the overall performance of the microreactors. The highest productivity was achieved in the monolith with the largest porosity, and not the largest surface area, which also offered the lowest pressure drop. The latter finding is also of major practical importance, and correlates very well with the observation most recently reported in [25].

2. Results

2.1. Characterization of the Silica Monoliths

Three silica monoliths designated as M1, M2, and M3 were fabricated using different synthesis protocols (see the Materials and Methods, Table 5). The monolith structure—in both the meso- and macropore scales—strongly depended on the composition of the reaction mixture and the synthesis process parameters thereof. The scanning electron microscopy images of the monoliths are displayed in Figure 1.

The images confirmed the presence of the bi-continuous, foam-like structure of the macropores in the monoliths. The characterization of the materials by low-temperature nitrogen adsorption and

mercury porosimetry (Figure 2) revealed pore system architecture in different size scales. Structural properties of the materials are summarized in Table 1.

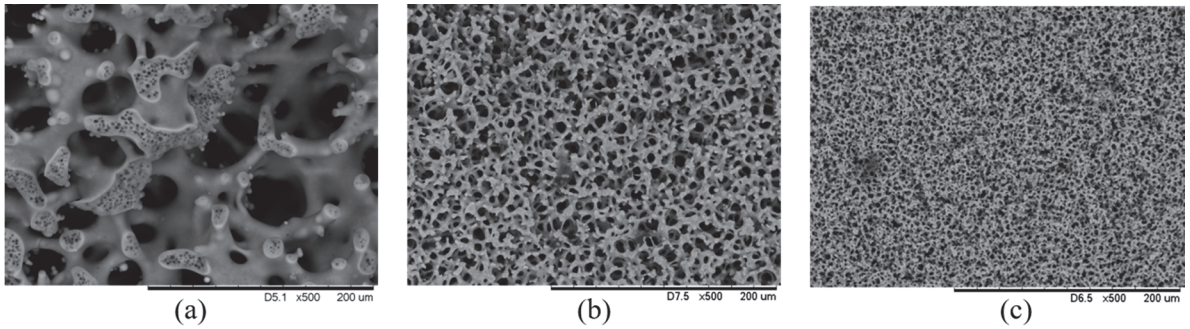

Figure 1. SEM images of (**a**) M1, (**b**) M2, and (**c**) M3 monoliths.

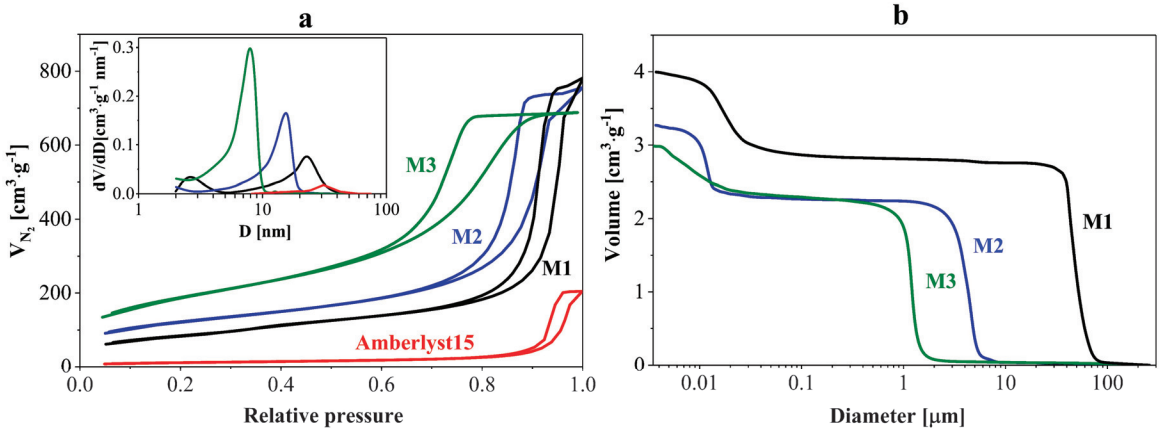

Figure 2. (**a**) N_2 adsorption/desorption isotherms and pore size distribution in monoliths and Amberlyst 15; (**b**) Cumulative pore volume curves determined by mercury porosimetry.

Table 1. Structural and acidic properties of the materials.

Sample	S_{BET} ($m^2 \cdot g^{-1}$)	Vp_{mes} ($cm^3 \cdot g^{-1}$)	V_T ($cm^3 \cdot g^{-1}$)	D_{mac} (μm)	D_{mes} [1] (nm)	H^+ ($mmol \cdot g^{-1}$)	A_{200}/A_{150} [4]
M1	328 (245) [2]	1.15 (0.91)	4 (3.72)	30–50 (30–50)	2.5/20 (20)	0.65	0.9
M2	413 (316)	1.12 (0.91)	3.27 3.01	4–6 4–6	15 (14.9)	0.85	0.9
M3	575 (427)	1.04 (0.74)	2.98 2.65	1.3 1.3	8.7 (7.9)	0.97	0.8
Amberlyst	40	0.33	-	-	31	4.7 [3]	n/a

[1] a maximum of the pore size distribution curve by BJH; [2] in parentheses, texture parameters after functionalization with acidic groups; [3] manufacturer's data; [4] relative strength of Brönsted acid sites (BAS).

Monolith M1 synthesized in the presence of surfactant and hydrothermally treated in ammonia solution at 90 °C featured bimodal mesopore structure (small mesopores with diameters of 2–4 nm and larger ones in the size of 10–35 nm) and large macropores with diameters in the range of 30–50 μm. The bimodal mesopore structure originated from the presence of a micelle-forming surfactant. Monolith M2 hydrothermally treated in ammonia solution at 80 °C had a uniform mesopore structure in the range of 10–20 nm and macropores with diameters ca. 5 μm. As reported earlier [26,27], the size

of the macropores decreased with the increase in the value of polyethylene glycol (PEG)/Si ratio (Table 1, Figure 2). In turn, the use of a higher concentration of nitric acid in the synthesis of monolith (sample M3) resulted in the formation of smaller macropores with a small effect on the volume of the macropores. This phenomenon was interpreted as an effect of a faster hydrolysis and slower condensation of siliceous species in acidic conditions [28]. The pore structure in the nanometer range was tailored by a post-gelation treatment of the silica monoliths in ammonia solution, as well as an application of a cationic surfactant. The total pore volume (V_T) of the monoliths was very large (in the range of 3–4 $cm^3 \cdot g^{-1}$), while the mesopore volume (Vp_{mes}) was comparable (ca. 1.1 $cm^3 \cdot g^{-1}$). Monolith M3 was characterized by the largest specific surface area (575 $m^2 \cdot g^{-1}$), which is associated with the presence of small mesopores. Monoliths M1 and M2 also differed in the structure of the silica skeleton. Monolith M2 was characterized by a uniform wall thickness (about 5 μm), while in monolith M1 there were visible structural elements of different thicknesses ranging from a few to tens of micrometers. Ion-exchange resin Amberlyst 15 exhibited large mesopores (cf. inset to Figure 2) of volume ca. 0.3 $cm^3 \cdot g^{-1}$ (i.e., four times smaller than in the synthesized monoliths).

Thermal stability of the catalyst is of primary importance—particularly when it contains organic groups. The thermal stability of arenesulphonic acid groups attached to the monoliths' surface and their amount were determined by thermogravimetric method. The results are shown in Figure 3 and in Table 1. All samples were stable up to 350 °C. The sharp weight loss below 120 °C corresponds to physisorbed water. The amount of incorporated acidic groups was calculated from mass loss in the range of 300–700 °C, resulting from thermal decomposition of functional groups. A strong relationship between specific surface area of silica skeleton and chemically bonded acidic groups was observed. Monolith M3 with the largest specific surface area had the highest amount of anchored acidic groups (Table 1), which correlates very well with the content of hydroxyls employed to attach functional groups [29].

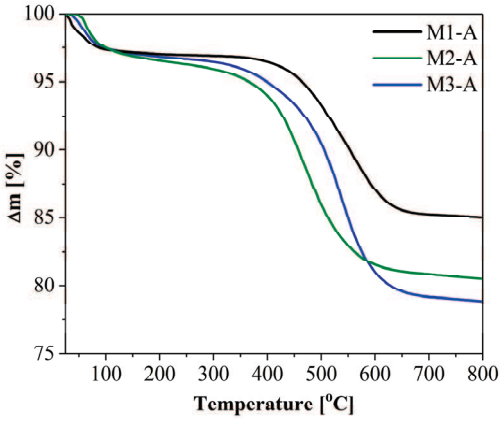

Figure 3. Thermogravimetric (TG) curves of the functionalized silica monoliths.

The identification of acid sites and their strength were studied using pyridine (Py) adsorption combined with Fourier transform infrared (FTIR) studies. The spectra recorded before and after the adsorption and desorption at different temperatures for M1 are depicted in Figure 4. The bands at 1488, 1542, and 1634 cm^{-1} derive from pyridinium ions bonded to Brönsted acid sites (BAS). The fact that the characteristic bands still remained after evacuation at 150 °C and 200 °C confirmed the presence of strong BAS. The band at 1443 cm^{-1}—visible after adsorption—disappeared at 150 °C, and it corresponds to hydrogen-bonded pyridine. The relative acid strength was calculated based on the intensity of the adsorption band centered at 1542 cm^{-1}. The ratio of the integrated area of the peaks obtained at 200 °C and 150 °C represents the fraction of acid sites still containing chemisorbed Py after evaluation at these temperatures and reduced pressure. The data in Table 1 confirmed that strength of

BAS is comparable for all the samples. The value of A_{200}/A_{150} nearly close to unity is characteristic of strong acid sites [30,31].

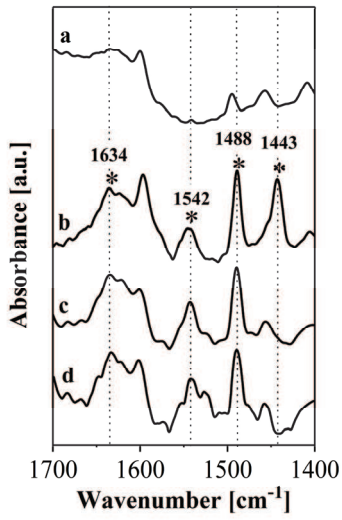

Figure 4. Fourier transform infrared (FTIR) spectra of M1-A: (**a**) before and (**b**) after pyridine adsorption, and after evacuation at (**c**) 150 °C and (**d**) 200 °C.

The relationship between the pressure drop and the flow rate is of practical significance, providing additional knowledge which is useful in assessing process economics. Thus, the pressure drop was measured for all monolithic microreactors and the packed bed reactor equipped with the Amberlyst 15 resin. It was found that it strongly depended on the size of the flow-through macropores, and a significant increase in pressure was recorded in the order M1 << M2 < M3 (Figure 5), which correlates very well with the decreasing pore size. The reduction in the size of the flow-through macropores (from ca. 50 μm to 1 μm) resulted in the increase in pressure drop of a few orders of magnitude. In the packed bed reactor, the pressure drop was twice as large as that recorded in the M1 microreactor.

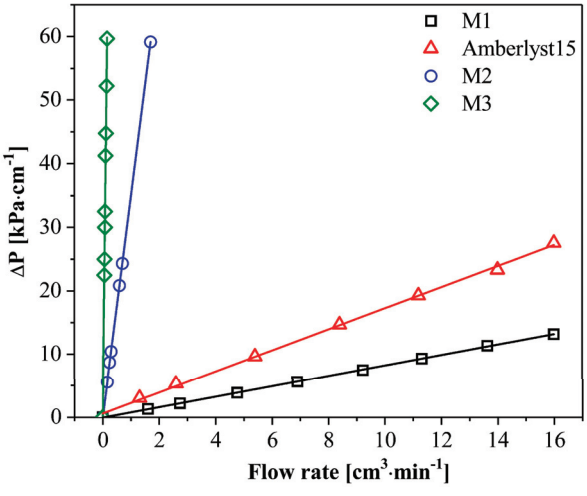

Figure 5. Pressure drop vs. flow rate in microreactors and the packed bed reactor with Amberlyst 15.

The permeability of the monoliths and the packed bed reactor (Amberlyst) was calculated using Darcy equation [25], and the results obtained are shown in Table 2. The permeability coefficient was three orders of magnitude lower in M3 than in M1, in perfect agreement with the smaller size of macropores in that material.

Table 2. Permeability of silica monoliths and Amberlyst 15.

Sample	Permeability $K \cdot 10^{12}$ (m^2)
M1	11.3
M2	0.27
M3	0.025
Amberlyst 15	5.4

2.2. Catalytic Performance

The performance of continuous-flow monolithic microreactors and the packed bed reactor with Amberlyst 15 resin was compared in the esterification of acetic acid with n-butanol. Catalytic tests were performed for at least 6 h, at a flow rate of 0.06 $cm^3 \cdot min^{-1}$ (representative graph for M1-A is shown in Figure 6). The flow rate was selected to achieve conversion smaller than 50% to discriminate efficacy of different structure.

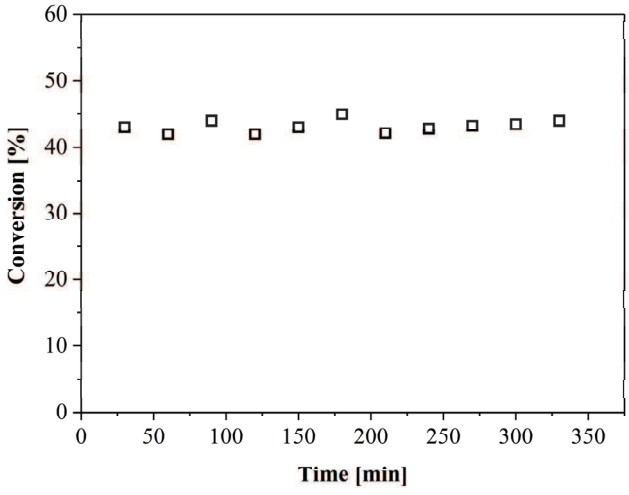

Figure 6. Conversion vs. time in the M1-A microreactor.

One of the key factors in continuous flow reactors' performance is the residence time (τ) of a reactant molecule in the active zone. According to Sachse et al. [32], for the monolithic reactor τ may be determined from the following expression:

$$\tau = xmV_T/F, \quad (1)$$

where x is monolith length, m is a weight per cm ($g \cdot cm^{-1}$), and F is the flow rate ($cm^3 \cdot min^{-1}$).

Thus, the more open the structure (as found in M1), the longer the residence time (Table 2) for the same flow rate.

The productivity—expressed in mol of product formed per kg of catalyst per h—was calculated from conversion (*Conv*) and initial concentration of reactant (C_0) using the equation:

$$P = C_0 Conv V_T/\tau. \quad (2)$$

The value of productivity calculated for all microreactors was similar and of ca. 68 $mol \cdot kg_{cat}^{-1} \cdot h^{-1}$ (Table 3). However, if the productivity was related to the concentration of active centers (mmol of product per mmol of active centers per hour), the M1-A microreactor showed superior performance. This can be ascribed to: (i) enhanced mass transfer from a core of reactants to the skeleton's surface, and (ii) easier access of reactants to active sites embedded in much larger mesopores of M1-A than in M2-A and M3-A. On the other hand, a greater density of active sites in M2-A and M3-A enabled compensation

for the higher activity of the M1-A catalytic sites. However, M1 monoliths revealed the largest permeability of liquids (Table 2), and this bears directly on pressure drop and hence power/energy input and also safety. Thus, bearing in mind all factors, we consider the M1-A microreactor as the most effective solution.

Table 3. Results from catalytic experiments.

Sample	Conversion (%)	τ (min)	Productivity ($mol \cdot kg_{cat}^{-1} \cdot h^{-1}$)	Productivity ($mol \cdot mol_{H}^{+-1} \cdot h^{-1}$)
M1-A	42	10	68.4	105.2
M2-A	41	8	67.2	79.2
M3-A	42	7.5	68.4	70.8
Amberlyst 15	38	4.2	61.8	13.2

The productivity in the reactor packed with Amberlyst 15 was about 86% of the M1-A microreactor, despite a similar conversion as in M-type reactors. It is important to emphasize that in the case of monolithic microreactors, higher conversions can be achieved by increasing the length of the microreactor or by applying numbering-up approach [5]. For example, by connecting two the M1-A reactors in series, a conversion of 62% was reached (data not shown here).

The M1-A performance also most favourably compares with other studies reported previously (Table 4).

Table 4. Comparison of acetic acid esterification with n-butanol in flow (entries 1–2) and batch (entries 3–5) reactors.

Entry	Catalyst	Conversion (%)	Productivity ($mol \cdot kg_{cat}^{-1} \cdot h^{-1}$)	Temp. (°C)	Time (min)	Ref.
1	M1-A	42	68.4	75	10 [2]	This work
2	Amberlyst 15 [1]	70	30	80	10 [2]	[33]
3	Al-MCM-41	50	29.4	150	360	[34]
4	H-USY-20	35	13.8	75	360	[35]
5	Smopex-101	65	37.8	75	360	[35]

[1] packed-bed column; [2] residence time; molar ratio of substrates—1:1.

3. Materials and Methods

3.1. Monoliths Synthesis and Activation

Three silica monoliths (M1–M3) in the form of rods with diameter of 4.5 mm were prepared using Nakanishi approach [13,14] with minor modifications [26,27]. In brief, polyethylene glycol (PEG 35000, Sigma-Aldrich, St. Louis, MO, USA) was dissolved in aqueous HNO_3 (Avantor, 65%, Gliwice, Poland), after which tetraethoxysilane (TEOS, ABCR, 99%, Karlsruhe, Germany) was added slowly to the PEG solution in an ice bath followed by the addition of cetyltrimethylammonium bromide (CTAB, Sigma-Aldrich) (sample M1). Details of the composition of the reagents are given in Table 5.

After treatment with ammonia (Avantor, 25%), the samples were washed with deionized water and dried for 3 days at 40 °C. Finally, the samples were calcined at 550 °C for 8 h (ramp 1 $°C \cdot min^{-1}$).

Single silica rods (ca. 4 cm long) were embedded into heat-shrinkable Teflon tubes, equipped with connectors to obtain a microreactor suitable for a continuous operation. Subsequently, silica monoliths were functionalized under flow (48 h, 60 °C) with arenesulphonic acid groups using solution of 2-(4-chlorosulfonylphenyl)ethyltrimethoxysilane (CSPTMS; 50 wt % solution in CH_2Cl_2, ABCR) dissolved in anhydrous ethanol. The functionalized monoliths were designated as M1-A, M2-A, and M3-A. The nominal content of organic groups was 1.5 $mmol \cdot g^{-1}$. After activation, the material was washed extensively with ethanol (Avantor, 99.8%) to remove a non-bonding precursor.

Table 5. Composition of reagents for monolith synthesis and conditions during ammonia aqueous solution treatment of monoliths prior to drying. PEG: polyethylene glycol.

Sample	TEOS (cm^3)	PEG (g)	H_2O (cm^3)	HNO_3 (cm^3)	CTAB (g)	Aging (Days)	Ammonia Treatment		
							Conc. (M)	Time (h)	Temp. (°C)
M1	26.1	2.73	30.10	2.18	1.2	7	1	8	90
M2	26.1	3.31	31.44	2.04	0	3	1	24	80
M3	26.1	3.32	32.05	2.39	0	3	0.1	20	40

3.2. Characterization of Materials

The mesoporous textural properties of the materials were determined from low-temperature nitrogen sorption (Micromeritics ASAP 2020, Norcross, GA, USA). The samples were outgassed in a vacuum for 24 h at 200 °C prior to the analysis. The specific surface area S_{BET} was determined using a standard BET method [36]. The mesopore volume and pore size distribution were calculated from the desorption branch of the isotherm using BJH model [37]. The macroporous network of pores in the silica monoliths was investigated by mercury porosimetry (PoreMaster 60, Quantachrome, Boynton Beach, FL, USA) and by scanning electron microscopy (TM 30000, Hitachi, Tokyo, Japan). Thermal properties and the amount of acidic groups attached to the silica carrier were studied by thermogravimetric analysis (STAR 853, Mettler Toledo, Greifensee, Switzerland). The type and strength of acid centres were determined using pyridine as a probe molecule and a FTIR-DRIFT spectrometer (NICOLET 6700, Thermo Fisher Scientific, Waltham, MA, USA) equipped with high temperature/vacuum chamber with ZnSe windows.

3.3. Catalytic Tests

The catalytic tests were performed in the esterification of acetic acid (Avantor, p.a) with n-butanol (Avantor, p.a) in a continuous-flow monolithic microreactor fabricated using monoliths M1–M3 and a packed bed reactor filled with Amberlyst 15 resin (particle size of 0.7 ± 0.1 mm, Sigma-Aldrich). The esterification process was examined for the molar ratio of substrates 1:1 and at 75 °C using flow rate of 0.06 $cm^3 \cdot min^{-1}$. The catalytic tests were carried out for 6 h. The progress of the reaction was monitored by gas chromatography (Agilent 7890 A; FID detector; HP-5 column, Agilent Technologies, Palo Alto, CA, USA).

4. Conclusions

The presented studies clearly showed that the performance of the continuous-flow monolithic microreactors strongly depended on the silica structure both on meso- and macro-scale. It was shown that slight changes in the synthesis procedure strongly affected the structure of monoliths, which translated directly into a significant effect of their flow characteristic. The extremely high pressure drop was recorded when decreasing the size of the macropores from ca. 50 μm to 1.3 μm. Furthermore, smaller mesopores were detected in monoliths with small macropores, which resulted in a considerable increase (ca. 60% of specific surface area). Consequently, a larger concentration of arenesulphonic groups (up to 50%) was identified in these monoliths. However, the microreactors with much larger macroporosity appeared to be the most effective; i.e., they were characterized by a lower pressure drop and higher productivity in the esterification process despite the smaller concentration of active groups. The studied microreactors have strong Brönsted acid sites and they can operate up to 300 °C. Moreover, the performance of the best microreactor appeared to be significantly better than that found for the reactor packed with Amberlyst 15.

Acknowledgments: This work was financed by the National Science Centre Project no DEC-2014/15/N/ST8/03171.

Author Contributions: A.C., K.M. and J.M.-B. conceived and designed the experiments, analysed the data and wrote the paper; J.J.M. wrote part of the manuscript.

Conflicts of Interest: The authors declare no conflict of interest.

References

1. Plumb, K. Continuous processing in the pharmaceutical industry—Changing the mind set. *Chem. Eng. Res. Des.* **2005**, *83*, 730–738. [CrossRef]
2. Malet-Sanz, L.; Susanne, F. Continuous flow synthesis. A pharma perspective. *J. Med. Chem.* **2012**, *55*, 4062–4098. [CrossRef] [PubMed]
3. Teoh, S.K.; Rathi, C.; Sharratt, P. Practical assessment methodology for converting fine chemicals processes from batch to continuous. *Org. Process Res. Dev.* **2016**, *20*, 414–431. [CrossRef]
4. Stankiewicz, A. Process intensification in in-line monolithic reactor. *Chem. Eng. Sci.* **2001**, *56*, 359–364. [CrossRef]
5. Ehrfeld, W.; Hessel, V.; Lowe, H. *Microreactors: New Technology for Modern Chemistry*; Willey-VCH: Weinheim, Germany, 2000.
6. Wirth, T. *Microreactors in Organic Chemistry and Catalysis*, 2nd ed.; Willey-VCH: Weinheim, Germany, 2013.
7. Peterson, D.S.; Rohr, T.; Svec, F.; Frechet, J.M.J. Enzymatic microreactor-on-a-chip: Protein mappingusing trypsin immobilized on porous polymer monoliths molded in channels of microfluidic devices. *Anal. Chem.* **2002**, *74*, 4081–4088. [CrossRef] [PubMed]
8. Poupart, P.; Le Droumaguet, B.; Guerrouache, M.; Carbonnier, B. Copper nanoparticles supported on permeable monolith with carboxylic acid surface functinality: Stability and catalytic properties under reductive conditions. *Mater. Chem. Phys.* **2015**, *163*, 446–452. [CrossRef]
9. Khalil, A.M.; Georgiadou, V.; Guerrouache, M.; Mahouche-Chergui, S.; Dendrinou-Samara, C.; Chehimi, M.M.; Carbonnier, B. Gold-decorated polymeric monoliths: In-situ vs. ex-situ immobilization strategies and flow through catalytic applications towards nitrophenol reduction. *Polymer* **2015**, *77*, 218–226. [CrossRef]
10. El Kadib, A.; Chimenton, R.; Sachse, A.; Fajula, F.; Galarneau, A.; Coq, B. Functionalized inorganic monolithic microreactors for high productivity in fine chemicals catalytic synthesis. *Angew. Chem. Int. Ed.* **2009**, *48*, 4969–4972. [CrossRef] [PubMed]
11. Sachse, A.; Galarneau, A.; Fajula, F.; Di Renzo, F.; Creux, P.; Coq, B. Functional silica monoliths with hierarchical uniform porosity as continuous flow catalytic reactors. *Microporous Mesoporous Mater.* **2011**, *140*, 58–68. [CrossRef]
12. Siouffi, A.M. Silica gel-based monoliths prepared by the sol-gel method: Facts and figures. *J. Chromatogr. A* **2003**, *1000*, 801–818. [CrossRef]
13. Nakanishi, K.; Minakuchi, H.; Soga, N.; Tanaka, N. Structure design of double-pore silica and its application to HPLC. *J. Sol. Gel Sci. Technol.* **1998**, *13*, 163–169. [CrossRef]
14. Nakanishi, K.; Kobayashi, Y.; Amatani, T.; Hirao, K.; Kodaira, T. Spontaneous formation of hierarchical macro-mesoporous ethane-silica monolith. *Chem. Mater.* **2004**, *16*, 3652–3658. [CrossRef]
15. Galarneau, A.; Iapichella, J.; Bonhomme, K.; Di Renzo, F.; Kooyman, P.; Terasaki, O.; Fajula, F. Controlling the morphology of mesostructured silicas by pseudomorphic transformation: A route towards applications. *Adv. Funct. Mater.* **2006**, *16*, 1657–1667. [CrossRef]
16. Martin, T.; Galarneau, A.; Di Renzo, F.; Fajula, F.; Plee, D. Morphological control of MCM-41 by pseudomorphic synthesis. *Angew. Chem. Int. Ed.* **2002**, *41*, 2590–2592. [CrossRef]
17. Na, K.; Jo, C.; Kim, J.; Cho, K.; Jung, J.; Seo, Y.; Messinger, R.J.; Chmelka, B.F.; Ryoo, R. Directing zeolite structures into hierarchically nanoporous architectures. *Science* **2011**, *333*, 328–332. [CrossRef] [PubMed]
18. Li, X.Y.; Sun, M.H.; Rooke, J.C.; Chen, L.H.; Su, B.L. Synthesis and applications of hierarchically porous catalysts. *Chin. J. Catal.* **2013**, *34*, 22–47. [CrossRef]
19. Hoffmann, F.; Cornelius, M.; Morell, J.; Froba, M. Silica-based mesoporous organic-inorganic hybrid materials. *Angew. Chem. Int. Ed.* **2006**, *45*, 3216–3251. [CrossRef] [PubMed]
20. Koreniuk, A.; Maresz, K.; Odrozek, K.; Jarzębski, A.B.; Mrowiec-Białoń, J. Highly effective continuous-flow monolithic silica microreactors for acid catalyzed processes. *Appl. Catal. A* **2015**, *489*, 203–208. [CrossRef]

21. Szymańska, K.; Pudło, W.; Mrowiec-Białoń, J.; Czardybon, A.; Kocurek, J.; Jarzębski, A.B. Immobilization of invertase on silica monoliths with hierarchical pore structure to obtain continuous flow enzymatic microreactors of high performance. *Microporous Mesoporous Mater.* **2013**, *170*, 75–82. [CrossRef]
22. Kawakami, K.; Sera, Y.; Sakai, S.; Ono, T.; Ijima, H. Development and characterization of a silica monolith immobilized enzyme micro-bioreactor. *Ind. Eng. Chem. Res.* **2005**, *44*, 236–240. [CrossRef]
23. Koreniuk, A.; Maresz, K.; Mrowiec-Białoń, J. Supported zirconium-based continuous-flow microreactor for effective Meerwein-Ponndorf-Verley reduction of cyclohexanone. *Catal. Commun.* **2015**, *64*, 48–51. [CrossRef]
24. Cheung, H.; Tanke, R.S.; Torrence, G.P. *Ullman's Encyclopedia of Industrial Chemistry*; Willey-VCH: Weinheim, Germany, 2012.
25. Szymańska, K.; Odrozek, K.; Zniszczoł, A.; Pudło, W.; Jarzębski, A.B. A novel hierarchically structured siliceous packing to boost the performance of rotating bed enzymatic reactors. *Chem. Eng. J.* **2017**, *315*, 18–24. [CrossRef]
26. Smått, J.H.; Schunk, S.; Linden, M. Versatile double-templating synthesis route to silica monoliths exhibiting a multimodal hierarchical porosity. *Chem. Mater.* **2003**, *15*, 2354–2361. [CrossRef]
27. Pudło, W.; Gawlik, W.; Mrowiec-Białoń, J.; Buczek, T.; Malinowski, J.J.; Jarzębski, A.B. Materials with multimodal hierarchical porosity. *Inzynieria Chemiczna i Procesowa* **2006**, *27*, 177–185.
28. Szymańska, K.; Pietrowska, M.; Kocurek, J.; Maresz, K.; Koreniuk, A.; Mrowiec-Białoń, J.; Widłak, P.; Magner, E.; Jarzębski, A. Low back-pressure hierarchically structured multichannel microfluidic bioreactors for rapid protein digestion—Proof of concept. *Chem. Eng. J.* **2016**, *287*, 148–154. [CrossRef]
29. Mrowiec-Białoń, J. Determination of hydroxyls density in the silica-mesostructured cellular foams by thermogravimetry. *Thermochim. Acta* **2006**, *443*, 49–52. [CrossRef]
30. Stawicka, K.; Diaz-Alvarez, A.E.; Calvino-Casilda, V.; Trejda, M.; Banares, M.A.; Ziolek, M. The role of Brönsted and Lewis acid sites in acetalization of glycerol over modified mesoporous cellular foams. *J. Phys. Chem. C* **2016**, *120*, 16699–16711. [CrossRef]
31. Datka, J.; Turek, A.M.; Jehng, J.M.; Wachs, I.E. Acidic properties of supported niobium oxide catalysts—An infrared-spectroscopy investigation. *J. Catal.* **1992**, *135*, 186–199. [CrossRef]
32. Sachse, A.; Hulea, V.; Finiels, A.; Coq, B.; Fajula, F.; Galarneau, A. Alumina-grafted macro-/mesoporous silica monoliths as continuous flow microreactors for the Diels-Alder reaction. *J. Catal.* **2012**, *287*, 62–67. [CrossRef]
33. Kulkarni, A.A.; Zeyer, K.P.; Jacobs, T.; Kienle, A. Miniaturized systems for homogeneously and heterogeneously catalyzed liquid-phase esterification reaction. *Ind. Eng. Chem. Res.* **2007**, *46*, 5271–5277. [CrossRef]
34. Jermy, B.R.; Pandurangan, A. A highly efficient catalyst for the esterification of acetic acid using n-butyl alcohol. *J. Mol. Catal. A Chem.* **2005**, *237*, 146–154. [CrossRef]
35. Peters, N.E.; Benes, N.E.; Holmen, A.; Keurentjes, J.T.F. Comparison of commercial solid acid catalysts for the esterification of acetic acid with butanol. *Appl. Catal. A* **2006**, *297*, 182–188. [CrossRef]
36. Brunauer, S.; Emmett, P.H.; Teller, E. Adsorption of gases in multimolecular layers. *J. Am. Chem. Soc.* **1938**, *60*, 309–319. [CrossRef]
37. Barrett, E.; Joyner, L.; Halenda, P. The determination of pore volume and area distributions in porous substances. Computations from nitrogen isotherms. *J. Am. Chem. Soc.* **1951**, *73*, 373–380. [CrossRef]

Chemical and Process Engineering 2018, 39 (1), 33–38
DOI: 10.24425/119097

COMPARATIVE STUDY OF CONTINUOUS-FLOW MICROREACTORS BASED ON SILICA MONOLITHS MODIFIED WITH LEWIS ACID CENTRES

Agnieszka Ciemięga*,[1], Katarzyna Maresz[1], Janusz J. Malinowski[1], Julita Mrowiec-Białoń[1,2]

[1] Institute of Chemical Engineering, Polish Academy of Sciences, Bałtycka 5, 44-100 Gliwice

[2] Department of Chemical Engineering and Process Design, Chemical Faculty, Silesian University of Technology, Ks. M. Strzody 9, 44-100 Gliwice

Silica multichannel monoliths modified with zirconia, titania and alumina have been used as reactive cores of microreactors and studied in chemoselective reduction (MPV) of cyclohexanon/benzaldehyde with 2-butanol as a hydrogen donor. The attachment of metal oxides to the silica surface was confirmed by FT–IR spectroscopy, and dispersion of metal oxides was studied by UV–Vis spectroscopy. the catalytic activity of the lewis acid centres in both chemical processes decreased in the order zirconia > alumina > titania. This activity is in good agreement with dispersion and coordination of metal species. good stability of zirconia-grafted reactors was confirmed. high porosity of the monoliths and the presence of large meandering flow-through channels with a diameter of ca. 30 μm facilitate fluid transport and very effective mixing in the microreactors. The whole synthesis process is perfectly in line with trends of modern flow chemistry.

Keywords: flow chemistry, silica monolith, Lewis acid centres, MPV reduction

1. INTRODUCTION

Chemoselective reduction of carbonyl compounds, known as Meerwein-Ponndorf-Verley (MPV) reaction is traditionally carried out in batch reactors. The MPV reaction is a highly selective reduction reaction involving hydrogen transfer mechanism between aldehydes and ketones and secondary alcohols (Zhang et al., 2012). In contrast to a reaction carried out in the presence of hydrogen or strong reducing agents – metal hydrides, the selective reduction of the carbonyl group, allows to obtain α, β – unsaturated alcohols, preserving all other functional groups in the molecule (Corma et al., 2003). This feature is of particular relevance for the pharmaceutical and chemical industries. The MPV reaction with Lewis-type acid centres coordinates only the carbonyl group while multiple bonds remain intact. The reduction is performed under mild process conditions and usually in the presence of metal alkoxides (Campbell et al., 2001). However, these highly selective homogeneous catalysts should be used in stoichiometric amounts relative to the substrates and difficulties in separation are a major limitation of their use. Replacement of the homogeneous catalysts with the heterogeneous ones eliminates some of the drawbacks. The main problem is, however, the sensitivity of immobilized metal alkoxides to moisture, causing a decrease in their activity or deactivation (Quignard et al., 1999).

* Corresponding author, e-mail: akoreniuk@iich.gliwice.pl

Recently, we have proposed a continuous-flow monolithic silica microreactor activated with anchored isolated zirconium species for the MPV reduction to overcome these drawbacks (Koreniuk et al., 2015). This approach fits modern flow chemistry carried out using microreactor technology, which is critical for both significant process intensification and miniaturization. It simplifies chemical processes, facilitates automation and better control, catalyst regeneration and storage, and allows to separate the catalyst from contact with adverse external factors. The microreactors provide a much larger surface area, compared to the conventional reactors, and a very high surface-to-volume ratio enhances heat exchange and mixing (Reschetilowski, 2013). In recent years process miniaturization has opened new paths towards creating a new generation of catalysts.

In this work we compare the performance of continuous-flow microreactors, with Lewis acid centres originated from zirconia, alumina and titania incorporated into silica multichannel monolith, in the MPV reduction of cyclohexanon/benzaldehyde with 2-butanol as a hydrogen donor. Structural, physicochemical properties and catalytic activity of the reactors were studied.

2. EXPERIMENTAL

Silica monolithic supports were synthesized according to a procedure described previously by Koreniuk (Koreniuk et al., 2015). Briefly, a mixture of PEG35000, nitric acid, water, CTAB and TEOS, after complete dissolution, was placed in polypropylene tubes at 40°C, and allowed to gel. The solid rods were treated in 1 M ammonia solution at 90°C, for 9 hours, washed with water and dried. Subsequently, organic template was removed by calcination in air at 550°C.

The monoliths were dried at 200°C prior to functionalization. Modification was carried out using the grafting method. Metal precursors: zirconium isopropoxide, aluminium di-s-butoxide ethylacetoacetate, titanium diisopropoxide bis (acetyloacetonate) were dissolved in ethanol. Monolithic carriers were soaked with the precursor solution to obtain metal/Si mass ratio equal to 0.05, treated one day at 70°C, washed with excess of anhydrous ethanol, evaporated and finally calcined at 500°C.

The structural properties of monoliths were determined using various instrumental techniques. The parameters of mesostructure were calculated from low-temperature nitrogen adsorption isotherms (Micromeritics, ASAP2010). Scanning electron microscopy (Hitachi HD-2300A) and mercury porosimetry (Quantachrome, PoreMaster 60) was applied to determine the size of the flow-through channels created by the system of connected macropores. Studies involving spectroscopic methods FT-IR (Nicolet6700, DRIFT collector) and UV-Vis (Varian, Carry 100, Labsphere DRA-CA-3300) provided information about the physicochemical properties of metal attached to the silica carrier.

Catalytic activity was investigated in Meerwein-Ponndorf-Verley reaction. 2-butanol was used as a hydrogen donor in the reduction of cyclohexanone and benzaldehyde. Experiments were conducted in 4 cm-long microreactors, at 95°C, with the flow rate of 0.03 ml/min. Carbonyl compound/alcohol molar ratio was fixed at 1 : 52. Process efficiency was monitored by gas chromatography (HP-5 column, FID detector). Pressure drop for a reagent mixture was measured using differential pressure controller (UNIC5000, Ex-Calibra).

3. RESULTS AND DISCUSSION

Silica monolithic materials with a trimodal pore structure were prepared using sol-gel process coupled with phase separation and pore templating. Polyethylene glycol undergoes phase separation, induced by

polymerization of TEOS and gives rise to a continuous structure of larger flow-through channels, whereas cationic surfactant used as the template promotes formation of mesopores.

SEM image depicted in Fig. 1 clearly demonstrates a bi-continuous structure consisting of connected macropores and silica skeleton. The highly open and tortuous structure facilitated fluid transport and effective mixing. The average macropore diameter, determined by the mercury porosimetry, was found to be 30 μm and the total pore volume in the monoliths was about 4.2 cm^3/g (Fig. 2).

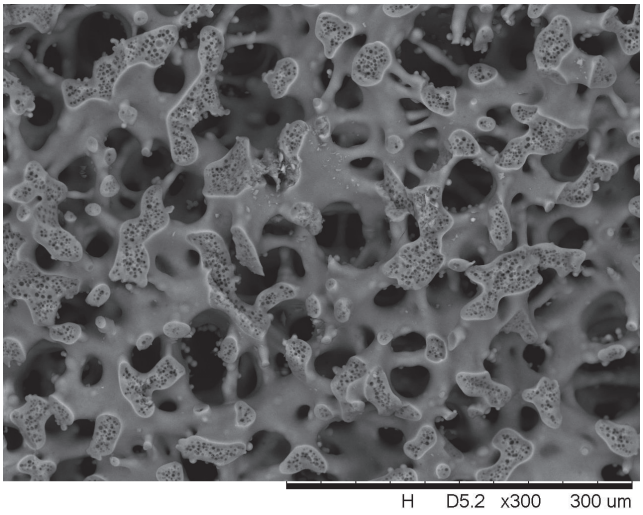

Fig. 1. SEM image of silica monolith

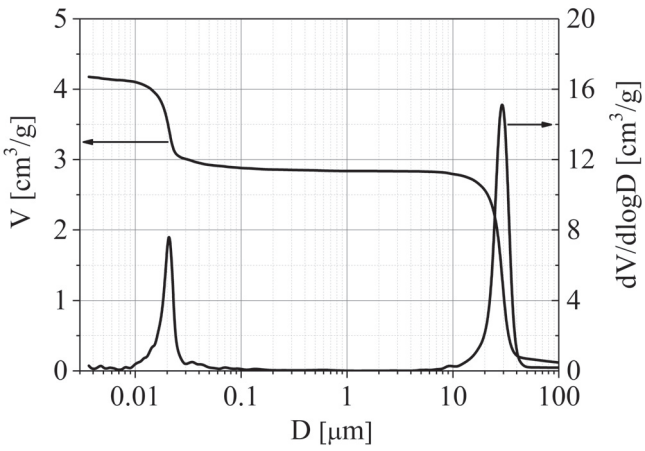

Fig. 2. Pore volume vs. pore diameter for silica monolith obtained by mercury porosimetry; cumulative and differential curves

Texture parameters of the samples were estimated from low temperature adsorption/desorption data. The isotherm, depicted in Fig. 3 is typical for mesoporous materials. Cylindrical pores of average diameters of about 2.5 and 23 nm, generated in silica skeleton, allowed to obtain a large surface area above 300 m^2/g and mesopore volume about 1 cm^3/g, that is still larger than in the most typical mesoporous materials.

FT-IR DRIFT spectra of all the modified samples in the wavelength range of 3700–3800 and 850–1400 cm^{-1} are shown in Fig. 4. The spectrum of untreated silica was used as a reference. A decrease in intensity or complete disappearance of the band at a wavelength of 960 cm^{-1}, assigned to stretching vibration of Si–OH bond, confirm the metal incorporation into the support surface. It is also corroborated by reduced band intensity at 3750 cm^{-1}, which corresponds to isolated hydroxyls on the silica. The broad band in the range of 1000–1250 cm^{-1}, characteristic for the Si–O–Si asymmetric stretching is clearly

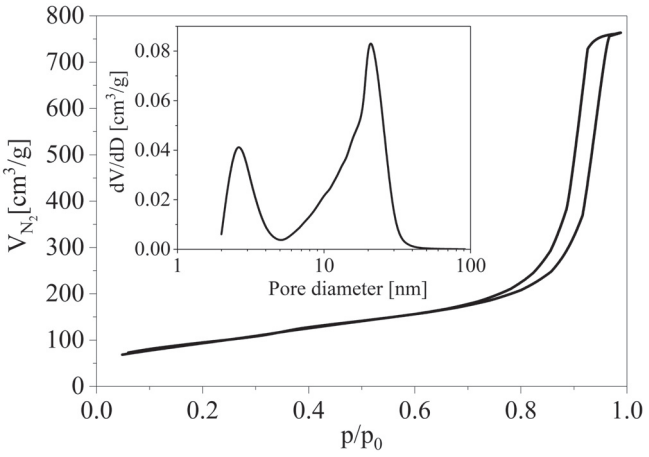

Fig. 3. Adsorption/desorption isotherm and mesopore size distribution of silica monolith

weakened. All these changes are due to Si–O–metal bond formation (Telalovic et al., 2011). Differences between spectra of Al, Zr and Ti functionalized samples can be attributed to a better dispersion of Al and Zr on silica surface. Titanium species tend to agglomerate owing to highly reactive nature of the metal precursor. This finding correlates well with the results obtained from UV–Vis analysis.

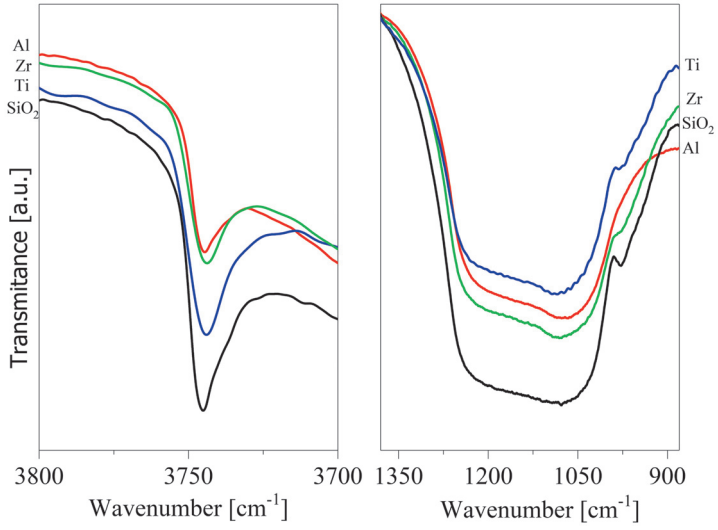

Fig. 4. DRIFT FT-IR spectra of Al-, Ti-, Zr-modified samples

Figure 5 shows UV–Vis spectra for the metal-modified samples. In zirconia-grafted monolith maximum absorption occurred at 209 nm, and it is attributed to ligand-to-metal charge transfer from oxygen ions to isolated zirconium cations in a tetrahedral coordination. The broad absorption band in the range of 200 to 350 nm recorded for titania-modified monolith confirmed the presence of oligomeric titanium-oxygen species in this material. Aluminium deposited onto silica surface was in tetrahedral coordination, confirmed by absorption band with maximum at 265 nm, which corroborates the good distribution of this metal onto silica surface (Beck et al., 2001; Morey et al., 1999).

The results of catalytic studies of the microreactors activated with Al, Zr, Ti oxides are summarized in Fig. 6. As can be seen the highest conversion in the MPV reduction of both cyclohexanone and benzaldehyde was achieved in ZrO_2 functionalized microreactors, and it was almost three times higher than that obtained in the alumina functionalized reactor. It can be related to a slightly better distribution of zirconium species onto the silica surface, and also propensity of the alumina to generate Brønsted acid sides, which do not catalyse the MPV reaction (Shylesh et al., 2009).

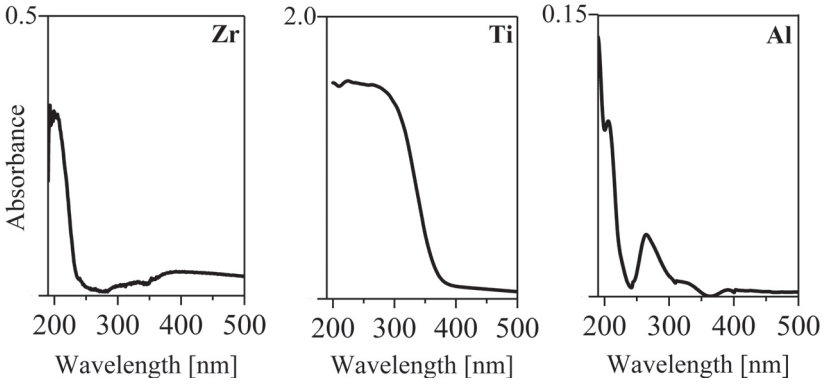

Fig. 5. UV-Vis spectra of Zr-, Ti-, Al-modified samples

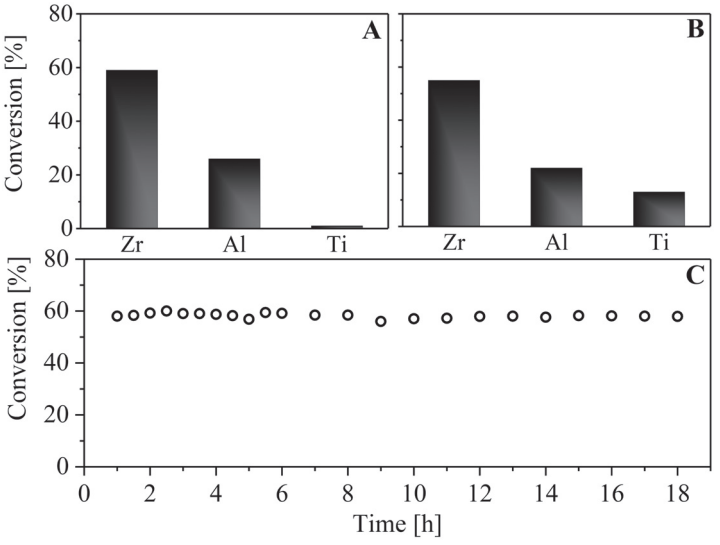

Fig. 6. Average conversion of cyclohexanone (A) and benzaldehyde (B) in zirconia-, alumina- and titania-doped microreactors under the same reaction conditions. Stability of Zr-modified microreactor (C)

Titanium-doped monolith was inactive in cyclohexanone reduction or showed poor activity in case of aldehyde. The formation of large TiO_2 agglomerates, which was confirmed by FT-IR and UV-Vis analysis, has detrimental impact on catalytic properties of the proposed microreactor. Moreover, according to Quignard (Quignard et al., 1999), Ti complexes appeared to be difficult for use in the processes involving alcohols, since they tend to leach into a protic solvent.

The zirconia-modified microreactor was tested in a 18 h-long experiment. It demonstrated good catalytic stability, and only small fluctuations of conversion, ca. 2%, were observed. Pressure drop was monitored during the process, and it was equal to 0.066 kPa/cm for the applied flow rate.

4. CONCLUSIONS

The performed studies clearly show that:

- silica multichannel monoliths can be easily functionalized with Lewis acid centres and used as a core of catalytic microreactors in the Meerwein–Ponndorf–Verley chemoselective reduction of ketones and aldehydes,

- the activity of acid centres in MPV reaction strongly depended on the nature of incorporated metals and their coordination and dispersion,
- the microreactors modified with zirconia, showed better activity in chemoselective reduction of cyclohexanone/benzaldehyde with 2-butanol as a hydrogen donor than those functionalized with alumina and titania,
- good stability of the zirconia-grafted reactors was confirmed.

This work was financed by the National Science Centre (Poland), project No. DEC-188 2014/15/N/ST8/03171.

REFERENCES

Beck C., Mallat T., Burgi T., Baiker A., 2001. Nature of active sites in sol-gel TiO_2–SiO_2 epoxidation catalysts. *J. Catal.*, 204, 428–439. DOI: 10.1006/jcat.2001.3407.

Campbell E.J., Zhou H.Y., Nguyen S.T., 2001. Catalytic Meerwein-Pondorf-Verley reduction by simple aluminum complexes. *Org. Lett.*, 3, 2391–2393. DOI: 10.1021/ol0162116.

Corma A., Domine M.E., Valencia S., 2003. Water-resistant solid lewis acid catalysts: Meerwein-Ponndorf-Verley and Oppenauer reactions catalyzed by tin-beta zeolite. *J. Catal.*, 215, 294–304. DOI: 10.1016/S0021-9517(03)00014-9.

Koreniuk A., Maresz K., Mrowiec-Białoń J., 2015. Supported zirconium-based continuous-flow microreactor for effective Meerwein-Ponndorf-Verley reduction of cyclohexanone. *Catal. Commun.*, 64, 48–51. DOI: 10.1016/j.catcom.2015.01.021.

Koreniuk A., Maresz K., Odrozek K., Jarzębski A. B., Mrowiec-Białoń J., 2015. Highly effective continuous-flow monolithic silica microreactors for acid catalyzed processes. *Appl. Catal. A*, 489, 203–208. DOI: 10.1016/j.apcata.2014.10.047.

Morey M.S., Stucky G.D., Schwarz S., Froba M., 1999. Isomorphic substitution and postsynthesis incorporation of zirconium into MCM-48 mesoporous silica. *J. Phys. Chem. B*, 103, 2037–2041. DOI: 10.1021/jp980844t.

Quignard F., Graziani O., Choplin A., 1999. Group 4 alkyl complexes as precursors of silica anchored molecular catalysts for the reduction of ketones by hydrogen transfer. *Appl. Catal. A.*, 182, 29–40. DOI: 10.1016/S0926-860X(98)00421-9.

Reschetilowski W., 2013. *Principles of microprocess technology. Microreactors in preparative chemistry: Practical aspects in bioprocessing, nanotechnology, catalysis and more*. Wiley-VCH Verlag GmbH & Co. KGaA. 1–12.

Shylesh S., Kapoor M.P., Juneja L.R., Samuel P.P., Srilakshmi Ch., Singh A. P., 2009. Catalytic Meerwein-Ponndorf-Verley reductions over mesoporous silica supports: Rational design of hydrophobic mesoporous silica for enhanced stability of aluminum doped mesoporous catalysts. *J. Mol. Catal. A: Chem.*, 301, 118–126. DOI: 10.1016/j.molcata.2008.11.020.

Telalovic S., Ramanathan A., Ng J. F., Maheswari R., Kwakernaak C., Soulimani F., Hanefeld U., 2011. On the synergistic catalytic properties of bimetallic mesoporous materials containing aluminum and zirconium: The prins cyclisation of citronellal. *Chem. Eur. J.*, 17, 2077–2088. DOI: 10.1002/chem.201002909.

Zhang, Bo, Tang, Minhui, Yuan, Jian, Wu, Lei., 2012. Support effect in Meerwein-Ponndorf-Verley reduction of benzaldehyde over supported zirconia catalysts. *Chin. J. Catal.*, 33, 914–922. DOI: 10.1016/S1872-2067(11)60370-7.

Received 15 October 2016
Received in revised form 09 January 2018
Accepted 12 January 2018

Applied Catalysis A, General 560 (2018) 111–118

Contents lists available at ScienceDirect

Applied Catalysis A, General

journal homepage: www.elsevier.com/locate/apcata

Meervein-Ponndorf-Vereley reduction of carbonyl compounds in monolithic siliceous microreactors doped with Lewis acid centres

Agnieszka Ciemięga[a], Katarzyna Maresz[a], Julita Mrowiec-Białoń[a,b,*]

[a] Institute of Chemical Engineering Polish Academy of Sciences, Bałtycka 5, 44-100 Gliwice, Poland
[b] Department of Chemical Engineering and Process Design, Faculty of Chemistry, Silesian University of Technology, Strzody 7, 44-100 Gliwice, Poland

ARTICLE INFO

Keywords:
MPV chemoselective reduction
Monolithic microreactors
Lewis acid catalysts

ABSTRACT

Meerwein-Ponndorf-Vereley chemoselective reduction of cyclohexanone and benzaldehyde was studied in monolithic continuous-flow microreactors, with various Lewis acid centres derived from different metal precursors, i.e. metal alkoxides, chelated metal alkoxides and salts. The productivities achieved in the microreactors, doped with metal centres terminated by propoxy ligands, were significantly higher, ca. 30%, than those obtained for oxides modified monoliths. The highest efficiency of Zr-doped microreactors was proved and their superiority over aluminium and titanium functionalized ones was demonstrated. Higher efficiency of microreactors compared to batch reactors with powdered catalysts has been shown. Stability of proposed materials has been demonstrated. The catalytic outcomes were correlated with structural and physicochemical properties of materials, obtained using low-temperature nitrogen adsorption, mercury porosimetry, SEM microscopy, ICP-MS, FTIR study and pyridine adsorption.

1. Introduction

In recent years, process miniaturization has opened up new directions in the development of industrial catalytic processes. Traditional systems, in some cases, can be replaced by smaller, more complex modules of microreactors, to provide greater process intensity with lower capital and operating costs. Intensive mixing and rapid heat transfer in the microreactor facilitate efficiency and selectivity of chemical reactions [1,2]. Moreover, the use of microreactors allows almost direct transfer of the laboratory-scale results into industry, and the possibility of combining them into larger segments (numbering-up) significantly simplifies adjusting the size of the installation to the requirements [3–5]. Structural reactors, currently used in industrial practice, have a surface to volume ratio about 20,000 m^2/m^3, and it is ten times more than for traditional packed-bed reactors. The use of opened-structure silica monolithic materials with expanded surface area, as reactive cores of microreactors, enables to increase this parameter by one order of magnitude [6]. The monoliths, obtained by phase separation combined with sol-gel method, featured highly open-structure which consists of connected flow-through macropores, separated by the struts with extended network of mesopores. The macropores, with diameters in the range of 30–50 μm, enable effortless reagents flow during process, while mesopores with bimodal pores diameter, ca. 2.5 and 20 nm, allow to achieve an adequate active species dispersion and to reduce of mass transport resistance, as well. The silica monolithic microreactors, modified with metal oxides [7,8], organic groups [9] or enzymes [10–12], have been successfully applied in a few continuous-flow chemical processes.

Here, we focus on the performance of the monolithic microreactors functionalized with Lewis acid sites in Meerwein-Ponndorf-Vereley (MPV) reduction of carbonyl compounds. This highly selective process allows to transform C=O while other possible reducible bonds, e.g. C=C, are retained [13]. It utilizes the mechanism of hydrogen transfer from secondary alcohol to carbonyl substrate to obtain appropriate, unsaturated alcohol. Corma at al. theoretically studied the mechanism of cyclohexanone reduction with 2-butanol, over Zr-beta zeolites and proved that among seven possible of reagents adsorption positions only the direct coordination of the carbonyl group to the Lewis site allows the reaction to proceed. They proposed mechanism which involves the following steps: adsorption of both ketone and alcohol on the Lewis acid centre, deprotonation of the alcohol, hydride transfer through six-member intermediate state complex and protonation of ketone to form an alcohol [14–17].

Previously, we reported that $Zr(OPr^i)$-based monolithic continuous-flow microreactor has been successfully employed for cyclohexanone reduction via MPV protocol [6,18]. The use of the monolithic microreactor allows to simple immobilization of metal alkoxide providing effective protection against hydrolysis during this modification as well

* Corresponding author at: Institute of Chemical Engineering Polish Academy of Sciences, Bałtycka 5, 44-100 Gliwice, Poland.
E-mail address: jmrowiec@polsl.pl (J. Mrowiec-Białoń).

https://doi.org/10.1016/j.apcata.2018.04.037
Received 16 February 2018; Received in revised form 12 April 2018; Accepted 26 April 2018
Available online 27 April 2018
0926-860X/

as during the reactor operation. It considerably facilitates preparing, operating, regenerating and storage of catalyst. Moreover the beneficial properties of silica carrier structure, preserved after modification with active species, enable to achieve high conversions and selectivity during long-term experiments and it offers trouble-free regeneration.

In the present study we functionalized monolithic supports with various aluminium, zirconium and titanium precursors to generate Lewis acid centres and study their activity in MPV reduction of ketone (cyclohexanone) and aldehyde (benzaldehyde) with 2-butanol and 2-propanol. The impact of metal precursor and metal chemical environment were discussed with respect to detailed structural and physicochemical characteristics. Flow process carried out in the monolithic microreactors was also compared with that realized in batch reactor working with powdered monoliths. A leaching of metals was studied both in continuous-flow and batch system as well.

2. Experimental

2.1. Materials

Synthesis of materials: poly(ethylene glycol) 35,000 (PEG), cetyltrimethylammonium bromide (CTAB), zirconium (IV) propoxide solution 70 wt. % in 1-propanol, aluminium isopropoxide > 98%, titanium diisopropoxide bis(acetylacetonate) 75% in isopropanol were purchased from Aldrich. Tetraethyl ortosilicate (TEOS) and aluminium di-sec-butoxide ethyl acetoacetate 95% were from ABCR, titanium (IV) isopropoxide 97% from Acros Organics, zirconium (IV) oxide chloride octahydrate, zirconium (IV) sulfate tetrahydrate from Alfa Aesar, aluminium nitrate nonahydrate, nitric acid, ammonia solution 25%, anhydrous ethanol from Avantor. All chemicals and solvent were of reagent grade and used without further purification.

Catalytic experiments: cyclohexanone and benzaldehyde were supplied by Aldrich, 2-butanol was from Acros Organics. All reagents used for catalytic studies were dried using 4A molecular sieves.

2.2. Monolith synthesis

Silica monoliths were synthesized following the procedure described in [7]. Briefly, PEG (0.39 g) was dissolved in 1 M HNO_3 (4.48 ml) at room temperature. The mixture was cooled down to 0 °C, and silica precursor (3.47 g) was added dropwise to obtain homogeneous solution. After that CTAB (0.17 g) was added into the mixture and stirred vigorously for 30 min. Glass vessel loaded with 4 cm long polypropylene tubes was filled with prepared solution, sealed and placed at 40 °C for 8 days. Next, the monoliths were put out from the moulds, washed with excess of deionized water and treated with 1 M ammonia solution at 90 °C for 9 h. After washing with distilled water they were dried in air at 40 °C for at least 3 days, followed by air calcination (5 h, 550 °C).

2.3. Catalysts preparation

Monoliths, were embedded into heat-shrinkable PTFE tubes, equipped with special connectors and dried at 200 °C in nitrogen atmosphere. All monoliths were functionalized by grafting method using metal precursor dissolved in ethanol or water. The metal/Si mass ratio was fixed at 0.05. Materials were kept at 70 °C for 24 h. Samples modified with metal alkoxide were washed with solvent, used during impregnation, to remove non-attached species. Finally, they were dried at 110 °C in nitrogen flow, and some of them were calcined at 500 °C for 5 h to obtain microreactors with zirconia, alumina and titania active centres. Silica functionalized with zirconium sulphate was calcined at 750 °C to complete decomposition of sulphate species. For batch experiments freshly prepared monoliths were milled and used as a fine powder catalyst.

The samples were designed using symbol of metal and abbreviation of ligands attached to the metal in precursors (Table 1), and superscript "C" refers to calcined samples.

Table 1
Description of the catalysts.

Sample name	Metal precursor	ICP determined metal/Si mass ratio	M wt.%*
Zr-Pr Zr-Pr^{C}	Zirconium(IV) propoxide	0.053	2.48
Zr-Cl^{C}	Zirconium(IV) oxide chloride octahydrate	0.036	1.69
Zr-Sul^{C}	Zirconium(IV) sulfate tetrahydrate	0.024	1.12
Al-BuEac Al-BuEac^{C}	Aluminum di-sec-butoxide ethylacetoacetate	0.027	1.29
Al-iPr^{C}	Aluminum isopropoxide	0.047	2.26
Al-Nit^{C}	Aluminium nitrate nonahydrate	0.049	2.35
Ti-iPAc Ti-PAc^{C}	Titanium diisopropoxide bis (acetylacetonate)	0.021	1.06
Ti-iPr^{C}	Titanium(IV) isopropoxide	0.046	2.33

^{C} –calcined sample; *related to mass of silica support.

2.4. Materials characterization

The structural properties of the proposed materials were investigated using a number of instrumental techniques. Mesostructured parameters of the monoliths, before and after functionalization, were determined from low-temperature nitrogen adsorption/desorption isotherms obtained at −196 °C (ASAP 2020, Micromeritics). Sample, before measurement, was degassed at 110 °C for 24 h. The specific surface area of materials was calculated using a standard BET method [19]. Pore size distribution and pore volume were determined by BJH method using data from desorption branch of isotherm [20]. The scanning electron microscopy (TM 30000, Hitachi) and mercury porosimetry (PoreMaster 50, Quantachrome) were employed to verify the size of the flow-through macropores. The amount of incorporated metal was determined by ICP-MS (NexION 300D PerkinElmer). FTIR DRIFT spectroscopy (Nicolet 6700, Thermo Line) was used to confirm the presence of functional groups. The studies of pyridine adsorption/desorption were carried out using procedure described in [21]. Briefly, the samples were prepared as self-supporting disc and placed inside IR cell. The spectra were recorded on Equinox 55 Bruker spectrometer with a resolution of 2 cm^{-1} and normalized to the 10 mg sample. Adsorption of pyridine was carried out at 150 °C, and desorption under vacuum at 150 °C and 300 °C. A leaching of the catalyst was checked by ICP-MS analysis of the reaction mixture collected after 8 h of reactor operation (fresh microreactor). Additionally, the continuous-flow process was also carried out in another fresh reactor at low conversion, ca. 35%, and next, the reaction mixture flowing out of the microreactor was placed in batch reactor to check the progress of the reaction without catalyst. Moreover, a leaching test with hot filtration during batch process was performed using crushed Zr-monoliths (fine powder of diameter 100 ± 10 μm).

2.5. Catalytic test

The continuous-flow microreactors with various catalytic centres were tested in Meerwein-Ponndorf-Verley reduction of cyclohexanone and benzaldehyde. 2-butanol was used as the hydrogen donor. The molar ratio of substrates was 1:52. Experiments were conducted for flow rate of 0.03 cm^3/min, at 95 °C. The batch experiments were carried out in three-neck reactor equipped with reflux condenser, thermocouple, heating jacket and sampling connector. Reaction conditions, i.e. temperature, molar ratio of substrate and catalyst loading were similar to those used in the continuous flow process.

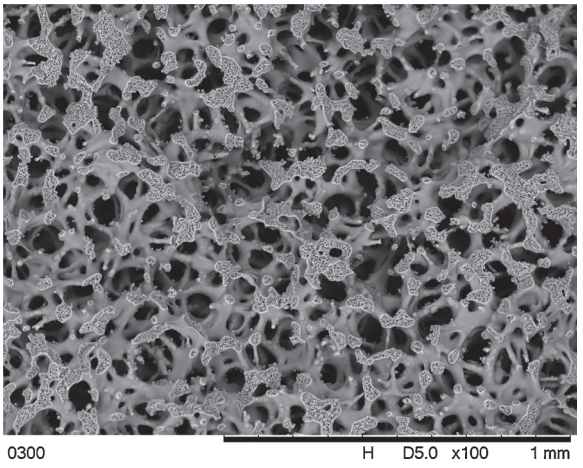

Fig. 1. SEM image of the monolith structure.

The progress of the reaction and selectivity were monitored by gas chromatography (Agilent 7890A, HP-5 column, FID detector).

3. Results

3.1. Structural and physicochemical properties

The structural properties of the monoliths were studied at meso- and macro-scales using different techniques. Tortuous network of flow-through macropores with dimensions in the range of 30–50 μm was confirmed by scanning electron microscopy (Fig. 1). The SEM observations were in line with data from mercury porosimetry (Fig. 2). Total pore volume was ca. 4 cm^3/g. The attractive features of the monoliths, i.e. interconnected macropores and large porosity, translated directly to low-flow-resistance in monolith-based microreactors, what has been shown in our previous papers [22].

Low-temperature nitrogen adsorption measurements complement detailed materials characterization. Isotherms displayed in Fig. 3 and Fig. 4, with the inflection at p/p_0 between 0.8 and 0.9 are typical for mesoporous materials. The sharp slope of this region and the shape of hysteresis loop correspond to cylindrical pores of relatively uniformed size. The values of specific surface area, mesopore volume and average pore diameter are reported in Table 2. Silica skeleton was formed by 30 μm–thick struts, containing two types of mesopores. BJH pore size distribution features the clearly seen maximum at 2.5 nm and 20 nm. Smaller pores originated from surfactant present in synthesis mixture,

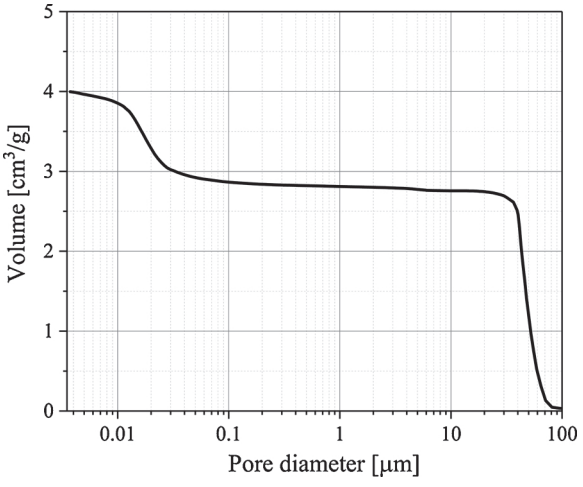

Fig. 2. Cumulative pore volume vs. pore diameter obtained from mercury porosimetry.

while the bigger ones designated as textural pores, were created by connected silica particles, arranged during hydrothermal treatment under basic conditions, owing to Ostwald ripening phenomenon. Both, textural and surfactant templated mesopores contributed to surface area extension and mass and heat limitations diminution, as well.

After functionalization, the volume of mesopores in calcined samples was slightly reduced, contrary to those non-calcined, in which ca. 10% decrease was observed (Table 2). This reduction was caused by the presence of large alkoxy groups and chelating ligands. Small changes in the pore size distribution and surface area recorded after calcination confirmed the uniform deposition of the metal oxide on the silica surface.

FTIR DRIFT spectra of silica and modified samples in the range of 3900 – 700 cm^{-1} are demonstrated in Fig. 5. The spectrum of pristine silica is characterised by broad band in the range of 3200–3700 cm^{-1} corresponding to asymmetric stretching of hydrogen bonded OH groups and bands around 1000–1250 cm^{-1}, 800 cm^{-1}, which are attributed to asymmetric and symmetric stretching vibrations of the Si-O-Si framework. Absorption band centred at 3745 cm^{-1} is characteristic for isolated silanols [20]. Well visible changes in all spectra were observed after modification of the monolithic support with metal species. Following from the left, the intensity of the band at 3745 cm^{-1} was reduced due to Si—O—metal bond formation. Characteristic peaks of asymmetric and symmetric stretching vibrations of C—H bonds in CH_3 group at 2962 and 2920 cm^{-1}, respectively, and at 2858 cm^{-1} for stretching vibration in CH_2 group originate from the unhydrolysed ligands. Spectrum of zirconium modified sample exhibits only peaks characteristic for vibration of propyl groups. In Al— and Ti— modified monoliths additional bands of asymmetric and symmetric C—O vibrations are visible in the region of 1650–1350 cm^{-1}. These bands originate from chelating ligands, i.e. ethylacetoacetate and acetylacetonate. In all modified samples the band accompanied to Si-O-Si is clearly weakened after functionalization. The peak located at 960 cm^{-1} is ascribed to concurrently overlapping bands, which correspond to the stretching of the non-condensed Si-OH groups and stretching mode of SiO_4 entities linked to Zr atoms (Si—O—Zr) [23]. After calcination, the bands assigned to organic ligands disappeared, which confirmed their complete decomposition. In summary, it can be concluded that catalytic centres have been successfully incorporated as metal-ligand and metal-oxide onto silica matrix.

Various metal contents were determined in the modified samples although the same concentration of metal deposited onto silica surface was assumed. The nominal content of all active centres expressed as a metal to silicon mass ratio was equal to 0.05. The amount determined by ICP strongly depended on the type of precursor used in the functionalization process (Table 1). It was almost equal to the nominal one only in samples functionalized with metal alkoxides. In the case of chelating alkoxides that value was twice smaller. It can be attributed to the presence of large ligands which hindered the bonding of part of the species to the silica surface.

The information about surface acidity, i.e. type of acidic centres and their strength was revealed from pyridine adsorption/desorption measurements of calcined materials. Fig. 6 shows the evolution of FTIR spectra recorded for the samples before and after adsorption/desorption. All samples are characterised by typical bands located at 1445 and 1594 cm^{-1}, assigned to pyridine species coordinated to Lewis acid sites, and at 1486 cm^{-1} associated with combination of Brønsted and Lewis acid sites. The concentration of acid sites and their strength are shown in the Table 3. The monolith functionalized with alumina was characterized by the highest concentration of Lewis acid sites, in agreement with largest concentration of the incorporated Al (express as μmol/g). Their acid strength was twice larger than those recorded for zirconia modified material. Moreover, from the number of acid centers, it may be inferred that only ca. 40% of metal atoms (Zr and Al) can be considered as those on the surface. On the other hand, it can be assumed that metal species deposited onto silica surface form a uniform

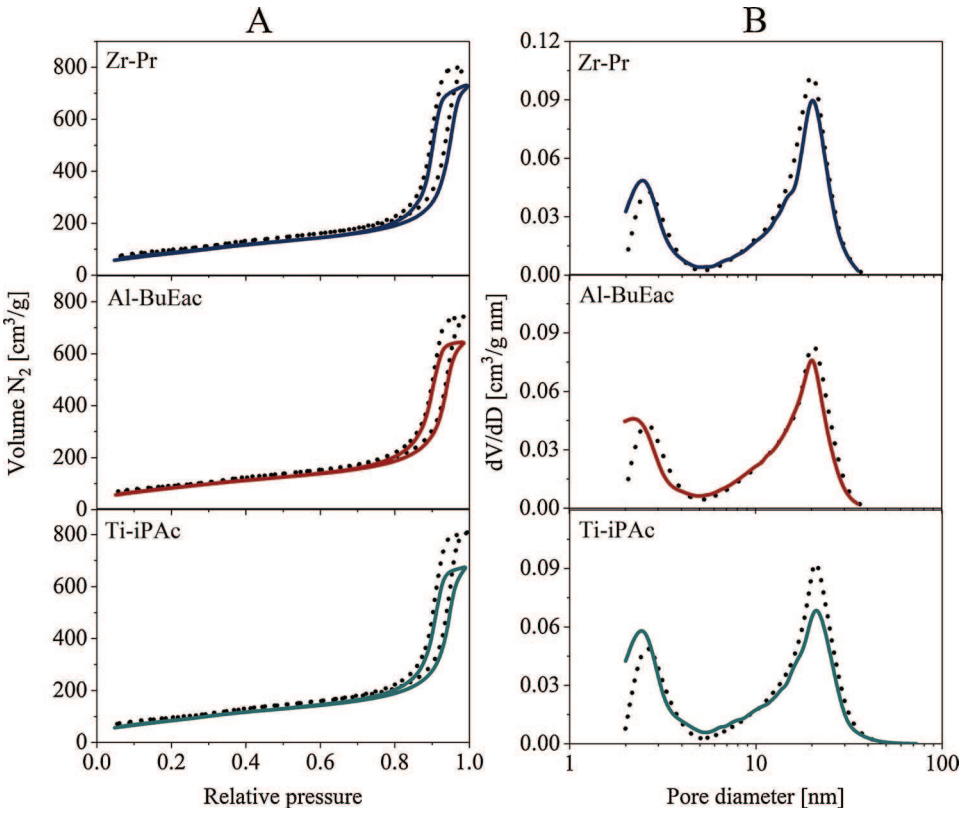

Fig. 3. Nitrogen adsorption/desorption isotherms (A) and pore size distributions (B) of Zr-Pr, Al-BuEac, Ti-iPAc; samples before (straight line) and after (dashed line) functionalisation.

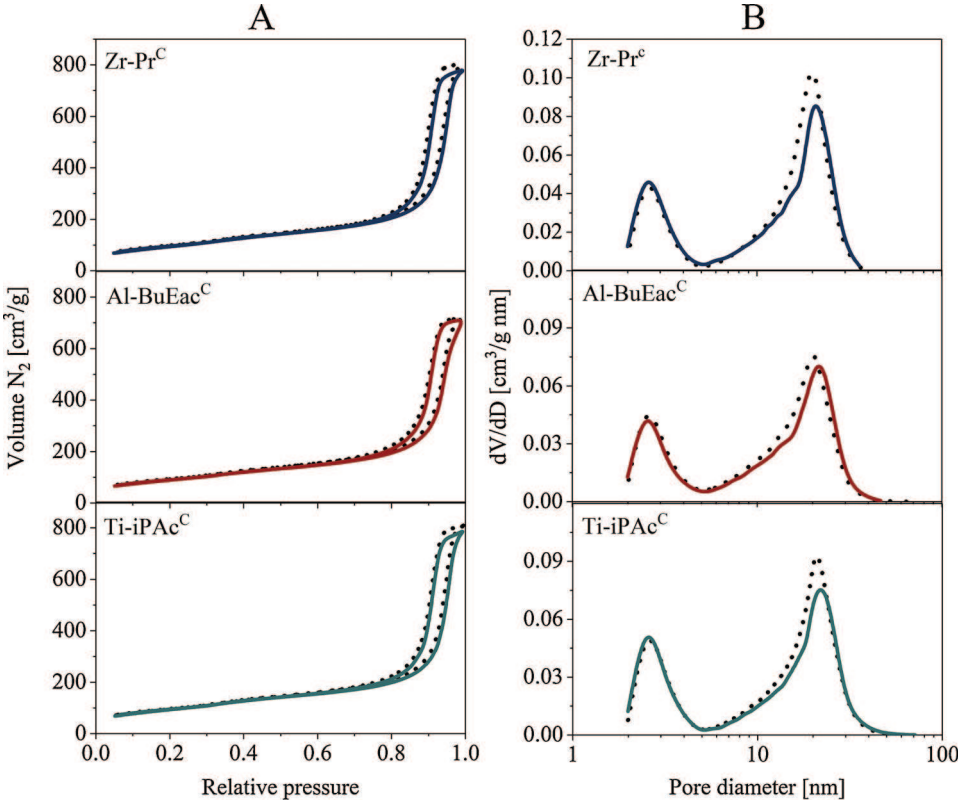

Fig. 4. Nitrogen adsorption/desorption isotherms (A) and pore size distributions (B) of Zr-Pr^{C}, Al-BuEac^{C}, Ti-PAc^{C}; samples before (straight line) and after (dashed line) functionalisation.

Table 2
Texture parameters of pristine monoliths (M) and after modifications with active centres.

Sample	S_{BET} [m^2/g]	V_p [cm^3/g]	d_p [nm]
M	343	1.23	2.6/20
Zr-Pr	322	1.10	2.5/20
M	343	1.23	2.6/20
Zr-Pr^C	337	1.18	2.6/21
M	324	1.14	2.6/20
Al-BuEac	316	0.99	2.2/20
M	326	1.11	2.6/20
Al-BuEac^C	316	1.09	2.5/22
M	338	1.24	2.6/21
Ti-iPrAc	323	1.03	2.4/21
M	338	1.24	2.6/21
Ti-iPrAc^C	333	1.19	2.6/22

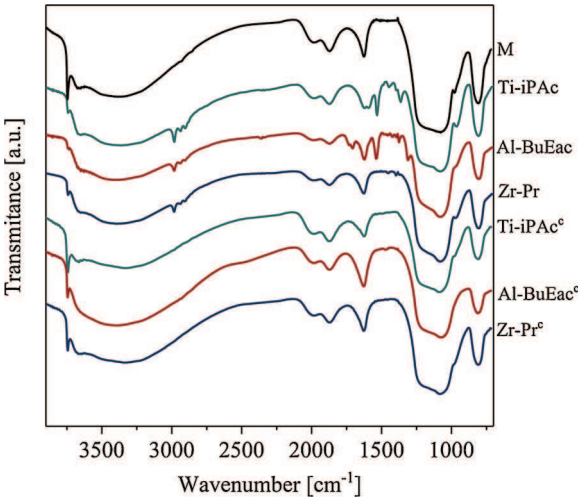

Fig. 5. FTIR spectra of pristine and modified monoliths.

thin layer. Good dispersion of zirconium was confirmed in our previous paper [6]. Titania modified material showed relatively low surface acidity. Monoliths modified with metal alkoxide/chelating metal alkoxide were not subjected to quantitative analysis of acid sites because the method used to determine them requires calcination at 450 °C prior to pyridine adsorption. Therefore, the qualitative analysis was made on the basis of pyridine adsorption at 25 °C. Measurement were carried out using FTIR DRIFT method. Prior to the adsorption samples were vacuum dried at 110 °C. The characteristic band of pyridine

Table 3
Acidic properties of materials.

Sample	Concentration of metal [μmol/g]	Concentration of acid sites [μmol/g]	Acid strength
Zr-Pr^C	260	95	0.30
Al-BuEac^C	444	180	0.65
Ti-iPrAc^C	200	35	0.35

coordinatively bonded to Lewis sites centered at 1454 cm^{-1} was well seen in all materials (Fig. 7). The spectra of samples after vacuum desorption at 150 °C were also recorded. However their course was disturbed not only by the pyridine desorption but also by the decomposition of organic groups.

3.2. Catalytic activity

We employed monolithic microreactors to the MPV reduction of cyclohexanone and benzaldehyde with 2-butanol and 2-propanol. Microreactor with unmodified core did not reveal any catalytic activity. First, we compared the performance of microreactors with metal oxides obtained after calcination of monoliths modified with various precursors (Zr, Al and Ti) in cyclohexanone reduction (Fig. 8). Bar in diagram corresponds to average value of conversion during 6-hours experiment. The highest conversion was observed for zirconia derived from propoxide. In family of zirconium modified microreactors the activity decreased in order Zr-Pr^C > Zr-Cl^C > Zr-Sul^C. However, the changes of activity were larger than those determined for the concentration ofzirconium (Table 1 and see also Table 4), which may indicates same differences in a distribution of metal atoms on the silica surface. The material functionalized with zirconium (IV) oxide chloride showed twice higher activity than that with zirconium (IV) sulphate. The microreactors functionalized with aluminium showed poor activity in cyclohexanone reduction. The best of them - Al-BuEac^C- achieved only about 20% conversion, which is almost three times lower than that recorded in the Zr-Pr^C microreactor. Moreover, its catalytic activity is not in line with the number of acid centers and their strength. Both values are twice as larger as those recorded in Zr-Pr^C (Table 3). Higher performance of zirconium grafted SBA-15 materials over those with aluminium in MPV reduction of various substrates was previously showed in the batch process [24]. A similar relationship was observed for zeolites [25]. The high activity of the ZrO_2 catalyst was attributed to the presence of weak acid – strong base sites that activate the methylene groups in 2-propanol bonded to Lewis acid sites [26]. Lower activity observed in Al-iPr^C than Al-BuEac^C could be assigned to polymerized form of aluminium isopropoxide [27], and, as a consequence, it

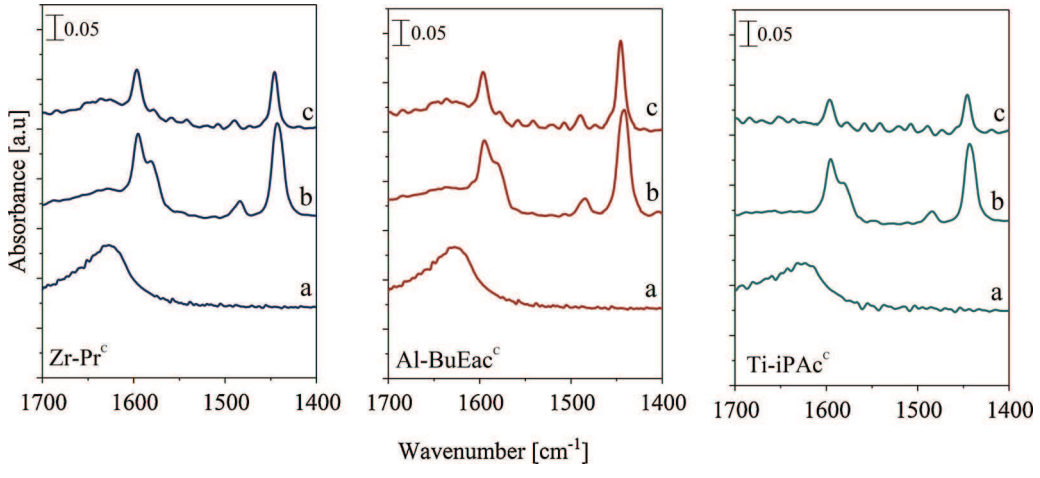

Fig. 6. FTIR spectra of calcined materials before adsorption of pyridine (a); after adsorption at 25 °C (b) and after desorption at 150 °C (c).

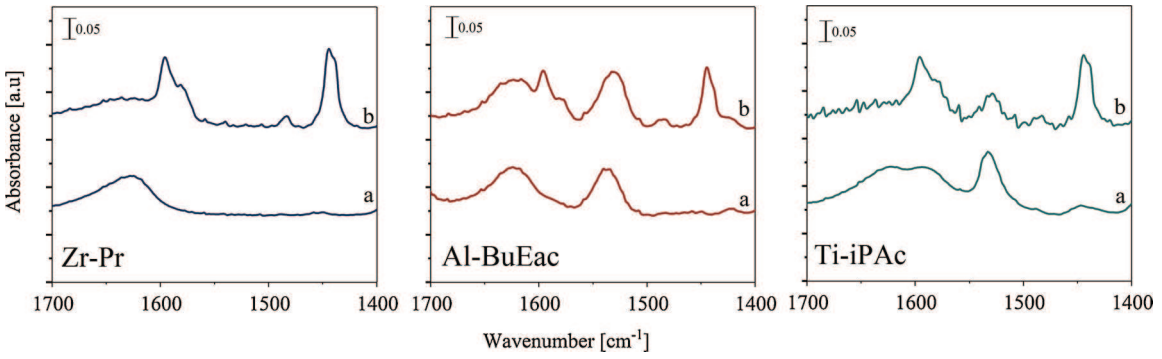

Fig. 7. FTIR DRIFT spectra of materials with organic groups: (a) pristine materials (b) after adsorption of pyridine at 25 °C.

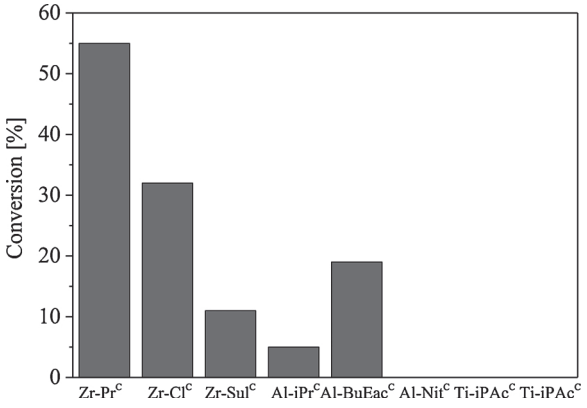

Fig. 8. Conversion of cyclohexanone in microreactors, derived from various metal precursors.

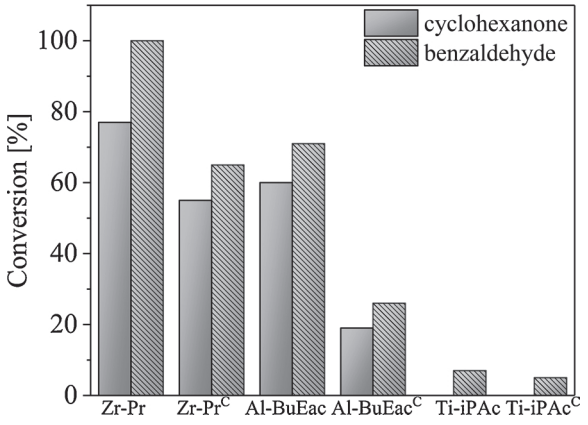

Fig. 9. Conversion of cyclohexanone and benzaldehyde in microreactors with different metal centres and various chemical surroundings.

Table 4
Productivity in reactors with different active species.

Microreactor	Productivity [mmol/gh]	Productivity [mmol/ $mmol_M h$]	Productivity [mmol/gh]	Productivity [mmol/ $mmol_M h$]
	Cyclohexanol		Benzyl alcohol	
Zr-Pr	1.90 (1.62)*	7.25 (6.22)*	2.61	9.96
Zr-Pr^C	1.40	5.38	1.62	6.19
Zr-Cl^C	0.78	4.33	nd	
Zr-Sul^C	0.26	2.17	nd	
Al-BuEac	1.42 (0.94)*	3.18 (2.12)*	1.79	4.0
Al-BuEac^C	0.49	1.09	0.66	1.47
Al-iPr^C	0.13	0.16	nd	
Ti-iPAc	0	0	0.18	0.94
Ti-iPAc^C	0	0	0.13	0.63

*Productivity in batch reactor; nd – not determined.

resulted probably in poorer dispersion of alumina. Al-Nit^C was found to be inactive in cyclohexanone reduction. Titanium functionalized microreactors did not show any activity in this reaction. Such behaviour is in line with data obtained for pure titania and zirconia catalysts in MPV reduction of cyclohexanone with 2-propanol [26].

Further catalytic experiments were carried out with microreactors modified with alkoxides, i.e. zirconium (IV) propoxide, aluminium di-sec-butoxide ethylacetoacetate and titanium diisopropoxide bis(acetylacetonate) using both calcined and non-calcined monoliths. Fig. 9 clearly shows higher activity of acidic sites in reduction of benzaldehyde than that of cyclohexanone, regardless of whether the metal was in the form of an oxide or as a complex with organic ligands. The microreactors with metal coordinated by oxo-ligands exhibited significantly lower activity than their non-calcined counterparts in both studied reactions. This was especially noticeable in the case of aluminium modified monoliths, i.e. an almost three-fold decrease in conversion was recorded. As it was reported in our previous paper [18] in zirconium modified samples, surface OR/OH groups facilitate ligand exchange between carbonyl compound and alcohol. The performance of the microreactors in cyclohexanone and benzaldehyde reduction confirmed that aldehyde can be easier transformed to the corresponded alcohols than ketone. Similar observation were done by Quignard at al. [28]. Furthermore, even the Ti-microreactor showed some activity in the benzaldehyde reduction. Molecular size of both substrates is smaller than 1 nm, therefore the pores in monoliths do not hinder an access of reagents to catalytic centres, and hence the performance of the microreactors should not be related to the monolith structure.

Productivity achieved in the microreactors, was calculated using Eq. (1) and collected in Table 3:

$$P = \frac{C_0 \bullet Conv \bullet F}{m_r} \left[\frac{mmol}{g \bullet h} \right] \quad (1)$$

where: C_0 - initial concentration [mmol/cm^3], Conv - conversion [-], F - flow rate [cm^3/h], m_r - mass of reactor's core [g]. Productivity was also referred to metal content [mmol/$mmol_M$ h].

Zirconium functionalized microreactors provided better productivities than those with aluminium. The highest value, of about 2.6 mmol/gh (9.96 mmol/$mmol_M$ h), was obtained for benzaldehyde reduction using Zr-Pr microreactor, due to the total substrate conversion. It should be noted that the productivity achieved in the microreactors, doped with centres terminated by OPr entities, was significantly higher, than those obtained for oxides modified monoliths. This relationships was observed for both substrates and all studied reactors. It evidences a superiority of the propoxy-surrounded centres in MPV reduction over other ones, which have been showed previously for zirconium species [18]. It seems, that activity probably depends on the coordination number (CN) of zirconium incorporated onto silica surface. In oxide CN

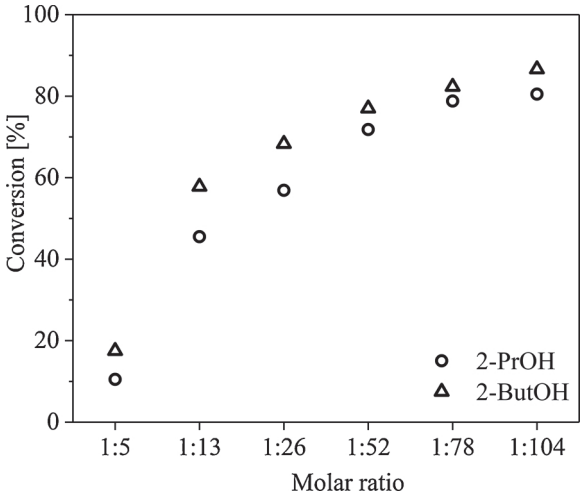

Fig. 10. Conversion of cyclohexanone vs. molar ratio of ketone to alcohol.

is equal 7 [29] or 8 [30], whereas the pristine CN = 4 of zirconium in the alkoxide was preserved in propoxy- and hydroxy-surrounded cations. Such behaviour was supported for zirconium modified monoliths using UV–vis analysis and showed in our previous publication in Microporous and Mesoporous Materials [6]. Lower CN of metal probably favors faster coordination of substrates by zirconium sites to form six-membered transition state ring, which is considered to be a determining step in the reaction rate [14,31]. Moreover, in case of modified aluminium and titanium alkoxide the chelating ligands allow better control of hydrolysis and thereby provide better distribution of active species onto silica surface.

We also compared the use of 2-butanol and 2-propanol in reduction of cyclohexanone and their molar ratio to ketone. The conversions obtained for 2-butanol were slightly higher than for 2-propanol throughout the wide range of substrate concentrations used in the experiments (Fig. 10). Moreover, the continuous growth of the conversion was observed with increasing concentration of alcohol. Thus, no maximum conversion was observed, which was found for tin modified mesoporous molecular sieves of MCM-41 type [32]. Possible explanation is that due to the fast transport in the large mesopores present in monoliths and under flow conditions no interference was observed in the coordination of ketone with Lewis acid sites.

Finally, the performances of flow and batch reactors were compared. Fig. 11 shows the conversions of cyclohexanone in batch reactors using crushed monoliths. The reaction conditions were identical for

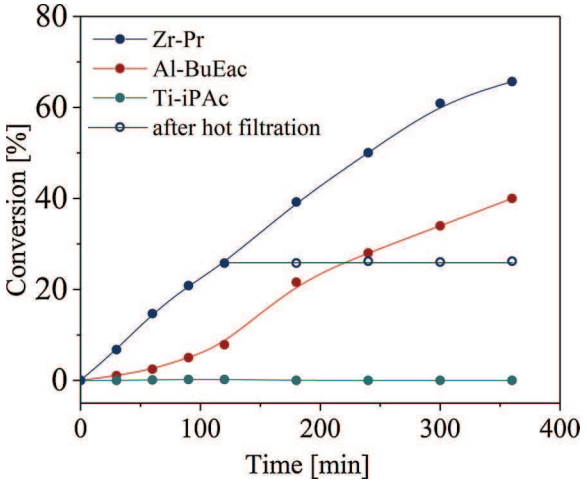

Fig. 11. Conversion of cyclohexanone in batch reactors vs. time, and after fast filtration (lines are only guides to the eye).

Table 5
Literature data on MPV process for different catalytic systems.

No.	Catalyst	Productivity [mmol/gh]	Reaction conditions: H-donor substrates molar ratio temperature	Lit.
	CYCLOHEXANOL			
1	10Zr@MCM-41	1.02	2-BuOH 1:50 100 °C	[35]
2	ZrO_2	0.66	2-PrOH 1:62, 120 °C	[26]
3	ZS-5	2.28	2-PrOH 1:64 82 °C	[36]
	BENZYL ALCOHOL			
4	5%ZrO_2/Si-MCM-41	1.10	2-PrOH 1:20 82 °C	[37]
5	SN/MCM-41(Me 2%)	0.96	2-BuOH 1:50 100 °C	[32]
6	ZrO_2	1.14	2-PrOH 1:52 60 °C	[38]

entry 1–5 – batch reactor; entry 6- packed-bed reactor.

both, flow and batch processes. Conversion in reactor with Zr-modified sample was 1.7 times higher than that in Al-catalyst, similar relationship was observed in the microreactors counterparts. The conversion and productivity in batch process (Table 3) were smaller than those achieved in the flow reactors. This confirms the observed process intensification in microreactors due to fast transport in thin fluid layers resulted in a notably decreased contact time [33], and thus higher performances in MPV process.

Literature data on MPV process carried out for five catalytic systems in batch reactor and one flow process performed in packed-bed reactor are shown in Table 5. The reaction conditions were quite similar to those used in our experiments. The data clearly support advantages of monolithic microreactors functionalized with zirconium and aluminium, i.e. higher productivity (excluding entry 3) of cyclohexanol and benzyl alcohol were obtained (Table 4).

3.3. Stability

Three approaches have been used to study the leaching of the metals incorporated into silica surface of the monoliths, i.e. i) ICP-MS analysis for the presence of metal ions in the products, ii) examination of the course of reaction after fast filtration of catalyst in batch process using crushed monoliths, and iii) examination of the course of reaction in batch process using reaction mixture flowing out of the microreactor (conversion achieved in microreactor was 35%). ICP-MS analysis showed that only leaching of the titanium ions occurred. After 8 h of the process, ca. 3 wt. % loss of Ti was determined. It is in line with previous studies showing the tendency of titanium leaching in polar solvents [28]. Aluminium and zirconium were not detected in the post-reaction solution of the processes carried out in the Zr-Pr and Al-BuEac microreactors. No reaction progress was recorded in the processes carried out after separation of the catalyst, both in the continuous and batch experiments (Fig. 11). It undoubtedly confirmed a lack of metal leaching in the Zr- and Al-modified microreactors.

Stability of the catalytic properties of for zirconium modified microreactors was confirmed in our previous papier [18] and also in manuscript recently accepted for publication [34]. We also compared structural properties (data from nitrogen adsorption) of fresh microreactor and after eighteen-hour catalytic process, and no noticeable

changes were found.

4. Conclusions

Comparative studies of the monolithic continuous-flow silica microreactors modified with different Lewis acids were performed in MPV reduction of cyclohexanone and benzaldehyde with 2-butalol and 2-propanol. The favourable structure of monoliths, which were applied as reactive cores, was preserved after functionalization. Strong impact of a metal type and its chemical environment were observed. All studied Lewis acid centres were more active in reduction of the benzaldehyde than for cyclohexanone. Regardless of the type of metal, the Lewis centres coordinated with alkoxy ligands showed higher activity, ca. 30% in benzaldehyde reduction than those of oxide type. The highest productivity was achieved in Zr-propoxide incorporated microreactor, and it was ca. twice larger than that recorded for aluminium Lewis acid sites. Titanium centres hardly revealed activity in aldehyde reduction. On the whole, the metal alkoxides appeared to be more effective precursors for creation of Lewis acid centres than inorganic salts which resulted in significantly higher activity of the catalysts. Lewis sites in the form of metals terminated by alkoxy/hydroxo groups preserved their low coordination number in contrast to the oxide forms. Smaller coordination numbers favored faster coordination of substrates to acid sites and thus higher reaction rate. FTIR studies, using pyridine as a probe molecule, indicated that Lewis acid centres were present in the synthesized materials, what resulted in an excellent selectivity of the studied reactions. Microreactors` benefits over batch reactors were pointed, including better catalytic performance due to favoured structure, which provides good mixing conditions and unrestricted mass and heat transfer. Good stability of zirconium and aluminium modified materials has been confirmed.

Acknowledgment

Financial support from the Polish National Science Centre (project no. DEC-2014/15/N/ST8/03171) is gratefully acknowledged.

References

[1] W. Reschetilowski, Principles of Microprocess Technology, Microreactors in Preparative Chemistry: Practical Aspects in Bioprocessing, Nanotechnology, Catalysis and More. Wiley-VCH Verlag GmbH & Co. KgaA, 2013.
[2] X. Wang, J. Zhu, H. Bau, R.J. Gorte, Catal. Lett. 77 (2001) 173–177.
[3] T. Wirth, Microreactors in Organic Chemistry and Catalysis, 2nd edition, Wiley-VCH, Weinheim, 2013.
[4] F.H. Kriel, S. Woollam, R.J. Gordon, R.A. Grant, C. Priest, Microfluid. Nanofluid. 20 (2016) 138.
[5] A. Nagaki, K. Hirose, O. Tonomura, S. Taniguchi, T. Taga, S. Hasebe, N. Ishizuka, J. Yoshida, Org. Proc. Res. Dev. 20 (2016) 687–691.
[6] A. Ciemięga, K. Maresz, J. Mrowiec-Białoń, Microporous Mesoporous Mater. 252 (2017) 140–145.
[7] A. Koreniuk, K. Maresz, K. Odrozek, J. Mrowiec-Białoń, Microporous Mesoporous Mater. 229 (2016) 98–105.
[8] A. Sachse, V. Hulea, A. Finiels, B. Coq, F. Fajula, A. Galarneau, J. Catal. 287 (2012) 62–67.
[9] A. Koreniuk, K. Maresz, K. Odrozek, A.B. Jarzębski, J. Mrowiec-Białoń, Appl. Catal. A Gen. 489 (2015) 203–208.
[10] K. Labus, K. Szymańska, J. Bryjak, A.B. Jarzębski, Chem. Pap. 69 (2015) 1058–1066.
[11] K. Szymańska, M. Pietrowska, J. Kocurek, K. Maresz, A. Koreniuk, J. Mrowiec-Białoń, P. Widłak, E. Magner, A. Jarzebski, Chem. Eng. J. 287 (2016) 148–154.
[12] K. Szymańska, K. Odrozek, A. Zniszczoł, G. Torrelo, V. Resch, U. Hanefeld, A.B. Jarzębski, Catal. Sci. Technol. 6 (2016) 4882–4888.
[13] M.A. Aramendia, V. Borau, C. Jimenez, J.M. Marinas, J.R. Ruiz, F. Urbano, Appl. Catal. A Gen. 249 (2003) 1–9.
[14] M. Boronat, A. Corma, M. Renz, J. Phys. Chem. B 110 (2006) 21168–21174.
[15] M. De bruyn, M. Limbourg, J. Denayer, G.V. Baron, V. Parvulescu, P.J. Grobet, D.E. De Vos, P.A. Jacobs, Appl. Catal. A Gen. 254 (2003) 189–201.
[16] J. Wang, K. Okumura, S. Jaenicke, G.K. Chuah, Appl. Catal. A Gen. 493 (2015) 112–120.
[17] Y. Zhu, S. Liu, S. Jaenicke, G. Chuah, Catal. Today 97 (2004) 249–255.
[18] A. Koreniuk, K. Maresz, J. Mrowiec-Białoń, Catal. Commun. 64 (2015) 48–51.
[19] S. Braunauer, P.H. Emmet, E. Teller, J. Am. Chem. Soc. (1938) 309–319.
[20] E. Barrett, L. Joyner, P. Halenda, J. Am. Chem. Soc. 73 (1951) 373–380.
[21] K. Góra-Marek, M. Derewiński, P. Sarv, J. Datka, Catal. Today 101 (2005) 131–138.
[22] A. Ciemięga, K. Maresz, J.J. Malinowski, J. Mrowiec-Białoń, Catalysts 7 (2017).
[23] A.Z. Jia, J. Li, Y.Q. Zhang, Y.J. Song, S.X. Liu, Mat. Sci. Eng. C 28 (2008) 1217–1226.
[24] Y.Z. Zhu, S. Jaenicke, G.K. Chuah, J. Catal. 218 (2003) 396–404.
[25] Y.Z. Zhu, G. Chuah, S. Jaenicke, J. Catal. 227 (2004) 1–10.
[26] T. Komanoya, K. Nakajima, M. Kitano, M. Hara, J. Phys. Chem. C 119 (2015) 26540–26546.
[27] N.Y. Turova, E.P. Turevskaya, V.G. Kessler, M.I. Yanovskaya, The Chemistry of Metal Alkoxides, Springer, 2002.
[28] F. Quignard, O. Graziani, A. Choplin, Appl. Catal. A Gen. 182 (1999) 29–40.
[29] Holleman-Wiberg, Inorganic Chemistry, Academic Press, 2001.
[30] J. Livage, Catal. Today 41 (1998) 3–19.
[31] A. Corma, M.E. Domine, S. Valencia, J. Catal. 215 (2003) 294–304.
[32] P.P. Samuel, S. Shylesh, A.P. Singh, J. Mol. Catal. A Chem. 266 (2007) 11–20.
[33] W. Ehrfeld, V. Hessel, H. Lowe, Microeactors: New Technology for Modern Chemistry, Willey-VCH, Weinheim, 2000.
[34] A. Ciemięga, K. Maresz, J.J. Malinowski, J. Mrowiec-Białoń, Chem. Process Eng. 39 (2018) 33–38.
[35] S. Shylesh, M.P. Kapoor, L.R. Juneja, P.P. Samuel, C. Srilakshmi, A.P. Singh, J. Mol. Catal. A Chem. 301 (2009) 118–126.
[36] G. Li, W.H. Fu, Y.M. Wang, Catal. Commun. 62 (2015) 10–13.
[37] B. Zhang, M. Tang, J. Yuan, L. Wu, Chin. J. Catal. 33 (2012) 914–922.
[38] C. Battilocchio, J.M. Hawkins, S.V. Ley, Org. Lett. 15 (2013) 2278–2281.

catalysts

MDPI

Article

Selective Reduction of Ketones and Aldehydes in Continuous-Flow Microreactor—Kinetic Studies

Katarzyna Maresz [1,*], Agnieszka Ciemięga [1] and Julita Mrowiec-Białoń [1,2]

[1] Institute of Chemical Engineering Polish Academy of Sciences, Bałtycka 5, 44-100 Gliwice, Poland; akoreniuk@iich.gliwice.pl (A.C.); jmrowiec@polsl.pl (J.M.-B.)

[2] Department of Chemical Engineering and Process Design, Silesian University of Technology, Ks. M. Strzody 7, 44-100 Gliwice, Poland

* Correspondence: k.kisz@iich.gliwce.pl; Tel.: +48-32-231-08-11

Received: 24 April 2018; Accepted: 18 May 2018; Published: 22 May 2018

Abstract: In this work, the kinetics of Meerwein–Ponndorf–Verley chemoselective reduction of carbonyl compounds was studied in monolithic continuous-flow microreactors. To the best of our knowledge, this is the first report on the MPV reaction kinetics performed in a flow process. The microreactors are a very attractive alternative to the batch reactors conventionally used in this process. The proposed micro-flow system for synthesis of unsaturated secondary alcohols proved to be very efficient and easily controlled. The microreactors had reactive cores made of zirconium-functionalized silica monoliths of excellent catalytic properties and flow characteristics. The catalytic experiments were carried out with the use of 2-butanol as a hydrogen donor. Herein, we present the kinetic parameters of cyclohexanone reduction in a flow reactor and data on the reaction rate for several important ketones and aldehydes. The lack of diffusion constraints in the microreactors was demonstrated. Our results were compared with those from other authors and demonstrate the great potential of microreactor applications in fine chemical and complex intermediate manufacturing.

Keywords: Meerwein–Ponndorf–Verley reduction; kinetics; flow microreactor

1. Introduction

A reduction of carbonyl bond is a widespread route for the synthesis of alcohols. However, the reaction, classically catalyzed by noble metals and carried out in the presence of molecular hydrogen, reveals significant limitations, including low selectivity, high sensitivity to sulfur-containing substrates, and high-pressure requirements. The pharmaceutical industry is concerned with the purity of its products. The Meerwein–Ponndorf–Verley (MPV) reaction is an attractive method of synthesizing unsaturated alcohols from ketones or aldehydes using secondary alcohols instead of gaseous hydrogen. According to a generally accepted mechanism of the MPV reaction, the carbonyl group acts as a hydrogen acceptor and alcohol as a hydrogen source. The hydrogen transfer occurs when both substrates are simultaneously coordinated to the same Lewis acidic site (Scheme 1). The formation of a six-membered transition state ring is considered to be a determining step in the reaction rate.

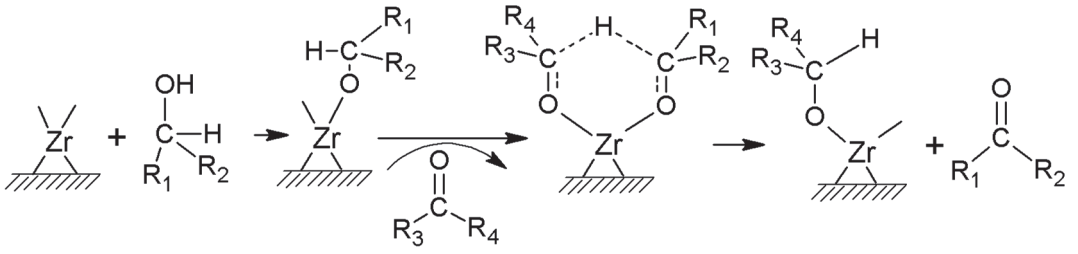

Scheme 1. The mechanism of Meerwein–Ponndorf–Verley (MPV) reduction.

Inexpensive and non-toxic hydrogen donors and catalysts, mild reaction conditions, and exceptional chemoselectivity render this method of reduction favorable over alternatives. Among many active species, such as Zr [1,2], Al [3,4], Mg [3,5], and B [6,7], which are considered to be active catalysts for MPV reduction, zirconium has been shown to be one of the most promising. In the literature, batch processes are predominantly described with the use of numerous catalysts, e.g., homogeneous alkoxides [8,9], zeolites [10,11], mesoporous sieves [12–14], and hydrotalcite [15]. Nevertheless, the tedious separation of homogenous catalysts at the end of the process leads to its deactivation and non-reusability. Powdered catalysts ensure significant benefits over its homogeneous counterparts. However, filtration is an additional time- and cost-consuming step in the technological line. Flow microreactors allow one to overcome these drawbacks and have additional advantages, i.e., high surface-to-volume ratio, improved reaction parameter control, a small equipment size, and a flexibility of module arrangement.

Flow chemistry is perspective and still not explored field in the area of chemoselective MPV reduction. Battilocchio et al. reported the protocol for synthesizing various alcohols from aromatic and aliphatic carbonyl compounds using a packed-bed reactor filled with zirconium hydroxide catalyst [16]. In our previous works [17–19], we demonstrated excellent activity of zirconium-doped silica monolithic microreactors in cyclohexanone reductions and their improved performance compared with the batch process. It was shown that zirconium species terminated with propoxy ligands featured the highest activity in MPV reduction among various Lewis centers immobilized onto monoliths' surfaces used as reactive cores in microreactors. Extensive studies of structural, physicochemical, and catalytic properties revealed the high efficiency of the proposed microreactors.

In this work, we present the kinetic studies of MPV reduction with the use of various carbonyl compounds and 2-butanol as a hydrogen donor. The experiments were performed in continuous-flow zirconium-propoxide-functionalized microreactors of different lengths.

We determined the kinetic parameters, hardly presented for the MPV reduction process carried out in a flow regime. The results of the flow and batch reactors were compared with those of other authors. The kinetic data are crucial to determine the optimum process conditions through the selection of appropriate catalysts and reaction parameters. The knowledge of basic issues related to the course of reactions allows one to set new, more effective paths for conducting processes. Despite the possibility of theoretical computer simulation of the behavior of the reaction system, the experimental determination of the kinetic equation parameters is still necessary for the development of the reactor model.

2. Results

The characterization of siliceous monolithic microreactors functionalized with zirconium species and their catalytic properties were described in our previous papers [17,18]. Kinetic studies were performed in the microreactors featured by the exceptionally low back-pressure. It resulted from the unique structure of cylindrical-shape monoliths applied as reactive cores [20]. Briefly, monoliths were characterized by a continuous, macroporous flow-through structure (macropores in the range of 30–50 μm), extended with mesopores of bimodal size distributions (3/20 nm) and a high surface area (340 $m^2 \cdot g^{-1}$) (Figure 1). The monoliths were functionalized with zirconium propoxide to obtained

Lewis acid sites on the silica surface. The zirconium cations were terminated by propoxy/hydroxo ligands, which appeared to be very active catalytic centers [18,19]. The concentration of zirconium, determined by ICP MS analysis, was 7.03 wt % (in relation to the mass of silica support) in all studied microreactors.

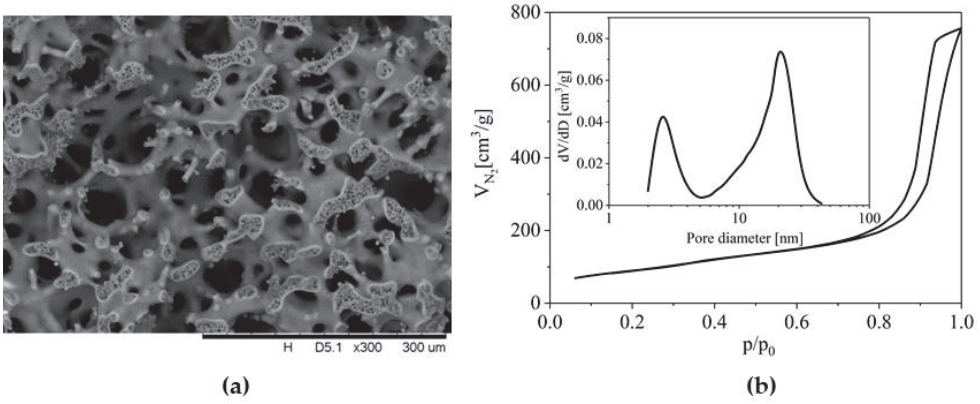

Figure 1. (**a**) SEM image of silica monolith structure; (**b**) nitrogen adsorption/desorption isotherm and pore size distribution (insert).

Material functionalization with zirconium precursor did not considerably influence the structural properties of the support. Only a small decline of the surface area and mesopore volume was observed. All features have been preserved after multiple reaction cycles.

Detailed studies of the kinetic experiment were performed for the MPV reduction of cyclohexanone with 2-butanol. First, we checked whether diffusion or activation controls the reaction rate. External mass transfer limitations are a common phenomenon in porous materials. To exclude the impact of diffusional effects on the reaction kinetics, the performance of microreactors with monolithic cores of different lengths were compared with respect to the same residence time, equal to 5 min. Similar conversions of cyclohexanone, about 40%, were achieved in all microreactors of a 1–8 cm length, which evidenced the lack of transport constraints (Figure 2).

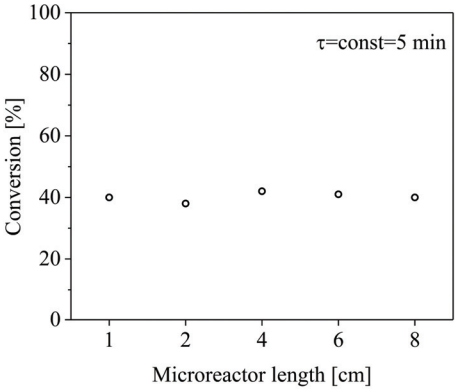

Figure 2. Conversion of cyclohexanone in microreactors of different lengths for a residence time of 5 min.

The results of kinetic experiments for cyclohexanone reduction are depicted in Figure 3. Figure 3a shows the single experimental run carried out for 6 h at 95 °C in a 6 cm long microreactor. The reaction rate constant (Figure 3c) was determined by assuming the first order kinetics and was calculated using Equation (1):

$$\ln(C_0/C) = k\tau \quad (1)$$

where C_0 [mmol·cm^{-3}] is the initial concentration of ketone, C [mmol·cm^{-3}] the substrate concentration after the reaction in the microreactor of a fixed length, k [min^{-1}] the rate constant, τ [min] the residence time.

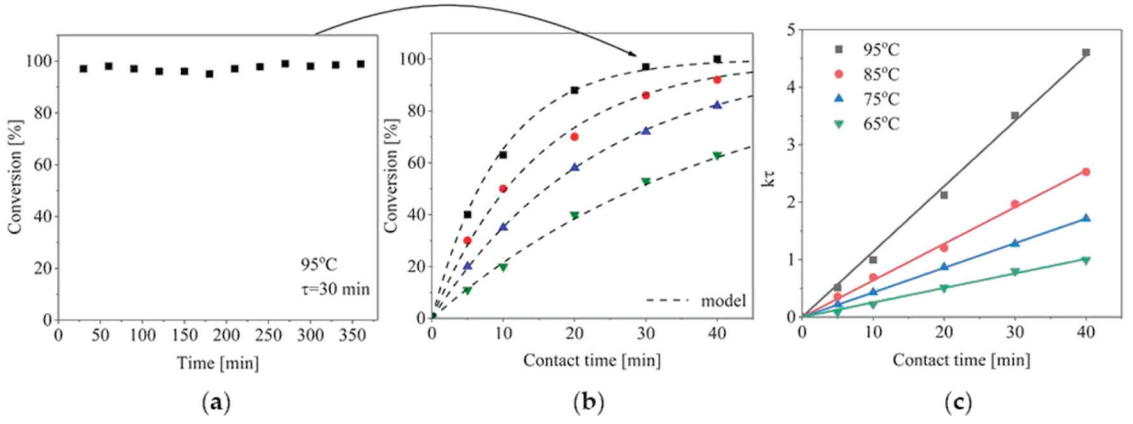

Figure 3. (**a**) Conversion of cyclohexanone in the 6-cm-long microreactor. (**b**) Catalytic results for MPV reduction at 65 °C (▼), 75 °C (▲), 85 °C (●), and 95 °C (■) in the microreactor (points—experiments, lines-model). (**c**) Plot of ln (C_0/C) versus contact time.

Figure 3b confirms good agreement between the experimental data and the model prediction of the first-order kinetics for the MPV process carried out at different temperatures and contact times in the range of 5–40 min. Each point corresponds to the average conversion obtained in microreactor during 6-h-long tests.

The linear relationship rate constant vs. the contact time was observed through the whole temperature range used in the experiments. The experimental data are in line with those calculated from first-order kinetics equation.

Temperature dependence of the rate constant was examined in the range of 65–95 °C and is shown in Figure 4. The activation energy was estimated from linear regression analysis, and it appeared to be 52 kJ·mol^{-1}, and frequency factor k∞ = 2.69 min^{-1}.

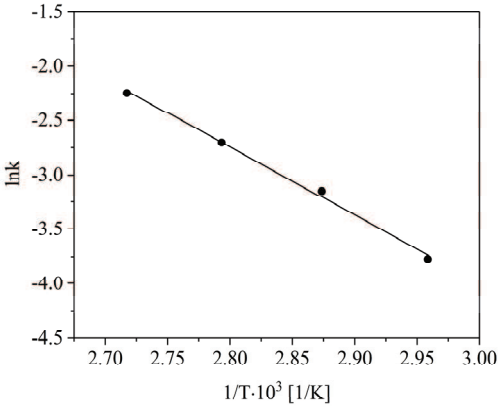

Figure 4. Arrhenius plot for the MPV reduction of cyclohexanone.

The studies of the MPV reduction in the flow process were extended to other ketones and aldehydes, and the results, i.e., the conversion, productivity, and reaction rate constant are summarized in Table 1. Analysis of these data shows that aldehydes are easier to be reduced than ketones. The reaction rate constant of benzaldehyde reduction was 0.212 min^{-1}, while that for cyclohexanone was twice lower. Battilocchio et al. also found that aldehydes, compared with aliphatic ketones,

required a shorter reaction time for complete conversion to alcohols [16]. Steric hindrance is a prevalent factor that affects the reactivity of the substrates. Citral is a mixture of cis- and trans-isomers signified as neral and geranial, respectively. The MPV reduction of citral reveals the preferential formation of its trans product. The yield of geraniol was 20% higher than nerol. The orientation of the carbonyl group to the molecular chain in geranial reduces steric limitations for binding between the Zr center and C=O.

Table 1. Data from catalytic experiments.

Substrate	K [1] [min^{-1}]	Conversion [1,*] [%]	Productivity [1,*] [$mmol \cdot g_{cat}^{-1} \cdot h^{-1}$]	Productivity [2] [$mmol \cdot g_{cat}^{-1} \cdot h^{-1}$]	Productivity [3] [$mmol \cdot g_{cat}^{-1} \cdot h^{-1}$]
	0.106	88	2.22	-	2.28 [21]
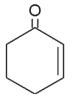	0.021	35	0.9	-	0.11 [15]
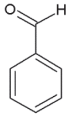	0.212	99	2.64	1.14 [16]	0.36 [10]
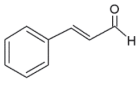	0.081	80	1.92	0.66 [16]	0.48 [5]
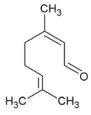	0.031/0.047 [4]	46/61	0.48/0.9	-	0.54 [5]
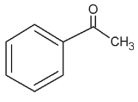	0.026	40	0.96	0.48 [16]	0.12 [22]
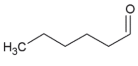	0.08	80	2.1	-	-
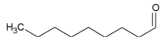	0.041	56	1.32	-	0.72 [23]

[1] this work (reaction temp. 95 °C), [2] in the flow process (data form literature), [3] in the batch process (data form literature); [4] nerol/geraniol; * data for the 4-cm-long microreactor.

The impact of both the steric and electronic effect can be observed in the case of cinnamaldehyde reduction. The low activity can be attributed to the presence of a bulky chain in this substrate and double bond. The productivity in the reduction process of cinnamaldehyde was significantly lower than that for benzaldehyde. The reduction of unsaturated ketone, 2-cyclohexen-1-on, is difficult without affecting the conjugated C=C bond. A significant decrease in conversion was observed compared to the saturated cyclic carbonyl compound (cyclohexanone); nevertheless, the product was obtained with 100% selectivity. Aromatic ketones, compared with cyclic ketones, are more difficult to reduce due to the resonance and inductive effect of the benzene ring [22]. It explains the difference in conversions of cyclohexanone and acetophenone. No products arising from the Tischenko cross reaction or from the aldol condensation [24], were detected for any of the investigated substrates. This evidenced the excellent selectivity of the proposed catalyst.

It should furthermore be highlighted that alcohols produced by the selective hydrogenation of carbonyl-bearing substrates are fine chemicals of primary interest. They are used as flavor additives, and intermediates in drug production. Products of the esterification of cinnamyl alcohol, indole-3-acetic acid, or α-lipoic acid were studied for their antioxidant and anti-inflammatory activity [25], and graniol was checked in colon cancer chemoprevention and treatment [26].

Our results were compared to the literature data for flow and batch processes. To the best of our knowledge, the MPV process using heterogeneous powdered catalyst at flow conditions has only been published in one paper [16]. The productivities of ZrO_2-based reactors toward benzyl alcohol, cinnamyl alcohol, and 1-phenylethanol are nearly 4 times lower than those achieved in the studied monolithic microreactors. Table 1 shows the productivities from batch reactors obtained by other research. They are significantly lower than those obtained in the proposed flow system (except one case). It was due to excellent mixing and mass transfer conditions, offered by innovative monolithic microreactor characterized by high surface-to-volume ratios. Application of the proposed continuous-flow microreactor for the MPV process offers not only enhanced productivity, but also facilitates process handling by excluding contact with reaction media. The latter is of importance when working with dangerous substances.

3. Materials and Methods

Microreactors were fabricated using silica monoliths as cores. The monoliths were obtained by combined sol-gel and phase separation methods described in details in [20]. Briefly, polyethylene glycol (PEG 35 000, Sigma-Aldrich, St. Louis, MO, USA) was dissolved in 1 M nitric acid (Avantor, 65%, Gliwice, Poland). The mixture was cooled in the ice bath and subsequently tetraethoxysilane (TEOS, ABCR, 99%, Karlsruhe, Germany) was added dropwise. After 30 min of stirring, cetyltrimethylammonium bromide (CTAB, Sigma-Aldrich) was added. After complete dissolution, the sol was transferred to the polypropylene molds and stored at 40 °C for 8 days for gelation and aging. Next, rod-shaped monoliths were washed with deionized water and treated with 1 M ammonia solution (Avantor, 25%) for 8 h at 90 °C. Afterward, the materials were washed, dried at 40 °C for 3 days, and finally calcined at 550 °C for 8 h to remove organic templates. The prepared monoliths of diameter 4.5 mm were put into heat-shrinkable tubes and equipped with connectors to obtain flow microreactors.

Zirconium propoxide moieties were grafted onto silica carriers, maintaining Zr/Si ratio fixed at 0.14 and using a solution of zirconium(IV) propoxide (Sigma Aldrich, 70% in 1-propanol) in anhydrous ethanol (Avantor, 99.8%). Reactive cores were impregnated with the solution and kept for 24 h at 70 °C. Finally, they were washed with ethanol and dried at 110 °C in nitrogen flow conditions.

Structural properties were analyzed by electron microscopy (TM 30000, Hitachi, Chiyoda, Tokyo, Japan) and adsorption–desorption measurements (ASAP 2020, Micromeritics, Norcross, GA, USA).

The continuous-flow microreactors were tested in the MPV reduction of various carbonyl compounds (cyclohexanone: Sigma Aldrich, 99%, benzaldehyde: Sigma-Aldrich, 99%, acetophenone: Acros, Geel, Belgium, 98%, cinnamaldehyde: Acros, 99%, citral: Roth, 95–98%, Karlsruhe, Germany, hexanal: Aldrich, Saint Louis, MO, USA, 98%, nonanal: Aldrich, 95%, 2-cyclohexen-1-one: Acros, 97%) with 2-butanol (Avantor 99%). The molar ratio of substrates was 1:52. The flow rate was changed in the range of 0.03–0.24 $cm^3 \cdot min^{-1}$. The progress and selectivity of the reaction were monitored by gas chromatography (FID detector, HP-5 column, 7890A, Agilent, Santa Clara, CA, USA).

The kinetic experiments were carried out in setup shown in Figure 5 for a flow rate fixed at 0.03 $cm^3 \cdot min^{-1}$, at the temperature range of 65–95 °C. The mass of the 1-cm-long microreactor was 0.0375 g. The length of reactive cores was changed from 1 to 8 cm (weight form 0.0375–0.3 g) and enabled the obtainment of data for different residence times, calculated using Equation (2):

$$\tau = \frac{m_k \cdot l \cdot V_T}{F} = \frac{0.0375 \cdot l \cdot V_T}{F} \quad (2)$$

where m_k is the mass of monolith per length unit [$g \cdot cm^{-1}$], l is the microreactor length [cm], V_T is the total pore volume, equal to -4 [$cm^3 \cdot g^{-1}$] (data from mercury porosimetry), and F is the flow rate [$cm^3 \cdot min^{-1}$].

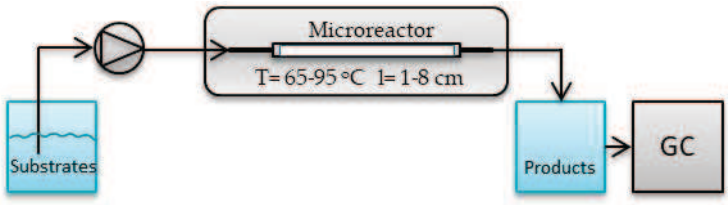

Figure 5. Scheme of the reaction setup.

4. Conclusions

The outstanding potential of continuous-flow microreactors in the area of selective reduction of carbonyl compounds was demonstrated. Broad-range and long-term experiments were conducted to determine the kinetics of the MPV reaction of cyclohexanone in the zirconium-functionalized flow microreactors. The lack of diffusion constraints in the microreactors was shown. The activation energy was calculated to be 52 kJ·mol^{-1}. Moreover, reaction rate constants for several ketones and aldehydes were collected. The rate of the process is necessary to design the apparatus and reaction systems. Significant differences in process efficiency were recorded for various carbonyl compounds. They were assigned to steric effects caused by bulky chains, electronic effects of an additional double bond, and an inductive effect of the benzene ring. We believe that the proposed system can be effectively exploited for fine chemical and pharmaceutical production.

Author Contributions: A.C. and K.M. conceived, designed, and performed the experiments; A.C., K.M., and J.M.-B. analyzed the data and wrote the paper.

Funding: This research was funded by the National Science Centre, Poland: DEC-2017/01/X/ST8/00083.

Acknowledgments: The financial support of the National Science Centre, Poland (project no. DEC-2017/01/X/ST8/00083), is gratefully acknowledged.

Conflicts of Interest: The authors declare no conflict of interest.

References

1. Liu, S.H.; Jaenicke, S.; Chuah, G.K. Hydrous zirconia as a selective catalyst for the Meerwein–Ponndorf–Verley reduction of cinnamaldehyde. *J. Catal.* **2002**, *206*, 321–330. [CrossRef]
2. Plessers, E.; Fu, G.X.; Tan, C.Y.X.; De Vos, D.E.; Roeffaers, M.B.J. Zr-based MOF-808 as Meerwein–Ponndorf–Verley reduction catalyst for challenging carbonyl compounds. *Catalysts* **2016**, *6*, 104. [CrossRef]
3. Axpuac, S.; Aramendía, M.A.; Hidalgo-Carrillo, J.; Marinas, A.; Marinas, J.M.; Montes-Jiménez, V.; Urbano, F.J.; Borau, V. Study of structure–performance relationships in Meerwein–Ponndorf–Verley reduction of crotonaldehyde on several magnesium and zirconium-based systems. *Catal. Today* **2012**, *187*, 183–190. [CrossRef]
4. Zapilko, C.; Liang, Y.C.; Nerdal, W.; Anwander, R. A general strategy for the rational design of size-selective mesoporous catalysts. *Chem. Eur. J.* **2007**, *13*, 3169–3176. [CrossRef] [PubMed]
5. Aramendía, M.A.A.; Borau, V.; Jiménez, C.; Marinas, J.M.; Ruiz, J.R.; Urbano, F. Reduction of α,β-unsaturated aldehydes with basic MgO/M_2O_3 catalysts (M=Al, Ga, In). *Appl. Catal. A Gen.* **2003**, *249*, 1–9. [CrossRef]
6. Uysal, B.; Oksal, B.S. A new method for the chemoselective reduction of aldehydes and ketones using boron tri-isopropoxide, $B(O^iPr)_3$: Comparison with boron tri-ethoxide, $B(OEt)_3$. *J. Chem. Sci.* **2011**, *123*, 681–685. [CrossRef]
7. Uysal, B.; Oksal, B.S. New heterogeneous $B(OEt)_3$-MCM-41 catalyst for preparation of α,β-unsaturated alcohols. *Res. Chem. Intermed.* **2015**, *41*, 3893–3911. [CrossRef]
8. Meerwein, H.; Schmidt, R. Ein neues verfahren zur reduktion von aldehyden und ketonen. *Justus Liebigs Ann. Chem.* **1925**, *444*, 221–238. [CrossRef]
9. Ooi, T.; Miura, T.; Takaya, K.; Ichikawa, H.; Maruoka, K. $Zr(OBut)_4$ as an effective promoter for the Meerwein–Ponndorf–Verley alkynylation and cyanation of aldehydes: Development of new asymmetric cyanohydrin synthesis. *Tetrahedron* **2001**, *57*, 867–873. [CrossRef]

10. Wang, J.; Okumura, K.; Jaenicke, S.; Chuah, G.K. Post-synthesized zirconium-containing beta zeolite in Meerwein–Ponndorf–Verley reduction: Pros and cons. *Appl. Catal. A Gen.* **2015**, *493*, 112–120. [CrossRef]
11. Creyghton, E.J.; Downing, R.S. Shape-selective hydrogenation and hydrogen transfer reactions over zeolite catalysts. *J. Mol. Catal. A Chem.* **1998**, *134*, 47–61. [CrossRef]
12. Zhang, B.; Xie, F.; Yuan, J.; Wang, L.; Deng, B.X. Meerwein–Ponndorf–Verley reaction of acetophenone over ZrO_2-La_2O_3/MCM-41: Influence of loading order of ZrO_2 and La_2O_3. *Catal. Commun.* **2017**, *92*, 46–50. [CrossRef]
13. Sushkevich, V.L.; Ivanova, I.I.; Tolborg, S.; Taarning, E. Meerwein–Ponndorf–Verley-Oppenauer reaction of crotonaldehyde with ethanol over Zr-containing catalysts. *J. Catal.* **2014**, *316*, 121–129. [CrossRef]
14. Rodriguez-Castellon, E.; Jimenez-Lopez, A.; Maireles-Torres, P.; Jones, D.I.; Roziere, J.; Trombetta, M.; Busca, G.; Lenarda, M.; Storaro, L. Textural and structural properties and surface acidity characterization of mesoporous silica-zirconia molecular sieves. *J. Solid State Chem.* **2003**, *175*, 159–169. [CrossRef]
15. Jimenez-Sanchidrian, C.; Ruiz, J.R. Tin-containing hydrotalcite-like compounds as catalysts for the Meerwein–Ponndorf–Verley reaction. *Appl. Catal. A Gen.* **2014**, *469*, 367–372. [CrossRef]
16. Battilocchio, C.; Hawkins, J.M.; Ley, S.V. A mild and efficient flow procedure for the transfer hydrogenation of ketones and aldehydes using hydrous zirconia. *Org. Lett.* **2013**, *15*, 2278–2281. [CrossRef] [PubMed]
17. Koreniuk, A.; Maresz, K.; Mrowiec-Białoń, J. Supported zirconium-based continuous-flow microreactor for effective Meerwein–Ponndorf–Verley reduction of cyclohexanone. *Catal. Commun.* **2015**, *64*, 48–51. [CrossRef]
18. Ciemięga, A.; Maresz, K.; Mrowiec-Białoń, J. Continuous-flow chemoselective reduction of cyclohexanone in a monolithic silica-supported $Zr(OPr^i)_4$ multichannel microreactor. *Microporous Mesoporous Mater.* **2017**, *252*, 140–145. [CrossRef]
19. Maresz, K.; Ciemięga, A.; Mrowiec-Białoń, J. Meervein–Ponndorf–Vereley reduction of carbonyl compounds in monolithic siliceous microreactors doped with Lewis acid centers. *Appl. Catal. A Gen.* **2018**, *560*, 111–118.
20. Ciemięga, A.; Maresz, K.; Malinowski, J.J.; Mrowiec-Białoń, J. Continuous-flow monolithic silica microreactors with arenesulfonic acid groups: Structure-catalytic activity relationships. *Catalysts* **2017**, *7*, 255. [CrossRef]
21. Li, G.; Fu, W.H.; Wang, Y.M. Meervvein–Ponndorf–Verley reduction of cyclohexanone catalyzed by partially crystalline zirconosilicate. *Catal. Commun.* **2015**, *62*, 10–13. [CrossRef]
22. Corma, A.; Domine, M.E.; Valencia, S. Water-resistant solid Lewis acid catalysts: Meerwein–Ponndorf–Verley and Oppenauer reactions catalyzed by tin-beta zeolite. *J. Catal.* **2003**, *215*, 294–304. [CrossRef]
23. Ruiz, J.R.; Jiménez-Sanchidrián, C.; Hidalgo, J.M.; Marinas, J.M. Reduction of ketones and aldehydes to alcohols with magnesium–aluminium mixed oxide and 2-propanol. *J. Mol. Catal. A Chem.* **2006**, *246*, 190–194. [CrossRef]
24. Aramendia, M.A.; Borau, V.; Jimenez, C.; Marinas, J.M.; Ruiz, J.R.; Urbano, F.J. Activity of basic catalysts in the Meerwein–Ponndorf–Verley reaction of benzaldehyde with ethanol. *J. Colloid Interface Sci.* **2001**, *238*, 385–389. [CrossRef] [PubMed]
25. Theodosis-Nobelos, P.; Kourti, M.; Tziona, P.; Kourounakis, P.N.; Rekka, E.A. Esters of some non-steroidal anti-inflammatory drugs with cinnamyl alcohol are potent lipoxygenase inhibitors with enhanced anti-inflammatory activity. *Bioorg. Med. Chem. Lett.* **2015**, *25*, 5028–5031. [CrossRef] [PubMed]
26. Carnesecchi, S.; Schneider, Y.; Ceraline, J.; Duranton, B.; Gosse, F.; Seiler, N.; Raul, F. Geraniol, a component of plant essential oils, inhibits growth and polyamine biosynthesis in human colon cancer cells. *J. Pharmacol. Exp. Ther.* **2001**, *298*, 197–200. [PubMed]

Dr hab. inż. Julita Mrowiec-Białoń

Instytut Inżynierii Chemicznej

Polskiej Akademii Nauk

Gliwice, 16.06.2018r.

OŚWIADCZENIE

Oświadczam, że w pracach:

1. Agnieszka Koreniuk, Katarzyna Maresz, Klaudia Odrozek, Andrzej B. Jarzębski, **Julita Mrowiec-Białoń**, *Highly effective continuous-flow monolithic silica microreactor for acid catalyzed processes,* Applied Catalysis A, General 489 (2015) 203-208
2. Małgorzata Berdys, Agnieszka Koreniuk, Katarzyna Maresz, Wojciech Pudło, Andrzej B. Jarzębski, **Julita Mrowiec-Białoń**, *Fabrication and performance of monolithic continuous-flow silica microreactors*, Chemical Engineering Journal 282 (2015) 137-141
3. Agnieszka Koreniuk, Katarzyna Maresz, **Julita Mrowiec-Białoń**, *Supported zirconium-based continuous-flow microreactor for effective Meerwein-Ponndorf-Verley reduction of cyclohexanone*, Catalysis Communications 64 (2015) 48-51
4. Agnieszka Koreniuk, Katarzyna Maresz, Klaudia Odrozek, **Julita Mrowiec-Białoń**, *Titania-silica monolithic multichannel microreactors. Proof of concept and fabrication/structure/catalytic properties in the oxidation of 2,3,6-trimethylphenol*, Microporous and Mesoporous Materials 229 (2016) 98-105
5. Agnieszka Ciemięga, Katarzyna Maresz, **Julita Mrowiec-Białoń**, *Continuous-flow chemoselective reduction of cyclohexanone in a monolithic silica-supported $Zr(OPr^i)_4$ multichannel microreactor*", Microporous and Mesoporous Materials 252 (2017) 140-145
6. Agnieszka Ciemięga, Katarzyna Maresz, Janusz J. Malinowski, **Julita Mrowiec-Białoń**, *Continuous-Flow Monolithic Silica Microreactors with Arenesulphonic Acid Groups: Structure-Catalytic Activity Relationships*, Catalysts 7 (2017) 255-265

7. Agnieszka Ciemięga, Katarzyna Maresz, Janusz J. Malinowski, **Julita Mrowiec-Białoń,** *Comparative study of continuous-flow microreactors based on silica monoliths modified with Lewis acid centres*, Chemical and Process Engineering 39 (2018) 33–38
8. Agnieszka Ciemięga, Katarzyna Maresz, **Julita Mrowiec-Białoń**, *Meerwein-Ponndorf-Verley reduction of carbonyl compounds in monolithic siliceous microreactors doped with Lewis acid centres*, Applied Catalysis A, General 560 (2018) 111–118
9. Katarzyna Maresz, Agnieszka Ciemięga, **Julita Mrowiec-Białoń**, *Selective Reduction of Ketones and Aldehydes in Continuous-Flow Microreactor - Kinetic Studies*, Catalysts 8 (2018) 221

mój wkład polegał na:

- nadzorze i opiece nad pracą doktorską jako promotor,

- ustaleniu tematyki i zakresu badań;

- współudziale w pisaniu manuskryptów publikacji i ich korekcie merytorycznej.

Dr inż. Katarzyna Maresz

Instytut Inżynierii Chemicznej

Polskiej Akademii Nauk

Gliwice, 16.06.2018r.

OŚWIADCZENIE

Oświadczam, że w pracach:

1. Agnieszka Koreniuk, **Katarzyna Maresz**, Klaudia Odrozek, Andrzej B. Jarzębski, Julita Mrowiec-Białoń, *Highly effective continuous-flow monolithic silica microreactor for acid catalyzed processes,* Applied Catalysis A, General 489 (2015) 203-208.
2. Małgorzata Berdys, Agnieszka Koreniuk, **Katarzyna Maresz**, Wojciech Pudło, Andrzej B. Jarzębski, Julita Mrowiec-Białoń, *Fabrication and performance of monolithic continuous-flow silica microreactors*, Chemical Engineering Journal 282 (2015) 137-141.
3. Agnieszka Koreniuk, **Katarzyna Maresz**, Julita Mrowiec-Białoń, *Supported zirconium-based continuous-flow microreactor for effective Meerwein-Ponndorf-Verley reduction of cyclohexanone*, Catalysis Communications 64 (2015) 48-51.
4. Agnieszka Koreniuk, **Katarzyna Maresz**, Klaudia Odrozek, Julita Mrowiec-Białoń, *Titania-silica monolithic multichannel microreactors. Proof of concept and fabrication/structure/catalytic properties in the oxidation of 2,3,6-trimethylphenol*, Microporous and Mesoporous Materials 229 (2016) 98-105.
5. Agnieszka Ciemięga, **Katarzyna Maresz**, Julita Mrowiec-Białoń, *Continuous-flow chemoselective reduction of cyclohexanone in a monolithic silica-supported $Zr(OPr^i)_4$ multichannel microreactor*", Microporous and Mesoporous Materials 252 (2017) 140-145.
6. Agnieszka Ciemięga, **Katarzyna Maresz**, Janusz J. Malinowski, Julita Mrowiec-Białoń, *Continuous-Flow Monolithic Silica Microreactors with Arenesulphonic Acid Groups: Structure-Catalytic Activity Relationships*, Catalysts 7 (2017) 255-265.
7. Agnieszka Ciemięga, **Katarzyna Maresz**, Janusz J. Malinowski, Julita Mrowiec-Białoń, *Comparative study of continuous-flow microreactors based on silica monoliths modified with Lewis acid centres*, Chemical and Process Engineering 39 (2018) 33–38.

Maresz

8. Agnieszka Ciemięga, **Katarzyna Maresz**, Julita Mrowiec-Białoń, *Meerwein-Ponndorf-Verley reduction of carbonyl compounds in monolithic siliceous microreactors doped with Lewis acid centres*, Applied Catalysis A, General 560 (2018) 111–118.
9. **Katarzyna Maresz**, Agnieszka Ciemięga, Julita Mrowiec-Białoń, *Selective Reduction of Ketones and Aldehydes in Continuous-Flow Microreactor - Kinetic Studies*, Catalysts 8 (2018) 221.

mój wkład polegał na:

- nadzorze i opiece nad pracą doktorską jako promotor pomocniczy,
- współudziale w zaplanowaniu i wykonaniu prac doświadczalnych
- współudziale w pisaniu manuskryptów publikacji.

Katarzyna Maresz

Prof. dr hab. inż. Andrzej Jarzębski

Katedra Inżynierii Chemicznej

i Projektowania Procesowego

Wydział Chemiczny

Politechnika Śląska

Gliwice, 16.06.2018r.

OŚWIADCZENIE

Oświadczam, że w pracach:

1. Agnieszka Koreniuk, Katarzyna Maresz, Klaudia Odrozek, **Andrzej B. Jarzębski**, Julita Mrowiec-Białoń, *Highly effective continuous-flow monolithic silica microreactor for acid catalyzed processes,* Applied Catalysis A, General 489 (2015) 203-208
2. Małgorzata Berdys, Agnieszka Koreniuk, Katarzyna Maresz, Wojciech Pudło, **Andrzej B. Jarzębski,** Julita Mrowiec-Białoń, *Fabrication and performance of monolithic continuous-flow silica microreactors*, Chemical Engineering Journal 282 (2015) 137-141

mój udział polegał na współredagowaniu i korekcie manuskryptów publikacji.

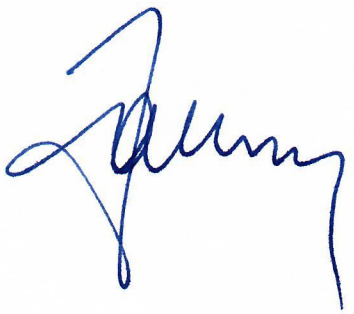

Dr Janusz J. Malinowski

Instytut Inżynierii Chemicznej

Polskiej Akademii Nauk

Gliwice, 16.06.2018r.

OŚWIADCZENIE

Oświadczam, że w pracach:

1. Agnieszka Ciemięga, Katarzyna Maresz, **Janusz J. Malinowski**, Julita Mrowiec-Białoń, *Continuous-Flow Monolithic Silica Microreactors with Arenesulphonic Acid Groups: Structure-Catalytic Activity Relationships*, Catalysts 7 (2017) 255-265.

   mój udział polegał na współredagowaniu manuskryptu.

2. Agnieszka Ciemięga, Katarzyna Maresz, **Janusz J. Malinowski**, Julita Mrowiec-Białoń, *Comparative study of continuous-flow microreactors based on silica monoliths modified with Lewis acid centres*, Chemical and Process Engineering 39 (2018) 33–38.

   mój wkład polegał na wykonaniu badań adsorpcji azotu.

Mgr inż. Małgorzata Berdys-Korkus

Katedra Inżynierii Chemicznej

i Projektowania Procesowego

Wydział Chemiczny

Politechnika Śląska

Gliwice, 16.06.2018r.

OŚWIADCZENIE

Oświadczam, że w pracy:

Małgorzata Berdys, Agnieszka Koreniuk, Katarzyna Maresz, Wojciech Pudło, Andrzej B. Jarzębski, Julita Mrowiec-Białoń, *Fabrication and performance of monolithic continuous-flow silica microreactors*, Chemical Engineering Journal 282 (2015) 137-141

mój udział polegał na opracowaniu metody generowania powierzchniowych hydroksyli w kordierytowym nośniku przed jego modyfikacją.

Dr inż. Klaudia Odrozek

Katedra Inżynierii Chemicznej

i Projektowania Procesowego

Wydział Chemiczny

Politechnika Śląska

Gliwice, 18.06.2018r.

OŚWIADCZENIE

Oświadczam, że w pracy:

Agnieszka Koreniuk, Katarzyna Maresz, **Klaudia Odrozek**, Andrzej B. Jarzębski, Julita Mrowiec-Białoń, *Highly effective continuous-flow monolithic silica microreactor for acid catalyzed processes,* Applied Catalysis A, General 489 (2015) 203-208

mój udział polegał na wykonaniu badań materiałów metodą skaningowej mikroskopii elektronowej.

Odrozek Klaudia

Dr inż. Wojciech Pudło

Katedra Inżynierii Chemicznej

i Projektowania Procesowego

Wydział Chemiczny

Politechnika Śląska

Gliwice, 18.06.2018r.

OŚWIADCZENIE

Oświadczam, że w pracy:

Małgorzata Berdys, Agnieszka Koreniuk, Katarzyna Maresz, **Wojciech Pudło**, Andrzej B. Jarzębski, Julita Mrowiec-Białoń, *Fabrication and performance of monolithic continuous-flow silica microreactors*, Chemical Engineering Journal 282 (2015) 137-141

mój wkład polegał na współudziale w opracowaniu metody generowania powierzchniowych hydroksyli w kordierytowym nośniku przed jego modyfikacją.